Design, synthesis and biological evaluation of two classes of antimycobacterial cyclic hexa(depsi)peptides

Dissertation

zur Erlangung des

Doktorgrades der Naturwissenschaften (Dr. rer. nat.)

der

Naturwissenschaftlichen Fakultät I – Biowissenschaften

der

Martin-Luther-Universität Halle-Wittenberg

vorgelegt von

Henok Asfaw Sahile

geboren am 02.12.1984 in Enewari, Äthiopien

Gutachter: Prof. Dr. habil. Peter Imming

Verteidigungsdatum:31.05.2017

Dedicated to my wife and my mother

Table of contents

List of abbreviations

2-CT	2-chlorotrityl chloride resin
ADP	adenosine diphosphate
Ala	alanine
allo-Ile	*allo*-isoleucine
AMP	antimicrobial peptide
Arg	arginine
Asn	asparagine
Asp	aspartic acid
ATP	adenosine triphosphate
AUC	area under curve
Boc	tert-butyloxycarbonyl
BOP.Cl	Bis(2-oxo-3-oxazolidinyl)phosphinic chloride
BTZ	benzothiazinone
Calc.	calculated
CFU	colony forming units
CGM	cyclohexylgriselimycin
CL_{int}	intrinsic microsomal clearance
CLND	chemiluminescent nitrogen detection
CL_{pred}	predicted microsomal clearance
DCC	dicyclohexylcarbodiimide
DCM	dichloromethane
DIC	diisopropylcarbodiimide
DIPEA	diisopropylethylamine
DMAP	dimethylaminopyridine
DMF	dimethylformamide
ADME	drug metabolism and pharmacokinetics
DNAUC	dose normalized area under curve
DPRE1	decaprenylphosphoryl-β-D-ribose oxidase
DVB	divinylbenzene
DVB-PS	divinylbenzene - polystyrene
EDC*HCl	1-Ethyl-3-(3-dimethylaminopropyl)carbodiimide hydrochloride
ESI-MS	electrospray ionization-mass spectroscopy
EtOAc	ethyl acetate
EtOH	ethanol
Fmoc	fluorenylmethyloxycarbonyl
Gln	glutamine

Glu	glutamic acid
Gly	glycine
GM	griselimycin
GSK	GlaxoSmithKline
HATU	N-{(dimethylamino)-1H-1,2,3-triazolo[4,5-b]-pyridino-1-ylmethylene}-N methylmethanaminium hexafluorophosphate
HepG2	human hepatocellular carcinoma cells
HFIP	hexafluoroisopropyl alcohol
HIV	human immunodeficiency virus
HKI	Hans-Knöll-Institut
HOAt	1-hydroxy-7-azabenzotriazole
HOBt	1-hydroxybenzotriazole
HPLC	high pressure liquid chromatography
HSA	Human serum albumin
IC_{50}	concentration that inhibits the growth of 50% of the population
INH	isoniazid
IP	intraperitoneal
Ile	isoleucine
LBF	liver blood flow
LC-MS	liquid chromatography-mass spectroscopy
Leu	leucine
LLOQ	lower limit of quantification
Lys	lysine
mAGP	mycolyl-arabinogalactan-peptidoglycan
Met	methionine
MDR	multi drug resistant
MeOH	methanol
MIC	minimum inhibitory concentration
MNBA	2-methyl-6-nitrobenzoic anhydride
mp	melting point
Mtb	*Mycobacterium tuberculosis*
NADH	nicotinamide adenine dinucleotide
NAG	N-acetylglocosamine
NAM	N-acetylmuramic acid
nd	not determined
NMP	N-Methyl-2-pyrrolidone (
NMR	nuclear magnetic resonance
Orn	ornithine

PAMPA	passive artificial membrane permeability assay
PASA	para amino salicylic acid
Pbf	2,2,4,7,6-pentamethyldihydrobenzofuran-5-sulfonyl
PG	peptidoglycan
Phe	phenylalanine
PoC	proof of concept
Pro	proline
PyBOP	Benzotriazol-1-yl-N-oxy-tris(pyrrolidino)phosphonium hexafluorophosphate
QC	quality control
qd	once a day
RNA	ribose nucleic acid
RT	retention time
rt	room temperature
SAR	structure activity relationship
Sar	sarcosine
Ser	serine
SPPS	solid phase peptide synthesis
TB	tuberculosis
TEA	triethylamine
TFA	trifluoroacetic acid
THF	tetrahydrofuran
Thr	threonine
TIPS	triisopropylsilane
TLC	thin layer chromatography
Trp	tryptophan
Trt	trityl
UDP	uridine diphosphate
UPLC-MS	ultra-performance liquid chromatography-mass spectroscopy
UV	ultraviolet
Val	valine
WHO	world health organization
XDR	extensively drug resistant
ZoI	growth inhibition zone

List of figures

List of tables

1. Introduction

1.1. Global tuberculosis burden

Tuberculosis (TB), still considered by some to be a disease of the past, is a cause of illness for more than 9 million people worldwide each year. In 2014 alone, 9.6 million people fell ill because of TB and out of which 1.1 million people lost their lives, an amount equivalent to the total population of Estonia[1]. TB is also the leading killer of HIV-positive people: in 2015, 1 in 3 HIV deaths was associated with TB. This made TB worldwide, along with HIV, to be the leading cause of death among infectious diseases. Though the majority of TB associated deaths occurred in low- and middle-income countries, developed nations are not immune from its incumbent threat. For example, in 2015, it was reported that the incidence rate of TB in some parts of London was higher than in Rwanda and Iraq[2]. Recently, an outbreak of TB in west Alabama (USA) was reported to kill three persons and sicken 26 and the infection rate in the town of Marion was found to be greater than those in many third world countries[3]. In Germany, in relation to the recent high immigrant influx, a large surge in the number of new TB cases was reported[4]. These facts indicate that despite the availability of effective diagnosis tools and effective cure for more than half a century, the danger imposed by the disease is still imminent. The problem is further complicated by the emergence and rapid distribution of multidrug and extensively resistant (MDR/XDR) bacteria. In 2014, an estimated 480,000 new cases of MDR-TB were reported and this was a cause of death for 190,000 people. On the other hand, the development of a new anti TB drug has been almost nonexistent, with only two new drug marketed in the past 40 years[5]. The gap clearly signifies the importance of developing new anti-tubercular agents to properly address the problem we are now facing.

1.2. Causative agent

The most common cause of human TB is *Mycobacterium tuberculosis* (*Mtb*) which is a rod shaped, obligate aerobic, intracellular acid fast bacillus. The structural feature of the bacterium that largely contributes to its pathogenicity and viability is the complex nature of its cell wall[6].

The cell wall of *Mtb* is composed of two distinct layers; the lower and upper segments (Figure 1). The lower segment is made up of three discrete macromolecules namely: peptidoglycan (PG), arabinogalactan and mycolic acids. These macromolecules are covalently linked to each other and form the main, insoluble, core of the cell wall which is also known as the mycolyl-arabinogalactan-peptidoglycan (mAGP) complex[7,8]. Surrounding the complex are non-covalently linked lipids, proteins and polysaccharides that form the soluble outer segment of the cell wall. These include free lipids that are composed of different chain length fatty acids, the cell-wall proteins, the phosphatidylinositol mannosides (PIMs), the phthiocerol- containing lipids, lipomannan (LM), and lipoarabinomannan (LAM)[8].
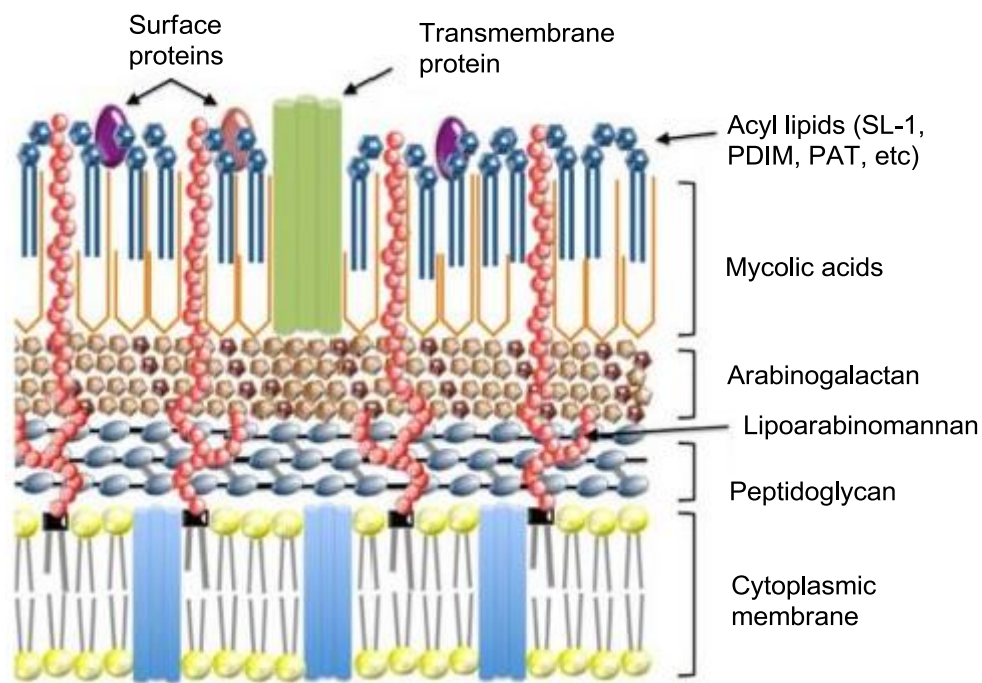
Figure 1: Schematic diagram of the components of Mycobacterium tuberculosis cell wall (the figure was taken from https://pharmchem.ucsf.edu/research/chembio/drug-targeting with permission).

PG constitutes a crucial component of the mycobacterial cell wall which provides structural support and is essential for its survival. The PG layer surrounds the plasma membrane and is made of long repeating polymers of the disaccharide *N*-acetyl glucosamine–*N*-acetyl muramic acid (NAG–NAM) that are linked via peptide bridges. The synthesis of PG takes place in three stages. The first stage involves the formation of the nucleotide-sugar linked precursors (UDP-NAM and UDP-NAG) and this occurs in the cytoplasm. The second synthetic stage occurs in the cell membrane, where the PG precursor lipid II is generated from the nucleotide-sugar units and a transport lipid (undecaprenyl pyrophosphate) found on the membrane. Lipid II is then transported across the periplasm by the transmembrane proteins and is incorporated into the nascent PG by the action of penicillin-binding proteins (PBPs)[9]. In the final stage, PBPs catalyze both transglycosylation and transpeptidation reactions, leading to the respective polymerization and crosslinking of the glycan strands via flexible peptides[10].

The PG layer of *Mtb* is linked to the outer mycolic acid moiety by a highly branched polysaccharide unit of arabinogalactan (AG). The galactan unit of AG comprises of repeating linear disaccharides unit of furanosyl galactose (Gal*f*) linked with an alternating β-(1-5) and β-(1-6) glycosidic linkage. The galactan moiety is modified with a long branched polymer of arabinan which is made of a repeating disaccharide unit of furanosyl arabinose (Ara*f*). A portion of the arabinan branch is also further modified by the addition of succinyl or unusual non-*N*-acetylated galactosamine (GalN) moieties[7,8].

On the termini of the arabinan part is a ligated long carbon chain mycolic acid. Mycolic acids are β-hydroxy fatty acids with a long α-alkyl side chain. The *Mtb* cell wall contains 3 classes of these acids: α-, keto-, and methoxymycolates. The mycolic acid moiety is responsible for the characteristic thick, waxy and impermeable nature of the mycobacterial cell wall and this is considered to be the major contributing factor for its virulence[11].

1.3. Pathophysiology of tuberculosis

Inhalation of aerosolized droplets that contain a small number of the bacilli is sufficient to initiate the infection[12]. Once the bacilli reach the lung alveoli, they encounter alveolar macrophages as a first line defense. They become internalized by the macrophages through phagocytosis. The entrance of *Mtb* to the alveolar macrophages is facilitated by two important factors: the presence of multiple cell surface receptors on the macrophages and the complex structure of the *Mtb* cell wall surface, which enables the bacteria to interact with these multiple receptors in various ways[13]. The cell surface receptors on macrophages through which *Mtb* enter include: complement receptors (CRs), mannose receptors (MR) and Fc receptors[14–16].

The fate of the internalized phagosome depends on the entrance point. For instance, if it enters through Fc receptors, respiratory burst occurs and an inflammatory response which results in activation of macrophages and complete destruction of the bacteria. On the other hand, if the entry occurs *via* other receptors like a complement receptor (CR3) or mannose receptor, it inhibits activation of the macrophages and ensures its survival[16,17]. The bacteria, inside non-activated macrophages, avoid destruction and ensure their survival through an arrest of phagosomal maturation[18,19].

Once arresting the phagosomal maturation, the bacteria continue to multiply within the macrophage and disseminate to the other parts of the lung or other organs through blood or local lymphatic system. At the later stage of the infection (usually after 3 weeks), the infected macrophages in the lymph nodes process and present the mycobacterial antigen to the T-cell. This leads to the initiation of adaptive immunity through generation of activated T-Cell effectors[20].

Activated macrophages exert both direct bactericidal action through generation of reactive free radicals and release more chemokines which facilities formation of granuloma through the recruitment of monocytes, lymphocytes and other types of cells[21,22]. A granuloma is constituted of infected macrophages at the center, surrounded by epithelioid macrophages, foam cells, and

occasional multinucleated giant cells of the Langhans type, with peripheral recruited lymphocytes and a fibrous capsule (Figure 2). This multicellular structure serves to wall off and contain the bacteria which continue growing and overwhelm the cells it has infected until they die. Over time, the center of the granuloma undergoes necrosis, and the high lipid and protein content of the dead macrophages results in the formation of caseous center[23,24].

In 90% all the cases, these necrotized lesions heal with some amount of scarring and calcification but not remain free of infection where the bacteria remain as dormant (latent) state for years and the individual remains asymptomatic. Approximately 10% of infected individuals, however, develop severe, life-threatening disease or primary progressive disease at this stage. This is believed to be caused by high bacterial load, increased bacterial virulence, immunosuppression, or genetic susceptibility[25].
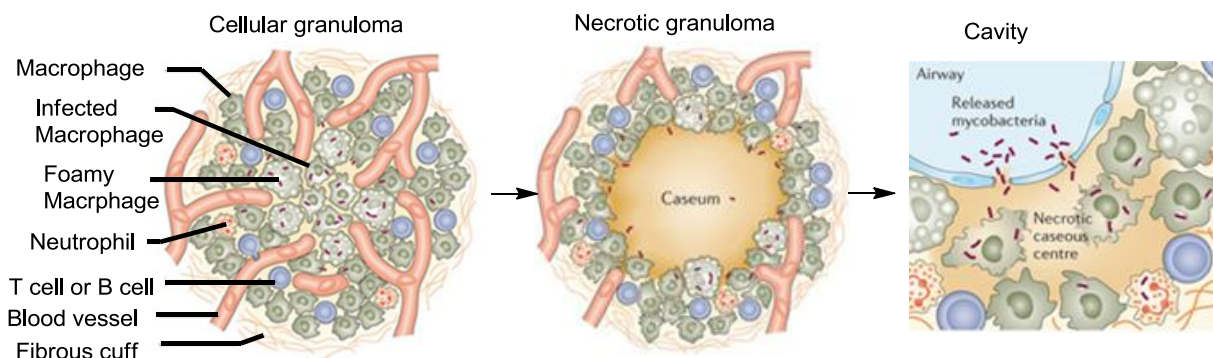
Figure 2: Stages in the pathogenesis of tuberculosis (the figure was taken from *Nat. Rev. Microbiol.* **2014**, 12, 159–167 with permission).

At some points in their life time, 10% of individuals with a latent infection develop a secondary disease and this is known to contribute about 80% of the clinical TB cases. Reactivation of the secondary TB could occur after re-infection with virulent strains or following weakening of the host immune system, for example because of HIV[25–27].

Granulomas of secondary TB are found most often in the lung apices or may be disseminated in the lungs, kidneys, meninges, marrow and other organs. Pulmonary lesions begin as an exudative bronchopneumonia and progress to classical caseous granuloma formation, followed by massive necrosis and cavity formation. Eventually, there is breakdown of the fibrous capsule and communication with airways. These events allow for rapid growth of extracellular bacilli and spread into airways, leading to transmission or intrapulmonary spread[28]. In immunocompetent individuals, secondary TB can result in dissemination and death in 50% of cases and chronicity in 25% to 30% of cases. If the host is able to reestablish immune control over the disease, recovery is also possible, as is seen in 20% to 25% of cases[25,29].

1.4. Currently available anti TB drugs

Drugs that are currently available for the treatment of TB are classified as first-line (Figure 3) and second-line (Figure 4) based on their efficacy, safety, cost and the status of the disease they are indicated. The drugs are either originally developed specifically for TB or repurposed to treat TB after they were initially developed for other bacterial infections. The general features of the most commonly used anti TB drugs are briefly summarized below[30].

1.4.1. First line anti TB drugs

Isoniazid (INH)

INH (**1**) is the most effective TB specific drug developed so far. It was developed in 1952 by researchers from three pharmaceutical companies – Roche, Bayer and Squibb – independently at the same time when they were looking for antitubercular compounds related to nicotinamide and thiosemicarbazones[31]. The drug has high potency with an MIC of 0.2 μM against rapidly growing *Mtb*. However, its activity against slowly growing *Mtb* is weak and it has practically no *in vitro* activity against anaerobically adapted bacteria[32].

INH works by inhibiting a principal enzyme, NADH-dependent enoyl-ACP reductase (InhA), involved in mycobacterial mycolic acid synthesis after it is activated to an isonicotinoyl radical

6

by mycobacterial KatG catalase enzyme[33–35]. Mycobacterial resistance to INH was reported shortly after it was introduced into the market. The major mechanism involved in INH resistance is mutations in katG and/or inhA enzymes[36,37]. Nonetheless, the drug still forms the backbone of both TB prophylaxis and treatment regimens in combination with other first line anti TB agents.

Rifampicin (R)

The first antimycobacterial rifamycin, rifamycin B, was isolated in 1957 from metabolites of *Amycolatopsis mediterranei* at the laboratory of Gruppo Lepetit SpA in Milan. However, the isolated rifamycin had weak potency and was only active when delivered intravenously[38]. Rifampin (**2**) was developed after putting a lot of effort to optimize the complex structure of rifamycin B for better potency and oral bioavailability[39]. Nowadays, rifampin represents one of the most active and widely used anti TB drugs. It is used for the treatment and prophylaxis of TB. The drug is also effective against a wide range of Gram positive and Gram negative bacteria.

Rifampin works by inhibiting the β-subunit of bacterial DNA-dependent RNA polymerase and stops the transcription of RNA. Accordingly, resistance to rifampin occurs primarily through point mutations acquired in the RNA polymerase ß-subunit gene, rpoB[40,41]. Resistance may also occur through ADP-ribosylation of the alcohol at position C(21)[42,43].

Pyrazinamide (Z)

Like INH, Pyrazinamide (**3**) is also a nicotinamide analogue that was discovered in 1952 in attempt to optimize the structure of nicotinamide for better anti TB activity[44]. Though its anti TB activity was discovered in 1952, the drug was included in the first line list in 1980s after studying its excellent potential to remarkably shorten the treatment duration from 1 year to 6 months when used in combination with rifampin and INH. Pyrazinamide has an excellent sterilizing effect on semi-dormant forms of the tubercle bacilli residing in macrophages[45].

The exact mechanism of action of pyrazinamide is not clear but there are studies which showed that it likely kills *Mtb* by intracellular acidification following hydrolysis by *Mtb*

nicotinamidase/pyrazinamidase[46]. Inhibition of fatty acid synthase has also been proposed as a mechanism[47].

Ethambutol (E)

The anti tuberculotic activity of ethambutol (**4**) was first reported in 1961 by Wilkinson *et al*[48]. In this work it was shown that the *dextro* form of 2,2'-(ethylenediimino)-di-l-butanol (ethambutol) had exhibited better potency and less toxicity profile than streptomycin (**5**) when administered parenterally and equivalent efficacy index with INH when taken orally[48]. It was also shown that ethambutol was active against streptomycin and INH resistant *Mtb* infection[48]. Soon after that (in 1966), ethambutol was included in the TB treatment regimen as a first line drug which is used when there is known resistance to INH.

Ethambutol works by inhibiting the enzyme arabinosyl transferase which is essential for synthesis of arabinoglycan unit of mycobacterial cell wall. This leads to inhibition of the mycolyl-arabinogalactan-peptidoglycan (mAGP) complex, the core of mycobacterial cell wall[49,50]. Ethambutol resistance has been reported to occur through mutation of the gene *emb*B at *emb*B306 position. embABC is a gene that is responsible to encode mycobacterial arabinosyl transferase enzyme[51].

Streptomycin (S)

The aminoglycoside streptomycin (**5**) is the first successful anti TB antibiotic to be introduced in the market. It was isolated in 1943 from a soil microorganism, *Streptomyces griseus*, in Waksman's laboratory by his doctoral student Albert Schatz in Rutgers University, New Jersey[52,53]. After the first clinical trial, results were published in 1945 and the drug was marketed by Merck in 1946. Apart from its strong activity against actively growing *Mtb* bacilli, streptomycin has a broad spectrum of action against a panel of Gram-positive and Gram-negative bacteria[54]. The use of streptomycin in the current TB treatment regimen is declined attributed to its ototoxicity and nephrotoxicity.

Streptomycin acts by inhibiting the 30S subunit of the ribosome at the ribosomal protein S12 and the 16S rRNA coded by the genes *rpsL* and *rrs*, respectively. By doing so, it interferes with bacterial protein synthesis which leads to cell death[55]. Consequently, mutations in *rpsL* and rrs are the major mechanisms of resistance to streptomycin[56,57].

INH **(1)**

Rifampin **(2)**

Pyrazinamide **(3)**

Ethambutol **(4)**

Streptomycin **(5)**
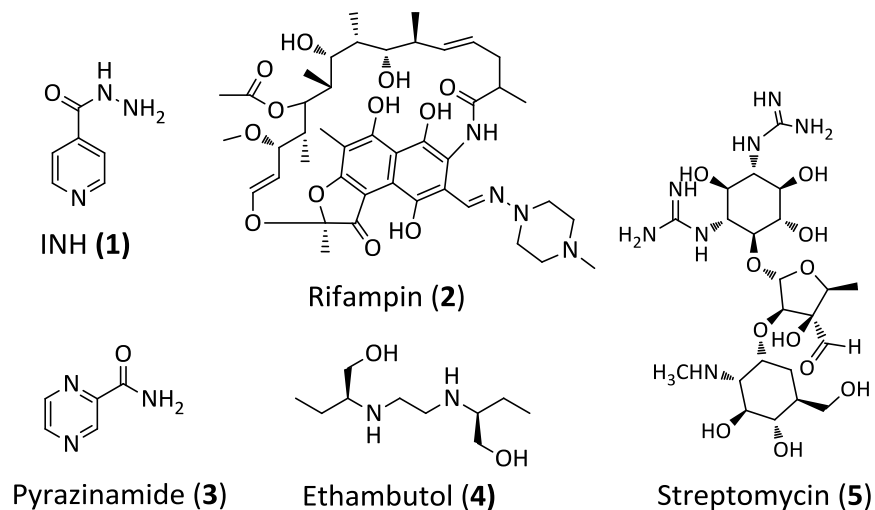
Figure 3: Chemical structures of first line anti TB drugs.

1.4.2. Second line anti TB drugs

Aminoglycosides

Two other second generations aminoglycosides, kanamycin (**6a-c**) and amikacin (**7**), are included as a second line anti TB agents for the treatment of MDR-TB[58–61]. These drugs were initially developed to circumvent the problem of drug resistant against streptomycin in other bacterial infections, not in *Mtb*. They were then repurposed to be used as anti TB agents.

Para-amino salicylic acid (PASA)

PASA (**8**) was the second anti TB drug to be marketed next to streptomycin. It is a synthetic drug that was developed in 1944 by the Danish professor of physiology Jorgen Lehmann at the central laboratory of Sahlgrenska University Hospital, Sweden. After finishing the clinical trial, the drug was then marketed in 1946.

PASA is now considered as a second line drug as part of the treatment regimen for MDR-TB[62]. The mechanism of action of PASA is proposed to be competitive inhibition of *para*-amino benzoic acid (PABA) incorporation by dihydropteroate synthase enzyme during the synthesis of *Mtb* folic acid. A mutation in the thyA gene, which encodes for thymidylate synthase, is known to confer PASA resistance[63,64].

Cycloserine

Cycloserine (**9**) is an oral bacteriostatic second line anti-tuberculosis drug used in MDR-TB treatment regimens. It is a natural product that was isolated from *Streptomyces sp*. in 1955 by research groups in two companies- Merck and El-Lilly-independently at a time[65]. Cycloserine works in two ways. The major action is mediated through inhibition of the enzyme alanine racemase, which is responsible for conversion of L-alanine to D-alanine during the synthesis of *Mtb* PG. It inhibits this enzyme by forming an irreversible isoxazole-pyridoxal adduct[66]. In addition, cycloserine also inhibits D-alanine–D-alanine ligase enzyme that is involved in synthesis of the terminal D-alanine–D-alanine of the peptidoglycan UDP-NAM[67]. Over

expression of *alr*A, the gene that encodes alanine racemase is reported to lead a cycloserine resistance in recombinant mutants of *M. smegmatis*[68].

Capreomycins

Capreomycins (**10a-b**) are a mixture of two cyclic pentapeptides isolated in 1960 from *Saccharothrix mutabolis* subspecies *capreolus*. They inhibit protein synthesis by binding at the interface between helix 44 of the 30S subunit and helix 69 of the 50S subunit of the bacterial ribosome[69]. Mutations in the *tlyA* gene have been shown to cause resistance to capreomycin. TlyA is an rRNA methyltransferase specific for 2'-O-methylation of ribose in rRNA. Mutations in t*lyA* determine the absence of methylation activity[70].

Fluoroquinolones

After being originally introduced as broad spectrum synthetic antibacterial agents, some members of the newer generation quinolones such as ofloxacin (**11**), moxifloxacin (**12**) and gatifloxacin (**13**) are being repurposed a second line anti TB agents for the treatment of MDR-TB[71,72]. Fluoroquinolones act by inhibiting the topoisomerase II (DNA gyrase) and topoisomerase IV, two principal enzymes for bacterial survival. These proteins are encoded by the genes *gyrA*, *gyrB*, *parC* and *parE*, respectively[73]. In *Mtb*, fluoroquinolones target only type II topoisomerase (DNA gyrase) as it has no the other enzyme (topoisomerase IV). *Mtb* acquire fluoroquinolone resistance by chromosomal mutations in the quinolone resistance determining region of *gyrA* or *gyrB* activity[74].

Kanamycin(**6**)

6a R$_1$= NH$_2$, R$_2$= OH

6b R$_1$= NH$_2$, R$_2$= NH$_2$

6c R$_1$= OH, R$_2$= NH$_2$

Amikacin (**7**)

PASA (**8**)

Cycloserine (**9**)

Capreomycin (**10**)

10a; R= OH

10b; R= H

Ofloxacin (**11**)

Moxifloxacin (**12**)

Gatifloxacin (**13**)
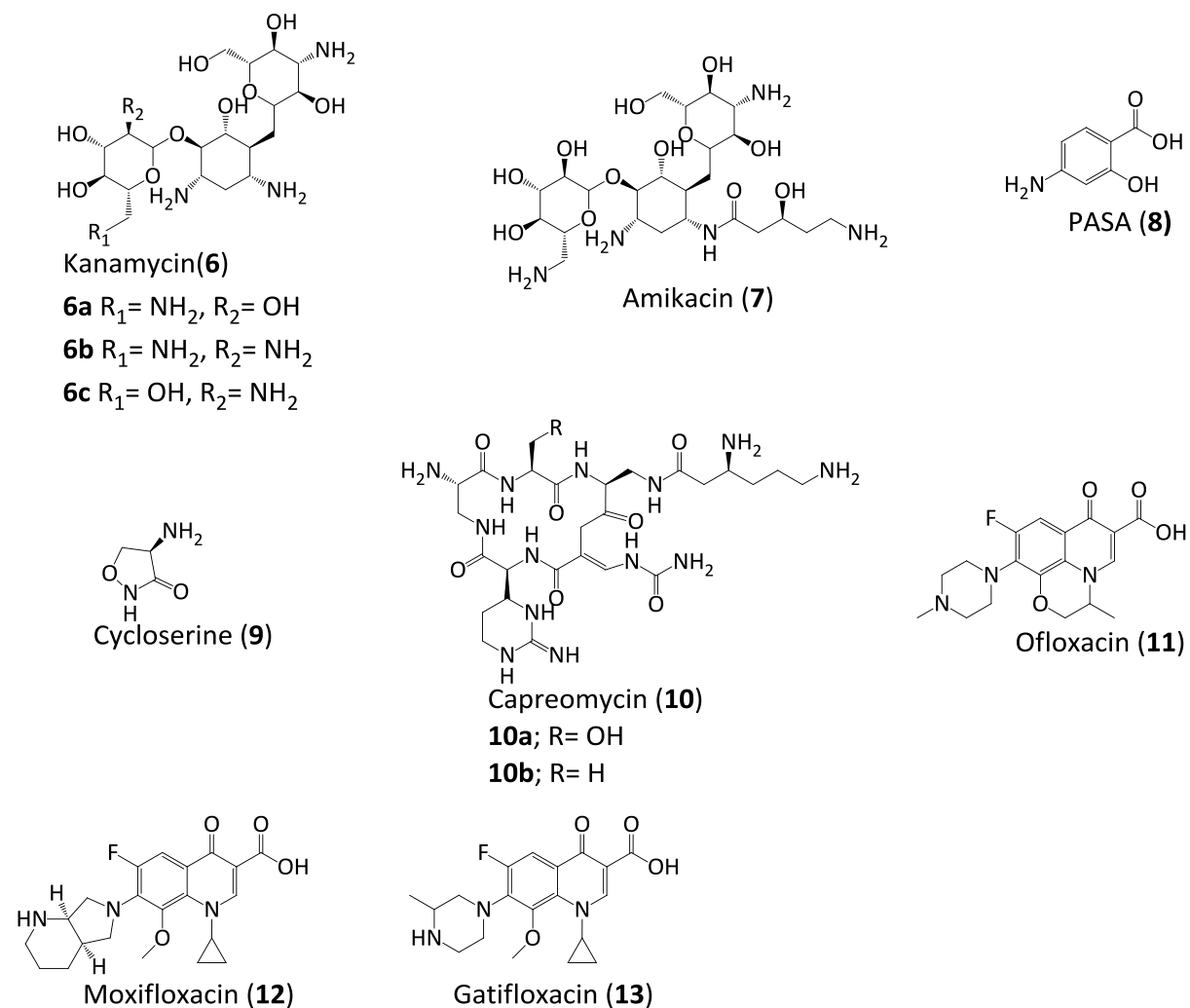
Figure 4: Chemical structures of second line anti TB drugs.

1.5. Newer Anti TB drugs

Bedaquiline (**14**) and delamanid (**15**) are the two newer anti TB drugs (Figure 5). In 2016, they were in confirmatory stages of phase III trials. Based on the data obtained in phase II trials, both of them got accelerated approval (bedaquiline in 2012 and delamanid in 2014) for the treatment of MDR TB in combination with other anti TB drugs[75]. Bedaquiline is a diarylquinoline anti TB drug that was identified in 2005 through high-throughput screening of thousands of compounds using *M. smegmatis* in a whole cell assay[76]. The mode of action of bedaquiline is inhibition of the ATP synthase of *Mtb*, which was a completely new target of action for an antimycobacterial drug[77].
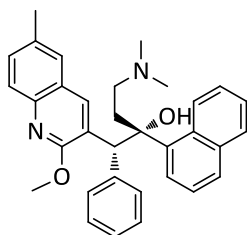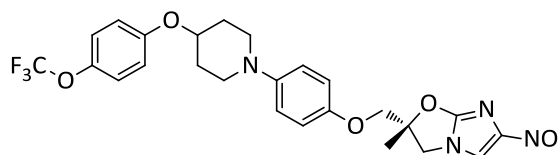
Bedaquiline (**14**)   Delamanid (**15**)

Figure 5: Chemical structures of recently approved anti TB drugs.

Nitroimidazole containing antibacterials such as metronidazole are known for their activity against anaerobic bacterial infections. Delamanid was discovered in 2006 in an attempt to explore the potential of these compounds against *Mtb*[78]. Delamanid is believed to act by inhibiting the synthesis of mycobacterial mycolic acids after it is activated through the reduction of the nitro group by the mycobacterial deazaflavin-dependent nitroreductase (Ddn)[79].

1.6. Drugs under development

There are also other classes of compounds which are currently in clinical trials (Figure 6). These include: PNU-100480 (an oxazolidinone, **16**), SQ109 (an ethylene diamine, **17**), and PA-824 (a nitroimidazole, **18**) which are in phase II clinical trial; BTZ043 (a benzothiazinone, **19**), TBA-354 (a nitroimidazole, **20**), and Q203 (an imidazopyridine, **21**) are being investigated in phase I trials[80].
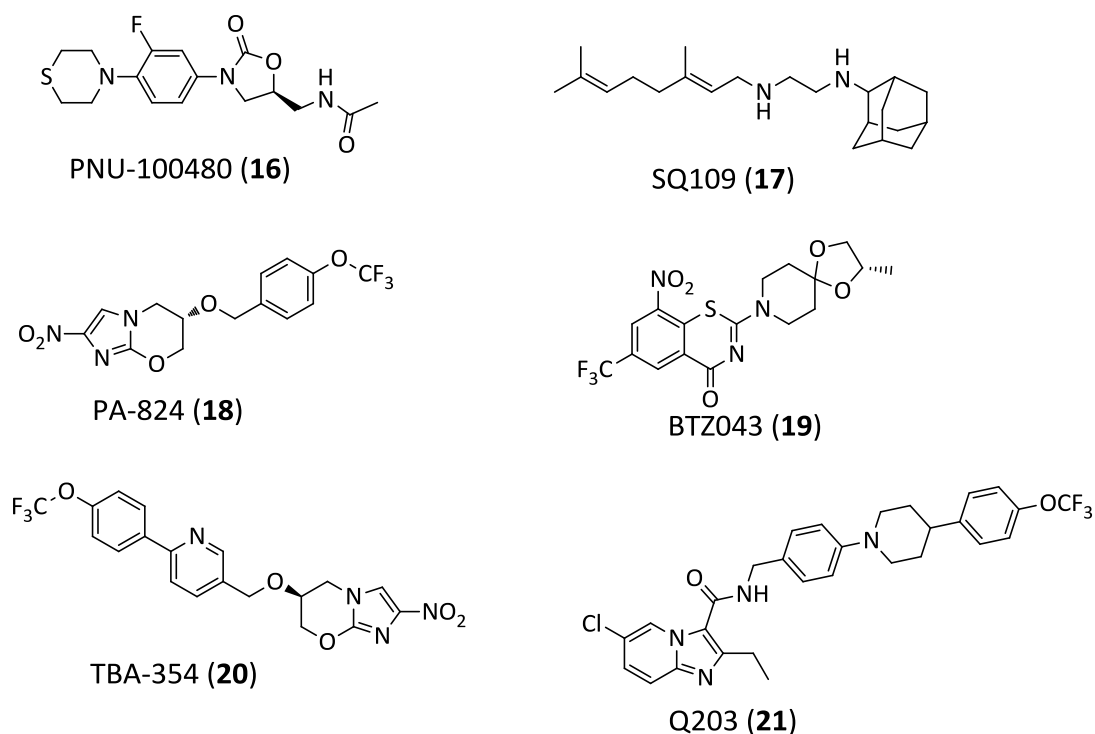
Figure 6: Anti TB drugs which are under clinical development.

1.7. Challenges of the current TB treatment approach

In the past four decades, with the use of the currently available anti TB drugs, remarkable success in the fight against TB was accomplished. Since 1990 alone, TB associated mortality had fallen nearly by half. With the use of these drugs, it was also possible to save the lives of 43 million people worldwide since 2000.

However, in spite of such great success, there are still challenges in properly addressing TB related casualities. The first issue is the challenge of further reducing the unacceptably high number of TB associated deaths occurring each year. It is very unfair and unacceptable to see that an infectious disease, with such a large number of available drugs, kills 1.5 million people each year throughout the globe. One reason for this problem stems from the lack of a very effective drug/drug combination that could cure the disease in a short period. In addition, the protracted treatment regimen makes TB treatment so expensive that many poor people are unable to afford and get the cure in time.

The second, probably the major, challenge in the current TB treatment approach is the problem of rapid emergence and spread of multidrug and extensively resistance (MDR/XDR) tuberculosis. MDR-TB is defined as a form of TB infection caused by bacteria that are resistant to treatment with at least two of the most powerful first-line anti TB drugs, INH and R. According to WHO estimate, in the year 2014, 3.3% of the new TB cases and 20% of the previously treated cases of TB were of MDR TB.

Hence, in order to achieve more success than we previously had and to circumvent the imminent threat of MDR/XDR TB, there is an urgent need to develop new drugs. The new drugs should have a novel mechanism to cure the disease within short time and significantly lower the treatment duration. In addition, these drugs shouldn't develop a rapid resistance and should be effective against the MDR TB. One of the potential sources of the new anti TB drugs with a novel mechanism of action and less prone to develop resistance are antimicrobial peptides (AMPs).

1.8. Antimycobacterial peptides as potential anti TB agents

Antimicrobial peptides (AMPs), also known as host defense peptides, are small molecular weight proteins that have a broad spectrum antimicrobial activities and immunomodulatory role. AMP occur naturally, in all forms of life, as a part of innate immunity or serve as a first line defense by exhibiting direct killing of a pathogen[81]. They start to attract a lot of attention in the area of new antimicrobial drug development against drug resistant microbes including *Mtb*. The features that made them to be attractive drug candidates include their; proven spectrum of action against a wide range of pathogens, selective affinity to prokaryotic negatively charged cell envelopes, rapid cell killing action against the pathogen, low immunogenicity and most importantly their unique mode of action that is less vulnerable for development of drug resistance[82–85].

The most common structural features of biologically active AMPs include cationicity with a net charge of at least +2 and amphiphilicity with considerably variable amino acid sequence and chain length (usually up to 50 amino acid chain)[86]. Most of the time, the cationicity of AMPs is attributed to the presence of positively charged amino acids Arg and/or Lys but in some instances, unnatural amino acids like Orn could contribute for that. About 50% percent of the peptide residues are made up of hydrophobic amino acids. The presence of such distinct hydrophobic and hydrophilic segments on AMP enables them to acquire amphiphilic nature especially when they come in contact with membranes[87].

These amphiphilic and cationic natures of AMPs are proved to be important factors for their antimicrobial action[88]. While a certain degree of cationicity is essential for initial selective binding of AMPs to the negatively charged lipid head groups of the outer surface of the cytoplasmic membrane of prokaryotes; the amphiphilic nature helps them to interfere with the cytoplasmic membrane which could lead to either membrane perturbation or self-promoting uptake of the peptides across the cellular membranes to exert their antimicrobial action inside the cytosolic targets[89,90].

Several AMP classes that exhibited activities against various mycobacterial species have been reported in the past few decades. Their source, structural features, antimycobacterial potency, possible mechanism of action and drug likeness were extensively reviewed recently[91–97]. Based on the size of the peptide, AMPs are broadly classified as large (50-100 aa), intermediate (25-50 aas), low (11-24 aas) and ultra-small (2-10 aas)[98]. Most of the peptides that were considerably investigated for their antimycobacterial activities belong to high and intermediate size peptides and are obtained from a mammalian host immune system or from bacteria. To mention some of them are, human neutrophile peptide[99], defensin[100], hepcidin[101], NK-lysin[102], granulysin[103], human host defense ribonuclases (RNase)[104], lysosomal ubiquitin derived peptide[105], lacticin 3147 [106]and E50-52[107]. In spite of their promising antimycobacterial activity, these classes of compounds have common limitations which include difficulty of isolation from their source, high production cost, not amenable to structural modification, extensive enzymatic degradation and possible immunogenicity.

Small and ultra-small cyclic antimycobacterial peptides could be good alternatives to larger ones as they basically contain the same structural features while avoiding most of the limitations mentioned. Ultra-small sized cyclic antimycobacterial peptides are fairly easy to construct with low cost, have adequate metabolic stability and have low immunogenicity. It is therefore very logical to work on such classes of AMPs in order to develop new anti TB agent. Several ultra-small sized cyclic peptides are also reported to exert antimycobacterial activities. Some of them include griselmycins[108], depsidomycin[109], hytramycin[110], brunsvicamides[111], pyridomycin[112], hirsutellide A[113] and wollamides[114].

Griselimycins

Griselimycins are Streptomycin derived cyclodecapeptides that were discovered in 1960s. Soon after their discovery, Sanofi had started investigating the antimycobacterial potency of Griselimycin (GM). Though GM (**25**) showed promising result when tested in human subjects, it revealed poor pharmacokinetic properties - particularly it had very short plasma half-life when administered orally. After some effort to optimize its pharmacokinetics, the program was

discontinued in 1970 mainly because of the introduction of another new anti TB drug, viz. rifampin. Recently, the company has reinitiated the development program because of earlier reports of the effectiveness of GM against drug-resistant *Mtb*. In an attempt to improve its metabolic stability, a lot of analogues were synthesized based on the GM scaffold where most of the modifications were performed on the Pro 8 moiety as it was proved to be responsible for its poor metabolic stability[108,115].

Among the synthesized analogues, CGM (**26**) with a cyclohexyl substituted amino acid at the Pro 8 position was found to be metabolically stable and orally available with enhanced potency compared to GM. The respective MIC values of CGM were 0.06 and 0.20 mg/mL for the drug susceptible *Mtb* H37Rv strain in broth culture and within macrophage-like (RAW264.7) cells. The molecular target of Griselimycins was identified to be the sliding clamp of the mycobacterial DNA polymerase (DNaN), a validated new novel target for future anti TB drug discovery[108].
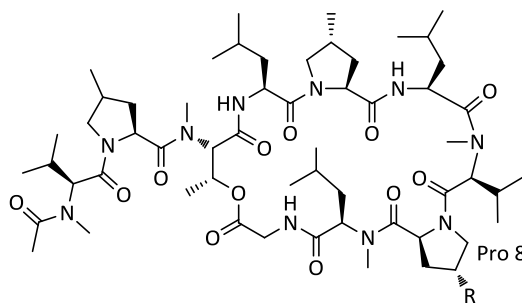
Griselimycin (**25**); R= H
Cyclohexylgriselimycin (**26**); R= Cyclohexyl

Brunsvicamides

Brunsvicamides (A-C) (**27-29**) are cyclic hexapeptides that were isolated in 2006 from the cyanobacterium *Tychonema sp*. Brunsvicamides B and C work by inhibiting the *Mtb* protein tyrosine phosphatase B (MptpB). MptpB is one of the enzymes that are secreted by *Mtb* while it

resides in macrophages. This enzyme helps the bacteria to survive inside the macrophages by preventing phagosomal maturation and hence it is a potential drug target. Brunsvicamides B and C were found to inhibit MptpB with an IC_{50} of 7.3 and 8.0 µMrespectively[111]. The structure-activity relationship (SAR) of brunsvicamide A was also studied after the synthesis of a library of its analogues. However, none of the tested analogues showed activity against MptpB at the maximum dose tested (100 µM)[116]. Brunsvicamides B and C were not synthetically further developed yet.

Brunsvicamide A (**27**); R= H
Brunsvicamide B (**28**); R= CH₃
Brunsvicamide C (**29**);

R= H
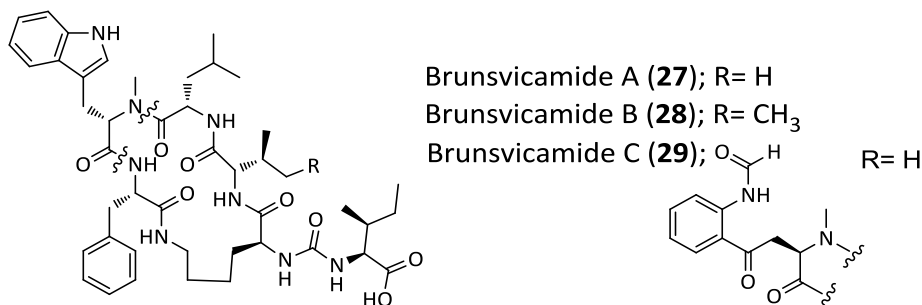
Hytramycins

Hytramycins V (**30**) and I (**31**) are two cyclic hexapeptide antimycobacterial antibiotics that were isolated in 2013 from *Streptomyces hygroscopicus* strain ECUM 14046. The compounds contained three unusual piperazic acid moieties and were found to be active against both replicating and non-replicating forms of *Mtb*. Hytramycin V displayed an activity against a replicating and non-replicating *Mtb* strain with an MIC of 11.3 and 2.4 µg/mL respectively. Similarly, hytramycin I was active against the replicating *Mtb* strain with an MIC of 6 µg/mL and its activity against the non-replicating strain was 1.5 µg/mL[110]. The potent activities of these compounds against the dormant forms of *Mtb*, coupled with the less explored piperazic acid moieties they contain, makes these compounds promising candidates for further development.
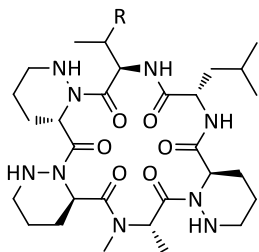
Hytramycin V (**30**); R= H
Hytramycin I (**31**): R= CH$_3$
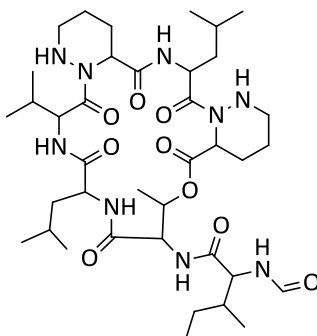
Depsidomycin (**32**)
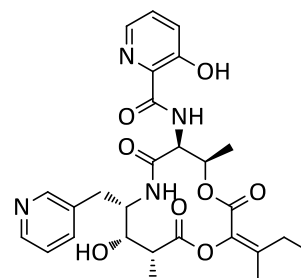
Pyridomycin (**33**)

Depsidomycin

Depsidomycin (**32**) is a cyclic heptadepsipeptide antibiotic that was isolated in 1990 from a cultured broth of *Streptomyces lavendofoliae* MI951-62F2. The compound showed an antimycobacterial activity against *M. Vaccae* with an MIC of 3.1 µg/mL. In addition, it was active against Gram-positive bacteria and had an immunosuppressive activity[109]. A total synthesis of one depsidomycin analogue in which 1,2-piperazine-3-carboxylic acid was substituted with proline was also reported. This analogue also exhibited antimycobacterial activity against both the standard drug susceptible (*Mtb* H37Rv) and multi drug resistant (MDR-*Mtb*) strains with an MIC of 4 and 16 µg/mL respectively[117].

Pyridomycin

The depsipeptide pyridomycin (**33**) was isolated in 1953 from *Streptomyces pyridomyceticus* strain 6706. The compound showed a potent *in vitro* antimycobacterial activity against *Mtb* with an MIC of 0.3 µg/mL and low systemic toxicity in mice[112]. The molecular target of pyridomycin was identified to be the mycobacterial NADH-dependent enoyl-[acyl-carrierprotein] reductase (InhA), which is also the target of INH. Pyridomycin is a competitive inhibitor at the NADH-binding site of InhA and it has not shown cross resistance with INH[118]. In attempt to define the SAR of pyridomycin, dihydropyridomycin analogues were synthesized and the result confirmed that the enol ester moiety in the natural product is not critical for its

biological activity[119]. Structural investigation of pyridomycin through the synthesis of more analogues is still an active area of research.
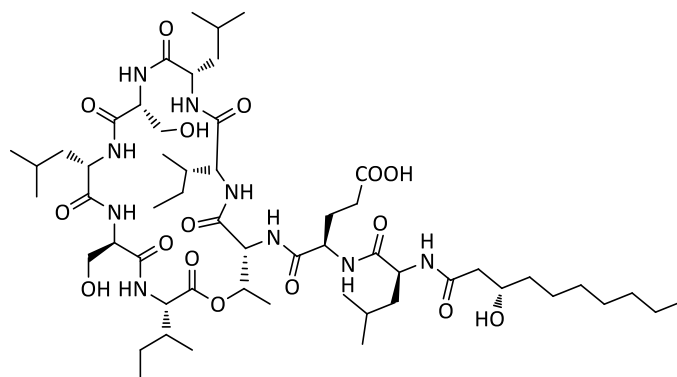
Massetolide A (**34**)

Massetolide A

Massetolide A is a cyclodepsipeptide that was isolated from a marine alga derived *Pseudomonas sp*. MK90e85. The *in vitro* antimycobacterial activity of massetolide A was tested against *Mtb* and *Mycobacterium avium-intracellulare* and it was found to be active with an MIC of 5-10 μg/mL and 2.5-5 μg/mL respectively. The compound was also shown to be nontoxic to mice when injected intraperitoneally at a single dose of 10 mg/kg. The other massetolides (B-H) that were isolated together with massetolide A didn't exhibit significant antimycobacterial activity[120].

Hirsutellide A

Hirsutellide A (**35**) is an 18-membered symmetrical cyclic hexadepsipeptide that was isolated from a cell extract of the entomopathogenic fungus *Hirsutella kobayasii* BCC 1660 and reported to exhibit antimycobacterial activity with an MIC of 6–12 μg/mL towards *Mtb* H37Ra. The structure of Hirsutellide A was elucidated by analyses of spectroscopic data and shown to

contain *allo*-isoleucine (*allo-Ile*), (R)-2-hydroxy-3-phenylpropanoic acid and sarcosine (Sar)[113]. The total synthesis of one of its stereoisomers, where *allo*-Ile replaced with Leucine (Leu), is reported[121].
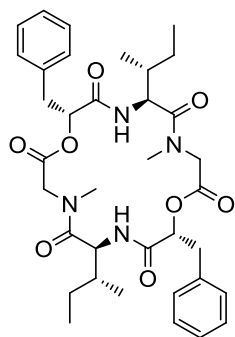
Hirsutellide A (**35**)
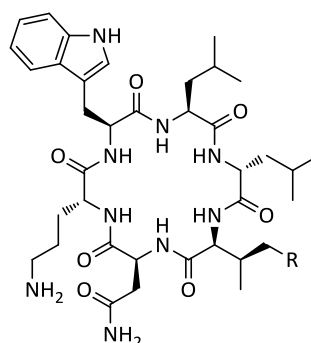
Wollamide A (**36**); R= CH$_3$
Wollamide B (**37**); R= H

Wollamides

Wollamides A (**36**) and B (**37**) are newer classes of cyclic hexapeptides that are isolated in 2014 from an Australian soil derived *Streptomyces nov.* sp. (MST-115088). The compounds are reported to exert antimycobacterial activities at 2.8 µM (wollamide A) and 3.1 µM (wollamide B) against *M. bovis*. In addition, wollamide B is found to reduce the intracellular mycobacterial survival in murine bone marrow-derived macrophages. Chemically, both wollamide A and B are eighteen-membered cyclic hexapeptides that consisted of four natural (L) and 2 unnatural (D) amino acids. The structural difference in the two classes of compounds is that, the *allo*-Ile moiety present at position IV in wollamide A is replaced by valine (Val) in wollamide B[114].

1.8.1. Mechanism of action of antimycobacterial peptides

The exact mechanism by which AMPs exert their antimycobacterial action is not clearly studied. However, a lot of studies demonstrated their membrane disruption/permeabilizing effect as major mechanism[94]. According to these studies, to exert their action AMPs have to first pass through the outer membrane of Mycobacteria which is believed to be achieved through self-promoting uptake. The net positive charge of AMPs ensures accumulation of the peptides at the negatively charged (lipopolysaccharides) cell surface of the bacterial cell wall. This causes neutralization of the outer charged membrane. Following that, a hydrophobic interaction between amphipathic AMPs and the lipid component of cell wall results in disruption of the matrix and formation of cracks through which the peptide will smuggle into the next cellular compartment[81,122].

Once the peptides pass the outer membrane, they interact with the anionic surface of the cell membrane and insert themselves in the interface of the hydrophilic head groups and the fatty acyl chains of membrane phospholipids. By insertion into the membrane they will either disrupt the physical integrity of the bilayer (via membrane thinning, transient poration and/or disruption of the barrier function) or translocate across the membrane and act on cytosolic targets[86].

Binding to bacterial membrane and delocalization of peripheral membrane proteins that are essential for respiration and cell wall biosynthesis was also proposed as a mechanism of action for small cationic AMPs[123].

2. Solid phase peptide synthesis: strategies and reagents

The concept of peptide synthesis, as well as the use of the term 'peptide', was first introduced nearly a century ago by E. Fischer. Fisher reported, in 1901, the synthesis of the first dipeptide (Gly-Gly) by hydrolysis of the diketopiperazine of glycine[124]. Following that, in 1931, M. Bergmann (the former student of E. Fisher) introduced the first temporary amino function protecting group, carbobenzoxy (Cbz), that can be removed fair easily by hydrogenation after making the peptide bond[124]. This discovery paved the way for the synthesis of several small peptides such as the therapeutically useful octapeptide hormone oxytocin[125]. The area was even further augmented in 1957 when Caprino *et al* invent a new acid liable amino functional protecting group, the tert-butyloxycarbonyl group (Boc), that is stable toward hydrogenation and therefore totally orthogonal to the Cbz (or modified Cbz) group[124].

A major breakthrough in the field took place in 1963 when Bruce Merrifield introduced the concept of solid phase peptide synthesis (SPPS)[126]. This approach has dramatically improved the efficiency and speed of the synthesis as it avoids the difficulty of isolation and purification of the intermediate peptides; the major limitation of solution phase peptide synthesis approach. The basic principle of SPPS and the reagents used are summarized briefly below.

2.1. General principle of SPPS

The general steps to be followed in the synthesis of peptides using SPPS approach is depicted in Figure 7. The synthesis is initiated through a temporary covalent attachment of the first N^α-protected amino acid, *via* its activated carboxy terminal, to a pre-swelled functionalized resin bed. This process, also termed as loading, is followed by removal of N^α-amino function protecting group after filtration of the excess reagents and a thorough washing of the resin. The next amino acid is then coupled, after activation of it carboxylic acid, to the loaded amino acid whose N^α-amino function is already freed. Deblocking of the N^α-amino function, washing of the resin and coupling of an activated amino acid will be then repeated as many as possible till a peptide of a required length is constructed. If the amino acid to be coupled to a growing

peptide chain has a reactive side chain that might interfere with coupling process, it is important to use a side chain protected amino acids and this protecting group should be resistant to the condition used to deprotect the N^α-amino function protecting group. Finally the assembled peptide is cleaved from the resin, along with the side chain protecting groups, and used for the intended purpose after purification.

2.1.1. The solid support

The most common type of solid support used in SPPS is polystyrene (PS) polymer that is cross-linked with either 1% or 2% divinylbenzene (DVB)[127]. Crosslinking of the PS is important as it alters the solubility of the linear uncross-linked polymer from being soluble in hydrophobic solvents to be practically insoluble in all commonly used solvents. These resins appear as spherical beads with two different particle sizes; the smaller one with a mesh size of 200-400 (35-75 μm) and the larger one with 100-200 (75-150 μm). A resin with the larger particle size is commonly used in synthesis owing to its good balance of reaction kinetic versus reliability.

The swelling properties of crosslinked PS resin beds in organic solvents is an important issue in SPPS as it determine the diffusion and accessibility of the reagents into the core of the polymer and thereby the efficiency of the synthesis. The swelling property is mainly dependent on the type of organic solvent used during the synthesis and the degree of crosslinking of the polymer. Generally a typical 1% DVB crosslinked PS resin goes from 5–6 times in THF, toluene, DCM, or dioxane, 4 times in DMF, 2 times in EtOH or CH_3CN, 1.6 times in MeOH up to no swelling in water. When the degree of crosslinking increases the volume of swelling is found to be smaller[128,129].

In addition to DBV-PS solid support, other types of resins based on polyamine and polyethylene glycol core are also introduced in SPPS. These types of resin were introduced to tackle some of the limitations associated with the use of DVB-PS resin which includes; (1) physicochemical incompatibility between the growing hydrophilic peptide chain and the rigid hydrophobic macromolecular environment created by DVB-PS network and (2) poor solvation of this type of resin in protic organic solvents[129].

2.1.2. The linker for SPPS

Linkers are chemical units that are used to anchor the first amino acid of the growing peptide to the resin bed. The first amino acid is covalently attached to these units *via* its carboxy function after being activated. The nature of the linkers determines the type of conditions to be used for cleaving of the peptide after it is being constructed on the solid support[130].
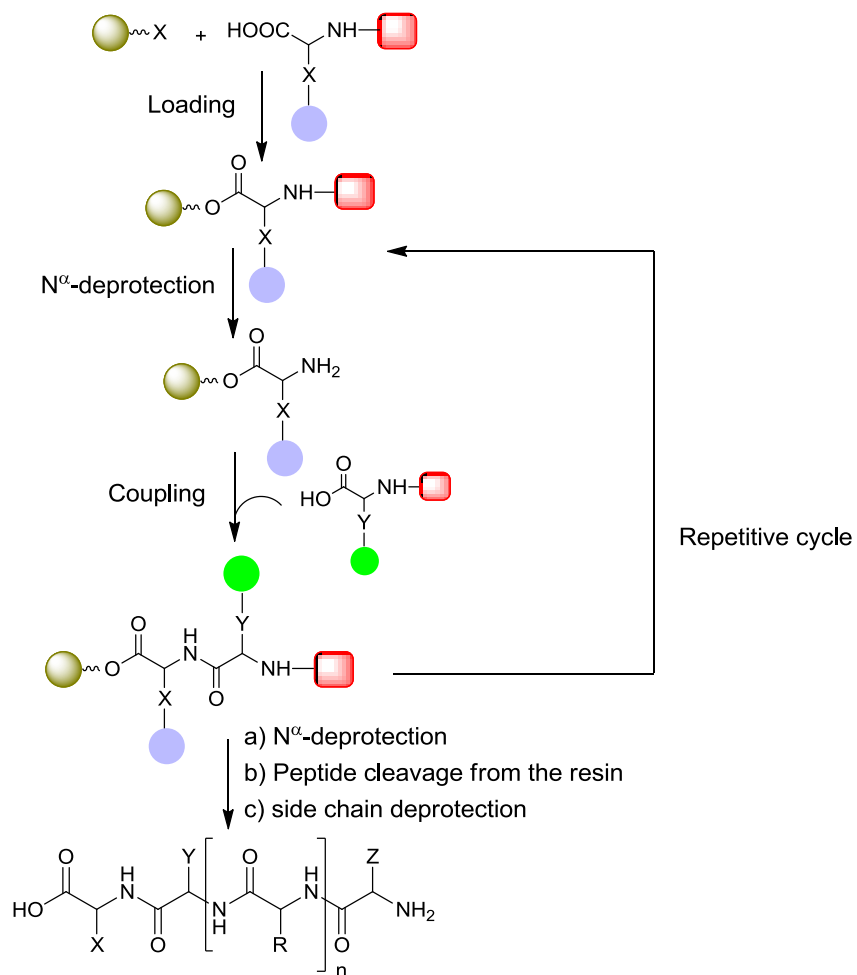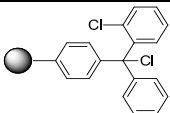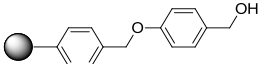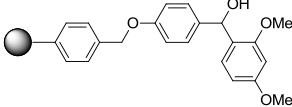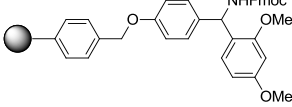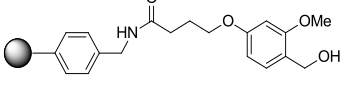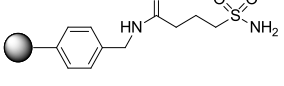
Figure 7: Scheme that shows the general principle of solid phase peptide synthesis.

Some of the various types of linkers that are developed on polystyrene resin core, together with their cleaving conditions are presented in Table 1. Among the various types of linkers, 2-chlorotrityl (2-CT) linkers are the most widely used. 2-CT resins are particularly useful when less acid labile protecting groups are required on the substrate following cleavage. It is also useful in cases where the growing peptide can cyclize on the anchoring linkage, usually through diketopiperazine formation, causing premature cleavage[131]. In such instances, the bulky 2-chlorotriphenylmethyl group prevents such attack through steric hindrance. Cleavage of side chain protected peptides can be achieved with the use of 20% (v/v) hexafluoroisopropyl alcohol (HFIP) in DCM with all the protecting groups intact.

Table 1: Some of the types of resins used in SPPS.

Resin-Linker	Resin Name	Cleavage conditions
	2-Chlorotrityl resin	1-5% TFA in DCM or 20% HFIP in DCM
	Wang resin	90-95% TFA in DCM
	Rink acid resin	1-5% TFA in DCM or 10% AcOH in DCM
	Rink amide resin	50% TFA in DCM
	HMPB resin	1% TFA in DCM
	Sulfonamide resin	1)ICH$_2$CN/DIPEA/NMP 2) Nucleophile, DMAP

2.1.3. N$^\alpha$-amino function protecting groups

The major feature that defines the chemistry of SPPS is the type of N$^\alpha$-amino function protecting groups used during the synthesis. The two most commonly used amine protecting groups are 9-fluorenylmethyloxy carbonyl (Fmoc)[132] and t-butyloxycarbonyl (Boc)[133]. Accordingly SPPS is classified as Fmoc-based and Boc-based SPPS. While removal of Fmoc group could be done in basic conditions using piperidine, Boc group requires acidic conditions, usually TFA, to be removed. The mechanism of deprotection is shown in Figure 8[129].
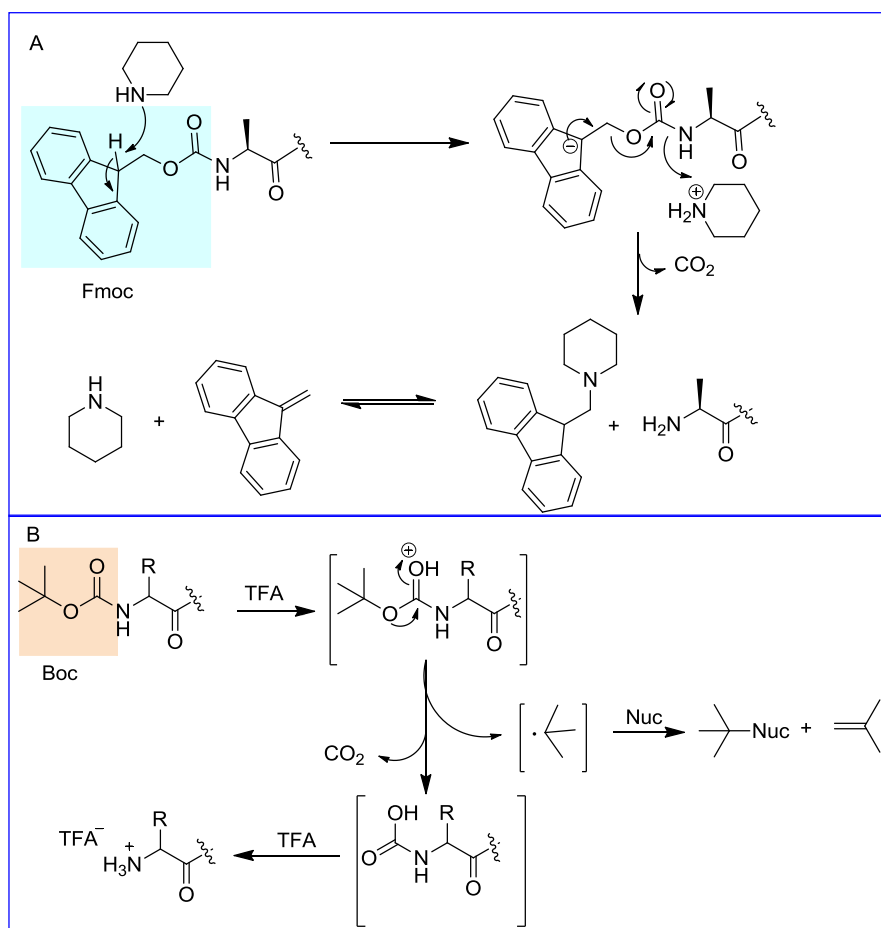
Figure 8: Mechanistic illustration for the deprotection of the two commonly used N$^\alpha$-amino function protecting groups. A) Fmoc deprotection mechanism. B) Boc deprotection mechanism.

Fmoc-based SPPS strategy is most commonly used for routine synthesis because this group could be easily removed under relatively mild condition in comparison to the Boc group. In addition, removal of Fmoc-protecting group can be done orthogonally with most reagents used to cleave the peptide from the resin and the side chain protecting groups of many amino acids.

2.1.4. Activation of the carboxyl group of the amino acids

Activation of the α-carbonyl function of amino acid is important during the coupling of an amino acid to the growing peptide to ensure a rapid and quantitative amide bond formation. This could be achieved using various types of activating agents that were developed over years. The commonly used activating agents in SPPS are listed below in Figure 9[134].

DCC DIC EDC

X = C; HOBt
X = N; HOAt

X = C; PyBOP
X = N; PyAOP

X = C; HBTU
X = N; HATU
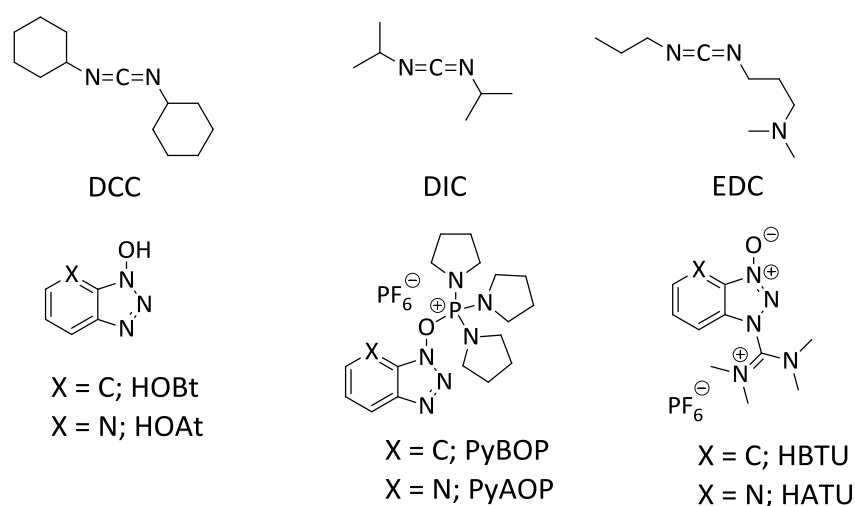
Figure 9: Commonly used α-carbonyl function activating agents in SPPS.

Dicyclohexylcarbodiimide (DCC) was the first activating agent to be used in SPPS by Merrifield. However the use of this reagent was shortly abandoned because of the problem of removing the insoluble dicyclohexylurea side product. Diisopropylcarbodiimide (DIC) is used instead in solid phase synthesis since its urea byproduct remains in solution. All carbodiimide based

coupling agents in general cause partial racemization of the amino acids during activation process. This happen due to the formation of highly reactive O-acylisourea intermediate that is prone to base catalyzed racemization. In order to suppress racemization, it is common practice to add an equivalent of 1-hydroxybenzotriazole (HOBt) or 1-hydroxy-7-azabenzotriazole (HOAt) as these reagents form an intermediate OBt/OAt esters with the acid that couples the primary amines with little racemization[135,136].

To minimize the racemization and other side reactions that occurs with carbodiimide based activating agents, other highly efficient coupling agents that generate OBt esters *in situ* are also introduced. Some of which includes; the phosphonium based Benzotriazol-1-yl-*N*-oxy-tris(pyrrolidino)phosphonium hexafluorophosphate (PyBOP), uronium/aminium based *N*-[(1*H*-Benzotriazol-1-yl)(dimethylamino)-methylene]-*N*-methylmethanaminium hexafluorophosphate *N*-oxide (HBTU) and *N*-{(dimethylamino)-1*H*-1,2,3-triazolo[4,5-b]-pyridino-1-ylmethylene}-*N*-methylmethanaminium hexafluorophosphate (HATU). For efficient coupling these salts must be combined with HOAt or HOBt in the presence of a base, usually *N,N*-diisopropylethylamine (DIPEA)[137,138]. The mechanism of activation of the α-carbonyl function of amino acid and subsequent coupling reaction with one of the most widely used coupling reagent HATU is shown in Figure 10[139].

2.1.5. Amino acid side-chain protecting groups

During peptide synthesis, it is important to protect a reactive amino acid side-residue as they could interfere with the coupling process. In Fmoc based SPPS approach, it is common to use an acid labile side-residues protecting groups as it is orthogonal to the basic condition used to remove the Fmoc group. The particular type of side-chain protecting groups to be used for each amino acid is however dependent on the nature of such residues. Some of the most commonly used side-residue protecting groups together with their removal condition is presented in Table 2[140].
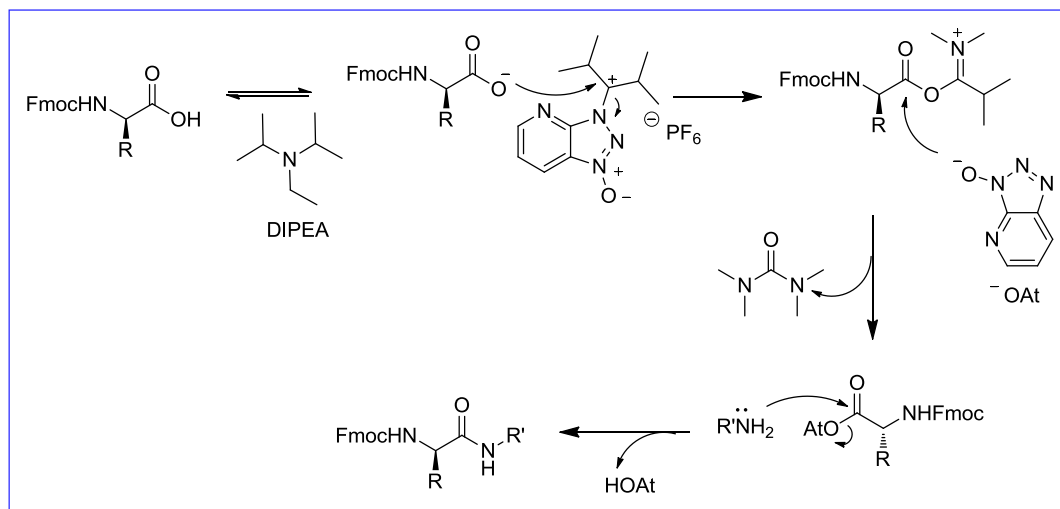
Figure 10: Mechanism of HATU mediated activation α-carbonyl function of amino acids and subsequent coupling to primary amines.

Table 2: Some of the amino acid side-chain protecting groups and the deprotection conditions.

Amino acid	Protecting group	Structure	Deprotection conditions
Arg	Pbf		TFA/TIS/H_2O (95:2.5:2.5)
Asn/Gln	Trt		TFA/TIS/H_2O (95:2.5:2.5)
Asp/Glu	Bn		Hydrogenation
Lys/Orn	Boc		TFA/DCM (1:1)
Ser/Thr	*t*-Bu		TFA/DCM (1:1)
Trp	Boc		TFA/DCM (1:1)

3. Objectives of the thesis

As summarized in section 1.8, antimycobacterial (depsi)peptides have great potential to be the next anti TB drugs owing to their rapid bactericidal action, high affinity and selectivity to the prokaryotic cell envelope, different mode of action from conventional antibiotics and their proven record of use as a permanent host first line defense without the development of notable bacterial resistance.

The main objective of the project was therefore to explore the anti TB potential of small cyclic (depsi) peptides by designing, synthesizing and evaluating their antimycobacterial activities using natural products as lead compounds.

Two biologically active antimycobacterial natural products that represent two different chemical classes - peptides and depsipeptides - were chosen as lead compounds for further development. The compounds were wollamide B (cyclic hexapeptide) and hirsutellide A (cyclic hexadepsipeptide). The two compounds were selected for development because (1) they had been reported to have appreciable antimycobacterial activity, (2) they are relatively easy to manipulate synthetically to prepare analogues and (3) they were not developed previously.

More specifically, the objectives included:

- Develop an optimized synthetic route and purification techniques for the target compounds
- Structural characterization of the synthesized target compounds using different spectroscopic methods
- *In vitro* Drug Metabolism Pharmacokinetic (ADME) profiling of the synthesized compounds
- Evaluate the *in vitro* antimycobacterial activities of the target compounds against different mycobacterial species (*M. tuberculosis, M. vaccae, M. smegmatis*…)
- Define the structure activity relationship (SAR) of the lead compounds
- Evaluate the *in vivo* antimycobacterial activity and toxicity of the most active analogue against *Mtb* infected mice as proof of concept study (PoC)

Part one:

Development of wollamide B and analogues

4. Wollamide B

Wollamide B represents one of the newer classes of cyclic peptides with good extracellular antimycobacterial activity against *M. bovis* (IC$_{50}$ of 3.1 µM). In addition, it was found to reduce the intracellular survival of Mycobacteria in murine bone marrow-derived macrophages[114]. However, its activity against the common disease causing pathogen, *Mtb* was not studied.

Structurally, wollamide B consists of two uncommon D-amino acids (D-Orn, D-Leu) and four L-amino acids (Figure 11). The presence of the basic amino acid D-Orn and clusters of lipophilic amino acids imparts the typical cationicity and amphiphilicity to the molecule. Desotamides, structurally related to wollamide B but lacking the basic amino acid D-Orn, were found to be inactive against Mycobacteria indicating the importance of this amino acid for activity[114]. Apart from this brief information, a detailed study of the structural activity relationship (SAR) of the compound remained unexplored.
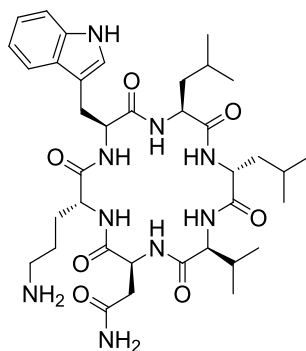
Figure 11: Chemical structure of wollamide B.

The aim of the first part of my PhD work was therefore (1) to study the SAR of wollamide B by designing, synthesizing and testing their *in vitro* antimycobacterial activities of its analogues and (2) to optimize its structure for better potency and pharmacokinetic properties.

4.1. Synthesis of wollamide B and its analogues

4.1.1. General synthetic approach

As the synthesis of wollamides was not reported previously, we devised a new synthetic approach illustrated in Figure 12. We envisioned that wollamide B (**1c)** would be available through global deprotection of the two Boc and a Trt side-residue protecting groups of cyclic precursor **1b.** Global deblockage of these protecting groups could be achieved by employing conditions for the removal of the Trt group (Table 2). Under this condition, the Boc protecting groups are also labile. The cyclic precursor **1b** in turn can be obtained through macrocyclization of the linear hexapeptide precursor **1a.** The macrocyclization can be done in solution phase at high dilution. **1a** could be obtained using Fmoc-based solid phase peptide approach. This synthetic approach was planned to be followed for wollamide B analogues.
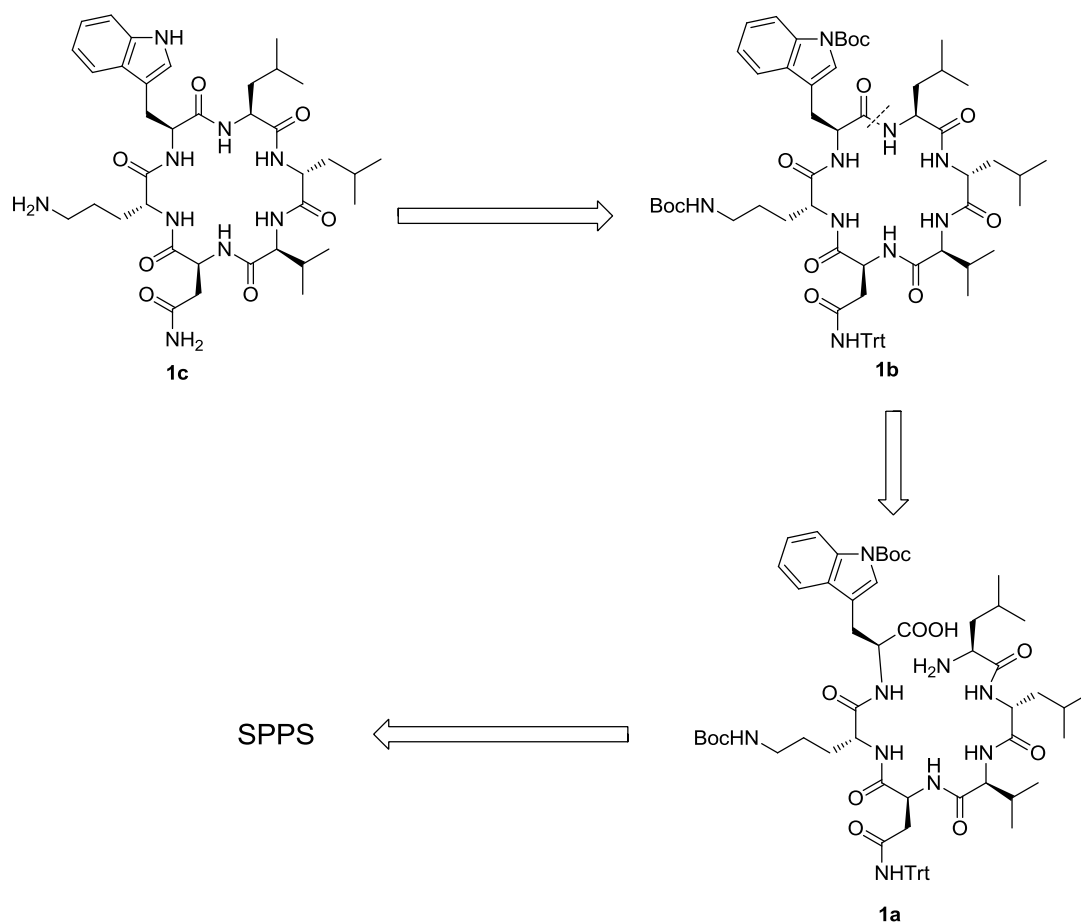
Figure 12: Synthetic approach of wollamide B (**1c**).

4.1.2. Synthesis of the linear hexapeptide precursors

All the linear peptide precursors (**1a-28a**) were synthesized following a standard Fmoc based solid phase peptide synthesis approach (SPPS) using a 2-chlorotrityl chloride (2-CT) DVB-PS resin as a solid support[141]. The general synthetic scheme and the list of the synthesized compounds are presented in Figure 13 and Table 3 respectively.
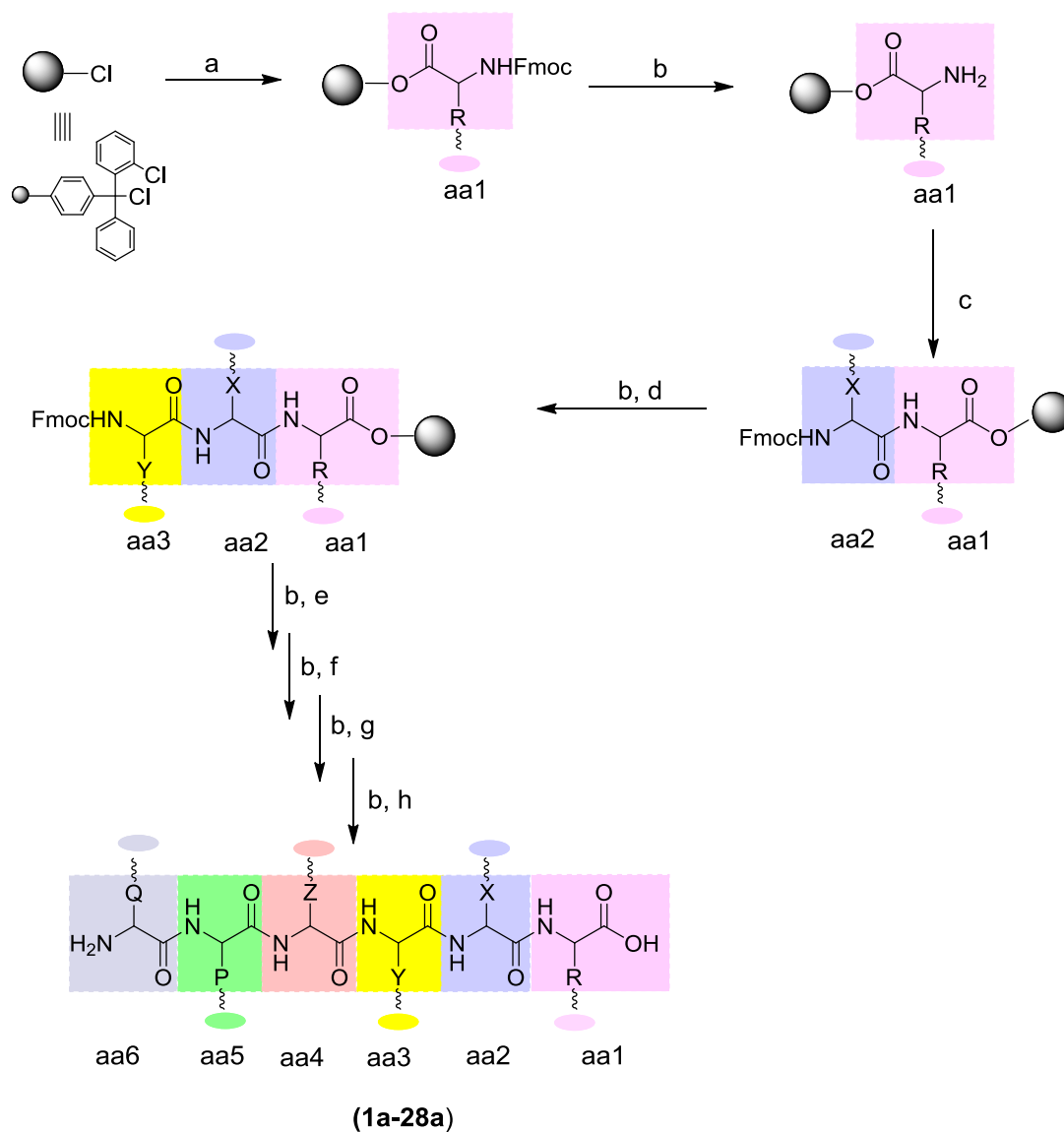
Figure 13: Synthetic pathway for the linear precursors (**2a**-**28a**) using SPPS.

Reagents and conditions: a) Fmoc-aa1-OH (1.2 eq.), DIPEA (2,5 eq.), DCM, 2 h; b) 20 % piperidine/DMF, 2X10 min; c) Fmoc-aa2-OH (3 eq.), HATU (3 eq.), DIPEA (6 eq.), NMP, 1 h; d) Fmoc-aa3-OH (3 eq.), HATU (3 eq.) , DIPEA (6 eq.), NMP, 1 h; e) Fmoc-aa4-OH (3 eq.), HATU (3 eq.), DIPEA (6 eq.), NMP, 1 h; f) Fmoc-aa5-OH (3 eq.), HATU (3 eq.), DIPEA (6 eq.), NMP, 1 h; g) Fmoc-aa6-OH (3 eq.), HATU (3 eq.), DIPEA (6 eq.), NMP, 1 h; h) 20 % HFIP/DCM, 1 h; i) HATU (3 eq.), HOBt (3 eq.), DIPEA (10 eq.), DMF, 3 d; rt.
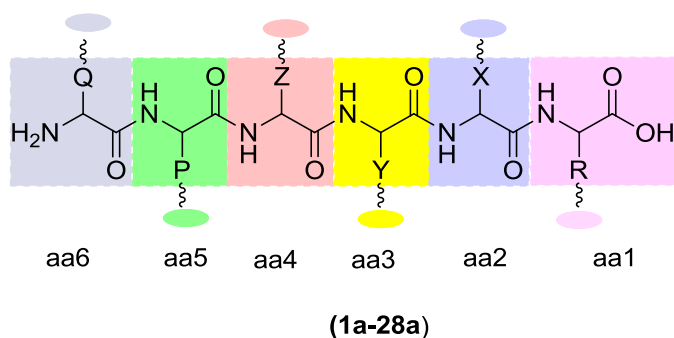
(**1a-28a**)

Table 3: List of the synthesized linear hexapeptides using SPPS approach (**1a**-**28a**).

Compound	aa1	aa2	aa3	aa4	aa5	aa6
1a	Leu	Trp (Boc)	D-Orn(Boc)	Asn(Trt)	Val	D-Leu
2a	Ala	Trp (Boc)	D-Orn(Boc)	Asn(Trt)	Val	D-Leu
3a	Leu	Ala	D-Orn(Boc)	Asn(Trt)	Val	D-Leu
4a	Leu	Trp (Boc)	D-Orn(Boc)	Ala	Val	D-Leu
5a	Leu	Trp (Boc)	D-Orn(Boc)	Asn(Trt)	Ala	D-Leu
6a	Leu	Trp (Boc)	D-Orn(Boc)	Asn(Trt)	Val	D-Ala
7a	Leu	Trp (Boc)	D-Orn(Boc)	Asn(Trt)	*allo*-Ile	D-Leu
8a	Leu	Trp (Boc)	D-Orn(Boc)	Asn(Trt)	Ile	D-Leu
9a	Leu	Trp (Boc)	D-Orn(Boc)	Asn(Trt)	Met	D-Leu
10a	D-Leu	Leu	Trp(Boc)	D-Orn(Boc)	Asn(Trt)	Asp(Bzl)
11a	Leu	Trp (Boc)	D-Orn(Boc)	D-Orn(Boc)	Val	D-Leu
12a	D-Orn(Boc)	Ser (t-Bu)	Ile	D-Leu	Leu	Trp(Boc)
13a	D-Orn(Boc)	Ser (t-Bu)	Ile	D-Leu	Leu	Trp(Boc)
14a	Leu	Trp (Boc)	D-Orn(Boc)	Ile	Ile	D-Leu
15a	Leu	D-Leu	D-Phe(4-Cl)	D-Orn(Boc)	Asn(Trt)	Val
16a	Leu	D-Phe (4-OMe)	D-Orn(Boc)	Asn(Trt)	Val	D-Leu
17a	Val	D-Leu	D-Phe(4-Cl)	Trp(Boc)	D-Orn(Boc)	Asn(Trt)
18a	Leu	Trp (Boc)	D-Orn(Boc)	Asn(Trt)	Val	D-Phe (4-Cl)
19a	Leu	Trp (Boc)	D-Orn(Boc)	D-Orn(Boc)	Ile	D-Phe (4-Cl)
20a	Val	D-Leu	Ile	Trp(Boc)	D-Orn(Boc)	Asn(Trt)
21a	Val	Ile	Leu	Trp(Boc)	D-Orn(Boc)	Asn(Trt)
22a	Leu	Trp (Boc)	D-Arg(Pbf)	Asn(Trt)	Ile	D-Leu
23a	Leu	Trp (Boc)	D-Orn(Boc)	Asn(Trt)	N-Me-Val	D-Leu
24a	D-Leu	N-Me-Leu	Trp(Boc)	D-Orn(Boc)	Asn(Trt)	N-Me-Val
25a	D-Orn(Boc)	Asn(Trt)	N-Me-Val	D-Leu	N-Me-Leu	Trp(Boc)
26a	D-Orn(Boc)	N-Me-Asn(Trt)	Val	N-Me-D-Leu	Leu	Trp(Boc)
27a	Leu	D-Leu	Val	Asn(Trt)	D-Orn(Boc)	Trp(Boc)
28a	Leu	D-Leu	Ala	Asn(Trt)	D-Orn(Boc)	Trp(Boc)

4.1.2.1. Resin loading

2-CT resin was chosen as a solid support because, being very acid sensitive, it enabled to cleave the final hexapeptides under mildly acidic conditions without causing harm to the acid labile side-chain protecting groups[142]. Loading of the first amino acid (Fmoc-XX-OH) was done on a pre-swelled resin in DCM, activated by DIPEA (2.5 eq.). Subsequent capping with methanol deactivated any un-reacted chlorotrityl group.

While DCM was used as a solvent for loading of the first amino acid, the actual peptide bond formation was performed in NMP. The choice of two different solvent systems during loading and subsequent coupling reactions arose from the difference in the swelling properties of the free vs. peptide-loaded resin. When it is unloaded, the resin tends to swells to a greater volume in DCM than in NMP/DMF and as the peptide chain grows during the synthesis, the swelling volume in DCM gradually decreases. The reverse happens in NMP/DMF solvent system. Hence, swelling the resin in DCM at the beginning and making the subsequent amide couplings in DMF/NMP gives an opportunity to efficiently load the amino acid and ensures more successful couplings[143].

Generally the efficiency of loading ranged from 70 to 90%. This was calculated based on the increase in the mass of the resin after loading[141]. The large variation in the loading efficiency seems to arise from batch to batch differences in the exact loading capacity of the resin. The loading capacity of commercial 2-CT resin is in the range of 1.0 to 1.6 mmol/g. Not to compromise the final yield, we took the maximum value as the theoretical loading capacity during the calculation of loading efficiency. The efficiencies of loading of resins which were taken from the same batch were nearly the same.

4.1.2.2. Fmoc deprotection

After loading the first Fmoc protected amino acid to the resin, the next step was to set its N^α-amino function free through removal of the Fmoc group. This was efficiently achieved using the common deblocking reagent used in SPPS, viz. 20% (v/v) piperidine in DMF solution.

In order to test the cleavage of the Fmoc group, the common practice is to use a Kaiser test. This test involves the use of ninhydrin to qualitatively determine the presence of free primary amines on the resin after Fmoc removal. However, occasionally false positives result when uncleaved Fmoc group gets removed by reacting with pyridine in the test reagent. In addition, this test cannot be used for secondary amines[127].

We used another simple and quick qualitative test to verify the removal of the Fmoc group. This involved an indirect detection of the dibenzofulvene-piperidine adducts by adding a fixed volume of water (hence named as 'water test') to the filtered cleavage solution. As this adduct was very lipophilic, it precipitated immediately upon addition of water. When the Fmoc group was completely removed (which always happened after two cleavage steps) the formation of the precipitate ceased confirming the completion of the deprotection.

4.1.2.3. Coupling of the amino acids

Following removal of the Fmoc group, subsequent elongation of the peptides was achieved through stepwise coupling of the next five Fmoc-amino acids. With N-nonmethylated amino acids, coupling of the next Fmoc-XX-OH was always done for one hour using HATU (3 eq.) as the coupling agent in NMP/DIPEA. The coupling time was doubled (2 h) and the coupling repeated twice in case of N-methylated amino acids,.

Monitoring of peptide coupling is usually performed qualitatively using a Kaiser test or quantitatively using HPLC after cleaving the peptide from portion of the resin. In both cases the objective is to ensure the complete coupling of each amino acid which otherwise will compromise the purity and the yield of the final peptide. This step is particularly important during synthesis of very long peptide chains as the efficiency of coupling was found to be progressively diminishing with increasing the chain length[144]. For short peptides, such as hexapeptides, doing the cleavage test after each coupling step is not economical, both in terms of money and time. Hence, instead of cleaving the peptide each time after coupling and doing HPLC analysis we used the 'water test' (described above) as a qualitative means to monitor the coupling.

4.1.2.4. Cleavage of the peptides from the resin

After removal of the last Fmoc protecting group, the hexapeptides were cleaved from the resin using 20% (v/v) hexafluoro-2-propanol (HFIP) in DCM for 1 h. While it is common to use 1% to 5% trifluoroacetic acid (TFA) in DCM for cleavage of a peptide from 2-CT resin, this could not be applied in our case as the sidechain protecting groups were sensitive to this condition. Premature removal of such groups might interfere with the subsequent macrocyclization. Hence, while cleaving the peptide, we needed to make sure that the sidechain protecting groups remained intact. The use of HFIP instead of TFA alleviated this problem as these side-chain protecting groups were stable under this condition[145].

Though not purified, the general crude yields of the constructed linear hexapeptides were greater than 75%. When the formation of the final peptides were confirmed with ESI-MS, it was only the product ion that always appeared as the major and dominant ion peak in both + and – spectra. Peaks that resulted from a deleted/incomplete sequence or any side products were hardly seen in all ESI-MS spectra except when preparing the linear hexapeptide **10a**.

As preparation of **10a** involved the use of Fmoc-Asp (Bzl)-OH as one of its amino acid constituents, the formation of an aspartimide side product was a major problem. Aspartimide formation is one of the most notorious side reactions that occur during SPPS[146,147]. This side reaction is a sequence dependent cyclization that is catalyzed by base or acid. ESI-MS spectra had shown that the dominant peak during the synthesis of **10a** was the hexapeptide that contained the aspartimide side product with little **10a**. One of the predisposing factors for aspartimide formation is repetitive piperidine (base) treatments during Fmoc removal[148]. To reduce the formation of this side product, we attached the Fmoc-Asn (Bzl)-OH last as this enabled to reduce the level of piperidine exposure. With this approach, though not completely avoided, it was possible to greatly reduce the amount of the side product. This was again confirmed through ESI-MS analysis of the dominant peaks where the major ion peak this time was the desired product.

4.1.3. Macrocyclization

Head to tail cyclization of the formed hexapeptides were performed in solution phase at high dilution (1 mM) using HATU/HOBt as α-carbonyl activating agent and DMF as a solvent (Figure 14). The structures of the synthesized macrocyclic peptides are listed in Table 4. Generally, performing macrocyclization under such a high dilution is a common practice in the synthesis of cyclic peptides as such condition favors intramolecular cyclization and prevents oligomerization (unwanted side reactions). However, too much dilution should also be avoided as it slows reaction by promoting solvent mediated decomposition of the activated α-carbonyl group before coupling[149].
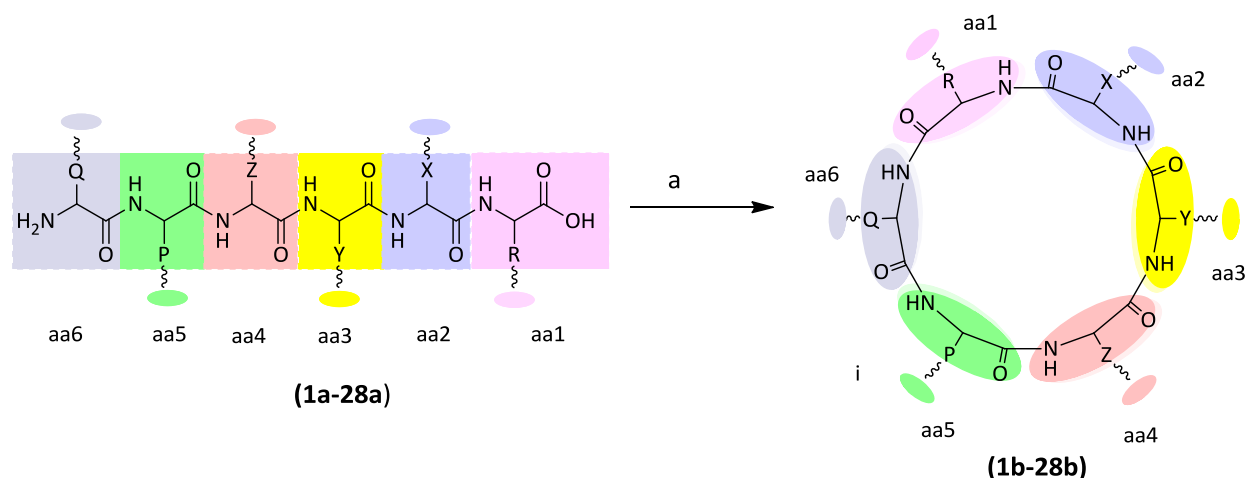
Figure 14: Macrocyclization of the linear hexapeptide precursors.

Reagents and conditions: a) HATU (3 eq.), HOBt (3 eq.), DIPEA (10 eq.), DMF, 3 d, rt.

Macrocyclization of the linear peptides took place in yield that ranged from 40% to 70%. Considering the challenges of cyclizing short chain peptides, this yield could be labeled as satisfactory[150]. Moreover all the performed cyclizations were free from oligomerization as

confirmed from the analysis of the products by ESI-MS, NMR and UPLS-MS. However, significant epimerization (20%) was observed during macrocyclization of **21a**. This was clearly visible both in the final ^{1}H NMR spectra and during purity checkup using UPLS-MS. The epimerization seems to be associated with replacing the D-Leu moiety of the lead with Ile.

After macrocyclization, all the products were purified by column chromatography using chloroform/methanol as a mobile phase and silica gel as a stationary phase and were directly used for the next step.
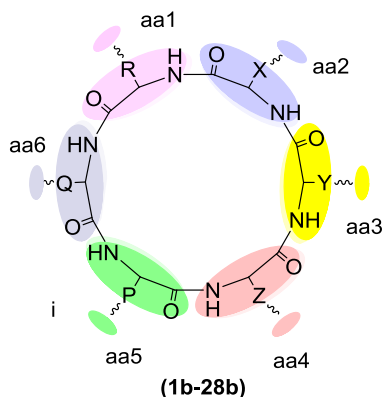
(1b-28b)

Table 4: List of the cyclic precursors of synthesized wollamide B analogues (**1b**-**28b**).

Compound	aa1	aa2	aa3	aa4	aa5	aa6
1b	Leu	Trp (Boc)	D-Orn(Boc)	Asn(Trt)	Val	D-Leu
2b	Ala	Trp (Boc)	D-Orn(Boc)	Asn(Trt)	Val	D-Leu
3b	Leu	Ala	D-Orn(Boc)	Asn(Trt)	Val	D-Leu
4b	Leu	Trp (Boc)	D-Orn(Boc)	Ala	Val	D-Leu
5b	Leu	Trp (Boc)	D-Orn(Boc)	Asn(Trt)	Ala	D-Leu
6b	Leu	Trp (Boc)	D-Orn(Boc)	Asn(Trt)	Val	D-Ala
7b	Leu	Trp (Boc)	D-Orn(Boc)	Asn(Trt)	*allo*-Ile	D-Leu
8b	Leu	Trp (Boc)	D-Orn(Boc)	Asn(Trt)	Ile	D-Leu
9b	Leu	Trp (Boc)	D-Orn(Boc)	Asn(Trt)	Met	D-Leu
10b	D-Leu	Leu	Trp(Boc)	D-Orn(Boc)	Asn(Trt)	Asp(Bzl)
11b	Leu	Trp (Boc)	D-Orn(Boc)	D-Orn(Boc)	Val	D-Leu
12b	D-Orn(Boc)	Ser (t-Bu)	Ile	D-Leu	Leu	Trp(Boc)
13b	D-Orn(Boc)	Ser (t-Bu)	Ile	D-Leu	Leu	Trp(Boc)
14b	Leu	Trp (Boc)	D-Orn(Boc)	Ile	Ile	D-Leu
15b	Leu	D-Leu	D-Phe(4-Cl)	D-Orn(Boc)	Asn(Trt)	Val
16b	Leu	D-Phe (4-OMe)	D-Orn(Boc)	Asn(Trt)	Val	D-Leu
17b	Val	D-Leu	D-Phe(4-Cl)	Trp(Boc)	D-Orn(Boc)	Asn(Trt)
18b	Leu	Trp (Boc)	D-Orn(Boc)	Asn(Trt)	Val	D-Phe (4-Cl)
19b	Leu	Trp (Boc)	D-Orn(Boc)	D-Orn(Boc)	Ile	D-Phe (4-Cl)
20b	Val	D-Leu	Ile	Trp(Boc)	D-Orn(Boc)	Asn(Trt)
21b	Val	Ile	Leu	Trp(Boc)	D-Orn(Boc)	Asn(Trt)
22b	Leu	Trp (Boc)	D-Arg(Pbf)	Asn(Trt)	Ile	D-Leu
23b	Leu	Trp (Boc)	D-Orn(Boc)	Asn(Trt)	N-Me-Val	D-Leu
24b	D-Leu	N-Me-Leu	Trp(Boc)	D-Orn(Boc)	Asn(Trt)	N-Me-Val
25b	D-Orn(Boc)	Asn(Trt)	N-Me-Val	D-Leu	N-Me-Leu	Trp(Boc)
26b	D-Orn(Boc)	N-Me-Asn(Trt)	Val	N-Me-D-Leu	Leu	Trp(Boc)
27b	Leu	D-Leu	Val	Asn(Trt)	D-Orn(Boc)	Trp(Boc)
28b	Leu	D-Leu	Ala	Asn(Trt)	D-Orn(Boc)	Trp(Boc)

4.1.4. Global deprotection of the side chain protecting groups

The final step in the synthesis of wollamides was global deprotection of all sidechain protecting groups. This afforded the final target compounds, except **10c** which was still an intermediate, that are listed in Table 5. Global deprotection of the sidechain protecting groups after macrocyclization was achieved with a cleaving cocktail made up of TFA/TIPS/H_2O (95:2.5/2.5/) for amino acids that contained Trt/Pbf protecting groups and with TFA/DCM (1:1) for amino acids containing Boc/tBu protecting groups[141] (Figure 15). The Triisopropylsilane (TIPS) scavenger was included in the cleaving cocktail mainly to trap the reactive Trt cation that was formed during the removal of the Asn side residue protecting group. The very reactive Trt cation, if not scavenged quickly, could modify the peptide through alkylation/arylation of the indole ring of Trp or could reattach itself to the amide sidechain of Asn[140].

While the entire deprotection step went smoothly for all the other analogues, the t-Bu protecting group of Ser was not completely removed when **12c** was synthesized. This generated side product **13c.** As it was possible to separate this side product in a pure form, it was submitted for activity testing.
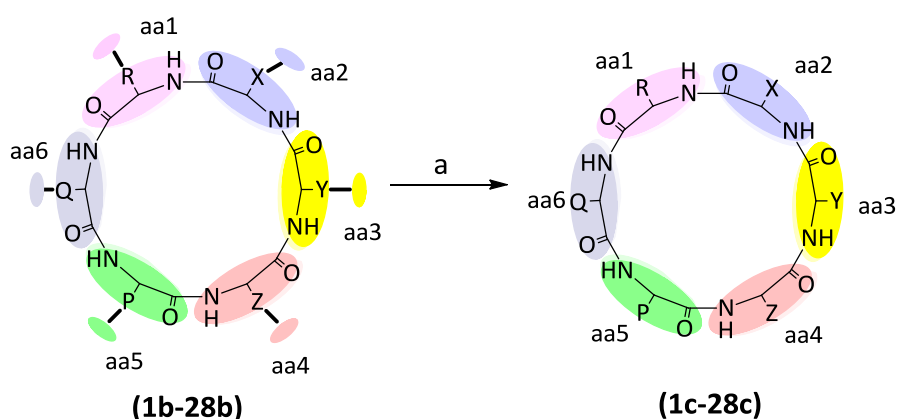
Figure 15: Global deprotection of the reactive amino acid sidechain protecting groups.

Reagents and conditions: a) TFA/TIPS/H_2O (95:2.5:2.5), 3 h, rt or TFA/DCM (1:1), 1 h, rt.

After removing the sidechain protecting groups, the purification of the final product was done by column chromatography using silica gel as a stationary phase and a polar mobile phase composed of chloroform/methanol (7:3).

Finally, the structure of all the compounds were verified using a combination of ESI-MS and NMR spectroscopy and purity were asserted by an independent QC unit GSK/ Stevenage using UPLC-MS The detailed procedures that were applied for the synthesis of the individual compounds are described in the experimental part (section 8.5).
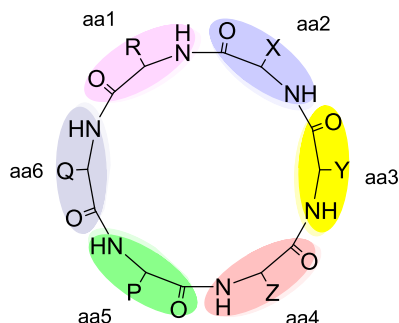
(1c-28c)

Table 5: Lists of the synthesized wollamide B analogues (**1c-28c**).

Compound	aa1	aa2	aa3	aa4	aa5	aa6
1c	Leu	Trp	D-Orn	Asn	Val	D-Leu
2c	Ala	Trp	D-Orn	Asn	Val	D-Leu
3c	Leu	Ala	D-Orn	Asn	Val	D-Leu
4c	Leu	Trp	D-Orn	Ala	Val	D-Leu
5c	Leu	Trp	D-Orn	Asn	Ala	D-Leu
6c	Leu	Trp	D-Orn	Asn	Val	D-Ala
7c	Leu	Trp	D-Orn	Asn	*allo*-Ile	D-Leu
8c	Leu	Trp	D-Orn	Asn	Ile	D-Leu
9c	Leu	Trp	D-Orn	Asn	Met	D-Leu
10c	D-Leu	Leu	Trp(Boc)	D-Orn(Boc)	Asn(Trt)	Asp
11c	Leu	Trp	D-Orn	D-Orn	Val	D-Leu
12c	D-Orn	Ser	Ile	D-Leu	Leu	Trp
13c	D-Orn	Ser (t-Bu)	Ile	D-Leu	Leu	Trp
14c	Leu	Trp	D-Orn	Ile	Ile	D-Leu
15c	Leu	D-Leu	D-Phe(4-Cl)	D-Orn	Asn	Val
16c	Leu	D-Phe (4-OMe)	D-Orn	Asn	Val	D-Leu
17c	Val	D-Leu	D-Phe(4-Cl)	Trp	D-Orn	Asn
18c	Leu	Trp	D-Orn	Asn	Val	D-Phe (4-Cl)
19c	Leu	Trp	D-Orn	D-Orn	Ile	D-Phe (4-Cl)
20c	Val	D-Leu	Ile	Trp	D-Orn	Asn
21c	Val	Ile	Leu	Trp	D-Orn	Asn
22c	Leu	Trp	D-Arg	Asn	Ile	D-Leu
23c	Leu	Trp	D-Orn	Asn	N-Me-Val	D-Leu
24c	D-Leu	N-Me-Leu	Trp	D-Orn	Asn	N-Me-Val
25c	D-Orn	Asn	N-Me-Val	D-Leu	N-Me-Leu	Trp
26c	D-Orn	N-Me-Asn	Val	N-Me-D-Leu	Leu	Trp
27c	Leu	D-Leu	Val	Asn	D-Orn	Trp
28c	Leu	D-Leu	Ala	Asn	D-Orn	Trp

Synthesis of **10e** needed a longer synthetic path than the other analogues as it required the introduction of the 2-(4-(4-aminobutanoyl)piperazin-1-yl)-8-nitro-6-(trifluoromethyl)-4H-benzo[e][1,3]thiazin-4-one (BTZ) group to the wollamide skeleton. This group was planned to be introduced through amide linkage after introducing the amino acid Asp in place of Val (**10c**). The BTZ was synthesized by one of my colleagues in our research group and kindly donated for this purpose.

The synthetic approach included preparation of the cyclic hexapeptide analogue of wollamide B through replacing Val with Asp. This was followed by the attachment of the BTZ group to the aspartyl side residue. The synthesis of the cyclic hexapeptide **10b** followed the standard course. After cyclization, the benzyl protecting group of the aspartyl side chain was selectively removed without affecting the other side-residue protecting groups (Boc and Trt). This was achieved by catalytic hydrogenation of **10c** (Figure 16). The deprotected carboxylic acid of the aspartyl side-chain was coupled to the BTZ group using HATU/DIPEA mediated amide coupling in DMF. The remaining side-residue protecting groups were removed as usual to afford **10e** after purification.
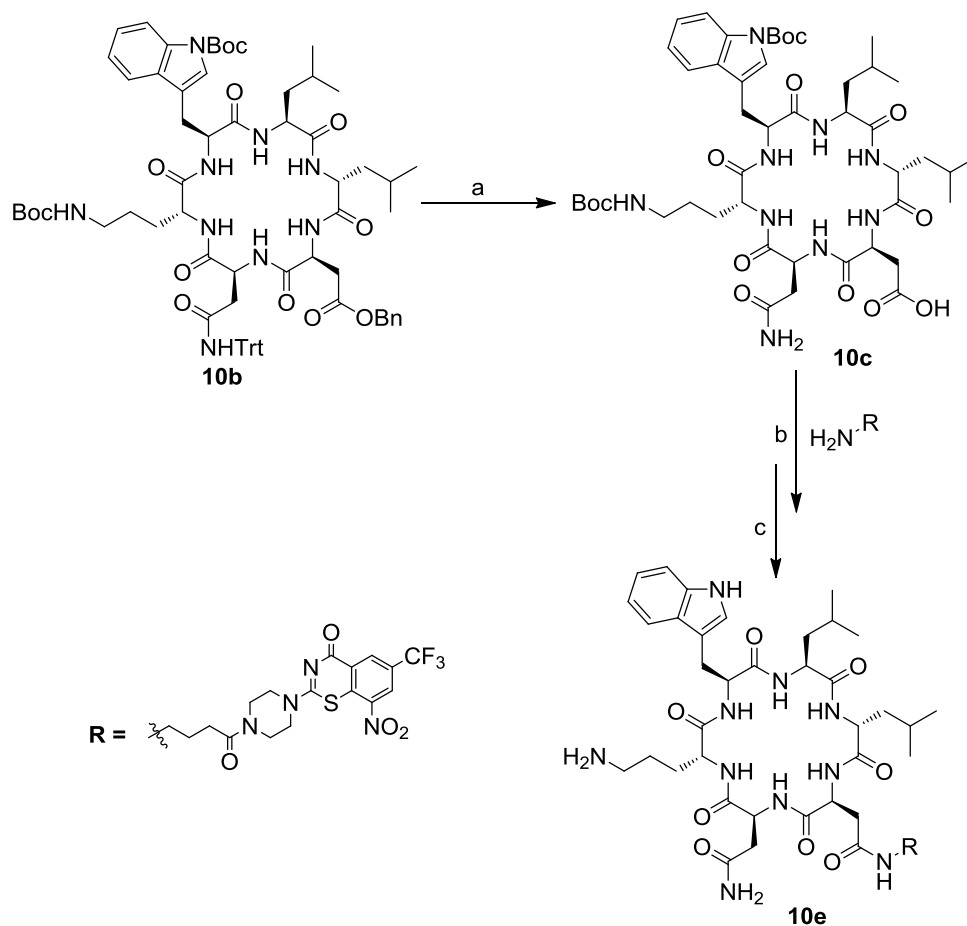
Figure 16: Synthesis scheme for compound **10e**.

Reagent and conditions: a) H$_2$, 10% Pd/C, EtOAc; b) HATU (3 eq.), HOBt (3 eq.), DIPEA (10 eq.), DMF, 12 h; c) TFA/TIPS/H$_2$O (95:2.5:2.5).

4.2. *In vitro* microbiological and toxicity assay of wollamides

In vitro experiments were done to evaluate the antimycobacterial activity and cytotoxicity of the synthesized wollamides. These tests were performed in cooperation with our partners, GlaxoSmithKline (GSK) Tres Cantos, Madrid (Spain) and Microbial Resource Collection, Leibniz-Institut für Naturstoff-Forschung und Infektionsbiologie - Hans-Knöll-Institut, Jena, Germany.

4.2.1. Agar diffusion test

An agar diffusion test served as a quick pilot method to evaluate the antimycobacterial activities of the synthesized analogues against non-pathogenic Mycobacterium species, namely *M. vaccae* and *M. smegmatis*. Both are known to have predictive value, that allow to decide for which compounds to determine MICs and which to take to the *Mtb* assays that require safety level 3 laboratories. The compounds were also tested against panels of different Gram negative and Gram positive bacterial strains. This test was done by placing the test compounds (100 µg/mL) into the wells of an agar plate that was previously inoculated with the test organism. After the end of incubation, mean diameters of growth inhibition zones (ZoI) were recorded.

The results of the testing are summarized in Table 6. Wollamide B (**1c**) showed small zone of inhibition against *M. vaccae* (ZoI = 17 mm), and no activity against *M. smegmatis*. Four test compounds (**6c**, **8c**, **10e** and **18c**) effected larger zones of inhibition against *M. vaccae* than **1c**, the maximum inhibition zone being recorded for **6c** (30 mm). All compounds that showed activity against *M. vaccae* were also active against *M. smegmatis*. The wollamides were also found to exhibit some antibacterial activities especially against the Gram negative *P. aeroginosa*.

While the diffusion assay shows if there is activity or not, it cannot be used to assess the extent of activity. This is because the size of the diffusion zone depends on diffusion rate in the agar media which in turn depends on compound polarity. Hence, after confirming their activity, the MICs of active compounds were determined by an agar dilution assay.

Table 6: *In vitro* antimicrobial activities of wollamide B and its synthetic analogues using agar diffusion assay.

Compound no.	Zone of inhibition at 100 µg/mL (mm)					
	M. smegmatis SG987	*M. vaccae* 10670	*B. subtilis* ATCC6633	*E.coli* SG458	*S. aureus* SG511	*P.aeruginosa* K799/61
1c	0	17	11	0	11	20
2c	0	0	0	0	0	0
3c	0	0	0	0	0	0
4c	0	0	0	0	0	0
5c	0	0	0	0	0	0
6c	0	30	0	0	0	0
7c	14	15	14	0	15	20
8c	0	18	12	0	12	24
9c	0	0	0	0	0	20
10e	11	24	11	0	11	16
11c	0	14	11	12	10	27
12c	nd	nd	nd	nd	nd	nd
13c	nd	nd	nd	nd	nd	nd
14c	nd	nd	nd	nd	nd	nd
15c	0	12	0	0	0	18
16c	0	0	0	0	0	0
17c	14	17	0	0	0	17
18c	19	23	14	0	13	23
19c	nd	nd	nd	nd	nd	nd
20c	0	0	0	0	0	20
21c	0	0	0	0	0	20
22c	15	16	13	0	15	17
23c	16	16	0	0	0	20
24c	0	0	0	0	0	14
25c	nd	nd	nd	nd	nd	nd
26c	nd	nd	nd	nd	nd	nd
27c	0	0	0	0	0	0
28c	0	0	0	0	0	0
References						
Ciprofloxacin[a]	23	24p	29	23/30p	19	28/35p
Solvent[b]	0	0	0	0	0	0

[a]Ciprofloxacin was tested at dose of 5 µg/mL; [b]The solvent used for blank control was DMSO/methanol (1:1); nd, not determined.

4.2.2. Minimum inhibitory concentration (MIC) and *in vitro* cytotoxicity

Determination of the minimum inhibitory concentrations (MICs) of the wollamides were done at two different sites against two different Mycobacterium strains. First, for all compounds that had shown activity against *M. vaccae* in the agar diffusion assay, MICs were determined against *M. vaccae* at Microbial Resource Collection, Leibniz-Institut für Naturstoff-Forschung und Infektionsbiologie - Hans-Knöll-Institut, Jena, Germany. Second, the MICs of all the synthesized compounds were determined against a standard drug susceptible *Mtb* H37Rv at the Open Lab facilities of GlaxoSmithKline (GSK), Tres Cantos (Spain). MIC determinations were carried out according to standard test protocols of the cooperation partners (see section 8.6).

The MICs were estimated by determination of the number of viable cells after incubation with the test compounds using a resazurin assay. The indicator dye resazurin was used to measure the metabolic capacity of cells, indicating cell viability. Viable cells of untreated controls retained the ability to reduce resazurin to resorufin which is highly fluorescent and visible by the change from blue to pink color. Non-viable cells rapidly lost metabolic capacity, did not reduce the indicator dye, and thus did not generate a fluorescent signal[151]. The MIC was defined as the lowest concentration of a test compound that did not produce a fluorescent signal and therefore prevented the color change from blue to pink[152].

Besides checking their antimycobacterial activities, the cytotoxicity of all the synthesized compounds were assessed using a human hepatocellular carcinoma cells (HepG2). All assays were conducted according to standard assay protocols of the cooperation partners (see section 8.6). The concentration of a compound that inhibits the growth of 50% of the HepG2 cells (IC_{50}) was used as a measure of toxicity. The IC_{50} of the compounds were assessed up to 100 µM beyond which the compound was declared nontoxic.

The results of the determined MICs together with their toxicity profiles are displayed in Table 7. The determined MIC values of all the compounds that were active against *M. vaccae* on agar diffusion assay were $\leq$ 12.50 µg/mL. Compound **18c** exhibited the strongest activity against *M. vaccae* with an MIC of 0.40 µg/mL. As expected, the antimycobacterial potencies of these

compounds were not proportional to the observed zones of inhibitions. For example **23c**, with a small zone of inhibition (16 mm) compared to **10e** (24 mm), exhibited a much stronger activity (MICs 0.78 and 3.13 µg/mL).

Table 7: *In vitro* antimycobacterial MICs and cytotoxicities of wollamides.

Compound no.	MICs		IC_{50} against
	Mtb H37Rv (µM)	*M. vaccae* (µg/mL)	Hep2G Cells (µM)
1c	0.60	6.25	56
2c	>80	nd	>100
3c	>80	nd	>100
4c	20	nd	>100
5c	>80	nd	>100
6c	>80	0.78	>100
7c	1.08	12.50	50
8c	1.08	6.25	51
9c	>80	nd	nd
10e	>80	3.13	>100
11c	2.50	nd	>100
12c	15	nd	>100
13c	40	nd	>100
14c	3.13	nd	>100
15c	40	nd	>100
16c	>80	nd	nd
17c	30	3.12	>100
18c	1.90	0.40	>100
19c	17.50	nd	>100
20c	7.50	nd	>100
21c	>80	nd	>100
22c	0.60	6.25	nd
23c	12.50	0.78	nd
24c	>80	nd	>100
25c	>80	nd	>100
26c	>80	nd	>100
27c	20	nd	>100
28c	>80	nd	>100

nd= not determined

Though it is a common practice to use *M. vaccae* as a surrogate to *Mtb* in initial screening of antimycobacterial compounds, this idea does not seem functional to our compounds[153]. As showed in Table 7, there exist no notable correlations between the activities of the compounds

against the two mycobacterial species. For example, compound **6c** did not show activity at the maximum testing dose (80 μM) against *Mtb* H37Rv, but had high potency against *M. vaccae* (MIC = 0.78 μg/mL).

The relationship between the observed antimycobacterial activities and the structural changes made on the lead compound are discussed separately in section 4.4.

The result of the cytotoxicity study done on the molecules showed that all the compounds were not toxic to the cells up to 50 μM. If we compare this with the activity of the most potent analogues, the selectivity index will be greater than 80 which indicate the general safety of the class.

4.2.3. Intracellular assay

Performing an intracellular assay against infected macrophages serves as a good predictive proof for the *in vivo* activity of antimycobacterial agents as the assay conditions resembles - in many ways - that of the host. For some of the analogues that showed good extracellular antimycobacterial activity, such test was done in *Mtb* H37Rv infected human macrophages[151].

The test was performed according to the protocols described by Pitta et al[154]. The result of the assay is displayed in Table 8. The tested analogues exhibited activities with IC_{90} values that were close to their extracellular MICs. This indicates their ability to cross cell membranes of macrophages to reach their target (internalized bacteria).

In this respect, **18c** performed best with an IC_{90} of 2.57 μM, almost similar to its extracellular MIC of 1.90 μM. The IC_{90} of the other three compounds (**7c**, **8c** and **11c**) were at least twice higher than their respective MICs (Table 8).

The similar intracellular and extracellular antimycobacterial potency of **18c** may be related to the lipophilic aromatic side chain of 4-chloro-D-Phe, facilitating permeability into the macrophages. The other three compounds that did not contain the aromatic substituent could not replicate their extracellular potency because of relatively low permeability.

Table 8: Results of the *in vitro* intracellular activities of selected wollamides against *Mtb* H37Rv.

Compound	IC_{50} (µM)	IC_{90} (µM)
7c	0.75	2.48
8c	0.73	2.63
11c	2.07	5.75
18c	1.02	2.57

4.3. *In vitro* drug metabolism and pharmacokinetic (ADME) profiling

An *in-vitro* drug metabolism pharmacokinetic (ADME) profiling was done for the synthesized analogues to evaluate their drug-likeness[155]. The ADME profiling was performed based on the internal protocols of the open lab foundation GSK, Tres Cantos (Spain) (section 8.7) and included the study of physicochemical properties, plasma stabilities and liver microsomal stabilities.

Physicochemical properties; the experimentally determined physicochemical parameters included, (1) kinetic aqueous solubility which was determined using chemiluminescent nitrogen detection (CLND), (2) membrane permeability that was determined using passive artificial membrane permeability assay (PAMPA), (3) percentage plasma albumin binding affinity and (4) lipophilicity (Log D) determined from the chromatographic retention properties of the test compounds. The results are summarily presented in Table 9.

Plasma stabilities: to assess the plasma stabilities the class in general, representative test compounds were incubated with human and mouse plasma for 2 hours at 37 °C. Following that, the percentage of compound remaining after the incubation was quantified with LC-MS. The results are presented in Table 10.

Microsomal stability: as a measure of their metabolic stability, the *in vitro* intrinsic clearances (CL_{int}) of the compounds and their half-lives were measured by incubating them with isolated human and mouse liver microsomes. Based on the measured *in vitro* intrinsic clearances, the *in vivo* clearances and the hepatic extraction ratios (% liver blood flow) were predicted taking the interspecies difference into account[156]. Results are displayed in Table 11.

The *in vitro* ADME profiles of the individual compounds in relation to their structural features and antimycobacterial activities will be discussed in depth in section 4.4.

Table 9: Physicochemical properties of the synthesized wollamides.

Compound	Solubility[a]* (μg/mL)	% HSA	Log D	Permeability[b]* (nm/sec)
1c	≥151	72.66	1.80	<3
2c	≥134	43.14	0.94	<10
3c	136	25.51	nd	nd
4c	143	82.76	2.00	<3
5c	129	56.76	1.32	<10
6c	≥196	42.21	1.04	<10
7c	nd	75.14	1.83	<10
8c	≥177	76.35	1.83	<10
9c	164	73.79	1.78	<10
10e	nd	95.26	2.20	15
11c	nd	86.46	1.32	10
12c	≥228	86.47	2.16	<10
13c	202	92.68	3.00	<3
14c	≥206	96.06	2.94	19
15c	≥218	70.25	1.90	<10
16c	≥189	46.55	1.73	<10
17c	≥230	93.83	2.12	17
18c	192	92.54	1.92	<3
19c	7	98.70	nd	nd
20c	≥183	67.10	1.73	<10
21c	≥195	83.67	1.83	<3
22c	≥189	87.55	2.05	11
23c	≥153	73.98	1.96	<10
24c	≥174	82.21	2.00	<10
25c	≥217	87.02	2.18	<10
26c	≥221	82.97	2.25	<10
27c	≥210	79.64	1.89	<3
28c	198	68.58	1.57	<3

[a]Refers to kinetic aqueous solubility determined by chemiluminescent nitrogen detection (CLND); [b]refers to passive artificial membrane permeability; HSA, human serum albumin binding; nd, not determined; *GSK cut-off values for solubility: > 100 μg/mL, high solubility; 30-100 μg/mL, intermediate solubility; <30 μg/mL, low solubility.: *GSK cut-off values for permeability: > 200 nm/sec, high permeability; 10-200 nm/sec, intermediate permeability; <10 μg/mL, low permeability.

Table 10: *In vitro* plasma stabilities of some selected wollamides.

Compound	Plasma stability (% remaining)*	
	Human	**Mouse**
1c	107	90
2c	107	93
3c	86	92
4c	95	100
5c	98	96
6c	95	102
7c	105	109
8c	99	98
10e	80	85
11c	100	100
15c	104	70
18c	99	98
27c	97	98
28c	87	85

*Estimated by quantifying the amount of a compound remaining after incubation with plasma for 2 h at 37 °C.

Table 11: *In vitro* determined and predicted *in vivo* microsomal stabilities of wollamides.

Compound	CL$_{int}$ (mL/min/g tissue)		CL$_{pred}$ (mL/min/kg)		% LBF		Microsomal t$_{1/2}$ (min)	
	Human	Mouse	Human	Mouse	Human	Mouse	Human	Mouse
1c	0.97	<0.50	10.24	<21.21	56.88	<16.83	56.80	>138.60
2c	<0.40	<0.48	6.31	<20.50	<35.08	<16.27	>138.60	>138.60
3c	<0.40	<0.48	6.31	<20.50	<35.08	<16.27	>138.60	>138.60
4c	<0.40	<0.48	6.31	<20.50	<35.08	<16.27	>138.60	>138.60
5c	<0.40	<0.48	6.31	<20.50	<35.08	<16.27	>138.60	>138.60
6c	0.73	<0.48	8.99	<20.50	49.94	<16.27	75.10	>138.60
7c	0.87	<0.48	9.74	<20.50	54.09	<16.30	63.58	>138.60
8c	1.70	<0.48	12.57	<20.50	69.81	<16.27	32.38	>138.60
9c	1.79	<0.48	12.76	<35.08	70.90	<16.30	30.66	>138.60
10e	1.33	0.96	11.61	35.23	64.48	27.96	41.25	69.40
11c	0.45	0.57	6.85	23.53	38.08	18.68	121.79	117.25
12c	9.77	<0.48	16.70	<20.50	93.00	<16.3	5.63	>138.60
13c	3.33	<0.48	14.70	<20.50	81.90	<16.3	16.54	>138.60
14c	5.93	<0.48	16.02	<20.50	88.98	<16.39	9.28	>138.60
15c	<0.40	<0.48	6.31	<20.50	<35.08	<16.27	>138.60	>138.60
16c	<0.40	0.78	<6.35	30.20	<35.08	24.00	>138.60	85.50
17c	<0.40	0.54	<6.35	22.60	<35.08	17.9	>138.60	123.50
18c	2.43	0.59	13.82	24.21	76.78	19.21	22.64	113.23
19c	1.06	0.98	10.65	35.80	59.15	28.4	51.72	67.90
20c	<0.40	<0.48	<6.35	<20.50	<35.08	<16.3	>138.60	>138.60
21c	<0.40	<0.48	<6.35	<20.50	<35.08	<16.3	>138.60	>138.60
22c	7.44	1.01	16.38	36.60	91.01	29.00	7.40	63.00
23c	<0.40	<0.48	<6.35	<20.50	<35.08	<16.3	>138.60	>138.60
24c	3.19	1.06	14.63	37.80	81.29	30.00	17.24	63.00
25c	3.51	1.79	14.90	52.90	82.70	42.0	37.26	15.68
26c	<0.40	<0.48	<6.35	<20.50	<35.08	<16.3	>138.60	>138.60
27c	<0.40	<0.50	<6.35	<21.21	<35.25	<16.83	>138.60	>138.60
28c	<0.40	<0.50	<6.35	<21.21	<35.25	<16.83	>138.60	>138.60

Cl$_{int}$, intrinsic microsomal clearance; CL$_{pred}$, predicted metabolic clearance; LBF, liver blood flow; nd, not determined; GSK cut-off values for % LBF: > ¾, high clearance; between 1/3 and ¾, intermediate clearance; <1/3, low clearance.

4.4. Discussion

4.4.1. The lead compound – wollamide B

The work started by synthesizing the lead compound itself and evaluating its antimycobacterial activities against *Mtb*. This was important to synthetically verify the structure of the natural product and to prove if it has also appreciable antimycobacterial activity and hence to testify the real potential of the compound for further development as an anti TB drug. Accordingly wollamide B (**1c**) was synthesized following the method described in section 4.1.

To substantiate the reported antimycobacterial activity (against *M. bovis*), the activity of the **1c** was tested against a standard drug susceptible *Mtb* H37Rv and *M. vaccae*. Wollamide B had very good activity against the tested strains with an MIC of 0.60 and 6.25 µM (Table 7). The toxicity assay that was done for this molecule against human HepG2 cells also confirmed that the compound did not show toxicity up to 50 µM. Consistent antimycobacterial activity accompanied by no host cell toxicity signaled a green light to further develop the molecule.

The results of *in-vitro* ADME profiling that were done for wollamide B (displayed in Tables 9-11) showed that it has good aqueous solubility (151 µg/mL), low affinity towards plasma protein albumin (73%), modest lipophilicity (Log D = 1.80 at pH = 7.4) but poor passive permeability through artificial membranes (< 3 nm/sec). More than 90% of the compound remained intact after 2 h incubation of the compound with mouse and human plasma at 37 °C showing its remarkable *in vitro* plasma stability. The predicted *in vivo* metabolic stability, expressed as % liver blood flow (LBF), was suitably high.

The favorable *in vitro* activity and ADME properties of wollamide B laid the basis for a rational optimization to achieve better antimycobacterial potency and pharmacokinetic properties.

4.4.2. Wollamide B analogues

Libraries of wollamide B analogues (**2c-28c**) were prepared following the same synthetic approach utilized for the synthesis of wollamide B. As presently there is no information about the target and mode of action of wollamides, the design of all the analogues was based on an approach commonly utilized to generate SAR of biologically active antimicrobial peptides.

4.4.2.1. Analogues synthesized through Ala scanning

The first generation wollamide B series, also known as 'Ala scan analogues' were designed and synthesized to identify the role (contribution) of each amino acid for the observed antimycobacterial activity. They were synthesized by sequentially replacing all the amino acids of wollamide B, except the D-Orn, with Ala. This technique is commonly used in the initial SAR investigation of peptide related compounds[157]. The D-Orn moiety was not replaced as the respective wollamide B analogue desotamide B had also been isolated and shown no antimycobacterial activity. Accordingly, five Ala scan analogues of wollamide B (**2c-6c**) (Figure 17) were synthesized at this stage.

The *in vitro* antimycobacterial activities of the Ala scan analogues were tested against *Mtb* H37Rv and *M. vaccae* 10670 (Table 7). Out of the tested five Ala scan analogues, it was only compound **4c** that exhibited moderate activity (20 µM) against *Mtb* H37Rv. This result infers that the side chains of all the amino acids present in the molecule contribute to activity either indirectly through dictating conformational space[158] or directly interacting with an assumed target. Regarding their activities against *M. vaccae* on the other hand, while all the four compounds were proved to be inactive at the maximum dose tested, one analogue (**6c**) displayed potent activity with an MIC of 0.78 µg/mL.

The *in vitro* plasma stability of all Ala scan derivatives was similar to wollamide B, i.e. more than 90% of all the compounds remained intact after 2 h incubation with human and mouse plasma at 37 °C (Table 10). This is another proof of the excellent stability of the class in general.
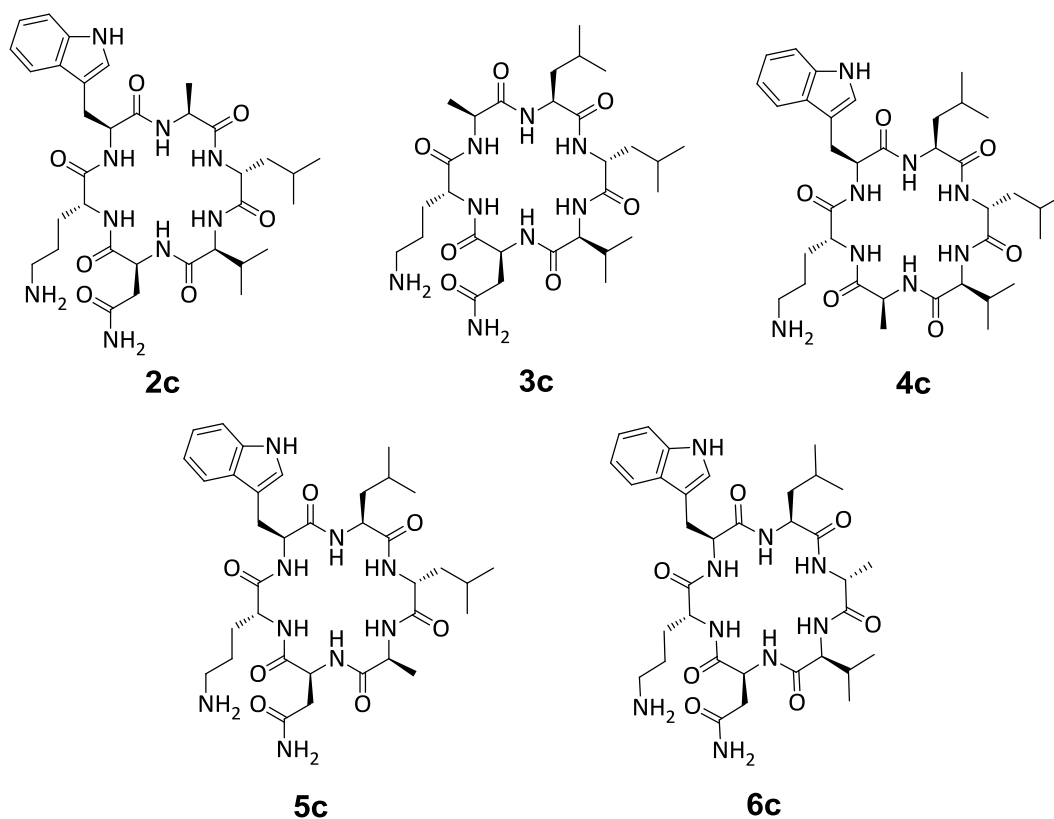
Figure 17: Structures of the alanine scan analogues.

The Ala scan analogues further shared higher metabolic stability and longer half-life compared to wollamide B. Based on the predicted hepatic clearance values, while wollamide B exhibited moderate metabolic stability (% LBF = 1/2), the Ala scan analogues were found in the range which is considered to be metabolically stable (% LBF < 1/3). Moreover, the half-lives of the Ala scan derivatives were doubled compared to wollamide B.

The determined Log D values ranged between 0.94 (**2c**) and 2.00 (**4c**) (Table 9). Considering their molecular weight, this value is not satisfactory for good cellular permeability[159]. Hence, further structural optimization of wollamide B should improve this issue. The experimentally determined human serum albumin binding affinity of the compounds showed large variation

ranging from 26% for **3c** to 83% for **4c**. This value seems correlated with the degree of lipophilicity and the presence or absence of the aromatic indole moiety. When the compound was more lipophilic and the indole moiety present, the binding affinity was found to be high. On the other hand, replacing Trp with Ala (**3c**) significantly lowered the affinity showing the contribution of the aromatic side chain for the relatively high serum albumin binding affinity of wollamide B.

In general, the major findings of the Ala scanning could be summarized as follows; (1) the result of the *in vitro* activity testing performed against *Mtb* H37Rv proved that all the amino acids of contributes towards to the observed activity of the lead (2) the finding that Asn substitution with Ala still retained some activity signals the possibility of further exploring this site for optimizing the structure for better potency and pharmacokinetic properties. (3) Very good stabilities (both plasma and metabolic) and physicochemical properties of such analogues, obtained through *in vitro* ADME profiling, continues to prove the drug likeness of the class.

4.4.2.2. Analogues synthesized through replacing the amino acid Val

Once we had checked the activity and the *in vitro* ADME profiles of the Ala scan analogues, we then closely examined the role of each of the six amino acids of wollamide B in view of improving potency and activity. Consequently, more analogues (second generation) were synthesized by replacing each residue with other proteinogenic and non proteinogenic amino acids.

We started the investigation on the Val moiety. Val could be a good site for variation because wollamide A (another naturally occurring wollamide) which have another amino acid at this site (*allo*-Ile) was also found to be active against *M. bovis* (2.8 µM)[114].

In accordance to this observation, analogues were synthesized through replacement of Val with *allo*-Ile (wollamide A), Ile, Met and a non proteogenic lipophilic substituent benzothiazinone (BTZ) (Figure 18).

Wollamide A (**7c**) was synthesized to confirm if it is still retains activity against *Mtb* like it did against *M. bovis.* Moreover, having wollamide A will also help to compare the antimycobacterial activities and drug-likeness of the two natural wollamides. This may helps further prioritization. As the *allo*-Ile moiety of wollamide A is quite expensive to use for routine synthesis, we also studied the effect of switching this moiety to Ile (**8c**). Moreover, to check if other lipophilic amino acid substituents are tolerable at this site, Met (**9c**) was introduced.
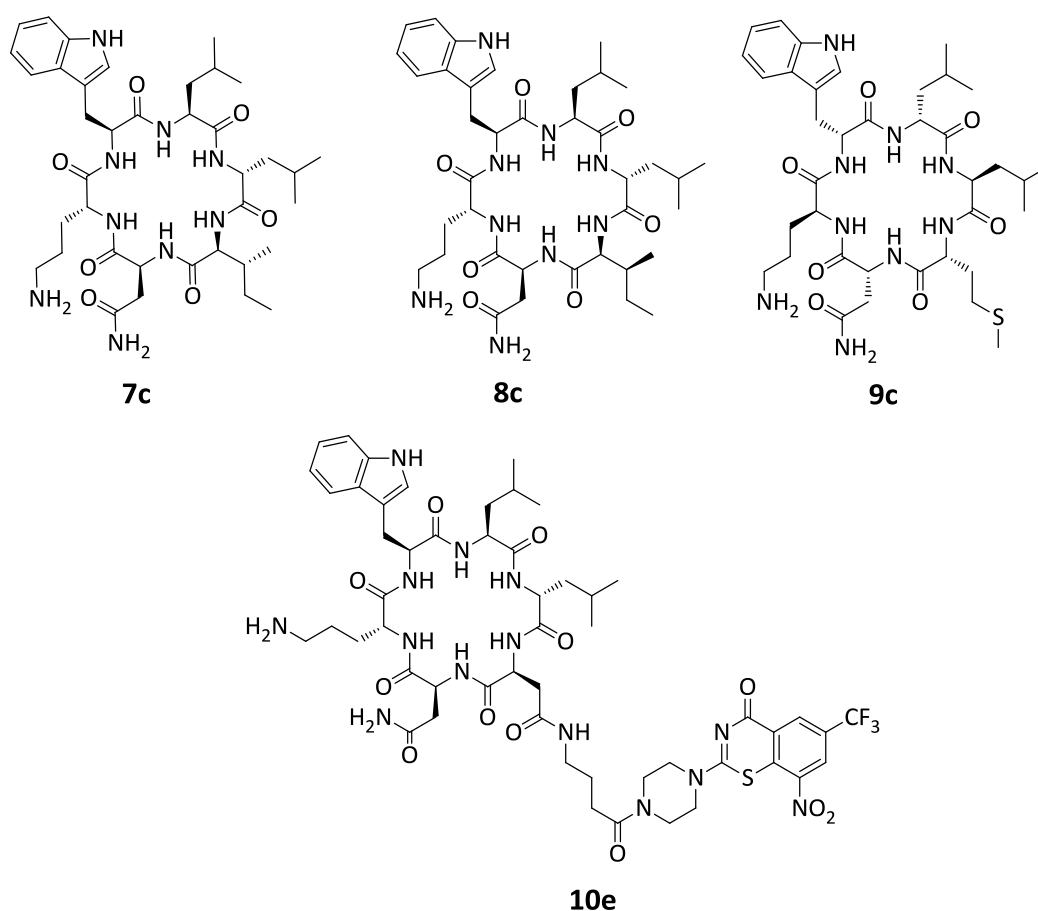

Figure 18: Wollamide B synthesized by replacing the valine amino acid.

There were two logics behind the preparations of a wollamide–BTZ (**10e**) hybrid. First, the incorporation of such a fairly lipophilic group to wollamide B structure will increase its lipophilicity. Increasing the lipophilicity of peptides is generally considered to be one of

theimportant factors for better antimicrobial activity[160]. Second, BTZs have already proved to be one of the most potent anti TB agents that target the enzyme DprE1. Studies have shown that their target DprE1 is also found in the outer membrane of the mycobacteria[161]. As the perceived sites of most of the studied AMPs are also on the cellular surface, this approach might help to localize BTZs on their target. As a result, the hybrid might have a dual action which could further improve its potency. The results of *in vitro* antimycobacterial activity test and ADME profiling of the four compounds, prepared through substituting the Val, are included in Table 7 and Tables 9-11.

Pertaining to their *in vitro* antimycobacterial activities against *Mtb* H37Rv, while **7c** and **8c** exhibited the same potency with an MIC of 1.08 µM, **9c** and **10c** were inactive at the maximum dose tested. The result confirmed that; while it is possible to retain the *in vitro* antimycobacterial activities of the natural wollamides (**1c** and **7c**) through replacement of Val or *allo*-Ile with Ile, further structural manipulations at this site is poorly tolerated. This finding, together with a similar result found by replacing Val with Ala (**5c**), could signify that the Val/Ile moiety have more important role than simply improving hydrophobicity at this site.

Among these series, while **10c** exhibited the best *in vitro* antimycobacterial activity against *M. vaccae* (MIC = 3.12 µg/mL), **9c** was the least active. Though their activity was not as potent as what was found against *Mtb*, both **7c** and **8c** were also active against *M. vaccae* with respective MICs of 12.50 and 6.25 µg/mL.

Like their antimycobacterial activities, wollamide A (**7c**) and B (**1c**) also showed quite similar *in vitro* stability (both plasma and metabolic) and physicochemical properties. Replacing the Val of wollamide B with *allo*-Ile had brought only very little improvement in the lipophilicity and metabolic stability. Hence, as the use of *allo*-Ile in place of Val didn't bring any significance improvement in both activity and drug-likeness, it is better to avoid such expensive building block in the future.

Similar to the result of their antimycobacterial activities, replacement of the expensive *allo*-Ile of **7c** by the Ile (**8c**) didn't alter the plasma stability and physicochemical properties of **7c**. However, such substitution was found to compromise the metabolic stability.

In vitro ADME profiling of **10c** has proved the initial assumption that improving the lipophilicity, and hence permeability, of wollamide B could be achieved through introduction of bulky lipophilic group. The compound had better lipophilicity and permeability than wollamide B. However, this was not very much exciting as it was achieved at the expense of antimycobacterial activity. The plasma stability of **10c** was also slightly compromised as a result of the BTZ side chain.

To sum up the major findings of Val substitutions; it was possible to come up with other active wollamide B analogues by replacing the Val moiety with *allo*-Ile (**7c**) and Ile (**8c**). However, all kind of lipophilic substitution at this site was not tolerated. This was confirmed with the obtained poor activity of other two analogues made through exchange of Val with Met (**9c**) and BTZ (**10c**) group.

4.4.2.3. Analogues synthesized through replacing the amino acid Asn

Based on the finding of the alanine scanning, the next amino acid that was subjected to modification was Asn. Among the five alanine scan analogues, the only compound that retains moderate activity (against *Mtb*) was obtained upon substitution of this amino acid. Hence, we wanted to further test the potential of this site in optimizing the activity and pharmacokinetics of the lead. Asn was replaced with positively charged amino acid D-Orn (**11c**), polar amino acid Ser (**12c**), lipophilic amino acids Ser (tBu) (**13c**) and Ile (**14c**). The structures of the synthesized analogues are showed in Figure 19.

Many naturally occurring antimycobacterial peptides contain a cationic center with at least a net charge of +2. To testify the effect of introducing a second positive charge on activity and stability of the lead, an analogue was synthesized by introducing another D-Orn in exchange for Asn (**11c**). The substitution was done in place of the polar amino acid Asn not to greatly

compromise the overall lipophilicity. Moreover, keeping the two D-Orn moieties adjacent to each other helps to maintain the amphiphilic nature.

This modification yielded a compound with an appreciable antimycobacterial activity (MIC_{Mtb} $_{H37Rv}$ = 2.50 µM) (Table 7). Of greater significance, compound **11c** exhibited a better *in vitro* microsomal stability (% LBF < 1/3) and its half-life was 2 times greater than that of the lead compound (Table 10). The finding showed the possibility of improving the microsomal stability in this class while still keeping high antimycobacterial activity.
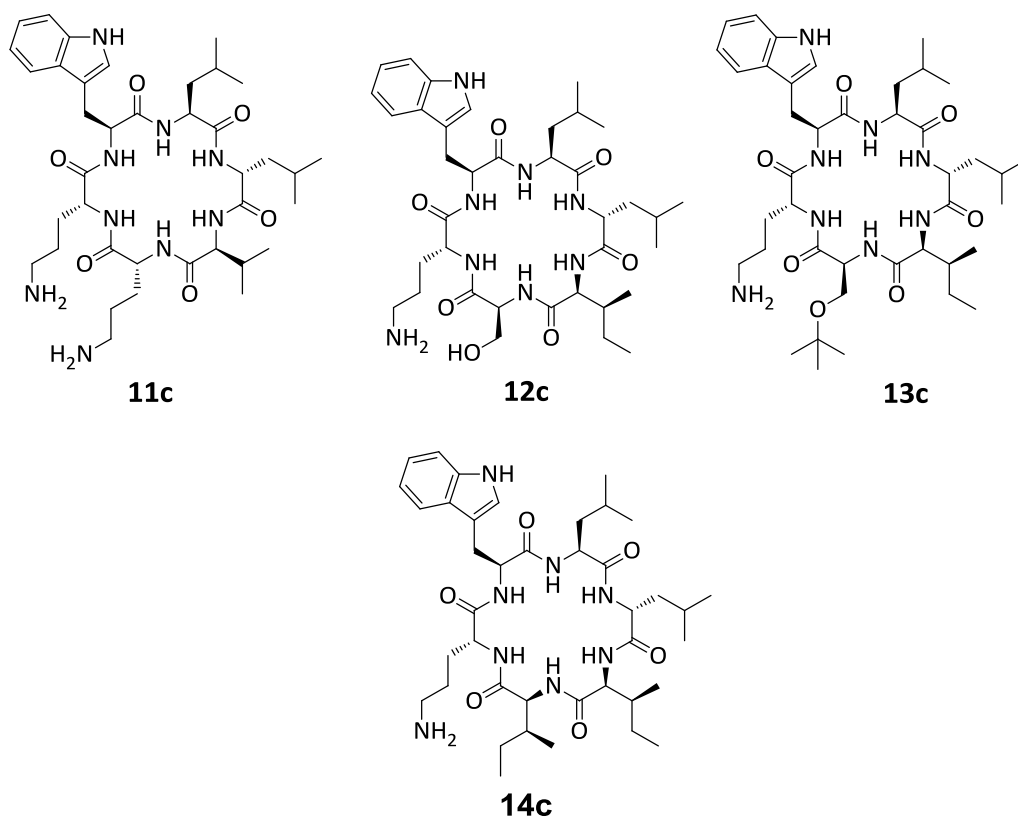

11c **12c** **13c**

14c

Figure 19: Wollamide B analogues synthesized by replacing the amino acid aspargine.

Asn was also replaced with the polar amino acid Ser (**12c**) and the lipophilic Ser (t-Bu) (**13c**) to explore the effect of varying the polarity of this position. While **10c** retained moderate

67

antimycobacterial activity with an MIC of 15 µM, compound **11c** was completely inactive (Table 7).

The result of the *in vitro* ADME profiling of compound **12c** showed that such modification did not affect the overall lipophilicity of wollamide B (Table 9). However, it had an adverse effect on the metabolic stability. Among all the synthesized analogues, this compound exhibited the lowest stability in human liver microsomes.

In view of improving the poor lipophilicity and permeability of the class in general, compound **14c** was prepared through exchanging both Asn and Val of the lead with the lipophilic amino acid Ile. While keeping significant antimycobacterial potency (MIC$_{Mtb\ H37Rv}$ = 3.13 µM) (Table 7), this change indeed produced the most lipophilic analogue so far (Table 9), While **14c** also exhibited better permeability than any of the synthesized analogues, it had high affinity to plasma proteins and a short microsomal half-life (Tables 9 and 11). This finding showed the possibility of improving passive membrane stability in this class while still keeping meaningful high antimycobacterial activity.

In summary, the result of Asn replacement with various charged, polar and lipophilic amino acid substituents showed that, while retaining appreciable antimycobacterial potency it is possible to use this site to improve the metabolic stability, lipophilicity and permeability of the lead compound. However, more work has to be done to find a substituent that demonstrates a right balance of metabolic stability and permeability.

4.4.2.4. Analogues synthesized through replacing the amino acids Trp, Leu and D-Leu

Another constitutional parameter for activity that we investigated was aromaticity. The number, type and arrangement of aromatic amino residues of antimicrobial peptides was shown to have an influence on their activities[162]. To testify if this also holds for wollamide B, we varied the type, number and arrangement of aromatic amino acids in the molecule.

Trp was swapped for Phe where the para positions of the phenyl side chain were blocked either with a chlorine (**15c**) or hydroxymethyl group (**16c**) (Figure 20). The *in vitro* metabolic study of these two compounds showed that the predicted metabolic clearances of both compounds were much lower than wollamide B (Table 11). The result of the *in vitro* ADME profiling also revealed that the two compounds exhibited nearly the same degree of lipophilicity with the lead. However, the antimycobacterial activities of **15c** and **16c** were much lower (Table 7). While **15c** showed only weak activity against *Mtb* H37Rv with an MIC of 40 µM, **16c** was completely inactive at the maximum dose tested. The loss of activities, in spite of maintaining comparable lipophilicity and greater metabolic stability, suggests that the role of Trp is far beyond contributing to the hydrophobicity of the molecule. This finding goes in line with a study made to examine the role of Trp for the antimicrobial activity in Arg and Trp rich peptides[163–165]. The study highlighted the unique properties of Trp to have a distinct preference for the interfacial region of lipid bilayers and its ability to participate in cation–π interactions, thereby facilitating enhanced peptide–membrane interactions.
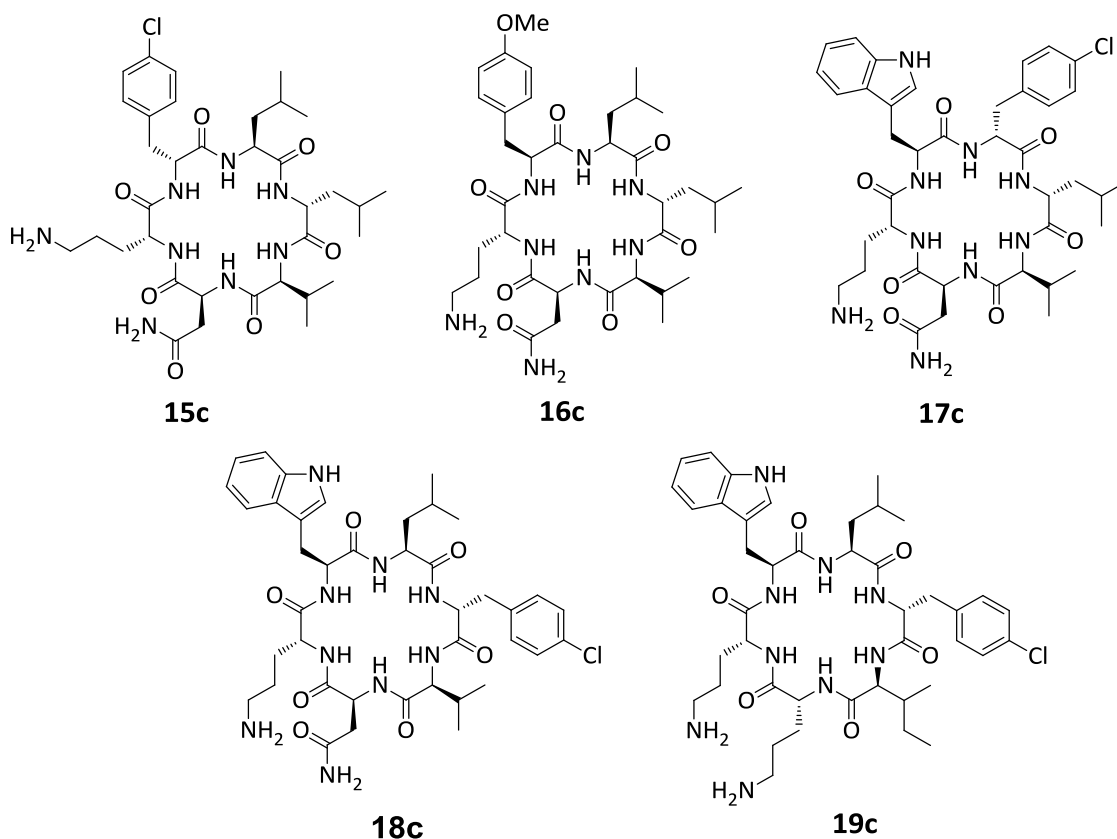
Figure 20: Wollamide B analogues synthesized through aromatic substitutions.

Two analogues were synthesized by introducing additional aromatic amino acids in the molecule, namely 4-chloro-D-Phe in place of both Leu (**17c**) and D-Leu (**18c**) (Figure 20). This was done to check the effect of having multiple aromatic amino acids with different arrangement in the molecule. While **18c** still maintained a notably high antimycobacterial activity **(**MIC$_{MtbH37Rv}$ = 1.90 µM**)**, the MIC of **17c** was 30 µM which is much lower than the lead (Table 7). Contrary to its good antimycobacterial potency, **18c** exhibited unfavorable pharmacokinetic properties with poor metabolic stability (% LBF > ¾), short half-life (< 30 min) and high human serum albumin binding (92%). The drop in the activity of **17c**, in spite of its better metabolic stability, might be attributed to the change in the stereochemistry of the amino acid from L to D, again suggesting that a specific interaction with a yet unknown target or targets causes activity in this cyclic peptide class.

70

Both **17c** and **18c** were also proved to exhibit a potent *in vitro* activity against *M. vaccae* with a respective MIC of 3.12and 0.40 µg/mL (Table 7).

Aiming at improving the poor *in vitro* metabolic stabilities of **18c**, **19c** was synthesized by incorporating a D-Orn in place Asn. This was based on the finding in compound **11c** where such change improved metabolic stability. Though the desired improvement in metabolic stability was achieved (Table 11), the antimycobacterial activity was greatly compromised ($MIC_{MtbH37Rv}$ = 17.50 µM).

20c   **21c**
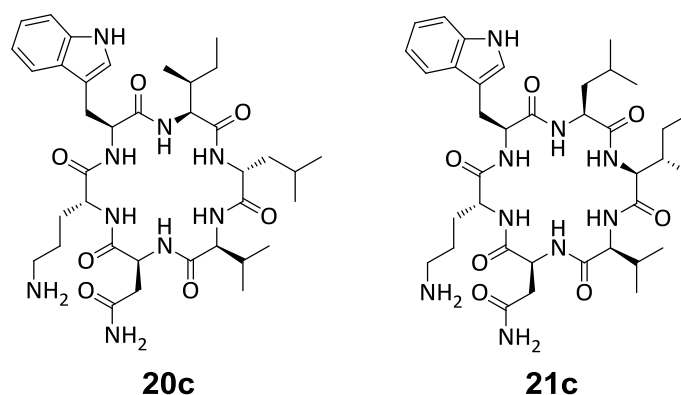
Figure 21: Wollamide B analogues synthesized through replacement of D-Leu and L-Leu.

Both the D- and Leu residues of wollamide B were further replaced with Ile (Figure 21) to check if such modification had similar outcome like the one obtained in compound **8c**. While replacing Leu with Ile (**20c**) retained moderate activity ($MIC_{Mtb\ H37Rv}$ = 7.50 µM) exchanging D-Leu for Ile (**21c**) completely abolished the activity. This was another instance that switching the stereo centers of these two amino acids gravely affects the activity of wollamide B. The predicted metabolic stabilities and the half-lives of both **20c** and **21c** were much better than the lead compound (Table 11). This is particularly interesting for **20c** as it still retained some antimycobacterial activity.

4.4.2.5. Analogues synthesized through replacing the D-Orn

Previous studies done on antimicrobial peptides showed that Arg containing peptides are generally more potent than the corresponding Lys or Orn analogues[162]. The higher antimicrobial activities of such peptides is attributed to the guanidinium group of Arg which allows more dispersed positive charge and offers greater directionality and possibility of hydrogen bonding with the surrounding water molecules. The Arg side chain allows the formation of more interactions compared to the mono charge present in Orn[164,166].

As we suspected introduction of the strongly basic guanidine side chain would greatly compromise lipophilicity, Val was simultaneously replaced by Ile. This afforded a very potent analogue (**22c**) with an MIC of 0.60 µM against *Mtb* H37Rv. This compound has also displayed a moderate activity against *M. vaccae* (MIC of 6.25 µM).
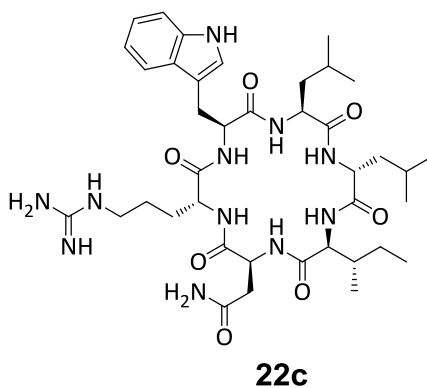

22c

Figure 22: Wollamide B analogue synthesized through replacing the D-ornithine amino acid.

On top of its remarkable activity, compound **22c** (Figure 22) exhibited higher lipophilicity (Log D = 2.05), permeability (11 nm/sec) and aqueous solubility (189 µg/mL) than wollamide B. The major shortcoming of this compound was its low stability in human liver microsome which we

associated with the metabolically labile guanidine group[167]. The stability of the compound in mouse microsome, on the other hand, was much better.

4.4.2.6. Analogues synthesized through N-methylation of wollamide B

Many studies showed N-methylation of cyclic peptides to offer a number of advantages, including (1) improvement of the therapeutic efficacy of peptides by fine-tuning their selectivity for a receptor[168], (2) enhancing the hydrophobicity by reducing the number of hydrogen-bond donors and by preventing the formation of intermolecular and intramolecular hydrogen bonds which in turn improves oral bioavailability[169], (3) Multiple *N*-methylation also introduce remarkable metabolic stability, even in the presence of gut peptidases, in comparison with cyclization only[170]. Hence, hoping to achieve one or more of the aforementioned goals, *mono-*, and *di-*-N-methylated analogues were synthesized (**23c-26c**) (Figure 23) and checked for their *in vitro* antimycobacterial activities, stabilities and physicochemical properties. Results are displayed in Tables 7 and Tables 9- 11.

The effect of N-methylation on the activity of the prepared analogues produced varying results. While the *mono*-N-methylated analogue (**23c**) retained moderate antimycobacterial activity (MIC$_{Mtb\ H37Rv}$ = 12.50 µM), the *di*-N-methylated analogues (**24c-26c**) were completely inactive irrespective of the position of the two methyl groups in the molecule.

As expected, N-methylation of the Val moiety of wollamide B increased lipophilicity and human liver microsomal stability. However, the contribution of this modification in improving the low permeability was not significant.

N,N-Dimethylated analogues displayed varying stability in human liver microsomes depending on the site of methylation. The metabolic stability was found to be compromised when the two methyl groups were introduced at Leu and Val (leading to **24c**) and on Leu and Asn (leading to **25c**). On the contrary, dimethylating the D-Leu and Asn to give **26c** increased microsomal stability.
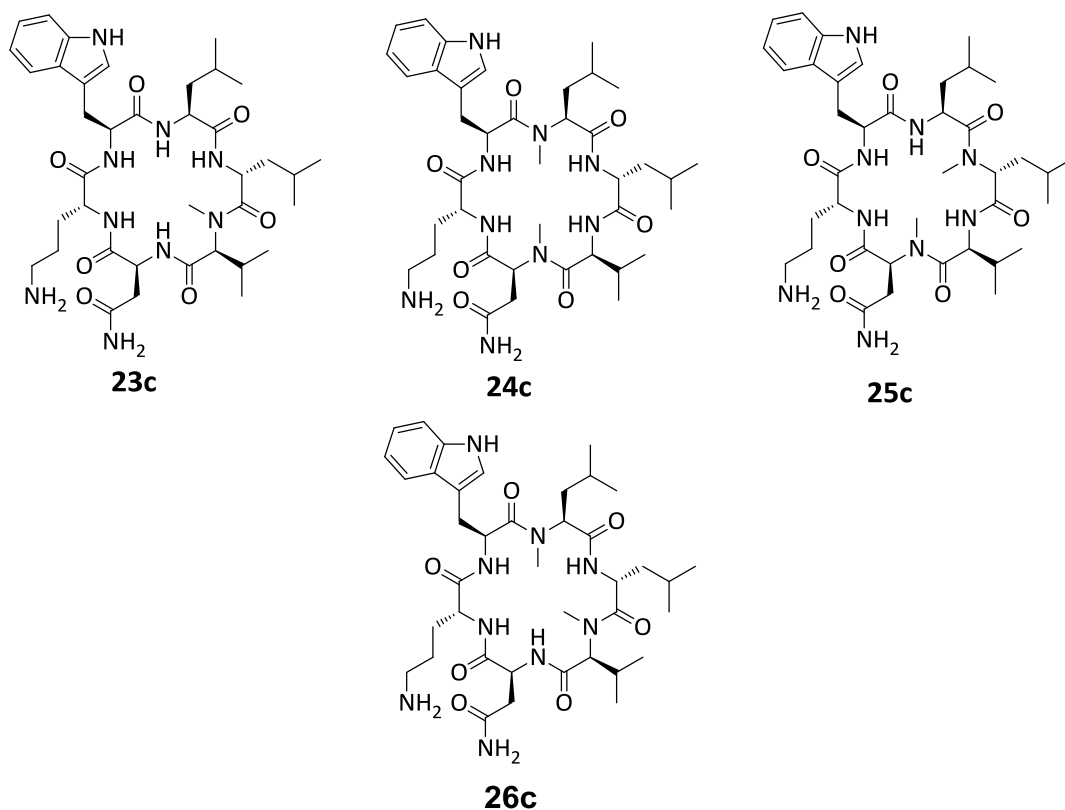
Figure 23: N-methylated wollamide B analogues.

The determined Log D values of the N-dimethylated analogues were also not identical, in spite of the introduction of the same functional groups. While **26c** exhibited the highest Log D value in these series (2.25), **24c** was found to be only slightly more lipophilic than its *mono*-N-methylated analogue (Log D = 2.0). Such differences in lipophilicity may be due to differences in the number of exposed polar surfaces because the molecules assume different conformations as a result of such methylations.

4.4.2.7. Analogues synthesized by swapping the positions of amino acids

To investigate the effect of changing the sequence of the amino acids in wollamide B, one of its stereo isomers (**21c**) was prepared through randomly exchanging the position of Trp for D-Leu (Figure 24). This compound exhibited different stability and physicochemical properties. While the change improved the experimental *in vitro* pharmacokinetic properties through increasing aqueous solubility, metabolic stability and half-life, the antimycobacterial activity was compromised. The compound showed activity against *Mtb* H37Rv with an MIC of 20 µM. Another compound (**28c**) that was synthesized through an exchange of the Val amino acid of **27c** with Ala was also found to be inactive. This finding indicates that the amino acids sequence is indeed crucial both for antimycobacterial activity and pharmacokinetic properties of wollamide B.
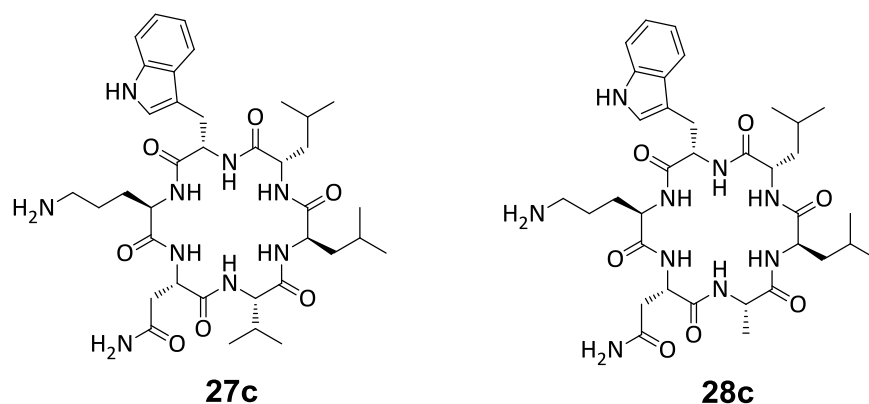

Figure 24: A stereoisomer of wollamide B and its analogue.

4.4.3. Summary of the SAR of wollamide B

Based on the results obtained from the synthesis, antimycobacterial activity testing and *in vitro*
ADME profiling of different analogues, the SAR of wollamide B can be summarized as follows
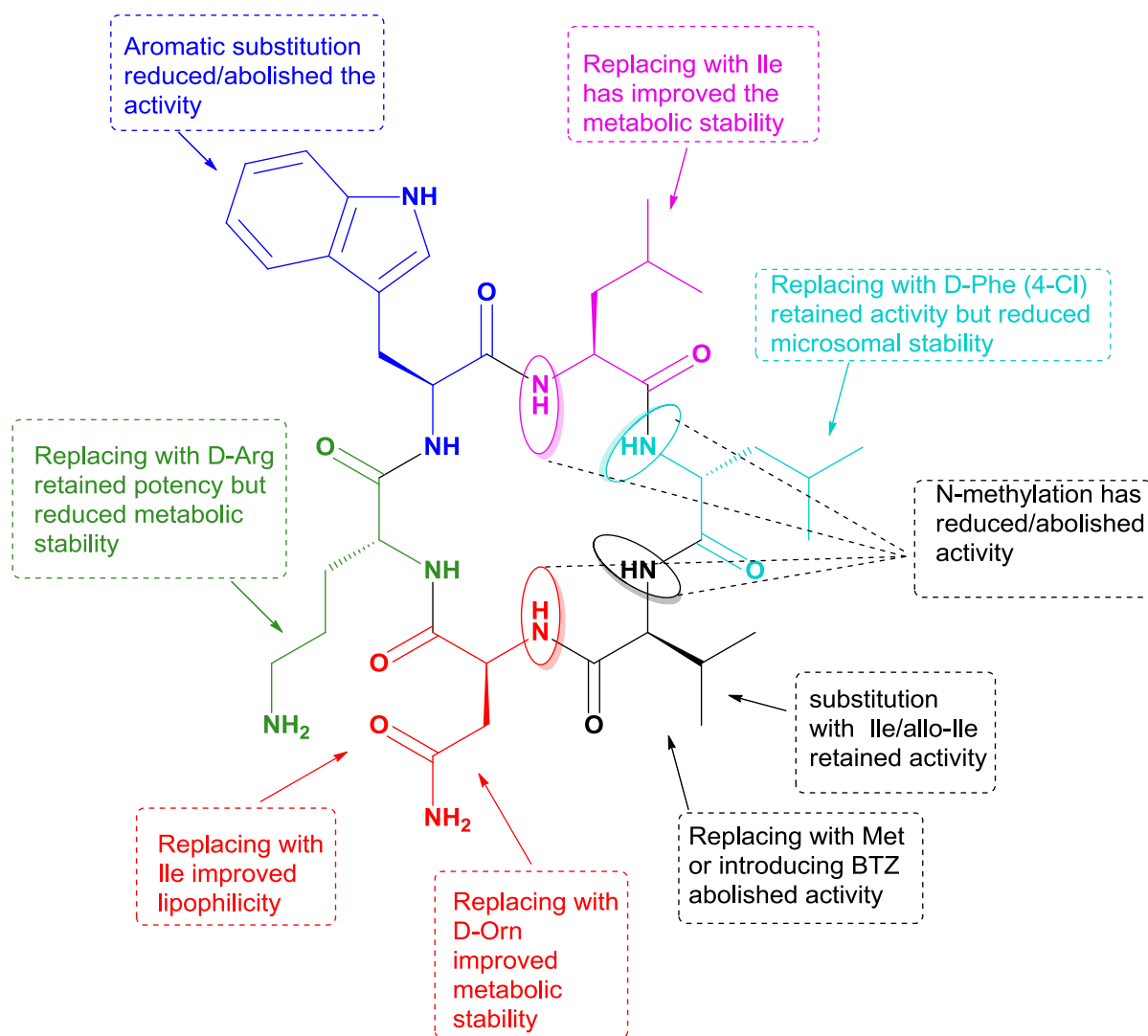(Figure 25).

Figure 25: General SAR of wollamide B.

a) The result of Ala scanning showed that each amino acid of wollamide B contributes towards the observed antimycobacterial activity

b) Replacement of Asn with a positively charged amino acid D-Orn and lipophilic amino acid Ile retained antimycobacterial potency. The D-Orn substitution also improved the microsomal stability.

c) Exchanging Asn with Ile significantly improved the lipophilicity of wollamide B. This substitution, however, reduced the *in vitro* microsomal stability.

d) Replacing Asn with other polar amino acid Ser and lipophilic amino acid Ala also afforded an analogues with moderate antimycobacterial activities.

e) While replacing the Val with Ile and *allo*-Ile retained the antimycobacterial potency, other lipophilic substituents like Met and benzothiazinone (BTZ) resulted in complete loss of activity.

f) Introduction of an aromatic amino acid 4-Chloro-D-Phe in place of D-Leu has also retained antimycobacterial potency and lipophilicity while reducing the *in vitro* microsomal stability. Exchanging D-Leu with Ile abolished the activity.

g) Exchanging the D-Orn with another basic amino acid D-Arg generated an analogue that had the same potency with wollamide B. This substitution also improved the lipophilicity and the aqueous solubility of the lead compound. However, the *in vitro* microsomal stability was reduced.

h) Replacement of Trp with other aromatic amino acids 4-Chloro-D-Phe and 4-Methoxy-Phe abolished the antimycobacterial potency showing the importance of the indole moiety.

i) N-methylation of some of the amino acids of wollamide B to produce *mono-* and *di-* N-methylated analogues reduced/abolished the antimycobacterial activity.

j) A stereoisomer of wollamide B that was synthesized through swapping the position of Trp for D-Leu had resulted in lower antimycobacterial potency than the lead.

4.4.4. Hit prioritization

Among the synthesized wollamides, 7 compounds that exhibited activities against *Mtb* H37Rv with MICs ≤ 3.13 µM were selected as possible hits. Prioritization among the hits was then made on the basis of their antimycobacterial potency and their drug-likeness. The list of the selected hits together with the properties used for prioritization is presented in Table 12. To facilitate the prioritization, a score was roughly assigned for each of the relevant properties a compound has displayed. The scoring for the *in vitro* ADME properties was based on pre-determined cut points developed by GSK. For the antimycobacterial activities, scoring was done by comparing their MICs with the commercially available anti TB drugs[171]. Compounds that exhibited MICs in a range of commercially available first line anti TB drugs were given the highest score (score = 5) and those whose MICs existed within ten fold dilutions were considered to be moderately active (score = 3).

Based on the cut off points developed by GSK, green color indicates a compound exhibits the desired level of that particular property (hence, highest score 5). For example, green color for metabolic stability means the compound has good metabolic stability; for permeability it means the compound has good level of permeability and so on. Similarly, a yellow color indicates an intermediate level of acceptance (score = 3) and a red color indicates that particular property is not within the acceptable range (score = 1).

Compounds **1c**, **7c**, **8c and 11c** are placed in the first priority list as they fulfilled most of the requirements (the highest score) needed to be good lead candidates. These compounds showed a good balance of antimycobacterial activity and *in vitro* microsomal stability. They also have good level of plasma stability and aqueous solubility, which is a common feature of all the selected hits. Since all the four compounds exhibited low level of passive membrane permeability, future optimization work should be concentrated on improving this property.

Table 12: Comparison of the selected hits based on their antimycobacterial activities and *in vitro* ADME properties.

Compound	Activity[a] (*Mtb* H37Rv)	Microsomal stability[b]	Plasma stability[c]	Aqueous solubility[d]	Passive Permeability[e]	Score
1c	green	yellow	green	green	red	19
7c	green	yellow	green	green	red	19
8c	green	yellow	green	green	red	19
11c	yellow	green	green	green	red	19
14c	yellow	red	green	green	yellow	17
18c	yellow	red	green	green	red	15
22c	green	red	green	green	red	17

[a]Antimycobacterial activity: green = high activity (5); yellow = moderate activity (3); red = low activity (1); [b]Microsomal and plasma stability: green = high stability (5); yellow = intermediate stability (3); red = low stability (1); [c,d]Aqueous solubility: green = high solubility (5); yellow = intermediate solubility (3); red = low solubility (1); [e]Passive permeability: green = high permeability (5); yellow = intermediate permeability (3); red = low permeability (1).

Compounds **14c** and **22c** are placed in the next priority list (score = 17). The common limitation of these two compounds was their poor stabilities in human liver microsomes. Apart from improving their microsomal stabilities, more work should be done focusing on improving the permeability of **22c** and the potency of **14c**. Among the selected hits, the only compound that exhibited moderate permeability was **14c**.

The compound with the lowest score and hence, the least prioritized lead was compound **18c**. This compound displayed a combination of low membrane permeability and microsomal stability apart from its moderate *in vitro* potency.

4.4.5. *In vivo* proof of concept (PoC) study

4.4.5.1. *In vivo* efficacy study in acute mouse model for 8c

As initial proof of concept, the first *in vivo* efficacy test was initiated for one of the active compounds, **8c.** This was done through intraperitoneal (IP) administration of the compound to female C57BL/6J mice infected with *Mtb* H37Rv according to a protocol described in section 8.6. The dose selected to be administered was 75 mg/kg. While doing the efficacy study, the blood exposure levels of the compound was assessed by taking blood samples at regular intervals. However, after withdrawing the sample for the first 3.5 hours, the entire test had to be terminated due to the observed severe toxicity signs which forced the mice to be sacrificed. The observed toxicity signs included abdominal pain and absence of righting reflex. The blood levels of the compound is displayed in Figure 26 and Table 13. **8c** was available in the blood at a concentration which is well above the determined MIC. The area under the curve (AUC) which measures the total amount of the compound that reaches the systemic circulation after IP administration also showed sufficient amount of the compound was available for 3.5 h.

Table 13: *In vivo* mice blood exposure level of **8c.**

Properties	Values
Cmax (ng/mL)	31300.0
Cmin (ng/mL)	12600.0 (at 3.5h)
AUC 3.5h (h*ng/mL)	71863.0
DNAUC 3.5h(h*ng/mL) per mg/Kg	958.2

AUC = area under the curve; DNAUC = dose normalized area under curve; Cmax, maximum blood concentration; Cmin, minimum blood concentration.
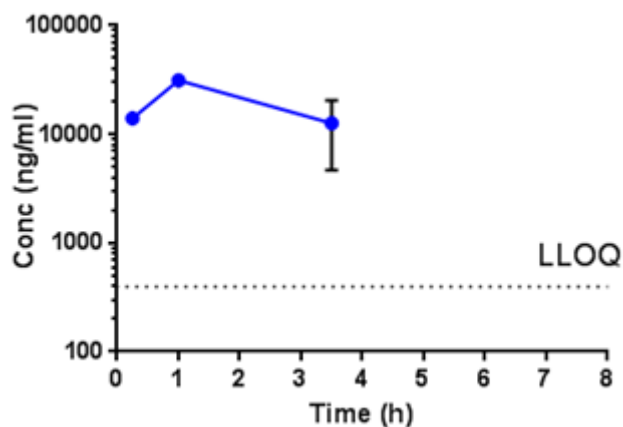
Figure 26: *In vivo* mice blood exposure level of **8c** after IP administration at a dose level of 75 mg/kg.

4.4.5.2. *In vivo* tolerability and blood level exposure assay

Since **8c** was toxic at 75 mg/kg, a tolerability assay had to be performed to select the optimal dose required for the *in vivo* efficacy study. Accordingly a tolerability study and determination of the blood exposure level was initiated for **8c** and **22c** (the other wollamide B analogue with the highest potency).

The study was done through IP administration of the compounds to three C57BL/6j female mice at two dose levels, 5 mg/kg and 25 mg/kg. The mice were inspected for any sign of toxicities using the Irwin test[172]. They did not demonstrate any behavioral changes and no signs of toxicity at both doses. The only concern upon administration of the two compounds at the 25 mg/kg dose level was consistent weight loss (10%) which occurred in the first 24 h after dosing. As such consistent weight loss might cause toxicity upon a repetitive dosing, a decision was made to perform the *in vivo* efficacy test by IP administration of both compounds at the lower dose of 5 mg/kg.

The result of the blood level exposure data after IP administration of the two compounds at 5 and 25 mg/kg dose level are shown in Figure 27 and Table 14. Both compounds exhibited slow *in vivo* clearance that was consistent with what was predicted by the *in vitro* ADME profiling. The magnitudes of the area under the curve (AUCs) that were determined over a period of 6 h after administration of the two compounds showed that, both compounds were available in the blood with a concentration that was close to their MICs. The dose normalized AUC (DNAUC) values for **8c** were closely similar for the two tested dose levels indicating that this compound shows good linearity between doses. Compound **22c**, on the other hand, exhibited nonlinear kinetics which might happened due to a saturation of metabolic pathway or clearance mechanism[173].
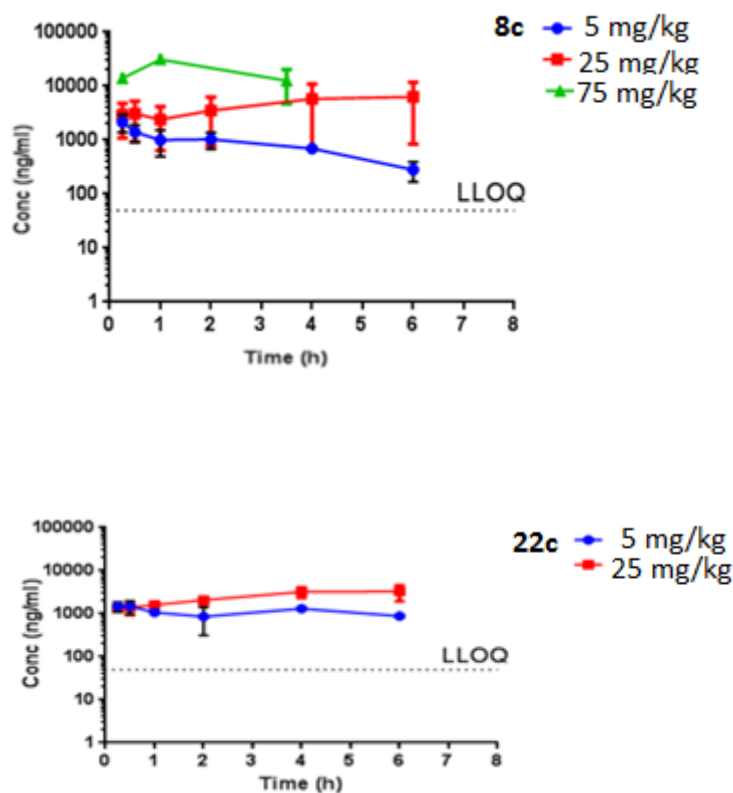
Figure 27: *In vivo* mice blood exposure level of a) **8c** and b) **22c** after IP administration.

Table 14: *In vivo* mice blood exposure level of **8c.**

Compound	Dose (mg/Kg)	Cmax (ng/ml)	Cmin (ng/ml)	AUC6h (h*ng/ml)	DNAUC6h(h*ng/ml) per mg/Kg
8c	5	2166.7	283.0	4785.0	957.0
	25	6328.7	2953.0	26596.0	1063.8
22c	5	1473.3	850.7	6293.0	1258.6
	25	3263.3	1320.0	14653.0	586.1

AUC = area under the curve; DNAUC = dose normalized area under curve; Cmax, maximum blood concentration; Cmin, minimum blood concentration.

4.4.5.3. *In vivo* efficacy study in acute mouse model for 8c and 22c

Based on the result of the tolerability assay **8c** and **22c** were evaluated for their *in vivo* efficacy in the acute mouse model. Detailed protocol of the test is described in section 8.6. The test was done by intraperitoneal administration of the two compounds at the dose levels of 5 mg/kg to female C57BL/6 mice infected with *Mtb* H37Rv.

Treatment was initiated the next day after infecting the mice with the bacteria and both **8c** and **22c** were administered once a day for 8 days. As an interassay control, moxifloxacin was administrated orally (30 mg/kg). On day 9 after the infection, all the mice were sacrificed and their lungs were harvested to inspect the outcome of the treatment. Evaluation of the treatment outcome was carried out by comparison of the lung mycobacterial burden (log10 CFUs/lungs) obtained from treated and untreated (control) mice. The results of the test is presented in Table 15 and Figure 28.

Both **8c** and **22c** did not demonstrate any hint of efficacy at the tested dose level (5 mg/kg) compared to the untreated mice. On the other hand, moxifloxacin treatment caused a 3.4 logCFU reduction of the bacterial lung count when compared to the untreated group which was statistically significant.

The blood exposure levels of the two compounds that were determined during the efficacy study showed that the compounds achieved a blood level just above their *in vitro* determined MICs. As the compounds exhibited poor *in vitro* membrane permeability, the effective

concentration of these compounds in the actual site (infected lung macrophages) may have been lower than what was achieved in the blood (MICs). Hence, the lack of efficacy with both compounds may be attributable to the rather low dose.

A = No treatment (day 9)

B = Moxifloxacin qd po 30 mg/Kg

C = **8c** qd IP 5 mg/Kg

D = **22c** qd IP 5 mg/Kg
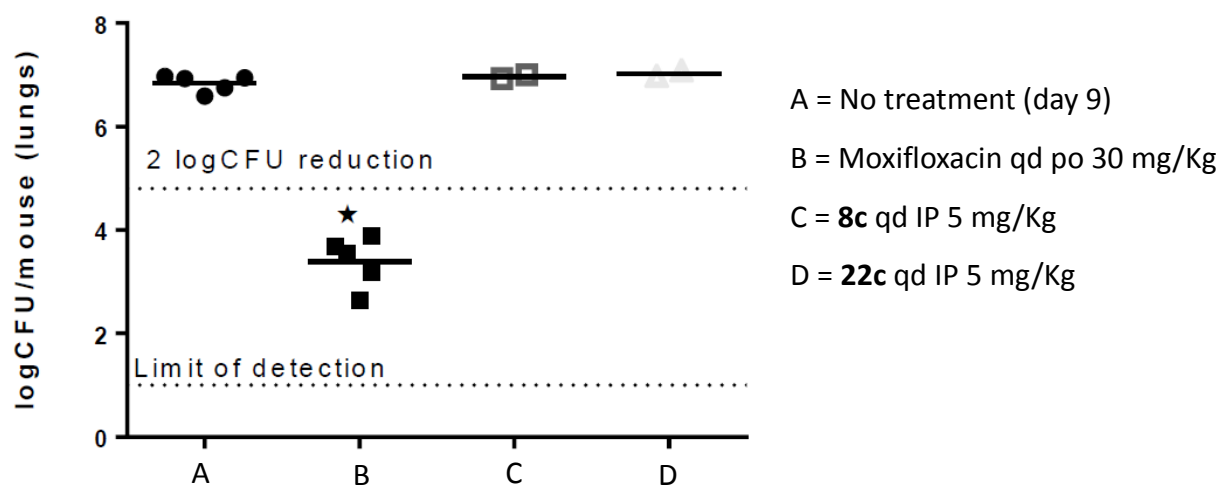
* P < 0.05, Anova analysis

Figure 28: Antitubercular efficacy in an acute infection murine model of tuberculosis. Each point represents data from an individual mouse that received each product administered in a once a day schedule (qd). 8c and 22c were administered for 8 days by intraperitoneal route and moxifloxacin was administered for 8 days by oral route.

Table 15: Result of the antimycobacterial efficacy study in acute *in vivo* mouse model for **8c** and **22c.**

Compound	Dose (mg/Kg)	Frequency of adminstration	Route of adminstration	LogCFU reduction[a]	p-value[b]
Moxifloxacin	30	qd (days 1-8)	oral	3.4	p < 0.05
8c	5	qd (days 1-8)	IP	-0.2	p > 0.05
22c	5	qd (days 1-8)	IP	-0.2	p > 0.05

[a]LogCFU reduction with respective to the untreated mice; [b] p < 0.05 was considered as significant; qd = once a day; IP = intraperitoneal route.

4.5. Conclusion

In conclusion, the reported chemical structure and antimycobacterial activity of wollamide B was verified by its independent synthesis and testing its activity against different Mycobacterium species, namely *Mtb* H37Rv, *M. vaccae* and *M. smegmatis*. The potent activity it showed against *Mtb* H37Rv (MIC = 0.60 μM) coupled with its little cytotoxicity against human HepG2 cells (IC_{50} = 50 μM) has proven its potential to be a good lead candidate for the development of an anti TB drug of a new class, small cyclopeptides. Results obtained during *in vitro* ADME profiling also proved the drug likeness of the molecule and strengthened the above claim.

The SAR study that was performed based on Ala scanning revealed that all amino acids of this cyclohexapeptide contributed to the observed activity. In addition to the Ala scanning, in depth SAR investigations were carried out by designing and synthesizing a library of wollamide B analogues and testing their antimycobacterial activities and drug likeness. The results of such structural modifications showed what features of wollamide B could be changed in view of improved potency and pharmacokinetic properties.

Among the synthesized 28 wollamides, seven (**1c**, **7c**, **8c**, **11c, 14c, 18c** and **22c**) showed antimycobacterial potency against *Mtb* H37Rv with an MIC $\leq$ 3.13 μM. For some of the active compounds, an intracellular assay was performed against *Mtb* H37Rv infected human macrophages. The results were consistent with the determined *in vitro* extracellular MICs. Compounds **22c** (MIC = 0.60 μM) and **8c** (MIC = 1.08 μM) that displayed a good balance of antimycobacterial activity and pharmacokinetic properties were also evaluated for their *in vivo* efficacy against *Mtb* H37Rv infected mice model at the dose level of 5 mg/kg. The first *in vivo* assay showed the dose to be too low.

Part Two:

Development of hirsutellide A and analogues

5. Hirsutellide A

The second part of my PhD work focused on the development of another small cyclic depsipeptide, hirsutellide A (Figure 29). Hirsutellide A is an 18-membered symmetrical cyclic depsipeptide that was isolated from the fungus *Hirsutella kobayasii* BCC 1660. The reported MIC of the compound against *Mtb* H37Ra was 6–12 µg/mL. Cytotoxicity study against Vero cell lines showed that the compound was not toxic at the maximum dose tested (50 µg/mL). The structure of hirsutellide A was reportedly elucidated by analyses of spectroscopic data and shown to contain *allo*-Ile, (R)-2-hydroxy-3-phenylpropanoic acid and Sar[113].
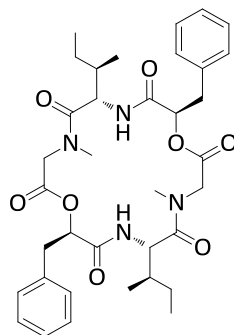
Figure 29: Structure of hirsutellide A.

Compared to other small cyclic antimycobacterial depsipeptides, e.g. depsidomycin[117] and massetolide A[120], the structure of hirsutellide A appears to be simple and easy to synthetically manipulate. This could help to synthesize many analogues to investigate its structure-activity relationships (SAR).

As this work was not done previously, the focus of the second part of my PhD work was to use hirsutellide A as a lead and to define its SAR. This was done by designing and synthesizing various depsipeptide and peptide analogs of the lead and testing the antimycobacterial activity and drug likeness, the final goal being finding a derivative that has superior potency and pharmacokinetic property than the lead.

5.1. Synthesis of hirsutellide A and its analogues

5.1.1. Synthesis of the depsipeptide analogues of hirsutellides

Hirsutellide A (**33e**) and its depsipeptide derivatives (**34e**-**36e** and **37b**) were synthesized using a solution phase peptide synthesis approach following a method described by Xu Y. *et al*[121]. The first step was diazotization hydrolysis of D-Phe to the corresponding α-hydroxyl carboxylic acid (**29**) (Figure 30). This type of reaction occurs with retention of configuration though the formation of trace amounts of racemate cannot completely be excluded[174,175]. To make sure the product had the required level of purity, it was carefully recrystallized from the crude mixture. The optical purity of **29** was asserted by comparing its specific optical rotation with a literature value. Following that, the free carboxyl function of **29** was temporarily protected as a benzyl ester **(30**) before coupling of the next amino acid. The benzyl ester of **29** was prepared by a reaction that involved esterification of **29** with benzyl alcohol in the presence of catalytic amount of 4-toluenesulfonic acid *(*TsOH)[176] (Figure 30).

The fully protected didepsipeptide **31** was obtained in a good yield (88%) using EDC*HCl/DMAP mediated coupling of **29** with N-Boc-Sar-OH. This reaction took only 2 h for completion. The same reaction that had been done previously using DCC (instead of EDC*HCl) took much longer duration (24 h) and lower yield (72%)[121,177]. The Boc protecting group of the didepsipeptides was then removed by treatment with TFA (6.5 eq.) to produce the amine TFA salt of compound **32** (Figure 30).

Coupling of the didepsipeptide **32** to N-Boc-protected aliphatic amino acids (*allo*-Ile, Leu, Val and Gly) using HATU/TEA as a coupling agent in DCM yielded the corresponding tridepsipeptides (**33-36)** whose reactive amino and carboxy terminals were protected **(**Figure 31**)**.
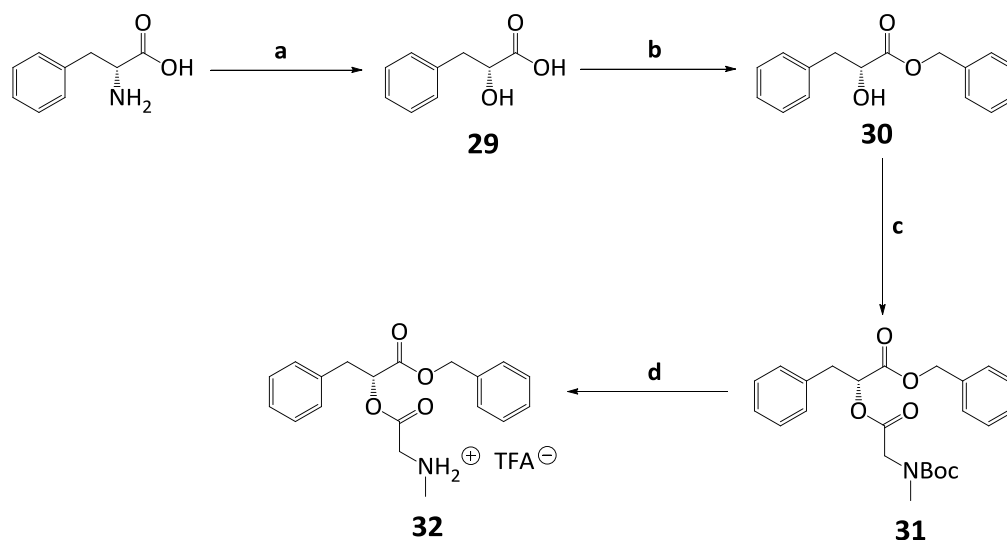
Figure 30: Synthetic pathway of the didepsipeptide precursor of hirsutellides.

Reagents and conditions: a) 40% NaNO$_2$, H$_2$SO$_4$, 36 h; b) BnOH, pTsOH, reflux, 4 h, toluene; c) EDC*HCl, DMAP, DCM, 0 °C to rt, 2 h; d) TFA, DCM, 0 °C to rt, 5 h, used directly in the next step.
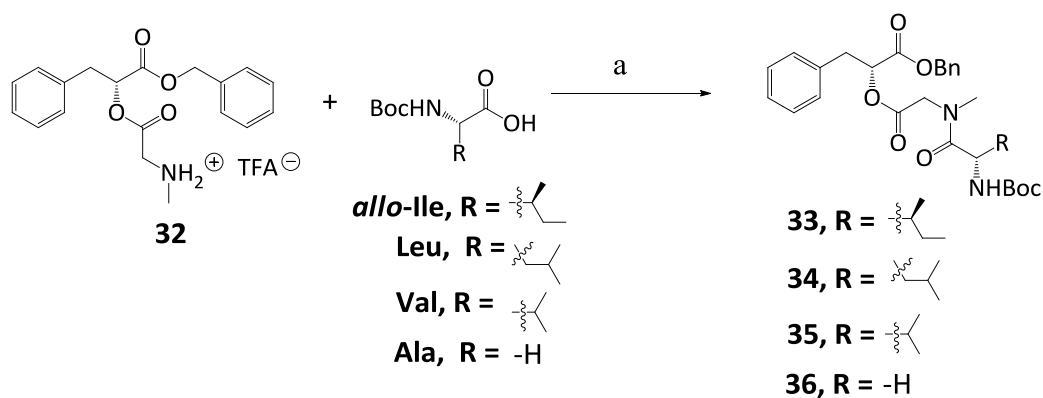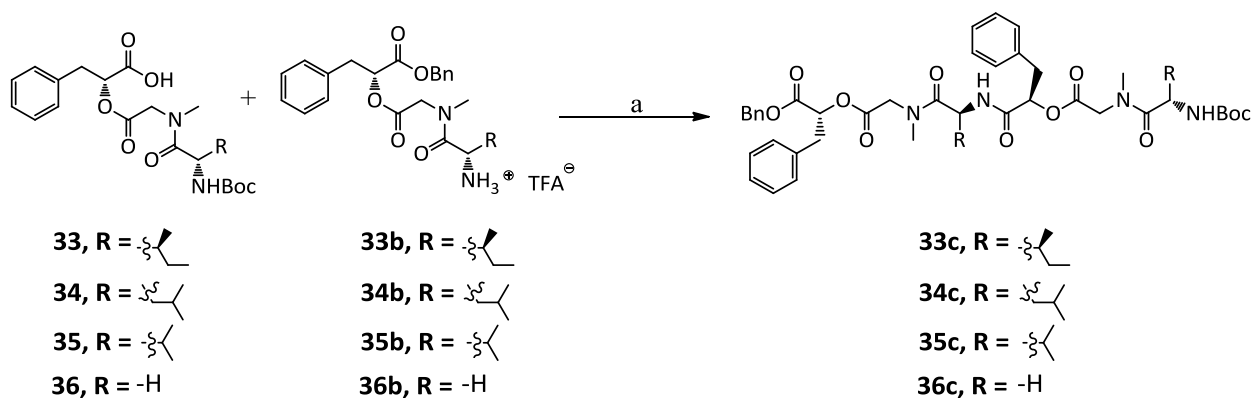

Figure 31: Synthetic pathway of the tridepsipeptide precursors of hirsutellides.

**Reagents and conditions:** a) HATU, TEA or DIPEA, DCM, 0 °C to rt, 12-24 h.

After purification, each of the tridepsipeptides was divided into two equal portions. The first portion was subjected to catalytic hydrogenation, using palladium/carbon (10%) as a catalyst, to remove the benzyl protecting group. This afforded compounds **33a-36a**. Similarly, the Boc protecting group of the second portion was removed by using TFA (6.5 eq.) and this yielded compounds **33b-36b** (Figure 32).
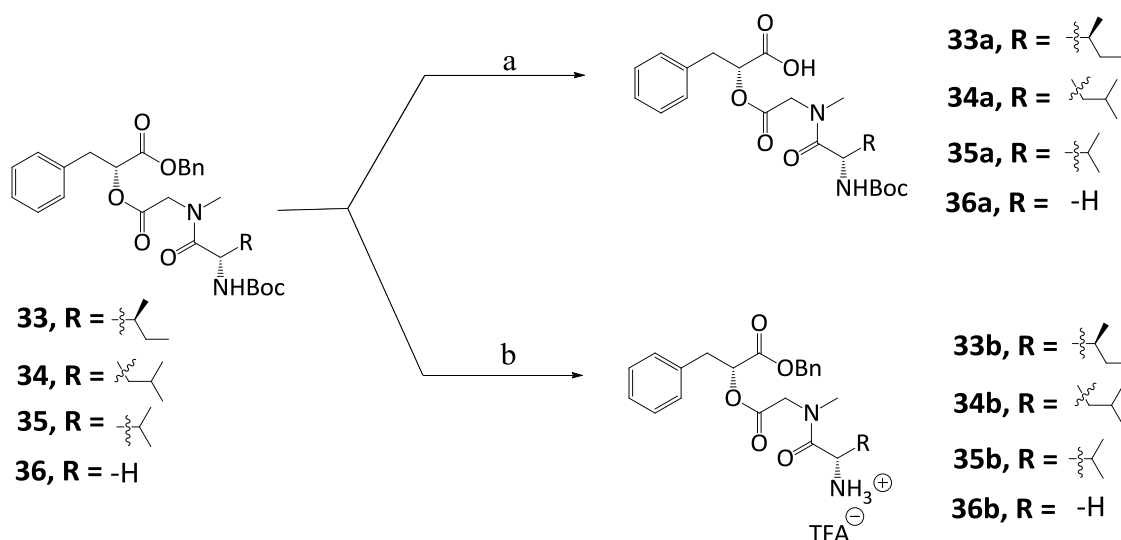
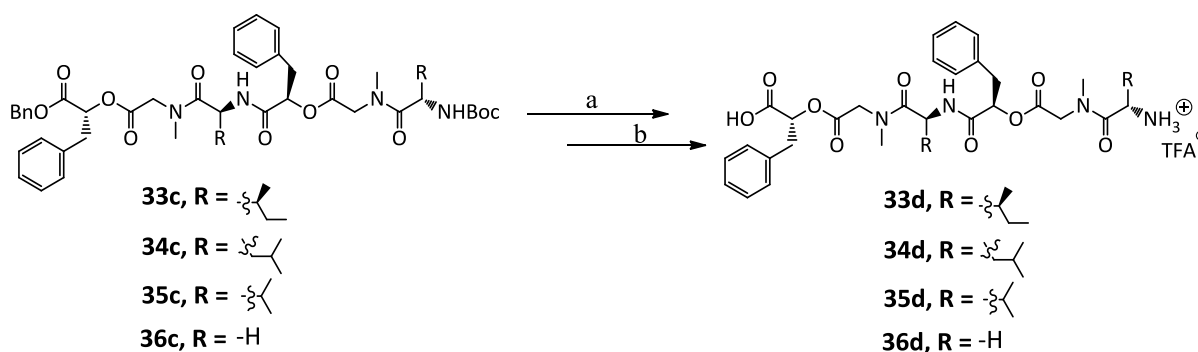**Figure 32:** Removal of the Bzl and Boc protecting groups from tridepsipeptide precursors.

Reagents and conditions: a) 10% Pd/C, H$_2$ (5 atm), EtOAc, rt, 12 h; b) TFA, DCM, 0 °C to rt, 5 h, used directly in the next step.

The syntheses of the linear hexadepsipeptides (**33c**-**36c**) were achieved through reactions that involved coupling of the two portions of tridepsipeptides (**33a-36a** and **33b-36b**). The coupling agent that best worked for the syntheses of these linear hexapeptides was BOP-Cl/DIPEA (Figure 33). The use of other coupling reagents such as HATU/DIPEA and PyBOP/DIPEA gave very little or no product[121].

The major side products of these reactions that were isolated during purification process were the corresponding diketopiperazines[178] and compound **30** (Figure 34). Formation of these side products appeared to occur when the free amine functions of **33b-36b** were released from their TFA salts upon addition of excess base, TEA/DIPEA. The efficiency of coupling with different coupling reagents seemed dependent on how fast the activated carbonyl group coupled to the freed amine. The fastest the reaction time is the lesser the formation of the side products. This could explain the difference in yields when using different types of coupling agents.

33, R = ⁙⟍ **33b, R =** ⁙⟍ **33c, R =** ⁙⟍

34, R = ⁙⟍⟨ **34b, R =** ⁙⟍⟨ **34c, R =** ⁙⟍⟨

35, R = ⁙⟨ **35b, R =** ⁙⟨ **35c, R =** ⁙⟨

36, R = -H **36b, R = -H** **36c, R = -H**

Figure 33: Synthetic pathway of the linear hexadepsipeptide precursors of hirsutellides.

Reagents and conditions: a) BOP-Cl, DIPEA, DCM, 0 °C to rt, 18-24 h.
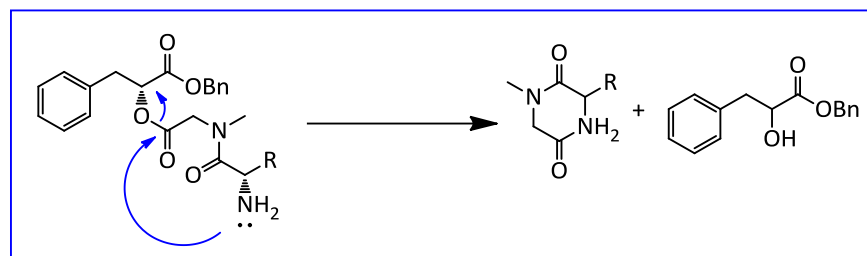
Figure 34: Competing side reactions (diketopiperazine formation) during synthesis of the fully protected linear hexadepsipeptides.

Subsequent reductive removal of the benzyl group and cleavage of the Boc group from compounds **33c**-**36c** led to the corresponding carboxylic acid amine TFA salts **33d-36d** (Figure 35).

Figure 35: Removal of the Bzl and Boc protecting groups from the linear hexadepsipeptide precursors.

Reagents and conditions: a) 10% Pd/C, H$_2$ (5 atm), EtOAc, rt, 24 h; b) TFA, DCM, 0 °C to rt, 8 h, used directly for the cyclization.

Finally, the desired cyclic depsipeptides (**33e-36e**) were obtained by macrocyclization of the linear hexadepsipeptides (**33d-36d**) using HATU/HOBt/DIPEA in DMF under highly diluted condition (1 mM) (Figure 36). Yield of the cyclization ranged from 25 to 50%.
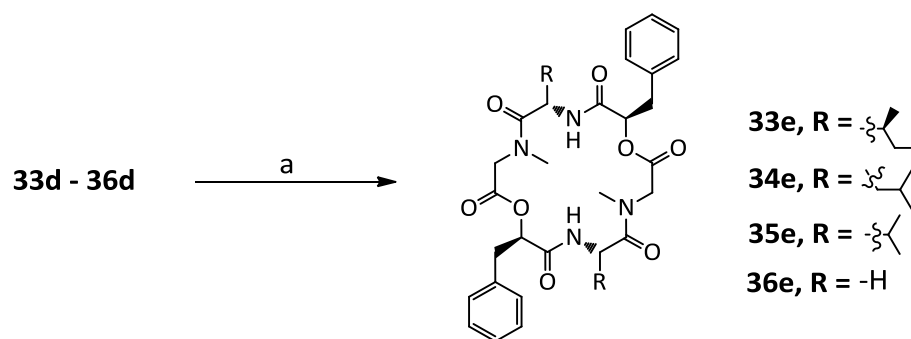
Figure 36: Macrocyclization of the linear hexadepsipeptide precursors of hirsutellides.

Reagents and conditions: a) HATU, HOBt, DIPEA, DMF, 0 °C to rt, 3 days.

Purification of all the final compounds was done by column chromatography using silica gel as a stationary phase and a mobile phase composed of EtOAc/heptane in different proportions. The structures of all compounds were verified using a combination of ESI-MS and NMR spectroscopy and purities were asserted by an independent QC unit GSK/ Stevenage using UPLC-MS and found to be more than 95% pure. The detailed procedures used to synthesize the individual compounds are described in the experimental part.

5.1.2. Synthesis of depsipeptide hirsutellide A analogues using SPPS

As an alternative to the lengthy solution phase synthetic approach, a procedure was developed to synthesize linear hexadepsipeptide precursors of hirsutellide A analogues using an SPPS approach. At the first trial, it was possible to synthesize one non-methylated linear hexadepsipeptide precursor (**37a**) which was used for the synthesis of compound **37b** (Figure 37).

The approach that was utilized for the preparation of the linear hexadepsipeptide **37a** was basically similar with what was discussed for wollamides in section 4.1 with only few modifications.

After loading of the first amino acid Fmoc-Gly-OH to the 2-CT resin, removal of the Fmoc protecting group was done using 20% piperidine/DMF (v/v). Following this, the second amino acid Fmoc-Ile-OH was coupled using HATU/DIPEA in NMP. HATU/DIPEA mediated coupling was repeated for the third building block, (R)-2-hydroxy-3-phenylpropanoic acid and this was achieved without protecting the free hydroxyl group. The depsipeptide (ester) bond formation was undertaken using EDC*HCl/DMAP as a coupling agent in DCM. This procedure was done for three hours and repeated twice to maximize the yield. Attempted ester formation with HATU/DIPEA yielded no product. Cleavage of the formed depsipeptide from the resin after the last coupling reaction was done using 3% TFA in DCM (Figure 38).

Finally, cyclization of the formed linear hexadepsipeptide **37a** to **37b** was achieved through lactonization using 2-methyl-6-nitrobenzoic anhydride (Shiina's reagent)/DMAP as a coupling agent in DMF[179]. The yield of the cyclization was found to be 43%.
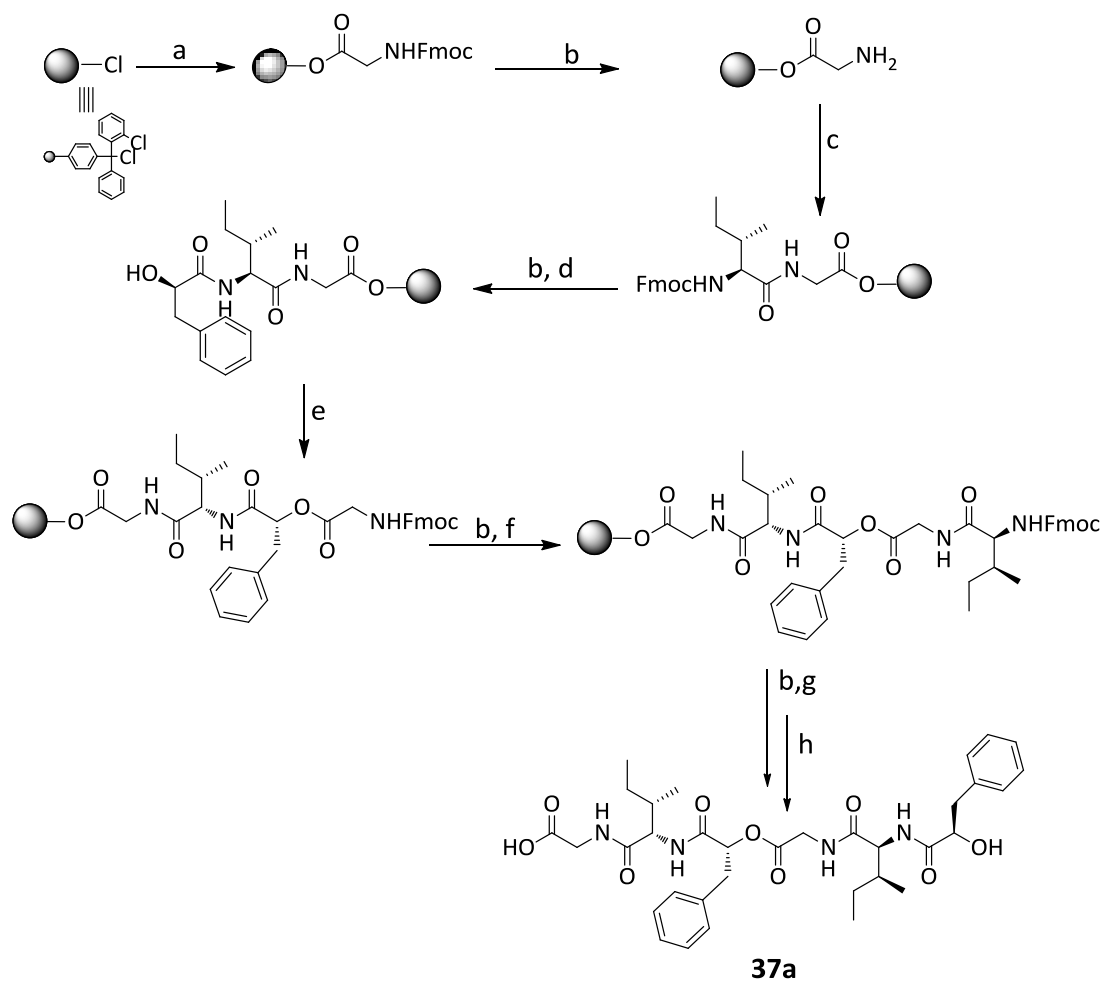
Figure 37: Synthesis of the depsipeptide precursor of **37b** *via* standard Fmoc-SPPS method.

Reagents and conditions: a)Fmoc-Gly-OH (1.2 eq.), DIPEA (2.5 eq.), DCM, 2 h; b) 20% Piperidine in DMF, 2X 10 min; c) Fmoc-Ile-OH (3 eq.), HATU (3 eq.), DIPEA (6 eq.), NMP, 1 h; d) (R)-2-hydroxy-3-phenylpropanoi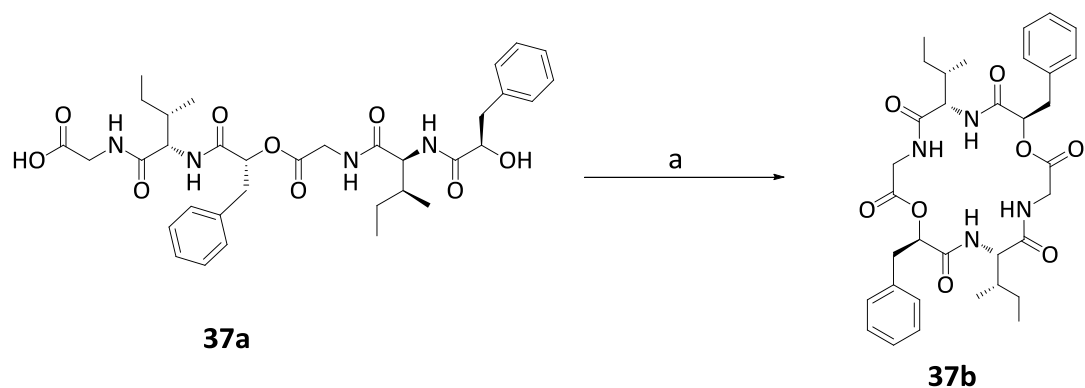c acid (3 eq.), HATU (3 eq.), DIPEA (6 eq.), NMP, 1 h; e) Fmoc-Gly-OH (3 eq.), EDC*HCl (3 eq.), DMAP (0.1 eq.), 2X3 h; f) Fmoc-Ile-OH (3 eq.), HATU (3 eq.), DIPEA (6 eq.), NMP, 1 h; g) (R)-2-hydroxy-3-phenylpropanoic acid (3 eq.), HATU (3 eq.), DIPEA (6 eq.), NMP, 1 h; h) 3% TFA in DCM, 2 h.

Figure 38: Macrocyclization of the linear hexadepsipeptide **37a** to **37b.**

Reagents and conditions: a) MNBA, DMAP, DCM, rt, 24 h.

Though the SPPS approach was found to be very simple and economical compared to the solution phase approach, it was not possible to apply it to the synthesis of the N,N-dimethylated hexadepsipeptide precursors. The major challenge was a very high level of diketopiperazine formation which rendered the formation of the final product totally impossible[180]. Though not as severe as the SPPS, diketopiperazine formation was also a problem in a solution phase synthesis (see section 5.1.1). To monitor the success of each coupling during SPPS, ESI-MS analysis of the formed (depsi)peptide was done by cleaving it from a portion of the resin. The result of the ESI-MS analysis showed that the required product was built till the pentadepsipeptide level (as shown in Figure 39). However, after coupling the last amino acid, the spectra showed only the formation of the tridepsipeptide. This happened because of the formation of a very stable diketopiperazine side product. The diketopiperazine was formed immediately when the amino function of the fifth amino acid was freed through the removal of its Fmoc protecting group (before coupling of the last amino acid).
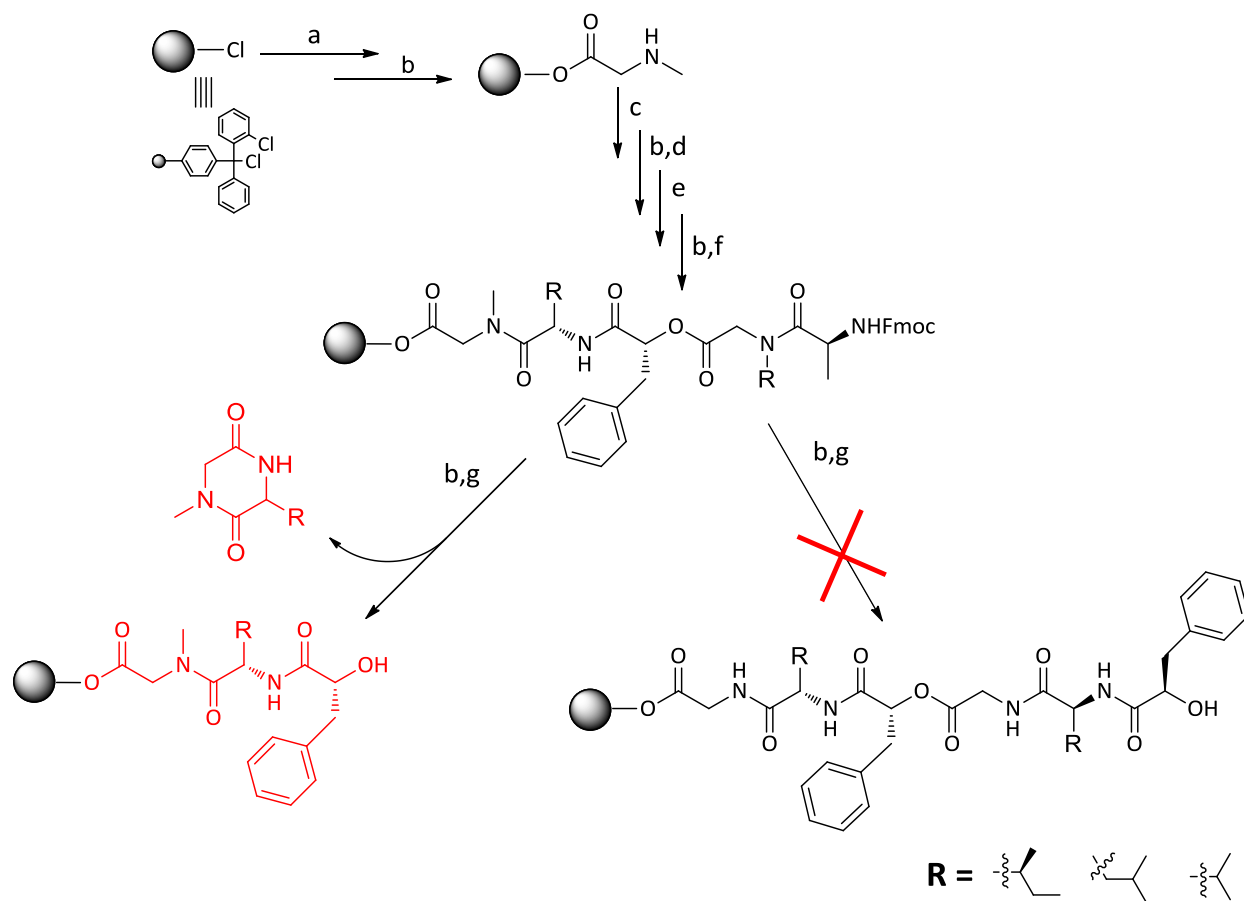
Figure 39: Synthesis of the N,N-dimethylated depsipeptide precursor of hirsutellides *via* standard Fmoc-SPPS method.

Reagents and conditions: a)Fmoc-Sar-OH (1.2 eq.), DIPEA (2.5 eq.), DCM, 2 h; b) 20% Piperidine in DMF, 2X 10 min; c) Fmoc-XX-OH (3 eq.), HATU (3 eq.), DIPEA (6 eq.), NMP, 1 h; d) (R)-2-hydroxy-3-phenylpropanoic acid (3 eq.), HATU (3 eq.), DIPEA (6 eq.), NMP, 1 h; e) Fmoc-Gly-OH (3 eq.), EDC*HCl (3 eq.), DMAP (0.1 eq.), 2X3 h; f) Fmoc-XX-OH (3 eq.), HATU (3 eq.), DIPEA (6 eq.), NMP, 1 h; g) (R)-2-hydroxy-3-phenylpropanoic acid (3 eq.), HATU (3 eq.), DIPEA (6 eq.), NMP, 1 h.

5.1.3. Synthesis of the peptide analogues of hirsutellide A

In addition to the depsipeptide analogues, some cyclic peptide analogues of hirsutellide A were synthesized as part of the SAR investigation. The syntheses of these analogues took place in two steps, (1) synthesis of the linear hexapeptide precursors (**38a-42a**) using Fmoc based SPPS approach using 2-chlorotrityl chloride resin followed by (2) cyclization in solution phase under high diluted condition (**38b-42b**). The reagents and reaction conditions utilized for the synthesis of both the linear precursors and cyclic peptides were similar to what was discussed for wollamides in section 4.1. The list of the synthesized cyclic peptide analogues are presented in Figure 40.

38b, R = H
39b, R = Cl
40b, R = OMe

41b

42b
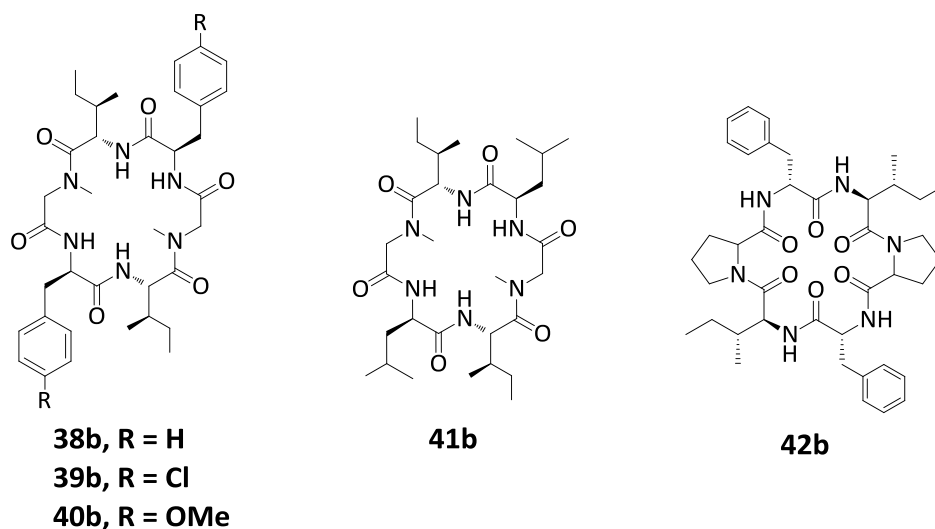
Figure 40: Structures of the synthesized cyclic peptide analogues of hirsutellide A.

5.2. *In vitro* microbiological and ADME profiling of hirsutellides

5.2.1. *In vitro* microbiological tests

Similar to what was done for wollamides, *in vitro* experiments were performed (section 4.3) to evaluate the antimycobacterial activities and cytotoxicities of the synthesized hirsutellides.

5.2.1.1. Agar diffusion test

Agar diffusion test was performed to evaluate the antimycobacterial activities of the synthesized analogues against non-pathogenic Mycobacterium species, namely *M. vaccae* and *M. smegmatis*. This test was done by placing the test compounds (100 µg/mL) into the wells of an agar plate that was previously inoculated with the test organism. The compounds were then allowed to diffuse into the agar and inhibit the growth of the test organisms. Finally after the end of the incubation, mean diameters of growth inhibition zones (ZoI) were recorded. The result of the testing is displayed in Table 16.

Among the tested compounds, four of them - including hirsutellide A (**33e**) - were found to exhibit activity against *M. vaccae* with a zone of inhibition that ranged from 12 to 15 mm. One of these four active compounds was **33c**, which is the fully protected linear hexadepsipeptide precursor of hirsutellide A. In addition to its activity against *M. vaccae*, compound **39b** (a peptide analogue of hirsutellide A) was also active against *M. smegmatis* and *M. aurum*.

5.2.1.2. Minimum inhibitory concentration (MIC)

In order to corroborate the result of the agar diffusion test, the MICs of the hirsutellides were determined against a standard drug susceptible *Mtb* H37Rv. This was done at the Open Lab facility of GlaxoSmithKline (GSK), Tres Cantos (Spain). Similarly, MICs determinations were carried out for compounds that showed activity against *M. vaccae* on agar diffusion assay at Microbial Resource Collection, Leibniz-Institut für Naturstoff-Forschung und Infektionsbiologie - Hans-Knöll-Institut, Jena, (Germany). The determined MICs together with a cytotoxicity study against human hepatocellular carcinoma cells (HepG2) are displayed in Table 17.

Table 16: *In vitro* antimicrobial activities of hirsutellide A and its synthetic analogues using an agar diffusion assay.

Compound no.	Zone of inhibition at 100 µg/mL (mm)		
	M. smegmatis SG987	*M. vaccae 10670*	*M. aurum SB66*
33c	0	15	0
33e	0	13	0
34e	0	12	0
35e	0	0	0
36e	0	0	0
37b	0	0	0
38b	0	0	0
39b	14	12	15
40b	0	0	0
41b	0	0	0
42b	0	0	0
References			
Ciprofloxacin[a]	19	21	34
Solvent[b]	0	0	0

[a]Ciprofloxacin was tested at 5 µg/mL dose; [b]The solvent used for blank control was DMSO/methanol (1:1); nd, not determined.

The only hirsutellide that exhibited weak activity against *Mtb* H37Rv was **39b** (MIC = 40 µM). All the other compounds, including hirsutellide A, showed no activity against *Mtb* H37Rv at the maximum dose tested (80 µM). The result contradicted the reported antimycobacterial activity of the lead compound (MIC$_{Mtb\ H37Ra}$ = 6-12 µg/mL)[113]. On the other hand, hirsutellide A exhibited an activity against a nonpathogenic mycobacteria *M. vaccae* with an MIC of 12.5 µg/mL. This value was similar to the reported activity against *Mtb* H37Ra. Compound **39b** also showed activity against *M. vaccae* with an MIC value that was more or less similar to the one it showed against *Mtb* H37Rv (MIC = 50 µg/mL). However, the IC$_{50}$ of this compound (26 µM) against the human HepG2 cells was lower than its MIC value which makes the compound toxic at the amount that is needed to kill the bacteria.

The compound that exhibit the best antimycobacterial activity against *M. vaccae* among the series was compound **33c** (MIC = 3.25 µg/mL) which is a linear hexadepsipeptide precursor of hirsutellide A.

Table 17: *In vitro* antimycobacterial MICs and cytotoxicity of hirsutellides.

Compound no.	MICs		IC$_{50}$ against
	Mtb H37Rv (µM)	*M. vaccae* (µg/mL)	Hep2G Cells (µM)
33c	nd	3.25	>100
33e	>80	12.50	>100
34e	>80	nd	25
35e	>80	nd	>100
36e	>80	nd	>100
37b	>80	nd	>100
38b	>80	nd	>100
39b	40	50	26
40b	>80	nd	>100
41b	>80	nd	>100
42b	>80	nd	>100

nd= not determined

5.2.2. *In vitro* ADME profiling of hirsutellides

An *in-vitro* ADME profiling was done for selected hirsutellide analogues to evaluate their drug-likeness[155]. The selected compounds represented three chemical subtypes of hirsutellides; (1) N,N-dimethylated cyclic depsipeptides (**33e** and **34e**), (2) a non-methylated cyclic depsipeptide (**37b**) and (3) N,N-dimethylated cyclic peptides (**41b** and **42b**) The ADME profiling was performed based on the internal protocols of the Open Lab Foundation of GSK, Tres Cantos (Spain) (section 8.6) and included the study of their physicochemical properties, plasma stabilities and liver microsomal stabilities. The results of the study are presented in Tables 18-20.

The results generally revealed that both peptide and depsipeptide hirsutellide derivatives exhibited good membrane permeability (>200 nm/sec) and low serum albumin binding affinities. While the peptide derivatives showed good aqueous solubility, the depsipeptide analogues had moderate or low solubility.

Table 18: Physicochemical properties of some selected hirsutellides.

Compound	Solubility[a*] (µg/mL)	Permeability[b*] (nm/sec)	%HSA	Log D
33e	ND	280	88.02	4.43
36e	81	ND	54.70	2.46
37b	6	470	91.02	3.68
41b	≥184	ND	37.15	ND
42b	≥254	330	84.22	ND

[a]Refers to kinetic aqueous solubility determined by chemiluminescent nitrogen detection (CLND); [b]refers to passive artificial membrane permeability; HSA, human serum albumin binding; nd, not determined. *GSK cut-off values for solubility: > 100 µg/mL, high solubility; 30-100 µg/mL, intermediate solubility; <30 µg/mL, low solubility. *GSK cut-off values for permeability: > 200 nm/sec, high permeability; 10-200 nm/sec, intermediate permeability; <10 µg/mL, low permeability.

All depsipeptide analogues were extremely unstable in mouse plasma (< 20%) but they exhibited good stability in human plasma (> 70%). The plasma stability of the peptide analogues was higher in both human and mouse plasma (> 85%).

Table 19: *In vitro* determined plasma stabilities of the synthesized hirsutellides.

Compound	Plasma stability (% remaining)*	
	Human	Mouse
33e	103	18.4
36e	67	0
37b	82	0
41b	90	88
42b	110	100

*Estimated by quantifying the amount of a compound remaining after incubation with plasma for 2 h at 37 °C.

All peptide and depsipeptide analogues of hirsutellide A were found to be highly unstable when *in vitro* metabolic stability was determined by incubating them in isolated human and mouse liver microsomes. The predicted *in vivo* clearance of all the compounds, in both species, was very fast (% LBF >3/4).

The *in vitro* ADME profiles of the selected compounds in relation to their structural features and antimycobacterial activities will be discussed in depth in section 5.3.

Table 20: *In vitro* determined and predicted *in vivo* microsomal stabilities of some hirsutellides.

Compound	CL_{int} (mL/min/g tissue)		CL_{pred} (mL/min/kg)		% LBF	
	Mouse	**Human**	**Mouse**	**Human**	**Mouse**	**Human**
33e	38.30	46.53	118.37	17.72	93.94	98.45
36e	52.00	34.00	120.29	17.62	95.46	97.88
37b	65.9	32.8	121.45	17.61	96.39	97.81
41b	5.79	6.07	88.32	16.06	70.10	89.20
42b	8.83	7.14	98.46	16.32	78.14	90.67

Cl_{int}, intrinsic microsomal clearance; CL_{pred}, predicted metabolic clearance; LBF, liver blood flow; nd, not determined; GSK cut-off values for % LBF: > ¾, high clearance; between 1/3 and ¾, intermediate clearance; <1/3, low clearance.

5.3. Discussion

5.3.1. The lead compound, hirsutellide A

The first attempt to synthesize hirsutellide A (**33e**) was reported in 2005 by Xu, Y. *et al*[121]. However, though they devised and followed a seemingly appropriate synthetic approach it was not successful. They rather ended up by synthesizing one of its stereoisomers[181]. This happened because they used a wrong building block (i.e. Ile instead of *allo*-Ile) during the construction of the fully protected tridepsipeptide (Figure 31). However, following the reported synthetic methodology, we were able to synthesize the lead compound (**33e**) for the first time. The physical properties and spectral data of the synthesized compound were similar with to what was described for the isolated natural product.

The antimycobacterial activity of **33e,** described in section 5.2.1.2, did not corroborate what was previously reported for the natural product. The likely reason for the discrepancy lies in the difference in the mycobacterial strains used. While the natural product was tested against the attenuated forms of *Mtb* (H37Ra), the synthesized hirsutellide A (**33e**) was tested against the virulent strain of *Mtb* (H37Rv). The fact that hirsutellide A was only active against the nonpathogenic (*M. vaccae*) and non-virulent (*Mtb* H37Ra) forms of Mycobacterium may indicate the ability of the virulent strain either to inactivate it quickly or remain totally unsusceptible towards to **33e**.

In vitro ADME profiling study done on **33e** has revealed some desirable features of the lead such as very good stability in human plasma (100% remained after 2 h incubation), very good permeability in artificial membrane (280 nm/sec) and low serum albumin binding affinity (88%). However, the microsomal stability of the compound was extremely low. Its predicted *in vivo* clearance was almost similar to the species liver blood flow (% LBF > 95%). In addition, **33e** exhibited very little stability in mouse plasma. The different stability profiles of the compound in human and mouse plasma indicates the difference in the susceptibility of the depsipeptide bonds of **33e** against various types of plasma esterases found in the two species.

5.3.2. Hirsutellide A analogues

5.3.2.1. Depsipeptide analogues

The design of the analogues (**34e-36e** and **37b**) focused on studying the effect of replacing the two *allo*-Ile moieties (Figure 41). This was based on the result obtained from testing the activity of one of the isomer synthesized previously through exchanging *allo*-Ile with Ile. This compound exhibited no significant antimycobacterial activity *in vitro* leading to the conclusion that the chiral center of 3'-C in hirsutellide A was one of the pivotal factors for the observed biological activity. To further evaluate this conclusion, compounds **34e-36e** (Figure 41) were synthesized through swapping the *allo*-Ile moieties with Leu, Val and Gly respectively. Compound **37b** was also synthesized through exchanging the *allo*-Ile for Ile and replacing the two Sar moieties with Gly.
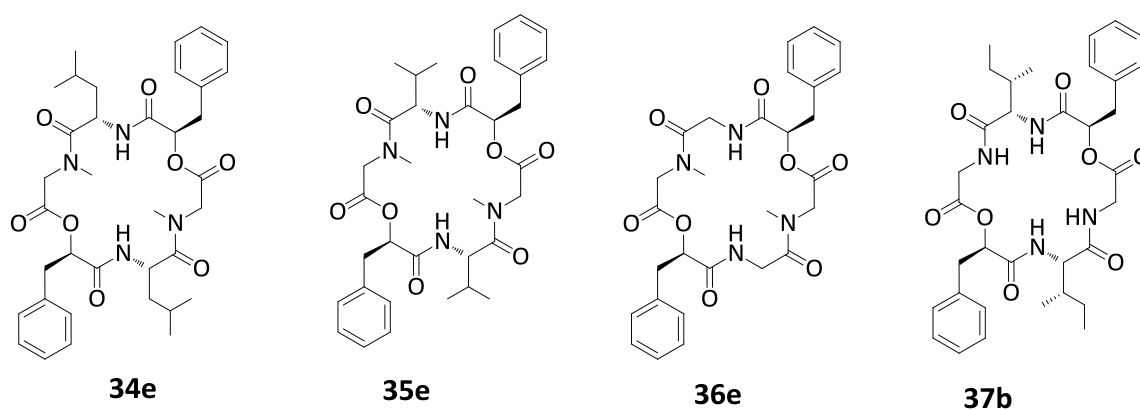
Figure 41: Synthesized depsipeptide analogues of hirsutellide A.

All of these compounds did not exhibit any activity against all tested Mycobacterium strains, proving the importance of the *allo*-Ile even for the observed weak activity of the lead compound against *M. vaccae*.

In vitro ADME profiling that was done for **36e** and **37b** showed that replacing the *allo*-Ile moiety with Gly caused a reduction in the lipophilicity, serum albumin binding affinity and plasma stability. Changing *allo*-Ile to Ile and Sar to Gly (**37b**) caused a significant improvement of permeability in artificial membrane (470 nm/sec) though its lipophilicity was diminished (Log D = 3.68). The metabolic stabilities of all the synthesized depsipeptide analogues were almost similar with the lead showing the poor metabolic stability of the class in general[182].

5.3.2.2. Peptide analogues

Hoping to improve the metabolic stability and potency of hirsutellide A, cyclic peptide analogues were synthesized (**38b-42b**). Based on the findings of the *allo*-Ile replacement, emphasis was given to study the effect of replacing other components of the lead, namely (R)-2-hydroxy-3-phenylpropanoic acid and Sar.

Compound **38b** was the peptide analogue of hirsutellide A that was synthesized through exchanging the (R)-2-hydroxy-3-phenylpropanoic acid moieties with D-Phe. Compounds **39b** and **40b** were synthesized by introducing D-Phe analogues whose phenyl side chains were blocked either with chlorine (**39b**) or methoxy group (**40b**) at the para position. This was done aiming at slowing down the metabolic clearances. Similarly, to investigate the importance of the aromatic side chains to the observed antimycobacterial activities, the two D-Phe were exchanged for aliphatic amino acid D-Leu (compound **41b**). The two Sar units of hirsutellide A were also replaced with Pro (**42b**) in order to evaluate the role of these amino acids.

Results of the antimycobacterial activity testing done for all the peptide analogues showed that all compounds - but **39b** - were inactive against the tested mycobacterial species (Tables 16 and 17). Compound **39b** showed weak activities against both the nonpathogenic (MIC$_{M.\ vaccae}$ = 50 µg/mL) and virulent (MIC$_{Mtb\ H37Rv}$ = 40 µM) mycobacterial species.

In vitro ADME profiling was carried out for two of the peptide analogues (**41b** and **42b**). Both compounds exhibited desirable physicochemical properties such as very good aqueous solubility (> 180 µg/mL) and low serum albumin binding. The determined membrane

permeability of **42b** was even higher (330 nm/sec) than the lead compound (280 nm/sec) which showed the possibility of improving the membrane permeability of cyclic hexapeptides without incorporating two ester groups. Like what was observed for wollamides, removal of the aromatic side chains significantly lowered the % albumin binding of **41b** (37%).

The other pharmacokinetic property that was improved through exchanging the two ester groups for amides was the mouse plasma stabilities. Both **41b** and **42b** exhibited much higher mouse plasma stabilities than the corresponding depsipeptide analogues (Table 19). However, the metabolic stabilities of both compounds were still poor (Table 20).

5.4. Conclusion

Following the synthetic route that was reported for the synthesis of one of its stereoisomers, the antimycobacterial cyclic hexadepsipeptide hirsutellide A was fully synthesized for the first time and its structure was verified using combinations of NMR and ESI-MS spectra. Side by side, other depsipeptide (**34e**-**36e** and **37b**) and peptide (**38b**-**42b**) analogues to hirsutellide A were synthesized in order to study its SAR. The antimycobacterial activities of all the compounds were tested against different mycobacterial species including *Mtb* H37Rv, *M.* vaccae, *M. smegmatis* and *M. aurum*.

The antimycobacterial activity testing against a virulent *Mtb* H37Rv strain showed that all the synthesized hirsutellides, except **39b,** were inactive at the maximum dose tested (80 µM). Compound **39b** showed weak activity with an MIC of 40 µM. The lead compound (**33e**) exhibited moderate activity against the nonpathogenic *M. vaccae* with an MIC (12.50 µg/mL) that was similar to the reported value against the attenuated Mycobacterium ($MIC_{MtbH37Ra}$ = 6-12 µg/mL). The result showed that hirsutellide A is only active against a nonpathogenic Mycobacterium.

In vitro ADME profiling that was done for some of the selected hirsutellides showed that the class in general has good stability in human plasma, good membrane permeability and lower albumin binding affinity. However, the determined microsomal stabilities of all the synthesized compounds were very little both in human and liver microsomes.

6. Summary

A rapid emergence and spread of multidrug resistant (MDR) mycobacterial strains is worsening the incumbent threat posed by tuberculosis (TB). To tackle the problem, there is a need to develop new anti TB drugs with novel mechanisms of action that are less vulnerable to the classical resistance mechanisms that microbes acquired to the currently used antibiotics. In this regard, antimicrobial (depsi)peptides offer good promise owing to their rapid bactericidal action, high affinity and selectivity to the prokaryotic cell envelope, different mode of action from conventional antimycobacterials and their proven record of use as a permanent host first line defense without the development of notable resistance.

The present work focused on exploring the anti TB potential of small cyclic (depsi)peptides by designing, synthesizing and evaluating their antimycobacterial activities. Two microbial antimycobacterial natural products served as leads. They represent two different chemical classes, viz. wollamides (cyclic hexapeptides) and hirsutellides (cyclic hexadepsipeptides).

The first part of the thesis set out from wollamide B (**1c**), a cationic antimycobacterial cyclohexapeptide that was isolated from Streptomyces nov. sp. (MST-115088) and reported to exert antimycobacterial activities against *M. bovis* (IC$_{50}$ of 3.1 µM). Aiming to define its structural activity relationship (SAR), optimizing potency and pharmacokinetic properties, libraries of analogues were synthesized following a standard Fmoc-based solid phase peptide synthesis approach. The antimycobacterial activities of wollamide B and all the synthesized analogues were tested against different Mycobacterium species namely, *Mtb* H37Rv, *M. vaccae* and *M. smegmatis*. Parallely, *in vitro* drug metabolism and pharmacokinetic (ADME) profiling was done for the synthesized compounds to evaluate their drug likeness. The result revealed the potent antimycobacterial activity of the lead against *Mtb* H37Rv (MIC=0.60 µM) and its druggability. From the outcome of the SAR investigation, it was also possible to figure out the features of the lead that could be changed in view of improved potency and pharmacokinetic properties. In addition, among the 27 synthesized wollamide B analogues six (**7c**, **8c**, **11c**, **14c**, **18c** and **22c**) showed potent activities against *Mtb* H37Rv with MICs $\leq$ 3.13 µM and found to be

nontoxic against human HepG2 cells up to 100 µM. The results of the *in vitro* ADME profiling also proved the drug likeness of the class in general with remarkable plasma stability, excellent aqueous solubility, and moderate to good metabolic stability. For some of the active compounds, an intracellular assay was performed against *Mtb H37Rv* infected human macrophages. The results were consistent with the *in vitro* extracellular MICs of these compounds. Compounds **8c** (MIC = 1.08 µM) and **22c** (MIC = 0.60 µM) that displayed a good balance of antimycobacterial activity and pharmacokinetic properties were also evaluated for their *in vivo* efficacy against *Mtb* H37Rv infected mice model at 5 mg/kg after a tolerability study. Both compounds were not effective at this low dose.

The second part of the thesis work focused on the development of hirsutellide A (**33e**), a cyclic hexadepsipeptide that was isolated from the fungus *Hirsutella kobayasii* BCC 1660. The reported MIC of the compound against *Mtb* H37Ra was 6–12 µg/mL. With the aim of defining its SAR and developing a more potent compound with enhanced pharmacokinetic properties, a series of depsipeptide and peptide analogues were synthesized and their *in vitro* antimycobacterial activities were tested against different mycobacterial species. *In vitro* ADME profiling of representative hirsutellides was also carried out. The results of antimycobacterial activity testing showed that all the synthesized hirsutellides, except **39b,** were inactive against *Mtb* H37Rv at the maximum dose tested (80 µM). The reported activity of hirsutellide A could not be reproduced in several assays. Compound **39b** showed weak activity with an MIC of 40 µM. Hirsutellide A only exhibited moderate activity against the nonpathogenic *M. vaccae* with an MIC (12.50 µg/mL) that was similar to the reported value against the attenuated Mycobacterium. *In vitro* ADME profiling of the selected hirsutellides showed that the class in general has good stability in human plasma, good membrane permeability and low albumin binding affinity. However, the microsomal stability of all hirsutellide analogues was poor both in human and mice liver microsomes.

7. Zusammenfassung

Das verstärkte Auftreten und die rasche Verbreitung multidrugresistenter (MDR) mykobakterieller Stämme vergrößert die durch Tuberkulose hervorgerufene Gefahr stetig. Zur Lösung dieses Problems werden dringend antituberkulöse Substanzen mit neuen Wirkmechanismen benötigt, die nicht durch bereits bestehende Resistenzen unbrauchbar sind. In dieser Hinsicht sind antimikrobielle (Depsi)peptide, die nachweislich eine große Rolle in der Immunantwort von Organismen spielen, eine vielversprechende Wirkstoffklasse. Diese zeichnet sich durch schnelle bakterizide Wirkung, hohe Affinität und Selektivität am prokaryotischen Zellapparat sowie einen alternativen Wirkmechanismus zu den konventionellen antimykobakteriellen Stoffen aus, ohne dass nennenswerte Resistenzen auftreten.

Die vorliegende Arbeit konzentrierte sich auf Design, Synthese und Wirksamkeitsbeurteilung kleiner cyclischer (Depsi)peptide. Zwei antimykobakterielle Naturstoffe aus Mikroorganismen dienten als Leitstrukturen. Sie stehen für zwei unterschiedliche chemische Klassen. Die nämlich Wollamide sind cyclische Hexapeptide; die Hirsutellide cyclische Hexadepsipeptide.

Wollamid B (**1c**), ein kationisches antimykobakterielles Cyclohexapeptid aus *Streptomyces nov. Sp.* (MST-115088) diente als Ausgangspunkt des ersten Teils der Arbeit. Von ihm wurde antimykobakterielle Aktivität gegen *M. bovis* mit einer IC_{50} von 3,1 µM berichtet. Um Struktur-Wirkungs-Beziehungen (SAR) zu erkunden und die Wirksamkeit sowie pharmakokinetische Eigenschaften zu verbessern, wurde eine Bibliothek von Substanzanaloga mittels Fmoc-basierter Festphasenmethode synthetisiert. Die antimykobakterielle Wirkung von Wollamid B und allen synthetisierten Analoga wurde gegen verschiedene Mykobakterienstämme getestet, namentlich *M. tuberculosis (Mtb)* H37Rv, *M. vaccae* und *M. smegmatis*. Im Hinblick auf die Eignung als Wirkstoff der *in-vitro*-Metabolismus und die pharmakokinetischen Eigenschaften (ADME) ermittelt. Die Leitverbindung erwies sich als stark wirksam gegen *Mtb* H37Rv (MHK = 0,6 µM) und sehr gut als Wirkstoff geeignet. Die SAR-Studie identifizierte die Positionen der Leitverbindung, welche zur Verbesserung der Wirkung und pharmakokinetischen Eigenschaften ausgetauscht werden können. Sechs der 27 synthetisierten Wollamidanaloga (**7c**, **8c**, **11c**, **14c**, **18c** und **22c**) zeigten gute Wirksamkeit gegen *Mtb* H37Rv (MHKs ≤ 3,1 µM) und waren bis zu

einer Konzentration von 100 µM nicht toxisch gegenüber humanen HepG2 Zellen. Die Resultate der *in vitro* ADME-Studie bewiesen ebenfalls die allgemeine Eignung der Wirkstoffklasse mit herausragender Plasmastabilität, exzellenter Wasserlöslichkeit und einer moderaten bis guten metabolischen Stabilität.

Mit einigen der aktiven Verbindungen wurde ein intrazellulärer Assay mit *Mtb* H37Rv infizierten humanen Makrophagen durchgeführt. Die Ergebnisse stimmten mit den MHKs überein, die durch extrazelluläre *in-vitro*-Assays gewonnen wurden. Nachdem eine Verträglichkeitsstudie durchgeführt worden war, wurden Substanz **8c** (MHK = 1,1 µM) und **22c** (MHK = 0,6 µM), die sowohl gute antimykobakterielle Wirksamkeit als auch gute pharmakokinetische Eigenschaften aufwiesen, auf ihre *in-vivo*-Wirksamkeit in Mäusen getestet, die mit *Mtb* H37Rv infiziert waren. Beide Substanzen waren bei der für diese Pilotstudie eingesetzten geringen Dosis von 5 mg/kg KG nicht wirksam.

Der zweite Teil der Arbeit befasste sich mit der Entwicklung von Hirsutellid A (**33e**), einem cyclischen Hexadepsipeptid, das aus dem Pilz *Hirsutella kobayasii* BCC 1660 isoliert wurde. Die publizierte Wirksamkeit des Stoffes gegen *Mtb* H37Ra lag bei 6 - 12 µg/mL. Mit dem Ziel, dessen SAR abzugrenzen, sowie eine wirksamere Substanz mit verbesserten pharmakokinetischen Eigenschaften zu entwickeln, wurde eine Serie von Depsipeptiden und Peptidanaloga synthetisiert und deren Wirksamkeit gegen verschiedene mykobakterielle Spezies *in vitro* getestet. Für ausgewählte Hirsutellidanaloga wurde außerdem das *in vitro* ADME-Profil erstellt. Die Ergebnisse der antimykobakteriellen Aktivitätstests zeigten, dass alle synthetisierten Hirsutellide, ausgenommen **39b**, bei der höchsten getesteten Konzentration von 80 µM gegen *Mtb* H37Rv inaktiv waren. Die publizierte Aktivität von Hirsutellid A konnte in mehreren Tests nicht bestätigt werden. Substanz **39b** zeigte eine schwache Aktivität (MHK = 40 µM). Hirsutellid A zeigte nur mäßige Aktivität gegen den nicht pathogenen Keim *M. vaccae* (MHK = 12,5 µg/mL), die dem publizierten Wert gegen das abgeschwächte Mykobakterium *Mtb* H37R**a** (MHK = 6 - 12 µg/mL) ähnlich war. Die *in vitro* ADME-Profile ausgewählter Wirkstoffklassenvertreter zeigten allgemein gute Stabilität in humanem Plasma, generell gute Membranpermeabilität sowie gemeinhin niedrige Albuminbindungsaffinitäten. Allerdings war

die mikrosomale Stabilität aller Hirsutellidanaloga sowohl in humanen als auch in murinen Lebermikrosomen gering.

8. Experimental

8.1. Materials and methods

8.1.1. General

All the chemicals and reagents used for synthesis and purification were purchased from a commercial source and used without further purification. A polypropylene syringe (Inject®, B.Braun Melsungen AG, Germany) fitted with a frits column plate was used for the solid phase synthesis of the linear hexapeptides. For a solution phase synthesis, a reaction progress was monitored by analytical TLC (Silica gel 60 F_{254}, Merk, Germany) and the purification of all the synthesized compounds were performed by a column chromatography using Silica gel 60 (0.063-0.200 mm, Merk) as a stationary phase. TLC plates were visualized by 254 nm UV light. Electrospray ionization mass spectra (ESI-MS) were acquired using SSQ 710 C mass Spektrometer, Finningen MAT GmbH, Bremen, Germany. NMR spectra were recorded on Bruker Varian Inova Unity 500 (operating frequency 300 or 500 MHz for ^{1}H-NMR and 101 or 126 MHz for ^{13}C-NMR), Kolthoff GmbH, Filsum, Germany. Proton and carbon chemical shifts are reported in ppm. ^{1}H NMR spectral data are reported as follows: chemical shift, multiplicity (s = singlet, d = doublet, t =triplet, q = quartet, m = multiplet, br = broad, ovlp = overlapping), coupling constant in Hz and integration.

Purity analysis of all the final target compounds was done by an independent QC team at GSK, Stevenage using UPLC-MS with UV diode array detection and MS used to confirm identity. ELSD was also used as an additional method of detection to confirm if there are nonechromophore impurities. Generally the purity of the synthesized final compounds was found $\geq$ 95%.

8.2. General procedure for solid phase peptide synthesis (SPPS)

8.2.1. General procedure for loading of 2-chlorotrityl chloride resin

The resin (1.0 g, 1.6 mmol/g loading capacity) was weighed, transferred to a syringe fitted with a filtering frit and was allowed to swell in dry DCM for 20 min while shaking on a mechanical shaker. The amino acid to be loaded (1.2 eq.) was separately dissolved in a vial with anhydrous DCM and well mixed with DIPEA (2.5 eq.). The solution was then transferred to the syringe and the loading was allowed to be taken place for 2 h. Following that, 1 mL distilled methanol was added to the contents of the syringe and continued to be shaken for additional 15 minutes to ensure the capping of remaining trityl chloride groups. The solvent and excess reactants were then filtered off from the syringe and the resin was thoroughly washed with DCM (5X), DCM/MeOH (1:1) (4X) and MeOH (2X). Finally, the resin was dried under vacuum pressure. Mass of the dried loaded resin was weighed and the loading efficiency was calculated from the increase in the mass of the loaded resin as follows.

$$loading(mmolg^{-1}) = \ (M_{total} - M_{resin}) \times 10^3)/(MW - 36.46) \times M_{total}$$

Where M_{total} = mass of the loaded resin, M_{resin} = mass of the unloaded resin, MW = molecular weight of the immobilized amino acid.

Generally, the loading efficiency was calculated to be in the range of 70-95%. A weighed amount of loaded resin mass that corresponds to 0.3 mmol of the loaded Fmoc-Xaa-OH was then used for the synthesis of each linear peptide.

8.2.2. General procedure for deblocking of Fmoc-protecting group

Removal of the Fmoc protecting group from the resin bound Fmoc peptide prior to coupling of the next amino acid was always achieved by treating the resin with a solution of 20% piperidine in DMF (v/v) for 10 minutes and this was repeated for the second time. The resin was washed with DMF (1X) between each deprotection step and after the final deprotection, the washing was done five times with DMF to make sure the complete removal of traces of piperidine.

8.2.3. General procedure for HATU mediated coupling of each amino acid

In 10 mL screw fitted vial, the Fmoc-Xaa-OH (3 eq.) and the coupling reagent HATU (3 eq.) were mixed and dissolved in NMP. DIPEA (6 eq.) was then added to the solution, well mixed by vortexing and the contents were transferred to a prewashed resin in a syringe. The peptide coupling was then allowed to taken place for 1h. Finally, the excess unreacted amino acid and other reagents were filtered-off from the syringe and resin was washed with DMF (4X) before proceeding to the next Fmoc cleavage.

8.2.4. General procedure for coupling to N-methylated peptide

A solution of Fmoc-Xaa-OH (3 eq.), HATU (3 eq.) and DIPEA (6 eq.) in NMP was added to the resin-bound N-methylamine peptide in the syringe and shaken for 2 h at room temperature. The excess unreacted amino acid and other reagents were filtered-off from the syringe and resin was washed with DMF (4X). The coupling was repeated for the second time.

8.2.5. General procedure for the formation of depsipeptide bond on a solid support

A solution of Fmoc-Xaa-OH (3 eq.), EDC*HCl (3 eq.) and DMAP (0.1 eq.) in DCM was added to the resin-bound N-methylamine peptide in the syringe and shaken for 3 h at room temperature. The excess unreacted amino acid and other reagents were filtered-off from the syringe and resin was washed with DMF (4X). The coupling was repeated for the second time.

8.2.6. General procedure for cleavage of the peptide from 2-chlorotrityl chloride resin

After the final Fmoc deprotection, the resin was washed with DMF (4X), dry DCM (2X) and allowed to swell in dry DCM for 20 min. A cleaving cocktail made of 20% HFIP in DCM (v/v) was then introduced into the syringe and the cleavage of the full-length hexapeptide was allowed to taken place for 1h. Following this, the filtrate was collected in already weighed round bottom

flask and the drained resin was further washed twice with DCM and all the washings were collected in the flask. Finally, the solvent was removed under vacuum and kept on the oil pump for prolonged period to exclude all the residual HFIP. The obtained solid mass was directly used for the next step without further purification.

8.3. General procedure for macrocyclization of the linear peptides

The linear hexapeptide prepared by SPPS approach was dissolved in DMF (1mM) and cooled to 0°C in an ice bath. To the solution was added HATU (3 equiv), and HOAt (3 equiv) under vigorous stirring. DIPEA (10 equiv) was then added to the dilute solution and the reaction mixture was allowed to warm slowly to the room temperature and kept stirring for 3 days. Following these, the solvent was removed under reduced pressure and the residue was dissolved in 40 mL saturated NaHCO$_3$ while stirring for about 10 minute. 20 mL of EtOAc was added to the mixture and stirred for further 5 minutes. The content was then transferred to a separatory funnel and the organic layer was collected. The aqueous phase was washed twice with 20 mL EtOAc. The combined EtOAc fraction was washed with brine, dried by anhydrous MgSO$_4$, filtered and concentrated under a reduced pressure. The obtained crude solid mass was purified by a column chromatography to give a pure cyclic hexapeptides whose reactive amino acid side chains were protected.

8.4. General procedure for deprotection of the reactive side chains protecting groups

The protecting groups from reactive amino acid side chains of the synthesized cyclic hexapeptides were removed with a cleaving cocktail made up of TFA/TIPS/H$_2$O (95:2.5/2.5/) for amino acids that contain Trt/Pbf protecting groups and with TFA/DCM (1:1) for amino acids containing Boc/tBu protecting group. The cleaving solution was then removed under a strong pressure and the residue was purified by column chromatography.

8.5. Synthetic protocols for individual compounds

8.5.1. Synthesis of wollamides

**Synthesis of H₂N-D-Leu-Val-Asn (Trt)-D-Orn (Boc)-Trp (Boc)-Leu-COOH (1a)**
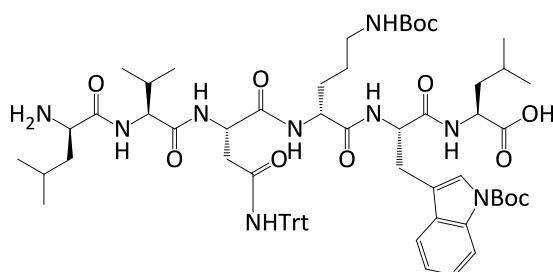
SPPS approach was used to prepare **1a** according to the general procedure described under section 8.2. The synthesis was initiated from a resin loaded with Fmoc-Leu-OH (0.43 g, 0.3 mmol). Crude % yield (87%), ESI-MS m/z calcd for $C_{66}H_{89}N_9O_{12}$:1199.66; found: 1200.47 $[M+H]^+$.

Synthesis of cyclo (Trp (Boc)-D-Orn (Boc)-Asn (Trt)-Val-D-Leu-Leu) (1b)
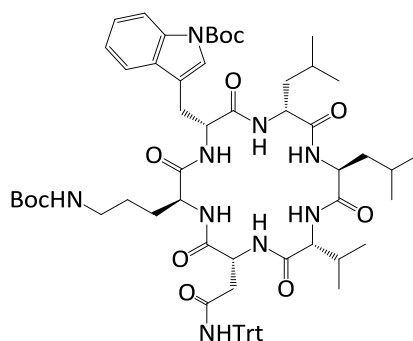
Compound **1b** was obtained through a macrocyclization of **1a** (0.2 g, 0.17 mmol) with HATU (0.19g, 0.51 mmol), HOBt (0.07 g, 0.51 mmol) and DIPEA (0.19 g, 1.7 mmol) according to the procedure described in section 8.3. The crude was purified by a column chromatography using a silica gel as a stationary phase and chloroform/methanol (49:1) as a mobile phase to give a white amorphous solid mass. Yield (68%), ESI-MS m/z calcd $C_{66}H_{87}N_9O_{11}$:1181.65; found: 1180.90 $[M-H]^-$. R_f = 0.23 in CHCl₃/MeOH (95:5).

**Synthesis of cyclo (Trp-D-Orn-Asn-Val-D-Leu-Leu) (1c)**
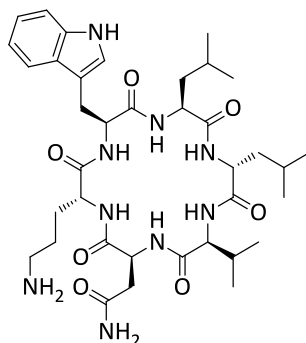
Compound **1b** (0.05 g, 0.05 mmol) was treated with 2 mL of TFA/TIPS/H$_2$O (95:2.5/2.5/) for 3 h. The cleaving solution was removed under a strong pressure and the residue was purified by column chromatography using a silica gel as a stationary phase and chloroform/methanol/ammonia solution (80:20:1) as a mobile phase to give a white amorphous solid mass. Yield (91%), mp 234-236 °C, UPLC-MS (UV) purity: 99.9%, RT:0.75 min, ESI-MS m/z calcd for C$_{37}$H$_{57}$N$_9$O$_7$: 739.44; found: 740.44 [M+H]$^+$. ^{1}H NMR (400 MHz, CD$_3$OD-d$_4$) δ 7.60 − 7.54 (m, 1H), 7.32 (dd, J = 8.0, 1.0 Hz, 1H), 7.13 (s, 1H), 7.12 − 7.06 (m, 1H), 7.01 (td, J = 7.4, 7.0, 1.0 Hz, 1H), 4.67 (dd, J = 6.0, 4.3 Hz, 1H), 4.57 (dd, J = 9.2, 5.1 Hz, 1H), 4.46 (dt, J = 17.3, 7.1 Hz, 2H), 4.37 (dd, J = 10.1, 4.8 Hz, 1H), 4.02 (d, J = 4.6 Hz, 1H), 3.25 (dd, J = 14.7, 5.1 Hz, 1H), 3.17 − 3.05 (m, 2H), 2.85 − 2.69 (m, 3H), 2.31 (pd, J = 6.9, 4.5 Hz, 1H), 1.89 − 1.78 (m, 1H), 1.71 (ddd, J = 14.1, 9.5, 4.7 Hz, 1H), 1.65 − 1.42 (m, 8H), 1.39 − 1.27 (m, 2H), 1.08 − 0.85 (m, 18H). ^{13}C NMR (126 MHz, CD$_3$OD-d$_4$) δ 175.09, 173.36, 172.61, 172.52, 172.33, 171.98, 171.97, 136.69, 127.07, 123.34, 121.11, 118.55, 117.96, 110.86, 109.19, 60.31, 55.93, 52.01, 51.89, 51.17, 50.01, 40.69, 39.48, 39.13, 35.67, 29.13, 27.17, 26.22, 24.67, 24.50, 24.42, 21.59, 21.57, 21.30, 21.07, 18.07, 16.54.

120

Synthesis of H$_2$N-D-Leu-Val-Asn (Trt)-D-Orn (Boc)-Trp (Boc)-Ala-COOH (2a)
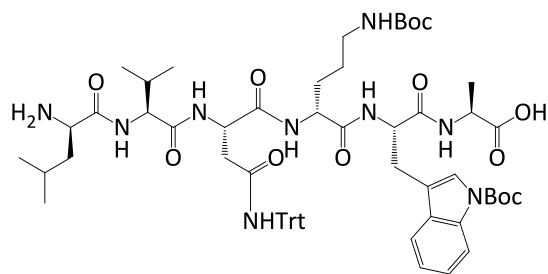

SPPS approach was used to prepare **2a** according to the general procedure described under section 8.2. The synthesis was initiated from a resin loaded with Fmoc-Ala-OH (0.28 g, 0.3 mmol). Crude % yield (97%), ESI-MS m/z calcd for C$_{63}$H$_{83}$N$_9$O$_{12}$: 1157.62; found: 1158.54 [M+H]$^+$.

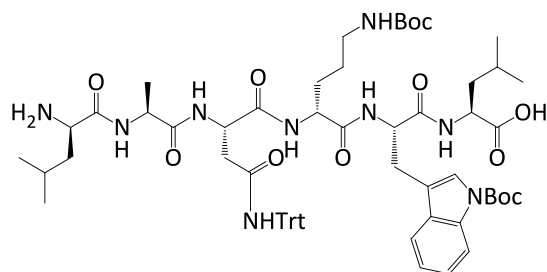**Synthesis of cyclo (Trp (Boc)-D-Orn (Boc)-Asn (Trt)-Val-D-Leu-Ala) (2b)**
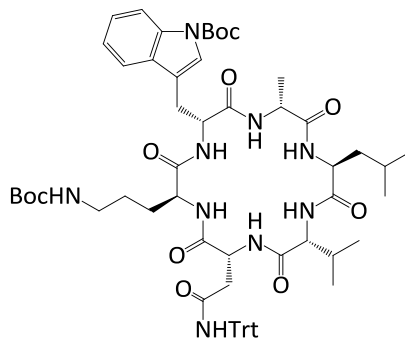
Compound 2b was obtained through a macrocyclization of **2a** (0.34 g, 0.3 mmol) with HATU (0.34 g, 0.9 mmol), HOBt (0.12 g, 0.9 mmol) and DIPEA (0.52 mL, 3.0 mmol) according to the procedure described in section 8.3. It was purified by a column chromatography using a silica gel as a stationary phase and chloroform/methanol (19:1) as a mobile phase to give a white amorphous solid mass. Yield (45%), ESI-MS m/z calcd for C$_{63}$H$_{81}$N$_9$O$_{11}$: 1139.61; found: 1162.59 [M+Na]$^+$. R$_f$ = 0.35 in CHCl$_3$/MeOH (95:5).

**Synthesis of cyclo (Trp-D-Orn-Asn-Val-D-Leu-Ala) (2c)**
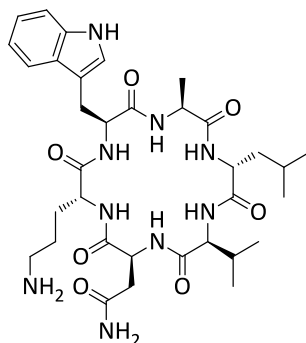
Compound 2b (0.08 g, 0.07 mmol) was treated with 1.5 mL of TFA/TIPS/H$_2$O (95:2.5/2.5/) for 3 h. The cleaving solution was removed under a strong pressure and the residue was purified by column chromatography using a silica gel as a stationary phase and chloroform/methanol/ammonia solution (80:20:1) as a mobile phase to give a white amorphous solid mass. Yield (80%), mp 230-232 °C, UPLC-MS (UV) purity: 98%, RT:0.64 min, ESI-MS m/z calcd for C$_{34}$H$_{51}$N$_9$O$_7$: 697.39; found: 698.39 [M+H]$^+$. ^{1}H NMR (500 MHz, CD$_3$OD-d$_4$) δ 7.56 (d, J = 7.9 Hz, 1H), 7.32 (d, J = 8.1 Hz, 1H), 7.14 (d, J = 2.4 Hz, 1H), 7.09 (t, J = 7.4 Hz, 1H), 7.01 (t, J = 7.6 Hz, 1H), 4.66 (t, J = 4.6 Hz, 1H), 4.58 − 4.44 (m, 3H), 4.38 (dd, J = 10.2, 4.9 Hz, 1H), 3.99 (dd, J = 4.9, 2.2 Hz, 1H), 3.25 (dd, J= 15.0, 4.5 Hz, 1H), 3.17 − 3.07 (m, 2H), 2.82 (dd, J = 17.0, 9.4 Hz, 2H), 2.71 − 2.63 (m, 1H), 2.33 − 2.21 (m, 1H), 1.83 (dt, J = 12.2, 7.0 Hz, 1H), 1.78 − 1.71 (m, 1H), 1.63 − 1.46 (m, 5H), 1.26 − 1.18 (m, 3H), 1.05 − 0.87 (m, 12H). ^{13}C NMR (126 MHz, CD$_3$OD-d$_4$) δ 175.13, 173.52, 172.72, 172.65, 172.21, 172.14, 172.01, 136.71, 127.06, 123.50, 121.15, 118.56, 117.95, 110.88, 108.93, 65.45, 60.68, 56.01, 51.70, 51.47, 49.85, 39.94, 38.80, 35.46, 29.07, 27.13, 25.79, 24.48, 23.30, 21.51, 21.27, 18.02, 16.78, 16.35.

**Synthesis of H₂N-ᴅ-Leu-Val-Asn (Trt)-ᴅ-Orn (Boc)-Ala-Leu-COOH (3a)**
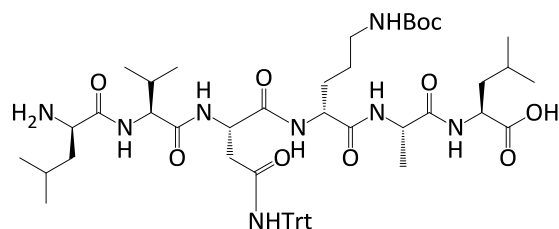
SPPS approach was used to prepare **3a** according to the general procedure described under section 8.2. The synthesis was initiated from a resin loaded with Fmoc-Leu-OH (0.34 g, 0.3 mmol). Crude % yield (103%), ESI-MS m/z calcd for $C_{53}H_{76}N_8O_{10}$: 984.57; found: 985.52 [M+H]$^+$.

Synthesis of cyclo (Ala-ᴅ-Orn (Boc)-Asn (Trt)-Val-ᴅ-Leu-Leu) (3b)
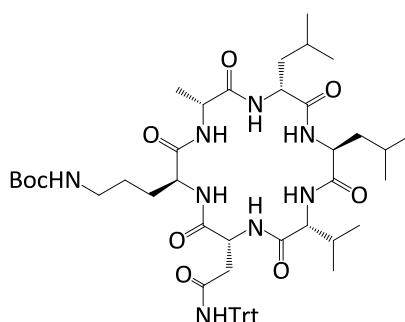
Compound **3b** was obtained through a macrocyclization of **3a** (0.36g, 0.37 mmol) with HATU (0.42g, 1.11 mmol), HOBt (0.15 g, 1.11 mmol) and DIPEA (0.65 mL, 3.7 mmol) according to the procedure described in section 8.3. It was purified by a column chromatography using a silica gel as a stationary phase and chloroform/methanol (19:1) as a mobile phase to give a white amorphous solid mass. Yield (43%), ESI-MS m/z calcd for $C_{53}H_{74}N_8O_9$: 966.56; found: 989.57 [M+Na]$^+$. R_f = 0.08 in CHCl₃/MeOH (95:5).

Synthesis of cyclo (Ala-D-Orn-Asn-Val-D-Leu-Leu) (3c)
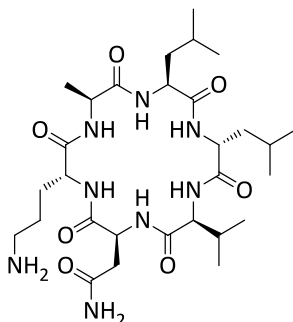
Compound **3b** (0.05 g, 0.05 mmol) was treated with 1.0 mL of TFA/TIPS/H$_2$O (95:2.5/2.5/) for 3 h. The cleaving solution was removed under a strong pressure and the residue was purified by column chromatography using a silica gel as a stationary phase and chloroform/methanol/ammonia solution (80:20:1) as a mobile phase to give a white amorphous solid mass. Yield (92%), mp 265-267 °C, UPLC-MS (UV) purity: 90%, RT:0.64 min, ESI-MS m/z calcd for C$_{29}$H$_{52}$N$_8$O$_7$: 624.40; found: 625.40 [M+H]$^+$. ^{1}H NMR (500 MHz, DMSO-d$_6$) δ 8.43 (d, J = 6.6 Hz, 1H), 8.29 − 8.16 (m, 2H), 7.93 (s, 1H), 7.74 (d, J = 7.0 Hz, 1H), 7.63 (s, 3H), 7.45 (d, J = 6.9 Hz, 2H), 7.24 (d, J = 8.2 Hz, 1H), 6.86 (s, 1H), 4.58 (d, J = 6.9 Hz, 2H), 4.39 (d, J = 7.7 Hz, 1H), 4.28 (d, J = 7.1 Hz, 1H), 4.20 (d, J = 7.5 Hz, 1H), 4.01 (dd, J = 7.3, 3.9 Hz, 2H), 2.76 (d, J = 8.5 Hz, 1H), 2.58 (d, J = 6.3 Hz, 2H), 2.23 (d, J = 9.4 Hz, 1H), 1.76 − 1.32 (m, 10H), 1.24 (d, J = 7.2 Hz, 3H), 0.86 (dt, J = 27.1, 6.2 Hz, 18H).

Synthesis of H₂N-D-Leu-Val-Ala-D-Orn (Boc)-Trp (Boc)-Leu-COOH (4a)
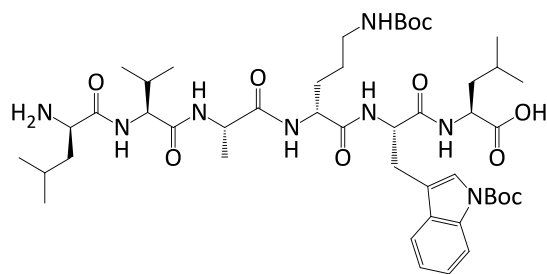
SPPS approach was used to prepare **4a** according to the general procedure described under section 8.2. The synthesis was initiated from a resin loaded with Fmoc-Leu-OH (0.34 g, 0.3 mmol). Crude % yield (99%), ESI-MS m/z calcd for $C_{46}H_{74}N_8O_{11}$: 914.55; found: 915.50 $[M+H]^+$.

**Synthesis of cyclo (Trp (Boc)-D-Orn (Boc)-Ala-Val-D-Leu-Leu) (4b)**
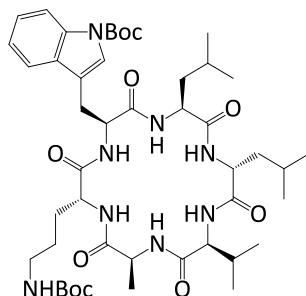
Compound **4b** was obtained through a macrocyclization of **4a** (0.27 g, 0.3 mmol) with HATU (0.34 g, 0.9 mmol), HOBt (0.12 g, 0.9 mmol) and DIPEA (0.52 mL, 3.0 mmol) according to the procedure described in section 8.3. It was purified by a column chromatography using a silica gel as a stationary phase and chloroform/methanol (19:1) as a mobile phase to give a white amorphous solid mass. Yield (56%), ESI-MS m/z calcd for $C_{46}H_{72}N_8O_{10}$: 896.54; found: 919.47 $[M+Na]^+$. R_f = 0.02 in CHCl₃/MeOH (96:4).

Synthesis of cyclo (Trp-D-Orn-Ala-Val-D-Leu-Leu) (4c)
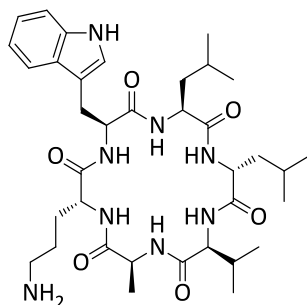
Compound **4b** (0.05 g, 0.06 mmol) was treated with 1.0 mL of TFA/TIPS/H$_2$O (95:2.5/2.5/) for 1 h. The cleaving solution was removed under a strong pressure and the residue was purified by column chromatography using a silica gel as a stationary phase and chloroform/methanol/ammonia solution (80:20:1) as a mobile phase to give a white amorphous solid mass. Yield (80%), mp 234-237 °C, UPLC-MS (UV) purity: 99.9%, RT:0.81 min, ESI-MS m/z calcd for C$_{36}$H$_{56}$N$_8$O$_6$: 696.43; found: 697.43[M+H]$^+$. ^{1}H NMR (500 MHz, CD$_3$OD-d$_4$) δ 7.56 (d, J = 7.9 Hz, 1H), 7.33 (d, J = 8.2 Hz, 1H), 7.19 (s, 1H), 7.09 (t, J = 7.7 Hz, 1H), 7.00 (t, J = 7.5 Hz, 1H), 4.51 (dd, J = 8.3, 4.4 Hz, 1H), 4.40 (q, J = 7.4 Hz, 2H), 4.29 (dt, J = 10.0, 4.7 Hz, 2H), 4.04 (d, J = 4.6 Hz, 1H), 3.18 (dd, J = 15.0, 8.3 Hz, 1H), 2.75 (dtt, J = 20.0, 13.1, 7.1 Hz, 3H), 2.30 (h, J = 6.5 Hz, 1H), 1.56 (dddd, J = 52.5, 31.1, 15.0, 7.7 Hz, 7H), 1.33 (dd, J = 24.0, 11.0 Hz, 6H), 1.01 – 0.74 (m, 18H). ^{13}C NMR (126 MHz, CD$_3$OD-d$_4$) δ 174.71, 173.35, 172.44, 172.15, 172.11, 171.95, 136.71, 127.17, 123.39, 121.28, 118.66, 118.12, 110.93, 108.95, 59.72, 55.10, 52.45, 52.18, 51.40, 48.96, 40.93, 39.29, 38.80, 29.00, 26.24, 26.13, 24.61, 24.41, 23.07, 21.56, 21.51, 21.33, 21.14, 18.22, 16.33, 16.29.

Synthesis of H₂N-D-Leu-Ala-Asn (Trt)-D-Orn (Boc)-Trp (Boc)-Leu-COOH (5a)


SPPS approach was used to prepare **5a** according to the general procedure described under section 8.2. The synthesis was initiated from a resin loaded with Fmoc-Leu-OH (0.34 g, 0.3 mmol). Crude % yield (86%), ESI-MS m/z calcd for $C_{64}H_{85}N_9O_{12}$: 1171.63; found: 1194.48 $[M+Na]^+$.

**Synthesis of cyclo (Trp (Boc)-D-Orn (Boc)-Asn (Trt)-Ala-D-Leu-Leu) (5b)**
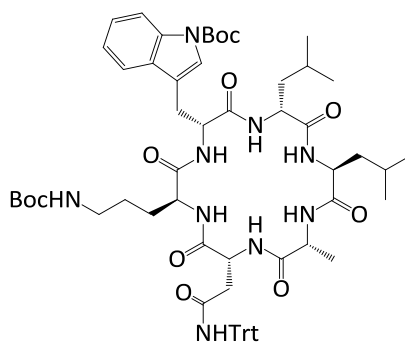
Compound **5b** was obtained through a macrocyclization of **5a** (0.3 g, 0.26 mmol) with HATU (0.3 g, 0.78 mmol), HOBt (0.11g, 0.78 mmol) and DIPEA (0.45 mL, 2.6 mmol) according to the procedure described in section 8.3. It was purified by a column chromatography using a silica gel as a stationary phase and chloroform/methanol (19:1) as a mobile phase to give a white amorphous solid mass. Yield (56%), ESI-MS m/z calcd for $C_{64}H_{83}N_9O_{11}$: 1153.62; found: 1176.57 $[M+Na]^+$. R_f = 0.29 in CHCl₃/MeOH (95:5).

Synthesis of cyclo (Trp-D-Orn-Asn-Ala-D-Leu-Leu) (5c)
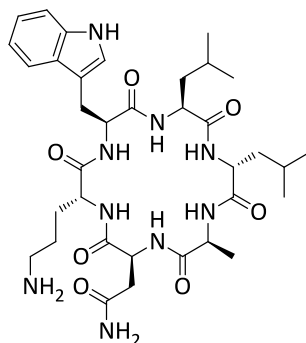
Compound **5b** (0.14 g, 0.12 mmol) was treated with 2.5 mL of TFA/TIPS/H$_2$O (95:2.5/2.5/) for 3 h. The cleaving solution was removed under a strong pressure and the residue was purified by column chromatography using a silica gel as a stationary phase and chloroform/methanol/ammonia solution (80:20:1) as a mobile phase to give a white amorphous solid mass. Yield (88%), mp 231-234 °C, UPLC-MS (UV) purity: 99.9%, RT:0.71 min, ESI-MS m/z calcd for C$_{35}$H$_{53}$N$_9$O$_7$: 711.41; found: 712.41[M+H]$^+$. ^{1}H NMR (400 MHz, CD$_3$OD-d$_4$) δ 7.57 (dq, J = 7.8, 1.1 Hz, 1H), 7.32 (dt, J = 8.1, 1.0 Hz, 1H), 7.13 (d, J = 6.0 Hz, 1H), 7.08 (ddd, J = 8.2, 7.0, 1.3 Hz, 1H), 7.01 (dddd, J = 8.0, 7.1, 2.4, 1.1 Hz, 1H), 4.70 – 4.61 (m, 1H), 4.57 (ddd, J = 9.0, 5.0, 3.8 Hz, 1H), 4.54 – 4.45 (m, 1H), 4.40 – 4.20 (m, 2H), 4.10 (q, J = 7.5 Hz, 1H), 3.29 – 3.20 (m, 1H), 3.18 – 2.96 (m, 3H), 2.81 – 2.64 (m, 2H), 1.88 – 1.79 (m, 1H), 1.76 – 1.25 (m, 12H), 1.03 – 0.79 (m, 12H). ^{13}C NMR (126 MHz, CD$_3$OD-d$_4$) δ 174.22, 173.60, 173.51, 172.65, 172.37, 172.25, 171.91, 136.69, 127.07, 123.40, 121.11, 118.55, 117.95, 110.88, 109.22, 55.74, 52.48, 51.97, 51.18, 50.66, 49.74, 40.50, 39.99, 39.52, 35.72, 27.21, 26.92, 26.53, 24.67, 24.52, 21.78, 21.63, 21.30, 20.85, 15.74.

**Synthesis of H$_2$N-D-Ala-Val-Asn (Trt)-D-Orn (Boc)-Trp (Boc)-Leu-COOH (6a)**
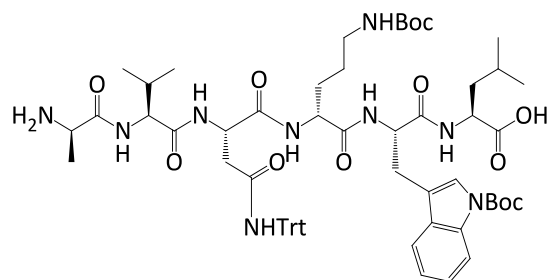
SPPS approach was used to prepare **6a** according to the general procedure described under section 8.2. The synthesis was initiated from a resin loaded with Fmoc-Leu-OH (0.43 g, 0.3 mmol). Crude % yield (72%), ESI-MS m/z calcd for C$_{63}$H$_{83}$N$_9$O$_{12}$: 1157.62; found: 1180.24 [M+Na]$^+$.

Synthesis of cyclo (Trp (Boc)-D-Orn (Boc)-Asn (Trt)-Val-D-Ala-Leu) (6b)
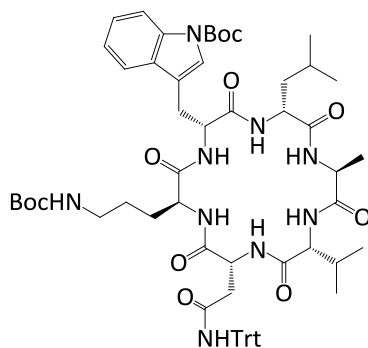
Compound **6b** was obtained through a macrocyclization of **6a** (0.23 g, 0.2 mmol) with HATU (0.23 g, 0.6 mmol), HOBt (0.08 g, 0.6 mmol) and DIPEA (0.35 mL, 2.0 mmol) according to the procedure described in section 8.3. It was purified by a column chromatography using a silica gel as a stationary phase and chloroform/methanol (97:3) as a mobile phase to give a white amorphous solid mass. Yield (64%), ESI-MS m/z calcd for C$_{63}$H$_{81}$N$_9$O$_{11}$: 1139.61; found: 1162.30 [M+Na]$^+$. R$_f$ = 0.09 in CHCl$_3$/MeOH (97:3).

**Synthesis of cyclo (Trp-D-Orn-Asn-Val-D-Ala-Leu) (6c)**
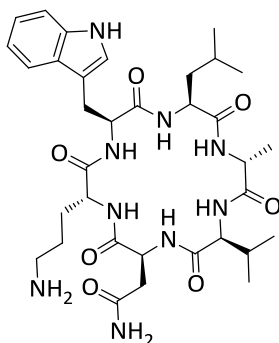
Compound **6c** (0.15 g, 0.13 mmol) was treated with 3.5 mL of TFA/TIPS/H$_2$O (95:2.5/2.5/) for 3 h. The cleaving solution was removed under a strong pressure and the residue was purified by column chromatography using a silica gel as a stationary phase and chloroform/methanol/ammonia solution (80:20:1) as a mobile phase to give a white amorphous solid mass. Yield (72%), mp 230-232 °C, UPLC-MS (UV) purity: 92%, RT:0.65 min, ESI-MS m/z calcd for C$_{34}$H$_{51}$N$_9$O$_7$: 697.39; found: 698.39[M+H]$^+$. ^{1}H NMR (400 MHz, CD$_3$OD-d$_4$) δ 7.57 (dt, J = 7.8, 1.0 Hz, 1H), 7.32 (dt, J = 8.1, 0.9 Hz, 1H), 7.13 (s, 1H), 7.08 (ddd, J = 8.1, 7.0, 1.2 Hz, 1H), 7.01 (ddd, J = 8.0, 7.0, 1.1 Hz, 1H), 4.69 (dd, J = 6.4, 4.6 Hz, 1H), 4.58 (dd, J = 9.1, 5.3 Hz, 1H), 4.47 − 4.34 (m, 3H), 4.03 − 3.95 (m, 1H), 3.29 − 3.22 (m, 1H), 3.12 (dd, J = 14.7, 9.1 Hz, 1H), 3.05 − 2.98 (m, 1H), 2.83 − 2.67 (m, 3H), 2.28 (pd, J = 7.0, 4.7 Hz, 1H), 1.83 (dddd, J = 14.2, 9.6, 6.8, 5.0 Hz, 1H), 1.68 (ddt, J = 14.2, 9.8, 4.8 Hz, 1H), 1.63 − 1.29 (m, 8H), 1.06 − 0.83 (m, 12H). ^{13}C NMR (101 MHz, CD$_3$OD-d$_4$) δ 175.64, 173.31, 172.60, 172.38, 172.32, 172.09, 171.74, 136.69, 127.07, 123.35, 121.11, 118.55, 117.95, 110.87, 109.14, 60.56, 55.92, 51.68, 51.19, 50.21, 49.07, 40.61, 38.82, 35.51, 29.22, 27.14, 26.22, 24.58, 23.49, 21.72, 21.19, 17.90, 16.61, 15.68.

**Synthesis of H$_2$N-D-Leu-*allo*-Ile-Asn (Trt)-D-Orn (Boc)-Trp (Boc)-Leu-COOH (7a)**
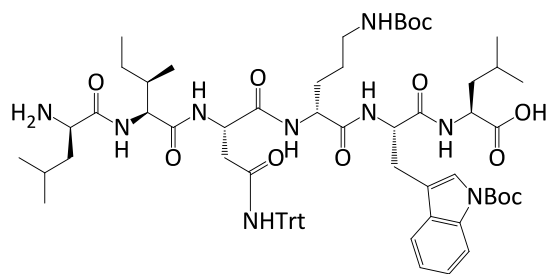
SPPS approach was used to prepare **7a** according to the general procedure described under section 8.2. The synthesis was initiated from a resin loaded with Fmoc-Leu-OH (0.43 g, 0.3 mmol). Crude % yield (91%), ESI-MS m/z calcd for C$_{67}$H$_{91}$N$_9$O$_{12}$: 1213.68; found: 1236.27 [M+Na]$^+$.

Synthesis of cyclo (Trp (Boc)-D-Orn (Boc)-Asn (Trt)-*allo*-Ile-D-Leu-Leu) (7b)
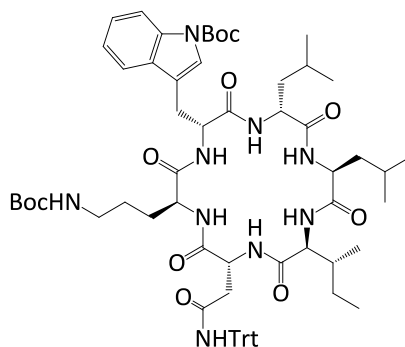
Compound **7b** was obtained through a macrocyclization of **7a** (0.4 g, 0.33 mmol) with HATU (0.38 g, 0.99 mmol), HOBt (0.13 g 0.99 mmol) and DIPEA (0.58 mL, 3.3 mmol) according to the procedure described in section 8.3. It was purified by a column chromatography using a silica gel as a stationary phase and chloroform/methanol (98:2) as a mobile phase to give a white amorphous solid mass. Yield (43%), ESI-MS m/z calcd for C$_{67}$H$_{89}$N$_9$O$_{11}$: 1195.67; found: 1218.32 [M+Na]$^+$. R$_f$ = 0.17 in CHCl$_3$/MeOH (98:2).

131

**Synthesis of cyclo (Trp-D-Orn-Asn-*allo*-Ile-D-Leu-Leu) (7c)**
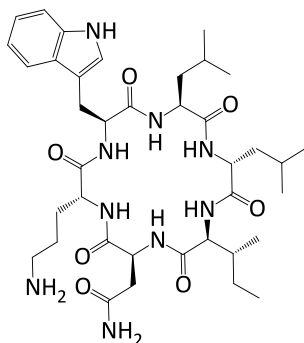
Compound **7b** (0.05 g, 0.04 mmol) was treated with 1.5 mL of TFA/TIPS/H$_2$O (95:2.5/2.5/) for 3 h. The cleaving solution was removed under a strong pressure and the residue was purified by column chromatography using a silica gel as a stationary phase and chloroform/methanol/ammonia solution (80:20:1) as a mobile phase to give a white amorphous solid mass. Yield (79%), mp 230-232 °C, UPLC-MS (UV) purity: 95%, RT:0.8 min, ESI-MS: m/z calcd for C$_{38}$H$_{59}$N$_9$O$_7$: 753.45; found: 754.45[M+H]$^+$. ^{1}H NMR (400 MHz, CD$_3$OD-d$_4$) δ 7.58 (dq, J = 8.0, 1.1 Hz, 1H), 7.32 (ddt, J = 8.1, 2.0, 0.9 Hz, 1H), 7.14 (d, J = 2.1 Hz, 1H), 7.12 − 7.04 (m, 1H), 7.01 (dddd, J = 8.0, 7.0, 2.5, 1.1 Hz, 1H), 4.78 − 4.70 (m, 1H), 4.58 (ddd, J = 9.5, 8.2, 4.6 Hz, 1H), 4.51 (dd, J = 7.7, 6.7 Hz, 1H), 4.42 (td, J = 7.4, 3.1 Hz, 1H), 4.31 − 4.20 (m, 2H), 3.18 − 3.02 (m, 2H), 2.94 (ddd, J = 18.8, 16.1, 6.2 Hz, 1H), 2.71 (dt, J = 16.0, 5.6 Hz, 1H), 2.61 − 2.47 (m, 2H), 2.10 (dtq, J = 11.0, 7.1, 3.5 Hz, 1H), 1.68 − 1.47 (m, 7H), 1.38 − 1.26 (m, 4H), 1.23 − 1.15 (m, 1H), 1.05 − 0.78 (m, 18H). ^{13}C NMR (101 MHz, CD$_3$OD-d$_4$) δ 174.80, 173.38, 172.58, 172.50, 172.48, 172.37, 171.66, 136.69, 127.10, 123.33, 121.09, 118.53, 117.99, 110.85, 109.35, 57.56, 55.56, 52.64, 52.07, 51.16, 49.88, 40.82, 40.05, 39.35, 36.13, 35.61, 27.09, 26.67, 25.90, 24.63, 24.49, 21.63, 21.49, 21.29, 21.16, 13.44, 10.64.

Synthesis of H₂N-D-Leu-Ile-Asn (Trt)-D-Orn (Boc)-Trp (Boc)-Leu-COOH (8a)
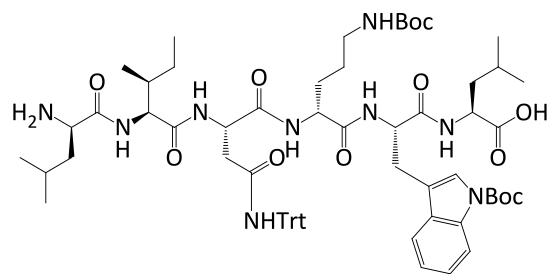

SPPS approach was used to prepare **8a** according to the general procedure described under section 8.2. The synthesis was initiated from a resin loaded with Fmoc- Leu-OH (0.43 g, 0.3 mmol). Crude yield (88%), ESI-MS m/z calcd for $C_{67}H_{91}N_9O_{12}$:1213.68; found: 1236.29 [M+Na]⁻.

Synthesis of cyclo (D-Leu-Ile-Asn (Trt)-D-Orn (Boc)-Trp (Boc)-Leu) (8b)
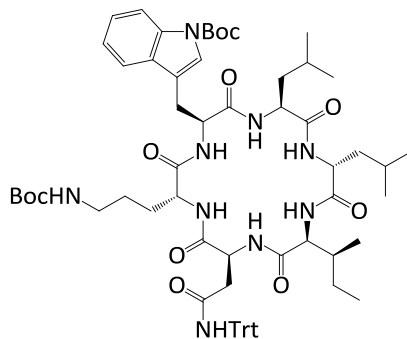
Compound **8b** was obtained through a macrocyclization of **8a** (0.32 g, 0.26 mmol) with HATU (0.3 g, 0.78 mmol), HOBt (0.11 g, 0.78 mmol) and DIPEA (0.45 mL, 2.6 mmol) according to the procedure described in section 8.3. The crude was purified by a column chromatography using a silica gel as a stationary phase and chloroform/methanol (49:1) as a mobile phase to give a white amorphous solid mass. Yield (52%), ESI-MS m/z calcd for $C_{66}H_{87}N_9O_{11}$:1195.67; found: 1194.49[M-H]⁻. R_f = 0.11 in CHCl₃/MeOH (49:1).

133

Synthesis of cyclo (D-Leu-Ile-Asn-D-Orn-Trp-Leu) (8c)
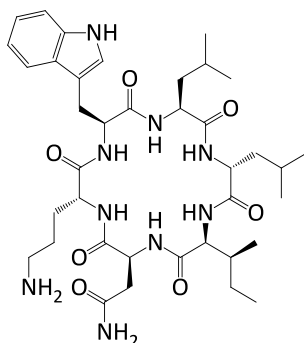

Compound **8b** (0.12 g, 0.1 mmol) was treated with 2.5 mL of TFA/TIPS/H$_2$O (95:2.5/2.5/) for 3 h. The cleaving solution was removed under a strong pressure and the residue was purified by column chromatography using a silica gel as a stationary phase and chloroform/methanol/ammonia solution (70:30:1) as a mobile phase to give a white amorphous solid mass. Yield (65%), mp 222-224 °C, UPLC-MS (UV) purity: 97%, RT:0.8 min, ESI-MS m/z calcd for C$_{38}$H$_{59}$N$_9$O$_7$: 753.45; found: 754.45 [M+H]$^+$. ^{1}H NMR (400 MHz, CD$_3$OD-d$_4$) δ 7.57 (dt, J = 7.8, 1.0 Hz, 1H), 7.32 (dt, J = 8.1, 0.9 Hz, 1H), 7.13 (s, 1H), 7.08 (ddd, J = 8.1, 7.0, 1.2 Hz, 1H), 7.01 (ddd, J = 8.0, 7.1, 1.1 Hz, 1H), 4.67 (dd, J = 6.0, 4.3 Hz, 1H), 4.56 (dd, J = 9.3, 5.1 Hz, 1H), 4.51 − 4.40 (m, 2H), 4.37 (dd, J = 10.0, 4.9 Hz, 1H), 4.07 (d, J = 4.5 Hz, 1H), 3.28 − 3.21 (m, 1H), 3.16 − 3.05 (m, 2H), 2.86 − 2.68 (m, 3H), 2.02 (ddt, J = 9.3, 6.9, 4.6 Hz, 1H), 1.87 − 1.80 (m, 1H), 1.72 − 1.44 (m, 8H), 1.36 − 1.28 (m, 3H), 1.03 − 0.83 (m, 18H). ^{13}C NMR (101 MHz, CD$_3$OD-d$_4$) δ 175.26, 173.35, 172.65, 172.49, 172.34, 172.13, 171.78, 136.70, 127.06, 123.34, 121.10, 118.56, 117.95, 110.85, 109.14, 59.72, 56.07, 52.01, 51.15, 50.04, 40.69, 39.52, 38.79, 35.97, 35.51, 27.23, 26.00, 24.69, 24.60, 24.52, 23.49, 22.32, 21.59, 21.57, 21.33, 21.03, 14.71, 10.76.

Synthesis of H$_2$N-D-Leu-Met-Asn (Trt)-D-Orn (Boc)-Trp (Boc)-Leu-COOH (9a)
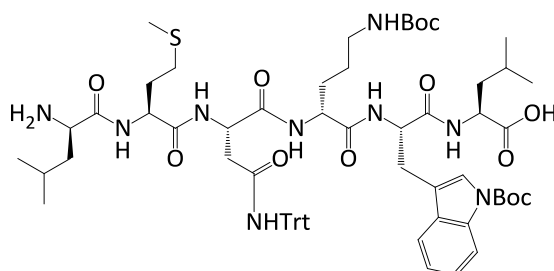

SPPS approach was used to prepare **9a** according to the general procedure described under section 8.2**.** The synthesis was initiated from a resin loaded with Fmoc-Leu-OH (0.31 g, 0.3 mmol). Crude yield (96%), ESI-MS m/z calcd for C$_{66}$H$_{89}$N$_9$O$_{12}$S: 1231.64; found: 1230.64 [M-H]$^-$.

**Synthesis of cyclo (D-Leu-Met-Asn (Trt)-D-Orn (Boc)-Trp (Boc)-Leu) (9b)**
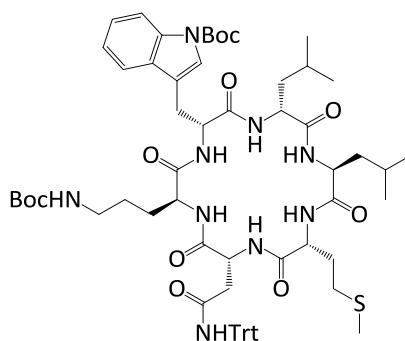
Compound **9b** was obtained through a macrocyclization of **9a** (0.36 g, 0.29 mmol) with HATU (0.33 g, 0.87 mmol), HOBt (0.12 g, 0.87 mmol) and DIPEA (0.51 mL, 2.9 mmol) according to the procedure described in section 8.3. The crude was purified by a column chromatography using a silica gel as a stationary phase and chloroform/methanol (49:1) as a mobile phase to give a white amorphous solid mass. Yield (40%), ESI-MS m/z calcd for C$_{66}$H$_{87}$N$_9$O$_{11}$S:1213.62; found: 1236.63 [M+Na]$^+$. R$_f$ = 0.1 in CHCl$_3$/MeOH (49:1).

Synthesis of cyclo (D-Leu–Met–Asn–D-Orn–Trp–Leu) (9c)
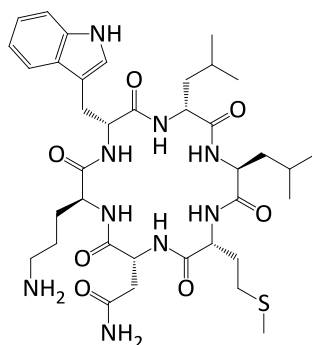
Compound **9b** (0.13 g, 0.11 mmol) was treated with 3 mL of TFA/TIPS/H$_2$O (95:2.5/2.5/) for 3 h. The cleaving solution was removed under a strong pressure and the residue was purified by column chromatography using a silica gel as a stationary phase and chloroform/methanol/ammonia solution (70:30:1) as a mobile phase to give a white amorphous solid mass. Yield (74%), mp 233-235 °C, UPLC-MS (UV) purity: 95%, RT:0.75 min, ESI-MS m/z calcd for C$_{37}$H$_{57}$N$_9$O$_7$S: 771.41; found: 772.41 [M+H]$^+$. ^{1}H NMR (400 MHz, CD$_3$OD-d$_4$) δ 7.58 (dt, *J* = 7.8, 1.0 Hz, 1H), 7.32 (dt, *J* = 8.1, 0.9 Hz, 1H), 7.12 (s, 1H), 7.08 (ddd, *J* = 8.2, 7.0, 1.2 Hz, 1H), 7.01 (ddd, *J* = 8.0, 7.0, 1.1 Hz, 1H), 4.69 (dd, *J* = 6.0, 4.5 Hz, 1H), 4.59 (dd, *J* = 9.3, 5.1 Hz, 1H), 4.49 (t, *J* = 7.1 Hz, 1H), 4.39 – 4.25 (m, 3H), 3.25 (ddd, *J* = 14.7, 5.2, 0.8 Hz, 1H), 3.16 – 3.04 (m, 2H), 2.85 – 2.71 (m, 3H), 2.65 (ddd, *J* = 13.0, 7.8, 4.9 Hz, 1H), 2.53 (ddd, *J* = 13.4, 8.3, 7.4 Hz, 1H), 2.19 (dtd, *J* = 14.3, 8.1, 4.3 Hz, 1H), 2.09 (s, 3H), 1.98 (dddd, *J* = 14.5, 9.8, 7.4, 4.9 Hz, 1H), 1.87 – 1.79 (m, 1H), 1.73 – 1.39 (m, 8H), 1.36 – 1.25 (m, 1H), 1.02 – 0.80 (m, 12H). ^{13}C NMR (126 MHz, CD$_3$OD-d$_4$) δ 175.03, 173.32, 173.12, 172.57, 172.51, 172.15, 171.56, 136.68, 127.09, 123.31, 121.08, 118.54, 117.97, 110.84, 109.23, 56.02, 53.54, 52.48, 51.55, 51.10, 50.10, 40.93, 39.48, 38.74, 35.42, 29.79, 29.68, 27.35, 25.94, 24.69, 24.52, 23.34, 21.53, 21.43, 21.16, 17.28, 15.85, 13.64.

Synthesis of H₂N-Asp (Bzl)-Asn (Trt)-D-Orn (Boc)-Trp (Boc)-Leu-D-Leu-COOH (10a)
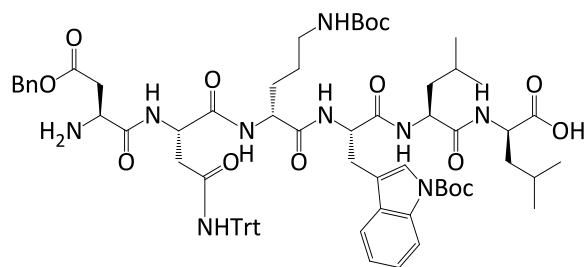
SPPS approach was used to prepare **10a** according to the general procedure described under section 8.2. The synthesis was initiated from a resin loaded with Fmoc-D-Leu-OH (0.52 g, 0.5 mmol). Crude % yield (72%), ESI-MS m/z calcd for $C_{72}H_{91}N_9O_{14}$:1305.67; found: 1328.21 $[M+Na]^+$.

Synthesis of cyclo(Asp (Bzl)-Asn (Trt)-D-Orn (Boc)-Trp (Boc)-Leu-D-Leu) (10b)
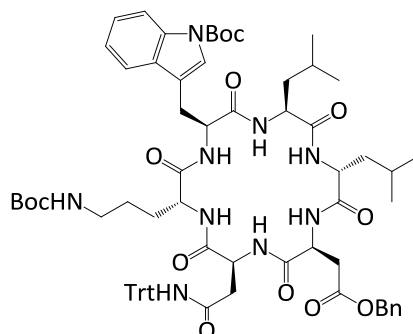
Compound **10b** was obtained through a macrocyclization of **10a** (0.4 g, 0.31 mmol) with HATU (0.35 g, 0.92 mmol), HOBt (0.12 g, 0.92 mmol) and DIPEA (0.54 mL, 3.1 mmol) according to the procedure described in section 8.3. The crude was purified by a column chromatography using a silica gel as a stationary phase and chloroform/methanol (49:1) as a mobile phase to give a white amorphous solid mass. Yield (40%), ESI-MS m/z calcd for $C_{72}H_{89}N_9O_{13}$: 1287.66; found: 1310.26 $[M+Na]^+$. R_f = 0.25 in CHCl₃/MeOH/NH₃ (97:3:1).

Synthesis of cyclo (Asp-Asn (Trt)-D-Orn (Boc)-Trp (Boc)-Leu-D-Leu) (10c)
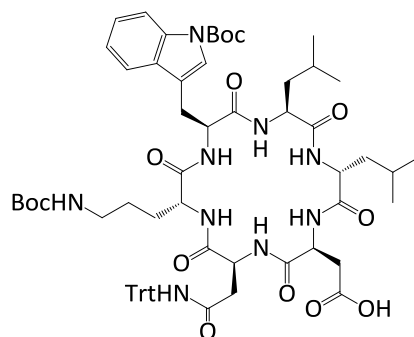
Compound **10c** was prepared through catalytic hydrogenation (H$_2$, 5 atm) of **10b** (0.14 g, 0.11 mmol) with 10% Pd/C (0.03 g) in EtOAc (50 mL). The reaction was allowed to be taken place overnight. After the completion of the reaction the Pd/C catalyst was filtered, the solvent evaporated under vacuum to give a white fluffy solid mass that was further purified by column chromatography using silica gel as a stationary phase and CHCl$_3$/MeOH (17:3) as a mobile phase. Yield (38%), ESI-MS m/z calcd for C$_{65}$H$_{83}$N$_9$O$_{13}$: 1197.61; found: 1220.25 [M+Na]$^+$. R$_f$ = 0.08 in CHCl$_3$/MeOH (9:1). ^{1}H NMR (400 MHz, CD$_3$OD-d$_4$) δ 8.10 − 8.03 (m, 1H), 7.62 − 7.57 (m, 1H), 7.55 (s, 1H), 7.31 − 7.14 (m, 17H), 4.73 (s, 3H), 4.64 (dd, J = 9.8, 4.3 Hz, 1H), 4.53 (d, J = 7.5 Hz, 1H), 4.15 − 4.03 (m, 2H), 3.35 (d, J = 11.9 Hz, 1H), 3.05 (dt, J = 16.7, 8.8 Hz, 2H), 2.82 (p, J = 11.7, 9.8 Hz, 3H), 2.56 (s, 2H), 1.66 (s, 9H), 1.60 (d, J = 27.1 Hz, 8H), 1.39 (s, 9H), 1.02 (s, 2H), 0.88 (ddd, J = 20.9, 16.9, 6.4 Hz, 12H).

Synthesis of cyclo (Asp (BTZ)-Asn (Trt)-D-Orn (Boc)-Trp (Boc)-Leu-D-Leu) (10d)

138
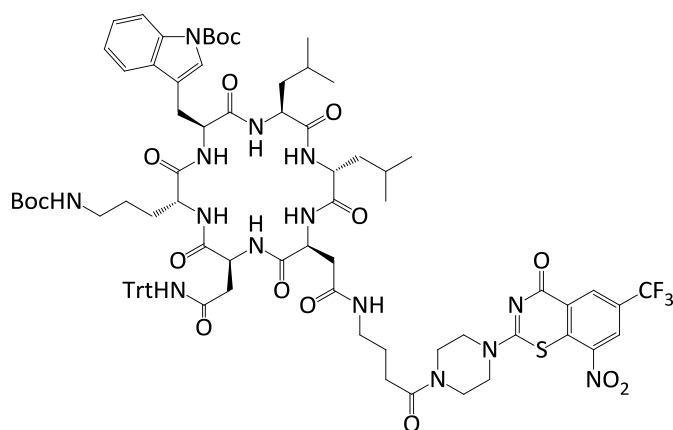
Compound **10d** was obtained by HATU (0.04 g, 0.11 mmol) mediated coupling of HA-3-29 (0.05 g, 0.04 mmol) and 2-(4-(4-aminobutanoyl)piperazin-1-yl)-8-nitro-6-(trifluoromethyl)-4H-benzo[e][1,3]thiazin-4-one (BTZ) (0.02 g, 0.04 mmol) in the presence of DIPEA (0.07 mL, 0.38 mmol) as a base and DMF (7 mL) as a solvent. The reaction was run for 20 h and the solvent was removed under strong vacuum. The obtained yellowish solid mass was then purified by column chromatography using silica gel as a stationary phase and $CHCl_3/MeOH$ (9:1) as a mobile phase. Yield (89%), ESI-MS m/z calcd for $C_{82}H_{99}F_3N_{14}O_{16}S$: 1624.7; found: 1623.46 [M-H]⁻. R_f = 0.24 in $CHCl_3/MeOH$ (9:1).

**Synthesis of cyclo (Asp (BTZ)-Asn-D-Orn-Trp-Leu-D-Leu) (10e)**
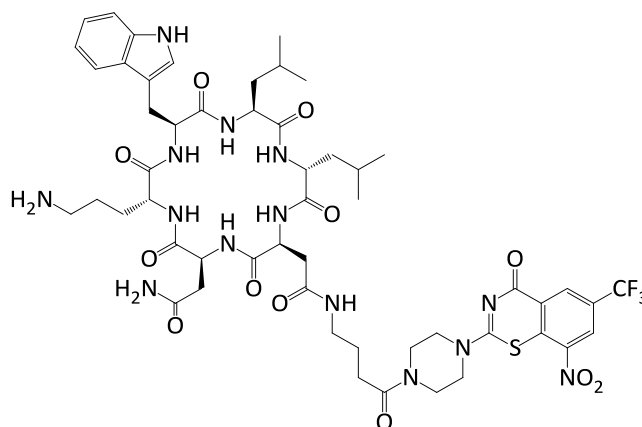
10d (0.06 g, 0.03 mmol) was treated with 2.0 mL of $TFA/TIPS/H_2O$ (95:2.5/2.5/) for 3 h. The cleaving solution was removed under a strong pressure and the product was washed with cold ether and kept under strong vacuum to give a yellowish amorphous solid mass. Yield (85%), mp 235-237 °C, UPLC-MS (UV) purity: 94%, RT:0.88 min, ESI-MS m/z calcd for $C_{53}H_{69}F_3N_{14}O_{12}S$:1182.49: found: 1183.49 [M+H]⁺. ¹H NMR (400 MHz, CD₃OD-d₄) δ 8.96 (dd, J = 2.1, 0.7 Hz, 1H), 8.87 (dd, J = 2.1, 0.8 Hz, 1H), 7.55 (dt, J = 7.8, 1.0 Hz, 1H), 7.31 − 7.26 (m, 1H), 7.09 (s, 1H), 7.05 (ddd, J = 8.1, 7.0, 1.2 Hz, 1H), 6.98 (ddd, J = 8.0, 7.1, 1.1 Hz, 1H), 4.68 (t, J = 5.3 Hz, 1H), 4.65 − 4.55 (m, 2H), 4.47 (td, J = 7.2, 5.2 Hz, 1H), 4.36 (dd, J = 9.9, 4.9 Hz, 1H), 4.24 (dd, J = 8.3, 6.5 Hz, 1H), 4.06 (s, 3H), 3.77 (dd, J = 12.2, 6.7 Hz, 3H), 3.29 − 3.17 (m, 3H), 3.15 − 3.01 (m, 2H), 2.88 − 2.70 (m, 4H), 2.64 (dd, J = 15.4, 7.8 Hz, 1H), 2.49 (t, J = 7.4 Hz, 2H), 1.83 (p, J = 6.7 Hz, 3H), 1.74 − 1.41 (m, 9H), 1.00 − 0.83 (m, 12H).

**Synthesis of H₂N-D-Leu-Val-D-Orn (Boc)-D-Orn (Boc)-Trp (Boc)-Leu-COOH (11a)**
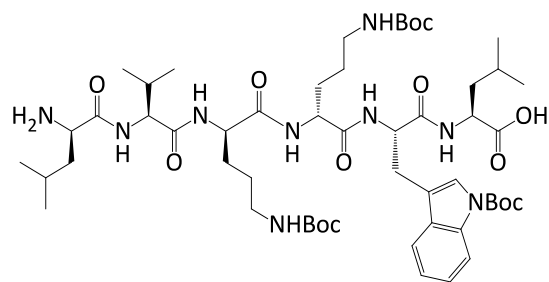
SPPS approach was used to prepare **11a** according to the general procedure described under section 8.2. The synthesis was initiated from a resin loaded with Fmoc- Leu-OH (0.3 g, 0.3 mmol). Crude % yield (95 %), ESI-MS m/z calcd for $C_{53}H_{87}N_9O_{13}$:1057.64: found: 1056.56 [M-H]⁻.

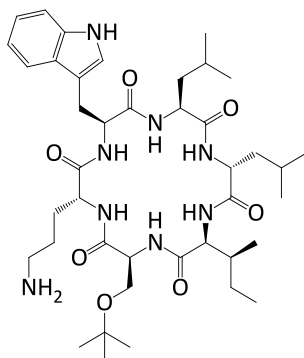**Synthesis of cyclo (D-Leu-Val-D-Orn (Boc)-D-Orn (Boc)-Trp (Boc)-Leu) (11b)**
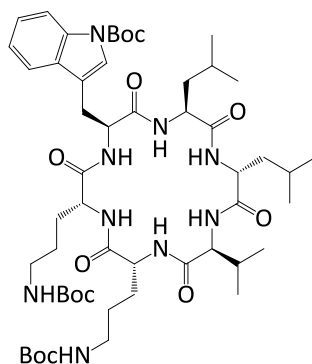
Compound **11b** was obtained through a macrocyclization of **11a** (0.3 g, 0.29 mmol) with HATU (0.3 g, 0.86 mmol), HOBt (0.12 g, 0.86 mmol) and DIPEA (0.5 mL, 2.87 mmol) according to the procedure described in section 8.3. The crude was purified by a column chromatography using a silica gel as a stationary phase and chloroform/methanol (49:1) as a mobile phase to give a white amorphous solid mass. Yield (40%), ESI-MS m/z calcd for $C_{53}H_{85}N_9O_{12}$: 1039.63; found: 1038.51 [M-H]⁻.R_f = 0.12 in CHCl₃/MeOH (49:1).

**Synthesis of cyclo (D-Leu-Val-D-Orn-D-Orn-Trp-Leu) (11c)**
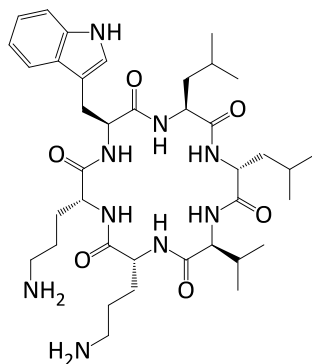
Compound **11b** (0.11 g, 0.11 mmol) was treated with 2.5 mL of TFA/DCM (95:2.5/2.5/) for 1 h. The cleaving solution was removed under a strong pressure and the product was washed with cold ether and kept under strong vacuum to give a white amorphous solid mass. Yield (70%), mp 235-237 °C, UPLC-MS (UV) purity: 97%, RT:0.68 min, ESI-MS m/z calcd for $C_{38}H_{61}N_9O_6$: 739.47; found: 740.47 [M+H]$^+$. ^{1}H NMR (400 MHz, CD_3OD-d_4) δ 7.61 (dt, J = 7.9, 1.0 Hz, 1H), 7.36 (dt, J = 8.1, 0.9 Hz, 1H), 7.22 (s, 1H), 7.12 (ddd, J = 8.2, 7.0, 1.2 Hz, 1H), 7.04 (ddd, J = 8.0, 7.1, 1.1 Hz, 1H), 4.55 − 4.37 (m, 4H), 4.23 (dd, J = 8.9, 3.9 Hz, 1H), 3.94 − 3.84 (m, 1H), 3.41 − 3.34 (m, 1H), 3.12 (dd, J = 14.8, 9.5 Hz, 1H), 2.93 (t, J = 7.3 Hz, 2H), 2.77 − 2.58 (m, 2H), 2.05 (ddd, J = 13.1, 9.1, 6.4 Hz, 2H), 1.79 − 1.48 (m, 9H), 1.45 − 1.24 (m, 4H), 1.08 − 0.73 (m, 18H). ^{13}C NMR (101 MHz, CD_3OD-d_4) δ 173.55, 173.07, 172.70, 172.52, 172.47, 171.88, 127.00, 123.46, 121.28, 118.68, 117.86, 111.03, 109.07, 60.74, 56.07, 53.40, 52.43, 51.48, 51.05, 50.31, 39.85, 39.55, 38.73, 29.03, 28.27, 27.94, 27.00, 24.46, 24.31, 23.75, 22.93, 22.08, 21.67, 21.19, 20.25, 18.30, 17.89.

141

Synthesis of H₂N-Trp (Boc)-Leu-D-Leu-Ile-Ser (tBu)-D-Orn (Boc)-COOH (12a)
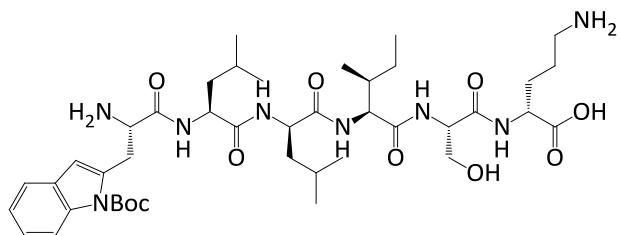
SPPS approach was used to prepare **12a** according to the general procedure described under section 8.2. The synthesis was initiated from a resin loaded with Fmoc- D-Orn (Boc)-OH (0.33 g, 0.3 mmol). Crude % yield (78%), ESI-MS m/z calcd for $C_{51}H_{84}N_8O_{12}$: 1000.62; found: 1023.74 $[M+Na]^+$.

Synthesis of cyclo (Trp (Boc)-Leu-D-Leu-Ile-Ser (tBu)-D-Orn (Boc)) (12b)
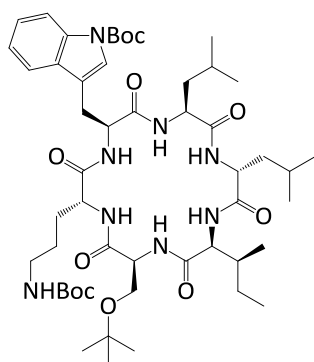
Compound **12b** was obtained through a macrocyclization of **12a** (0.23 g, 0.23 mmol) with HATU (0.27 g, 0.67 mmol), HOBt (0.09 g, 0.67 mmol) and DIPEA (0.41 mL, 2.33 mmol) according to the procedure described in section 8.3. The crude was purified by a column chromatography using a silica gel as a stationary phase and chloroform/methanol (49:1) as a mobile phase to give a white amorphous solid mass. Yield (68%), ESI-MS m/z calcd for $C_{51}H_{82}N_8O_{11}$: 982.61; found: 1005.75 $[M+Na]^+$. R_f = 0.04in CHCl₃/MeOH (49:1).

Synthesis of cyclo (Trp-Leu-D-Leu-Ile-Ser-D-Orn) (12c)
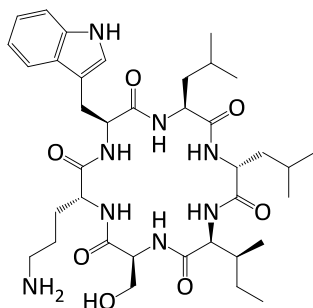
Compound **12b** (0.14 g, 0.14 mmol) was treated with 4 mL of TFA/DCM (1:1) for 1 h. The cleaving solution was removed under a strong pressure and the residue was purified by column chromatography using a silica gel as a stationary phase and chloroform/methanol/ammonia solution (80:20:1) as a mobile phase to give a white amorphous solid mass. Yield (45%), mp 95-97 °C, UPLC-MS (UV) purity: 98%, RT:0.8 min, ESI-MS m/z calcd for $C_{34}H_{52}N_8O_7$: 726.44; found: 727.44 [M+H][+]. ^{1}H NMR (400 MHz, CD$_3$OD-d$_4$) δ 7.57 (dt, J = 7.9, 1.0 Hz, 1H), 7.38 − 7.32 (m, 1H), 7.17 (s, 1H), 7.09 (ddd, J = 8.1, 6.9, 1.1 Hz, 1H), 7.00 (ddd, J = 7.9, 7.0, 1.0 Hz, 1H), 4.51 (dd, J = 9.3, 4.7 Hz, 1H), 4.44 (dt, J = 9.2, 5.2 Hz, 2H), 4.35 (dt, J = 14.5, 7.4 Hz, 2H), 4.11 (d, J = 4.7 Hz, 1H), 3.98 (dd, J = 11.3, 5.0 Hz, 1H), 3.83 (dd, J = 11.3, 4.2 Hz, 1H), 3.08 (dd, J = 14.8, 9.4 Hz, 1H), 2.77 (qdd, J = 12.6, 8.6, 6.3 Hz, 2H), 2.04 (ddt, J = 9.3, 6.9, 4.5 Hz, 1H), 1.72 − 1.23 (m, 12H), 1.02 − 0.75 (m, 18H). ^{13}C NMR (101 MHz, CD$_3$OD-d$_4$) δ 174.91, 172.74, 172.49, 172.41, 172.12, 171.05, 136.74, 127.02, 123.37, 121.19, 118.58, 117.88, 110.99, 109.07, 61.76, 59.53, 56.91, 55.59, 52.50, 52.06, 51.26, 48.22, 48.01, 47.79, 47.79, 47.61, 47.58, 47.37, 47.16, 46.94, 40.71, 39.43, 38.72, 35.76, 26.72, 26.23, 24.58, 24.52, 24.46, 23.08, 21.51, 21.49, 21.27, 21.18, 16.94, 14.82, 10.72.

Synthesis of cyclo (Trp-Leu-ᴅ-Leu-Ile-Ser (t-Bu)-ᴅ-Orn) (13c)

11c was isolated as a side product when **10c** was prepared due to incomplete deprotection of the t-Bu protecting group of serine. Yield (30%), mp 104-107 °C, UPLC-MS (UV) purity: 97%, RT:0.92 min, ESI-MS m/z calcd for $C_{41}H_{66}N_8O_7$: 782.51; found: 783.51 [M-H]⁻. ^{1}H NMR (500 MHz, CD_3OD-d_4) δ 7.57 (dt, J = 7.9, 1.0 Hz, 1H), 7.33 (dt, J = 8.2, 0.9 Hz, 1H), 7.18 (s, 1H), 7.09 (ddd, J = 8.2, 7.0, 1.2 Hz, 1H), 7.01 (ddd, J = 7.9, 7.1, 1.0 Hz, 1H), 4.56 (dd, J = 9.0, 4.2 Hz, 1H), 4.44 (dd, J = 7.3, 6.1 Hz, 2H), 4.33 (dd, J = 8.0, 6.9 Hz, 1H), 4.14 (t, J = 7.5 Hz, 1H), 4.09 (d, J = 4.5 Hz, 1H), 3.63 (dd, J = 8.9, 6.0 Hz, 1H), 3.57 − 3.47 (m, 1H), 3.42 − 3.33 (m, 1H), 3.15 (dd, J = 14.9, 9.0 Hz, 1H), 2.61 − 2.50 (m, 2H), 2.00 (ddt, J = 9.2, 6.9, 4.2 Hz, 1H), 1.66 − 1.18 (m, 12H), 1.14 (s, 9H), 0.98 − 0.76 (m, 18H). ^{13}C NMR (126 MHz, CD_3OD-d_4) δ 174.25, 172.69, 172.46, 172.11, 172.05, 170.59, 136.69, 127.16, 123.54, 121.21, 118.63, 118.15, 110.96, 109.20, 73.17, 60.88, 59.27, 54.77, 53.85, 53.15, 52.08, 51.48, 40.88, 39.70, 39.70, 39.03, 35.88, 26.54, 26.43, 26.34, 26.31, 25.82, 24.62, 24.36, 21.59, 21.45, 21.38, 21.08, 14.93, 10.81.

**Synthesis of H$_2$N-D-Leu-Ile-Ile-D-Orn (Boc)-Trp (Boc)-Leu-COOH (14a)**
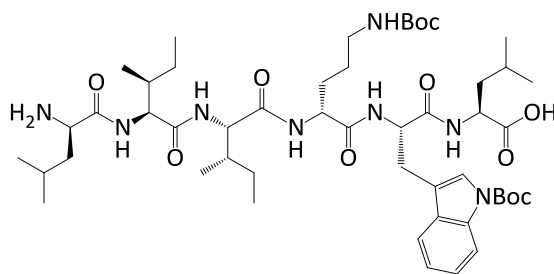
SPPS approach was used to prepare **14a** according to the general procedure described under section 8.2. The synthesis was initiated from a resin loaded with Fmoc- Leu-OH (0.3 g, 0.3 mmol). Crude % yield (104%), ESI-MS m/z calcd for C$_{50}$H$_{82}$N$_8$O$_{11}$: 970.61; found: 970.00 [M-H]$^-$.

**Synthesis of cyclo (D-Leu-Ile-Ile-D-Orn (Boc)-Trp (Boc)-Leu) (14b)**
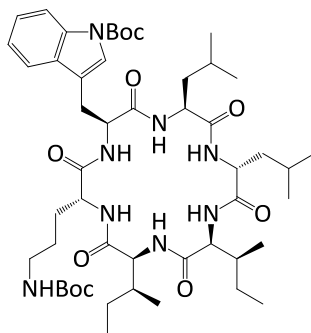
Compound **14b** was obtained through a macrocyclization of **14a** (0.44 g, 0.46 mmol) with HATU (0.52 g, 1.37 mmol), HOBt (0.18 g, 1.37 mmol) and DIPEA (0.79 mL, 4.6 mmol) according to the procedure described in section 8.3. The crude was purified by a column chromatography using a silica gel as a stationary phase and chloroform/methanol (49:1) as a mobile phase to give a white amorphous solid mass. Yield (54%), ESI-MS m/z calcd for C$_{50}$H$_{80}$N$_8$O$_{10}$: 952.60; found: 953.58 [M+H]$^+$. R$_f$ = 0.09 in CHCl$_3$/MeOH (49:1).

145

Synthesis of cyclo (D-Leu-Ile-Ile-D-Orn-Trp-Leu) (14c)
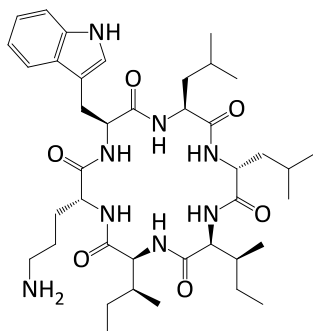
Compound **14b** (0.21 g, 0.22 mmol) was treated with 4 mL of TFA/DCM (1:1) for 1 h. The cleaving solution was removed under a strong pressure and the residue was purified by column chromatography using a silica gel as a stationary phase and chloroform/methanol/ammonia solution (85:15:1) as a mobile phase to give a white amorphous solid mass. Yield (70%), mp: 165 °C, UPLC-MS (UV) purity: 99.9%, RT:0.92 min, ESI-MS m/z calcd for $C_{40}H_{64}N_8O_6$: 752.49; found: 753.50 $[M+H]^+$. ^{1}H NMR (400 MHz, CD$_3$OD-d$_4$) δ 7.60 (d, J = 7.9 Hz, 1H), 7.33 (d, J = 8.1 Hz, 1H), 7.15 (s, 1H), 7.12 − 7.04 (m, 1H), 7.03 − 6.94 (m, 1H), 4.61 (dd, J = 10.6, 3.7 Hz, 1H), 4.55 (t, J = 7.4 Hz, 1H), 4.43 (t, J = 7.4 Hz, 1H), 4.36 (d, J = 8.0 Hz, 1H), 4.12 (d, J = 5.3 Hz, 1H), 3.89 (dd, J = 8.5, 6.5 Hz, 1H), 3.51 (dd, J = 14.8, 3.7 Hz, 1H), 3.03 (dd, J = 14.8, 10.7 Hz, 1H), 2.53 − 2.35 (m, 2H), 1.97 (ddd, J = 16.1, 8.3, 4.4 Hz, 1H), 1.91 − 1.79 (m, 1H), 1.73 − 1.40 (m, 9H), 1.32 − 1.05 (m, 4H), 1.03 − 0.83 (m, 24H), 0.81 − 0.70 (m, 1H). ^{13}C NMR (101 MHz, CD$_3$OD-d$_4$) δ 173.21, 173.02, 172.60, 172.35, 171.66, 171.47, 136.75, 127.03, 123.46, 121.18, 118.55, 118.02, 110.98, 109.86, 59.26, 56.58, 54.51, 54.38, 51.66, 51.34, 40.45, 39.70, 38.99, 36.99, 35.97, 27.02, 26.59, 25.69, 24.76, 24.75, 24.51, 24.41, 21.91, 21.61, 21.25, 20.86, 14.88, 14.15, 10.59, 9.88.

Synthesis of H$_2$N-Val-Asn (Trt)-D-Orn (Boc)-Phe (4-Cl)-Leu-D-Leu-COOH (15a)
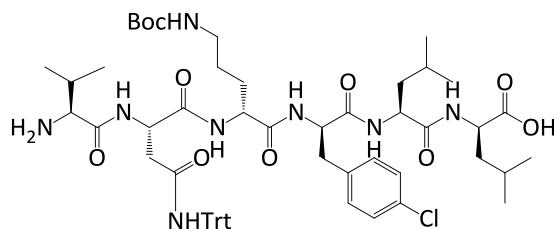

SPPS approach was used to prepare **15a** according to the general procedure described under section 8.2. The synthesis was initiated from a resin loaded with Fmoc-D-Leu-OH (0.3 g, 0.3 mmol). Crude % yield (100%), ESI-MS m/z calcd for C$_{59}$H$_{79}$N$_8$O$_{10}$: 1094.56; found: 1117.21 [M+Na]$^+$.

Synthesis of cyclo (D-Phe (4-Cl)-D-Orn (Boc)-Asn (Trt)-Val-D-Leu-Leu) (15b)
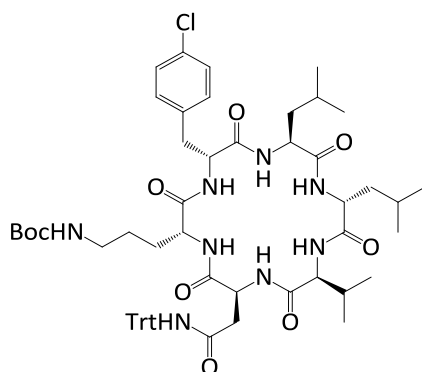
Compound **15b** was obtained through a macrocyclization of **15a** (0.33 g, 0.3 mmol) with HATU (0.34 g, 0.9 mmol), HOBt (0.12 g, 0.9 mmol) and DIPEA (0.52 mL, 3.0 mmol) according to the procedure described in section 8.3. It was purified by a column chromatography using a silica gel as a stationary phase and chloroform/methanol (97:3) as a mobile phase to give a white amorphous solid mass. Yield (43%), ESI-MS m/z calcd for C$_{59}$H$_{77}$ClN$_8$O$_9$: 1076.55; found: 1099.27 [M+Na]$^+$ R$_f$ = 0.14 in CHCl$_3$/MeOH (98:2).

Synthesis of cyclo (D-Phe (4-Cl)-D-Orn-Asn-Val-D-Leu-Leu) (15c)
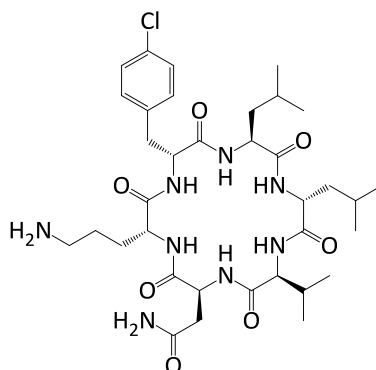
Compound **15b** (0.12 g, 0.11 mmol) was treated with 2.5 mL of TFA/TIPS/H$_2$O (95:2.5/2.5/) for 3 h. The cleaving solution was removed under a strong pressure and the residue was purified by column chromatography using a silica gel as a stationary phase and chloroform/methanol/ammonia solution (80:20:1) as a mobile phase to give a white amorphous solid mass. Yield (91%), mp 255-258 °C, UPLC-MS (UV) purity: 99.9%, RT:0.81 min, ESI-MS m/z calcd for C$_{35}$H$_{55}$ ClN$_8$O$_7$: 734.39; found: 735.39 [M+H]$^+$. ^{1}H NMR (400 MHz, CD$_3$OD-d$_4$) δ 7.32 − 7.26 (m, 2H), 7.21 − 7.16 (m, 2H), 4.68 (dd, J = 7.6, 6.2 Hz, 1H), 4.41 (ddd, J = 11.7, 8.6, 6.5 Hz, 3H), 4.20 (dd, J = 8.6, 5.3 Hz, 1H), 4.14 (d, J = 5.2 Hz, 1H), 3.20 (dd, J = 13.7, 6.9 Hz, 1H), 3.07 (dd, J = 13.7, 8.5 Hz, 1H), 2.91 − 2.83 (m, 2H), 2.81 (d, J = 7.6 Hz, 1H), 2.74 (dd, J = 15.6, 6.2 Hz, 1H), 2.28 − 2.19 (m, 1H), 1.69 − 1.54 (m, 8H), 1.39 (ddd, J = 13.4, 8.9, 5.8 Hz, 1H), 1.28 (dt, J = 13.5, 6.9 Hz, 1H), 1.04 − 0.80 (m, 18H). ^{13}C NMR (101 MHz, CD$_3$OD-d$_4$) δ 173.94, 173.37, 172.75, 172.33, 172.06, 171.92, 170.84, 136.21, 132.15, 130.58, 128.18, 59.15, 55.06, 53.01, 52.27, 51.21, 50.53, 39.65, 39.60, 38.57, 35.97, 35.47, 30.21, 27.95, 24.55, 24.29, 23.32, 21.73, 21.02, 20.85, 18.24, 16.40.

Synthesis of H₂N-D-Leu-Val-Asn (Trt)-D-Orn (Boc)- Phe (4-OMe)-Leu- COOH (16a)
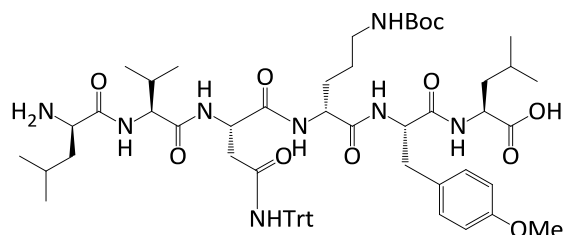
SPPS approach was used to prepare **16a** according to the general procedure described under section 8.2. The synthesis was initiated from a resin loaded with Fmoc- Leu-OH (0.31 g, 0.3 mmol). Crude % yield (96%), ESI-MS m/z calcd for $C_{60}H_{82}N_8O_{11}$:1090.61; found: 1089.59 [M-H]⁻.

**Synthesis of cyclo (D-Leu-Val-Asn (Trt)-D-Orn (Boc)-Phe (4-OMe)-Leu) (16b)**
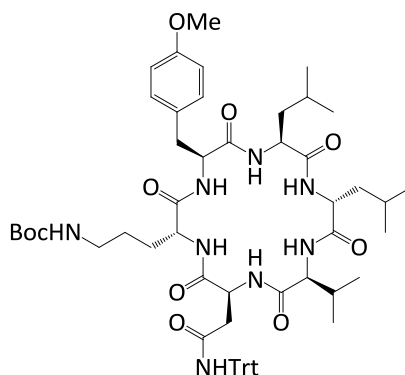
Compound **16b** was obtained through a macrocyclization of **16a** (0.35 g, 0.32 mmol) with HATU (0.37 g, 0.96 mmol), HOBt (0.13 g, 0.96 mmol) and DIPEA (0.56 mL, 3.2 mmol) according to the procedure described in section 8.3. The crude was purified by a column chromatography using a silica gel as a stationary phase and chloroform/methanol (49:1) as a mobile phase to give a white amorphous solid mass. Yield (41%), ESI-MS m/z calcd for $C_{60}H_{80}N_8O_{10}$:1072.60; found: 1095.60[M+Na]⁺. R_f = 0.09 in CHCl₃/MeOH (49:1).

Synthesis of cyclo (D-Leu-Val-Asn-D-Orn-Phe (4-OMe)-Leu) (16c)
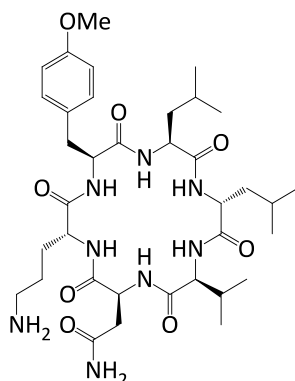
Compound **16b** (0.06 g, 0.06 mmol) was treated with 3 mL of TFA/TIPS/H_2O (95:2.5/2.5/) for 3 h. The cleaving solution was removed under a strong pressure and the residue was purified by column chromatography using a silica gel as a stationary phase and chloroform/methanol/ammonia solution (85:15:1) as a mobile phase to give a white amorphous solid mass. Yield (82%), mp 243-245 °C, UPLC-MS (UV) purity: 99.9%, RT:0.74 min, ESI-MS m/z calcd for $C_{36}H_{58}N_8O_8$: 730.44; found: 731.44 [M+H]$^+$. ^{1}H NMR (400 MHz, CD$_3$OD-d$_4$) δ 7.17 − 7.08 (m, 2H), 6.87 − 6.79 (m, 2H), 4.68 (dd, *J* = 5.7, 4.6 Hz, 1H), 4.53 − 4.38 (m, 3H), 4.31 (dd, *J* = 9.9, 5.1 Hz, 1H), 4.05 (d, *J* = 4.6 Hz, 1H), 3.75 (s, 3H), 3.17 − 3.01 (m, 2H), 2.86 (dd, *J* = 14.0, 10.2 Hz, 1H), 2.80 − 2.69 (m, 3H), 2.36 − 2.27 (m, 1H), 1.87 − 1.80 (m, 1H), 1.74 − 1.35 (m, 9H), 1.04 − 0.87 (m, 18H). ^{13}C NMR (101 MHz, CD$_3$OD-d$_4$) δ 175.20, 173.39, 172.41, 172.38, 172.15, 172.02, 171.84, 158.68, 129.89, 128.61, 113.52, 60.26, 56.81, 54.22, 52.12, 51.99, 51.22, 50.04, 40.89, 39.53, 39.21, 36.34, 35.68, 29.16, 26.33, 24.73, 24.70, 24.52, 22.80, 21.66, 21.57, 21.36, 21.07, 18.11, 16.95, 16.49.

Synthesis of H₂N-Asn (Trt)-D-Orn (Boc)-Trp (Boc)-D-Phe (4-Cl)-D-Leu-Val-COOH (17a)
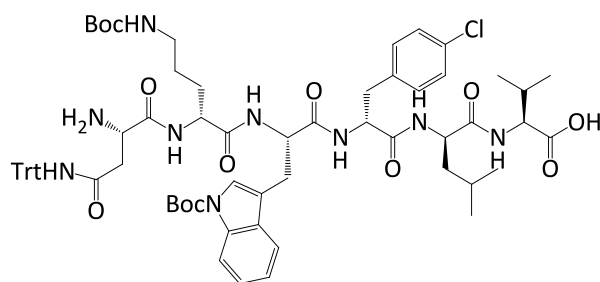
SPPS approach was used to prepare **17a** according to the general procedure described under section 8.2. The synthesis was initiated from a resin loaded with Fmoc-Val-OH (0.29 g, 0.25 mmol). Crude % yield (80%), ESI-MS m/z calcd for $C_{69}H_{86}ClN_9O_{12}$: 1267.61; found: 1290.61 [M+Na]$^{+}$.

**Synthesis of cyclo (Asn (Trt)-D-Orn (Boc)-Trp (Boc)-D-Phe (4-Cl)-D-Leu-Val) (17b)**
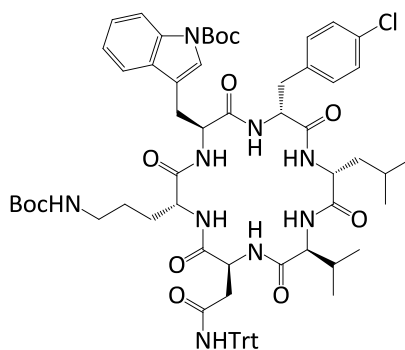
Compound **17b** was obtained through a macrocyclization of **17a** (0.25 g, 0.2 mmol) with HATU (0.23 g, 0.6 mmol), HOBt (0.08 g 0.6 mmol) and DIPEA (0.35 mL, 2.0 mmol) according to the procedure described in section 8.3. It was purified by a column chromatography using a silica gel as a stationary phase and chloroform/methanol (98:2) as a mobile phase to give a white amorphous solid mass. Yield (54%), ESI-MS m/z calcd for $C_{69}H_{84}ClN_9O_{11}$: 1249.60; found: 1272.81 [M+Na]$^{+}$.

Synthesis of cyclo (Asn-D-Orn-Trp-D-Phe (4-Cl)-D-Leu-Val) (17c)
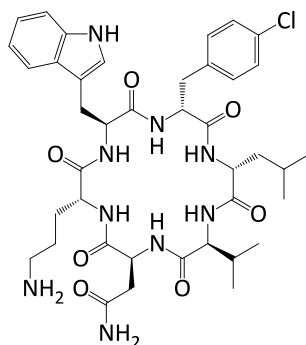
Compound **17b** (0.12 g, 0.09 mmol) was treated with 3.0 mL of TFA/TIPS/H$_2$O (95:2.5/2.5/) for 3 h. The cleaving solution was removed under a strong pressure and the residue was purified by column chromatography using a silica gel as a stationary phase and chloroform/methanol/ammonia solution (85:15:1) as a mobile phase to give a white amorphous solid mass. Yield (80%), mp 240-243°C, UPLC-MS (UV) purity: 99.9%, RT:0.82 min, ESI-MS m/z calcd for C$_{40}$H$_{54}$ClN$_9$O$_7$: 807.38; found: 808.38 [M+H]$^+$. ^{1}H NMR (400 MHz, CD$_3$OD-d$_4$) δ 7.55 (dt, J = 7.9, 1.0 Hz, 1H), 7.39 (dt, J = 8.2, 0.9 Hz, 1H), 7.14 (ddd, J = 8.2, 7.0, 1.1 Hz, 1H), 7.07 − 7.02 (m, 3H), 7.00 (s, 1H), 6.75 − 6.69 (m, 2H), 4.71 − 4.62 (m, 2H), 4.55 − 4.43 (m, 3H), 3.86 (d, J = 5.7 Hz, 1H), 3.11 (dd, J = 14.0, 9.1 Hz, 1H), 3.00 (ddd, J = 14.0, 6.3, 0.9 Hz, 1H), 2.96 − 2.81 (m, 3H), 2.81 − 2.76 (m, 2H), 2.72 (dd, J = 14.1, 4.7 Hz, 1H), 2.22 − 2.12 (m, 1H), 1.92 − 1.83 (m, 1H), 1.77 (ddd, J = 14.1, 9.5, 4.9 Hz, 1H), 1.69 − 1.52 (m, 3H), 1.47 − 1.40 (m, 1H), 1.38 − 1.34 (m, 1H), 1.05 − 0.84 (m, 12H). ^{13}C NMR (101 MHz, CD$_3$OD-d$_4$) δ 174.07, 173.57, 172.71, 172.04, 171.68, 171.48, 171.16, 136.63, 135.11, 132.18, 130.28, 128.04, 127.10, 123.31, 121.13, 118.49, 117.91, 111.15, 109.08, 61.30, 55.19, 54.57, 51.66, 51.44, 50.78, 41.45, 38.84, 35.68, 35.36, 29.42, 27.61, 26.28, 24.23, 23.29, 21.88, 21.23, 18.04, 17.24.

**Synthesis of H₂N-D-Phe (4-Cl)-Val-Asn (Trt)-D-Orn (Boc)-Trp (Boc)-Leu-COOH (18a)**
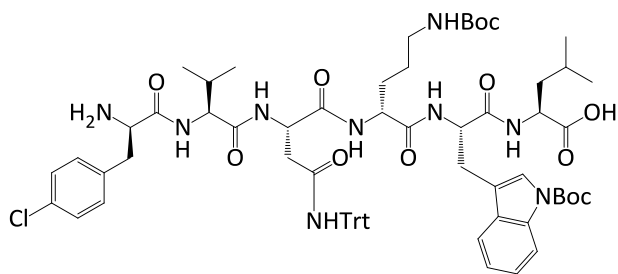
SPPS approach was used to prepare **18a** according to the general procedure described under section 8.2. The synthesis was initiated from a resin loaded with Fmoc- Leu-OH (0.143 g, 0.1 mmol). Crude % yield (70%), ESI-MS m/z calcd for $C_{70}H_{88}ClN_9O_{12}$: 1267.61; found: 1266.83 [M-H]⁻.

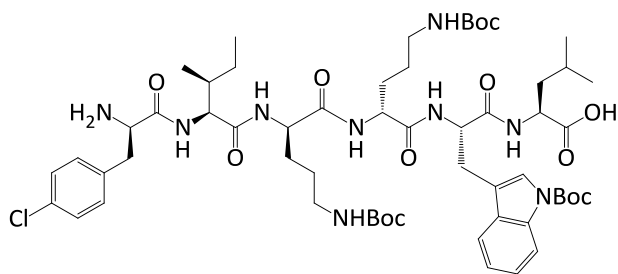**Synthesis of cyclo (D-Phe (4-Cl)-Val-Asn (Trt)-D-Orn (Boc)-Trp (Boc)-Leu) (18b)**
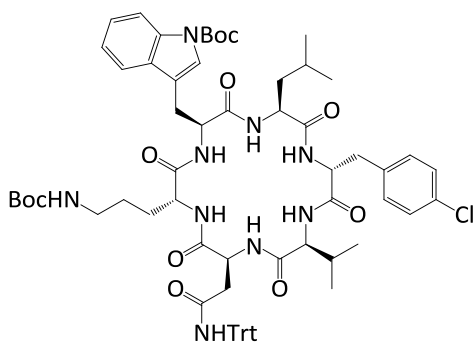
Compound **18b** was obtained through a macrocyclization of **16a** (0.09 g, 0.07 mmol) with HATU (0.08 g, 0.2 mmol), HOBt (0.03 g, 0.2 mmol) and DIPEA (0.12 mL, 0.68 mmol) according to the procedure described in section 8.3. The crude was purified by a column chromatography using a silica gel as a stationary phase and chloroform/methanol (49:1) as a mobile phase to give a white amorphous solid mass. Yield (53%), ESI-MS m/z calcd for $C_{70}H_{86}ClN_9O_{11}$:1249.60; found: 1272.65 [M+Na]⁺. R_f = 0.08 in CHCl₃/MeOH (49:1).

153

Synthesis of cyclo (D-Phe (4-Cl)-Val-Asn-D-Orn-Trp-Leu) (18c)
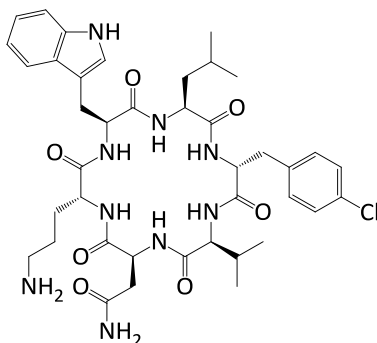
Compound **18b** (0.05 g, 0.04 mmol) was treated with 1.5 mL of TFA/TIPS/H$_2$O (95:2.5/2.5/) for 3 h. The cleaving solution was removed under a strong pressure and the product was washed with cold ether and kept under strong vacuum to give a white amorphous solid mass. Yield (75%), mp 280-282 °C, UPLC-MS (UV) purity: 91%, RT:0.82 min, ESI-MS m/z calcd for C$_{40}$H$_{54}$ClN$_9$O$_7$: 807.38; found: 808.378 [M+H]$^+$. ^{1}H NMR (400 MHz, CD$_3$OD-d$_4$) δ 7.58 (dt, J = 7.8, 1.0 Hz, 1H), 7.32 (dt, J = 8.2, 1.0 Hz, 1H), 7.30 − 7.25 (m, 2H), 7.24 − 7.18 (m, 2H), 7.12 (s, 1H), 7.09 (ddd, J = 8.2, 6.9, 1.2 Hz, 1H), 7.02 (ddd, J = 7.9, 7.1, 1.1 Hz, 1H), 4.70 − 4.51 (m, 3H), 4.45 − 4.35 (m, 2H), 3.77 (d, J = 4.7 Hz, 1H), 3.24 (dd, J = 14.7, 5.3 Hz, 1H), 3.16 − 3.06 (m, 2H), 3.03 − 2.92 (m, 2H), 2.84 (dq, J = 8.7, 6.2 Hz, 2H), 2.70 (dd, J = 16.8, 4.2 Hz, 1H), 2.16 − 2.08 (m, 1H), 1.91 − 1.28 (m, 7H), 0.97 − 0.68 (m, 12H). ^{13}C NMR (101 MHz, CD$_3$OD-d$_4$) δ 174.00, 173.40, 172.62, 172.40, 172.34, 172.14, 171.74, 135.10, 132.51, 130.59, 128.22, 127.05, 123.32, 121.11, 118.56, 117.92, 110.85, 109.09, 93.19, 60.56, 56.13, 54.94, 51.54, 51.11, 49.97, 40.51, 38.78, 36.05, 35.39, 29.00, 27.25, 26.05, 24.58, 23.33, 21.56, 21.23, 17.76, 16.38.

Synthesis of H₂N-D-Phe (4-Cl)-Ile-D-Orn (Boc)-D-Orn (Boc)-Trp (Boc)-Leu-COOH (19a)


SPPS approach was used to prepare **19a** according to the general procedure described under section 8.2. The synthesis was initiated from a resin loaded with Fmoc- Leu-OH (0.43 g, 0.44 mmol). Crude % yield (99%), ESI-MS m/z calcd for $C_{57}H_{86}ClN_9O_{13}$: 1139.60; found: 1140.62 [M+H]⁺.

**Synthesis of cyclo (D-Phe (4-Cl)-Ile-D-Orn (Boc)-D-Orn (Boc)-Trp (Boc)-Leu) (19b)**
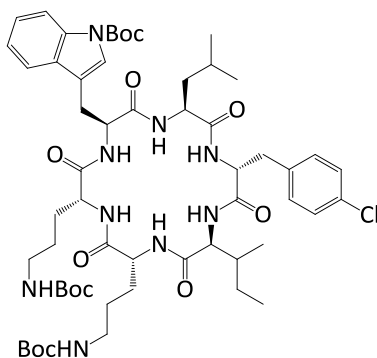
Compound **19b** was obtained through a macrocyclization of **19a** (0.3 g, 0.26 mmol) with HATU (0.3 g, 0.79 mmol), HOBt (0.11 g, 0.79 mmol) and DIPEA (0.46 mL, 2.63 mmol) according to the procedure described in section 8.3. The crude was purified by a column chromatography using a silica gel as a stationary phase and chloroform/methanol (49:1) as a mobile phase to give a white amorphous solid mass. Yield (55%), ESI-MS m/z calcd for $C_{57}H_{84}ClN_9O_{12}$: 1121.59; found, 1144.51 [M+Na]⁺. R_f = 0.26 in CHCl₃/MeOH (49:1).

**Synthesis of cyclo (D-Phe (4-Cl)-Ile-D-Orn-D-Orn-Trp-Leu) (19c)**
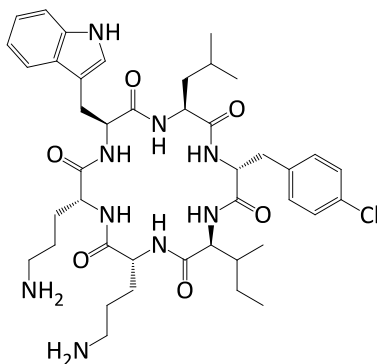
Compound **19b** (0.11 g, 0.1 mmol) was treated with 3 mL of TFA/TIPS/H$_2$O (95:2.5/2.5/) for 1 h. The cleaving solution was removed under a strong pressure and the residue was purified by column chromatography using a silica gel as a stationary phase and chloroform/methanol/ammonia solution (70:30:1) as a mobile phase to give a white amorphous solid mass. Yield (50%), mp 290-292 °C, UPLC-MS (UV) purity: 96%, RT:0.73 min, ESI-MS m/z calcd for C$_{42}$H$_{60}$ClN$_9$O$_6$: 821.44; found: 822.44 [M+H]$^+$. ^{1}H NMR (400 MHz, DMSO-d$_6$) δ 10.86 (s, 1H), 8.60 (d, J = 7.9 Hz, 1H), 8.30 (d, J = 6.1 Hz, 1H), 8.14 (d, J = 7.7 Hz, 1H), 7.94 (d, J = 8.5 Hz, 1H), 7.51 (d, J = 7.7 Hz, 1H), 7.33 − 7.24 (m, 3H), 7.21 (s, 1H), 7.19 − 7.13 (m, 2H), 7.07 − 7.01 (m, 1H), 7.00 − 6.93 (m, 1H), 4.61 − 4.49 (m, 1H), 4.35 − 4.15 (m, 3H), 3.96 (dt, J = 10.1, 4.9 Hz, 1H), 3.89 − 3.77 (m, 1H), 3.22 (d, J = 3.6 Hz, 1H), 2.96 − 2.81 (m, 2H), 2.78 − 2.69 (m, 1H), 2.44 (d, J = 6.7 Hz, 2H), 2.16 (t, J = 7.0 Hz, 2H), 1.81 − 1.14 (m, 13H), 1.04 − 0.91 (m, 1H), 0.86 − 0.54 (m, 12H). ^{13}C NMR (101 MHz, DMSO-d$_6$) δ 172.03, 171.91, 171.77, 171.68, 171.47, 169.87, 136.66, 131.51, 131.47, 128.38, 127.23, 124.52, 121.31, 118.74, 118.36, 111.79, 110.33, 67.45, 57.78, 56.23, 54.48, 53.97, 52.89, 51.03, 41.39, 41.06, 40.65, 40.60, 37.84, 34.76, 29.99, 29.40, 27.98, 27.58, 26.59, 25.56, 24.69, 24.63, 23.45, 21.88, 15.46, 10.58.

Synthesis of H₂N-Asn (Trt)-D-Orn (Boc)-Trp (Boc)-Ile-D-Leu-Val-COOH (20a)
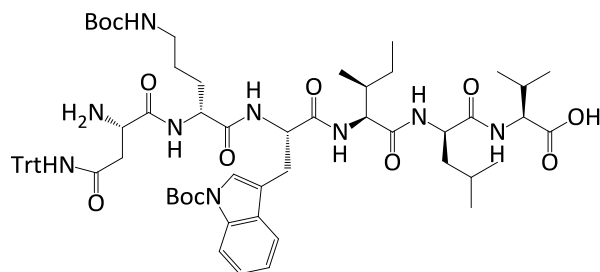

SPPS approach was used to prepare **20a** according to the general procedure described under section 8.2. The synthesis was initiated from a resin loaded with Fmoc-Val-OH (0.29 g, 0.25 mmol). Crude % yield (89%), ESI-MS m/z calcd for $C_{66}H_{89}N_9O_{12}$: 1199.66; found: 1200.59 $[M+H]^+$.

Synthesis of cyclo (Asn (Trt)-D-Orn (Boc)-Trp (Boc)-Ile-D-Leu-Val) (20b)
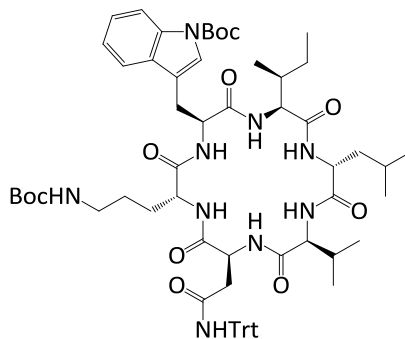
Compound **20b** was obtained through a macrocyclization of **20a** (0.27 g, 0.22 mmol) with HATU (0.25 g, 0.67 mmol), HOBt (0.09 g 0.67 mmol) and DIPEA (0.39 mL, 6.65 mmol) according to the procedure described in section 8.3. It was purified by a column chromatography using a silica gel as a stationary phase and chloroform/methanol (98:2) as a mobile phase to give a white amorphous solid mass. Yield (47%), ESI-MS m/z calcd for $C_{66}H_{87}N_9O_{11}$: 1181.65; found: 1204.56 $[M+Na]^+$. R_f = 0.08 in $CHCl_3$/MeOH (98:2).

**Synthesis of cyclo (Asn-D-Orn-Trp-Ile-D-Leu-Val) (20c)**
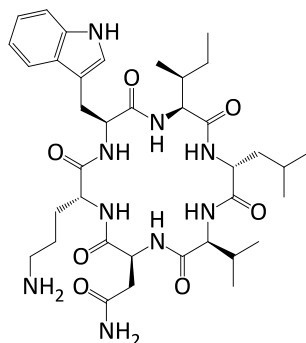
Compound **20b** (0.11 g, 0.09 mmol) was treated with 2.5 mL of TFA/TIPS/H_2O (95:2.5/2.5/) for 3 h. The cleaving solution was removed under a strong pressure and the residue was washed with cold ether to give a white amorphous solid mass. Yield (96%), mp 175-177 °C, UPLC-MS (UV) purity: 95%, RT:0.74 min, ESI-MS m/z calcd for $C_{37}H_{57}N_9O_7$: 739.44; found: 740.44 [M+H]$^+$. ^{1}H NMR (400 MHz, DMSO-d_6) δ 10.80 (d, J = 2.5 Hz, 2H), 8.44 (d, J = 4.8 Hz, 1H), 8.34 (dd, J = 16.0, 8.2 Hz, 2H), 7.56 (ddd, J = 22.1, 13.8, 7.2 Hz, 5H), 7.31 (d, J = 8.2 Hz, 2H), 7.12 (d, J = 2.3 Hz, 1H), 7.07 − 7.00 (m, 1H), 6.99 − 6.92 (m, 2H), 4.61 (dt, J = 8.4, 6.2 Hz, 1H), 4.37 − 4.12 (m, 4H), 4.05 (dd, J = 8.0, 4.1 Hz, 1H), 3.18 (dd, J = 14.6, 4.5 Hz, 1H), 2.96 (dd, J = 14.8, 10.4 Hz, 1H), 2.71 − 2.56 (m, 3H), 2.36 − 2.23 (m, 1H), 1.82 − 1.18 (m, 10H), 1.01 − 0.68 (m, 18H). ^{13}C NMR (101 MHz, DMSO-d_6) δ 173.99, 172.20, 171.31, 171.27, 171.26, 171.25, 170.92, 136.57, 127.46, 124.04, 121.33, 118.79, 118.59, 111.80, 110.62, 58.65, 56.16, 55.88, 52.60, 52.05, 50.07, 38.75, 38.20, 37.62, 29.24, 27.99, 27.09, 25.56, 25.07, 24.53, 23.66, 22.86, 22.50, 19.62, 17.29, 15.35, 11.66.

**Synthesis of H₂N-Asn (Trt)-D-Orn (Boc)-Trp (Boc)-Leu-Ile-Val-COOH (21a)**
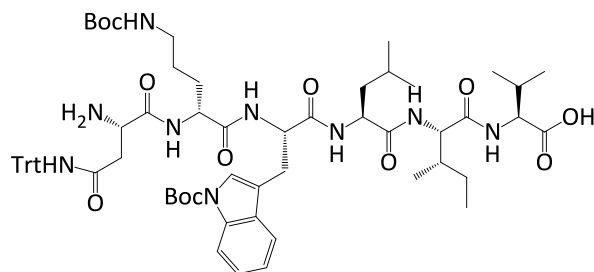
SPPS approach was used to prepare **21a** according to the general procedure described under section 8.2. The synthesis was initiated from a resin loaded with Fmoc-Val-OH (0.30 g, 0.25 mmol). Crude % yield (85%), ESI-MS m/z calcd for $C_{66}H_{89}N_9O_{12}$: 1199.66; found: 1222.71 $[M+Na]^+$.

Synthesis of cyclo (Asn (Trt)-D-Orn (Boc)-Trp (Boc)-Leu-Ile-Val) (21b)
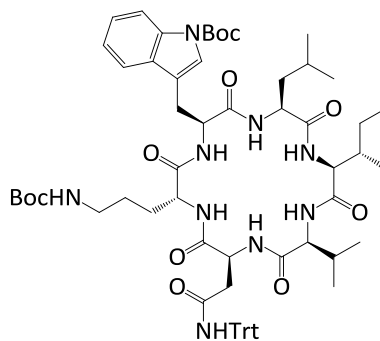
Compound **21b** was obtained through a macrocyclization of **21a** (0.26 g, 0.21 mmol) with HATU (0.24 g, 0.64 mmol), HOBt (0.07 g 0.64 mmol) and DIPEA (0.37 mL, 6.36 mmol) according to the procedure described in section 8.3. It was purified by a column chromatography using a silica gel as a stationary phase and chloroform/methanol (98:2) as a mobile phase to give a white amorphous solid mass. Yield (47%), ESI-MS m/z calcd for $C_{66}H_{87}N_9O_{11}$: 1181.65; found: 1204.65 $[M+Na]^+$. R_f = 0.1 in CHCl₃/MeOH (97:3).

Synthesis of cyclo (Asn-D-Orn-Trp-Leu-Ile-Val) (21c)
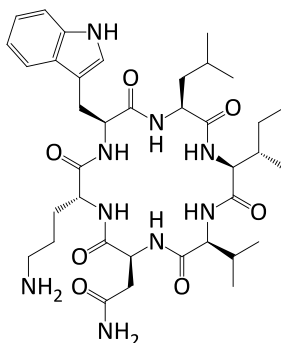
Compound **21b** (0.13 g, 0.11 mmol) was treated with 2.5 mL of TFA/TIPS/H_2O (95:2.5/2.5) for 3 h. The cleaving solution was removed under a strong pressure and the residue was purified by column chromatography using a silica gel as a stationary phase and chloroform/methanol/ammonia solution (80:20:1) as a mobile phase to give a white amorphous solid mass that contains a mixture two stereoisomers (3:1 ratio) . Yield (72%), mp 166-169 °C, UPLC-MS (UV) purity: 95%, RT:0.77 min, ESI-MS m/z calcd for $C_{37}H_{57}N_9O_7$: 739.44; found: 740.44[M+H]$^+$. ^{1}H NMR (400 MHz, CD_3OD-d_4) δ 7.63 (dd, *J* = 7.9, 3.7 Hz, 2H), 7.36 − 7.29 (m, 2H), 7.15 (d, *J* = 5.6 Hz, 1H), 7.12 − 7.05 (m, 2H), 7.05 − 6.98 (m, 2H), 4.71 − 4.64 (m, 2H), 4.60 (dd, *J* = 10.0, 4.6 Hz, 1H), 4.49 (dd, *J* = 11.4, 3.9 Hz, 1H), 4.43 (t, *J* = 7.8 Hz, 1H), 4.34 (dd, *J* = 8.4, 5.2 Hz, 1H), 4.13 (t, *J* = 7.4 Hz, 1H), 4.08 (d, *J* = 5.2 Hz, 1H), 3.76 (d, *J* = 8.1 Hz, 1H), 3.43 − 3.34 (m, 1H), 3.11 (ddd, *J* = 15.2, 9.4, 6.1 Hz, 2H), 3.02 (dd, *J* = 16.1, 4.7 Hz, 1H), 2.90 − 2.78 (m, 3H), 2.77 − 2.61 (m, 3H), 2.20 (ddt, *J* = 20.8, 14.4, 6.4 Hz, 2H), 1.92 − 1.38 (m, 14H), 1.08 − 0.77 (m, 24H). ^{13}C NMR (101 MHz, CD_3OD-d_4) δ 174.64, 173.93, 173.80, 173.73, 173.53, 173.52, 173.42, 172.52, 171.98, 171.95, 171.74, 136.71, 127.08, 127.05, 123.24, 123.16, 121.15, 121.12, 118.52, 117.93, 110.97, 110.92, 109.98, 109.46, 78.03, 62.28, 59.84, 59.78, 58.57, 55.84, 55.31, 53.64, 52.32, 52.13, 50.96, 50.44, 40.22, 39.43, 38.82, 38.54, 36.33, 34.87, 29.96, 28.64, 26.87, 26.54, 25.38, 24.55, 23.14, 22.34, 22.29, 21.87, 19.96, 19.80, 18.67, 18.38, 17.12, 16.21, 14.64, 14.40, 9.81, 9.64.

Preparation of H₂N-D-Leu-Ile-Asn (Trt)-D-Arg (Pbf)-Trp (Boc)-Leu-COOH (22a)
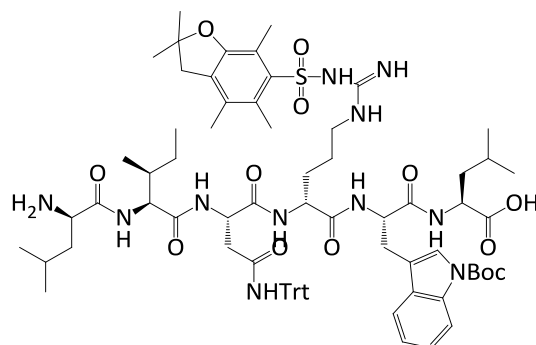
SPPS approach was used to prepare **22a** according to the general procedure described under section 8.2. The synthesis was initiated from a resin loaded with Fmoc- Leu-OH (0.3 g, 0.3 mmol). Crude % yield (96%), ESI-MS m/z calcd for $C_{75}H_{99}N_{11}O_{13}S$: 1407.73; found: 1408.89 $[M+H]^+$.

Synthesis of cyclo (D-Leu-Ile-Asn (Trt)-D-Arg (Pbf)-Trp (Boc)-Leu) (22b)
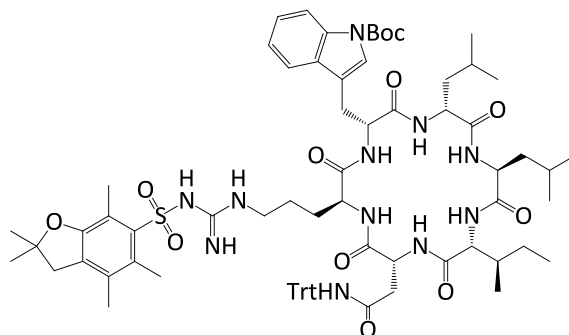
Compound **22b** was obtained through a macrocyclization of **13a** (0.52 g, 0.37 mmol) with HATU (0.42 g, 1.1 mmol), HOBt (0.15 g, 1.1 mmol) and DIPEA (0.65 mL, 3.7 mmol) according to the procedure described in section 8.3. The crude was purified by a column chromatography using a silica gel as a stationary phase and chloroform/methanol (49:1) as a mobile phase to give a white amorphous solid mass. Yield (70%), ESI-MS: m/z calcd for $C_{76}H_{99}N_{11}O_{12}S$: 1389.72; found: 1412.84 $[M+Na]^+$. R_f = 0.77 in $CHCl_3$/MeOH (4:1).

**Synthesis of cyclo (D-Leu-Ile-Asn-D-Arg-Trp-Leu) (22c)**
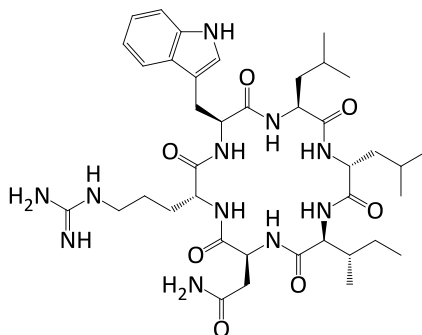
Compound **22b** (0.32 g, 0.23 mmol) was treated with 5 mL of TFA/TIPS/H$_2$O (95:2.5/2.5/) for 3 h. The cleaving solution was removed under a strong pressure and the product was washed with cold ether and kept under strong vacuum to give a white amorphous solid mass. Yield (70%), mp 271-273 °C, UPLC-MS (UV) purity: 96%, RT:0.79 min, ESI-MS m/z calcd for C$_{39}$H$_{61}$N$_{11}$O$_7$: 795.48; found: 796.488 [M+H]$^+$. ^{1}H NMR (400 MHz, DMSO-d$_6$) δ 11.08 (s, 1H), 8.42 (d, *J* = 8.0 Hz, 1H), 8.25 (t, *J* = 6.6 Hz, 2H), 7.96 (s, 1H), 7.85 (d, *J* = 6.4 Hz, 1H), 7.46 (dd, *J* = 16.8, 7.8 Hz, 4H), 7.35 (d, *J* = 8.1 Hz, 1H), 7.31 − 7.17 (m, 3H), 7.13 (d, *J* = 2.3 Hz, 1H), 7.01 (t, *J* = 7.5 Hz, 1H), 6.97 − 6.88 (m, 2H), 4.57 (q, *J* = 6.7 Hz, 1H), 4.42 (q, *J* = 7.2 Hz, 1H), 4.35 − 4.21 (m, 2H), 4.12 − 3.96 (m, 2H), 3.27 − 3.18 (m, 1H), 2.91 (dd, *J* = 14.6, 9.7 Hz, 3H), 2.57 (d, *J* = 6.5 Hz, 2H), 1.95 (dq, *J* = 11.0, 5.7, 5.0 Hz, 1H), 1.63 − 1.12 (m, 12H), 0.97 − 0.70 (m, 16H). ^{13}C NMR (101 MHz, DMSO-d$_6$) δ 173.57, 172.05, 171.94, 171.92, 171.28, 170.91, 170.82, 157.19, 136.65, 127.32, 124.27, 121.14, 118.62, 118.32, 112.01, 110.35, 67.46, 65.35, 58.55, 55.42, 53.14, 52.15, 51.09, 49.92, 42.29, 37.90, 35.96, 27.69, 27.50, 25.04, 24.88, 24.54, 24.35, 23.03, 22.97, 22.50, 16.12, 15.61, 12.20.

Synthesis of H$_2$N-D-Leu-N-Me-Val-Asn (Trt)-D-Orn (Boc)-Trp (Boc)-Leu-COOH (23a)
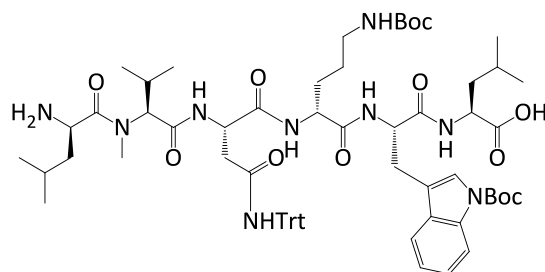

SPPS approach was used to prepare **23a** according to the general procedure described under section 8.2. The synthesis was initiated from a resin loaded with Fmoc-Leu-OH (0.31 g, 0.3 mmol). Crude % yield (93%), ESI-MS m/z calcd for C$_{66}$H$_{89}$N$_9$O$_{12}$: 1213.68; found: 1214.83 [M+H]$^{+}$.

Synthesis of cyclo (D-Leu-N-Me-Val-Asn (Trt)-D-Orn (Boc)-Trp (Boc)-Leu) (23b)
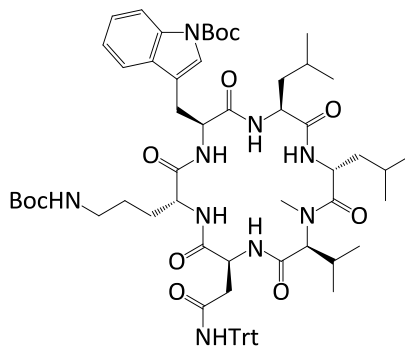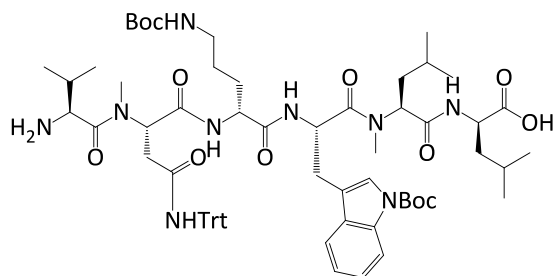

Compound **23b** was obtained through a macrocyclization of **23a** (0.34 g, 0.28 mmol) with HATU (0.32 g, 0.84 mmol), HOBt (0.11 g, 0.84 mmol) and DIPEA (0.49 mL, 2.8 mmol) according to the procedure described in section 8.3. The crude was purified by a column chromatography using a silica gel as a stationary phase and chloroform/methanol (49:1) as a mobile phase to give a white amorphous solid mass. Yield (60%), ESI-MS m/z calcd for C$_{67}$H$_{89}$N$_9$O$_{11}$: 1195.67; found: 1218.70 [M+Na]$^{+}$. R$_f$ = 0.1 in CHCl$_3$/MeOH (98:2).

## Synthesis of cyclo (D-Leu-N-Me-Val-Asn-D-Orn-Trp-Leu) (23c)
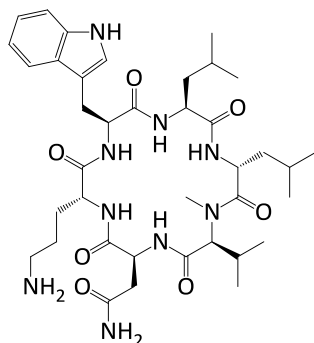
Compound **23b** (0.24 g, 0.2 mmol) was treated with 2.5 mL of TFA/TIPS/H$_2$O (95:2.5/2.5/) for 3 h. The cleaving solution was removed under a strong pressure and the residue was purified by column chromatography using a silica gel as a stationary phase and chloroform/methanol/ammonia solution (80:20:1) as a mobile phase to give a white amorphous solid mass. Yield (71%), mp 92-95 °C, UPLC-MS (UV) purity: 98%, RT:0.78 min, ESI-MS m/z calcd for C$_{38}$H$_{59}$N$_9$O$_7$: 753.45; found: 754.45 [M+H]$^+$. ^{1}H NMR (400 MHz, CD$_3$OD-d$_4$) δ 7.59 (dt, J = 7.9, 1.0 Hz, 1H), 7.34 (dt, J = 8.1, 0.9 Hz, 1H), 7.18 (s, 1H), 7.09 (ddd, J = 8.2, 7.0, 1.2 Hz, 1H), 7.01 (ddd, J = 8.0, 7.1, 1.1 Hz, 1H), 4.74 – 4.63 (m, 3H), 4.61 – 4.49 (m, 2H), 4.38 (dd, J = 8.2, 5.7 Hz, 1H), 3.37 (ddd, J = 14.7, 4.4, 0.9 Hz, 1H), 3.12 (dd, J = 14.8, 9.7 Hz, 1H), 3.03 (s, 2H), 2.98 – 2.81 (m, 2H), 2.69 (dddd, J = 36.2, 12.6, 8.5, 6.3 Hz, 2H), 2.24 (dp, J = 9.6, 6.6 Hz, 1H), 1.72 – 1.20 (m, 10H), 1.10 – 0.81 (m, 18H). ^{13}C NMR (101 MHz, CD$_3$OD-d$_4$) δ 174.13, 173.87, 172.83, 172.61, 172.12, 171.41, 171.02, 136.68, 127.14, 123.44, 121.11, 118.56, 117.96, 110.98, 109.46, 65.46, 62.96, 55.69, 52.33, 51.20, 50.16, 41.18, 39.52, 38.63, 35.55, 31.08, 27.68, 27.27, 26.72, 24.47, 24.38, 23.03, 21.98, 21.88, 20.90, 20.85, 19.64, 18.66.

Synthesis of H₂N-Val-N-Me-Asn (Trt)-D-Orn (Boc)-Trp (Boc)-N-Me-Leu-D-Leu-COOH (24a)


SPPS approach was used to prepare **24a** according to the general procedure described under section 8.2. The synthesis was initiated from a resin loaded with Fmoc-D-Leu-OH (0.31 g, 0.3 mmol). Crude % yield (103%), ESI-MS m/z calcd for $C_{68}H_{93}N_9O_{12}$:1227.69; found: 1250.70 $[M+Na]^+$.

Synthesis of cyclo (Val-N-Me-Asn (Trt)-D-Orn (Boc)-Trp (Boc)-N-Me-Leu-D-Leu) (24b)
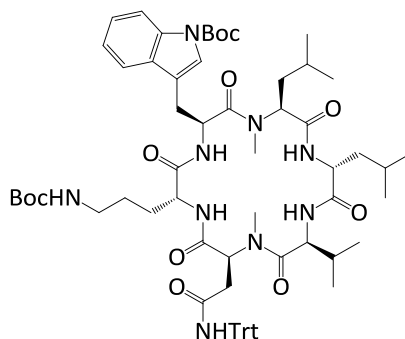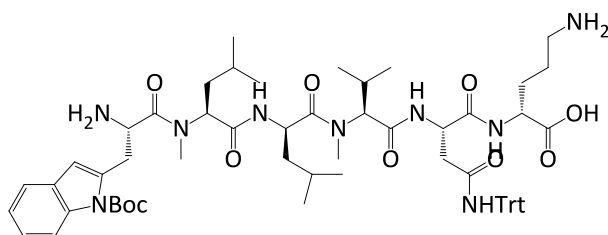

Compound **24b** was obtained through a macrocyclization of **24a** (0.38 g, 0.3 mmol) with HATU (0.34 g, 0.9 mmol), HOBt (0.12 g, 0.9 mmol) and DIPEA (0.52 mL, 3.0 mmol) according to the procedure described in section 8.3. The crude was purified by a column chromatography using a silica gel as a stationary phase and chloroform/methanol (49:1) as a mobile phase to give a white amorphous solid mass. Yield (80%), ESI-MS m/z calcd for $C_{68}H_{91}N_9O_{11}$: 1209.68; found: 1232.68 $[M+Na]^+$. R_f = 0.12 in $CHCl_3$/MeOH (99:1).

**Synthesis of cyclo (Val-N-Me-Asn-D-Orn-Trp-N-Me-Leu-D-Leu) (24c)**
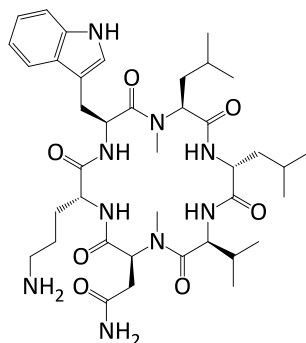
Compound **24b** (0.29 g, 0.24 mmol) was treated with 2.5 mL of TFA/TIPS/H_2O (95:2.5/2.5/) for 3 h. The cleaving solution was removed under a strong pressure and the residue was purified by column chromatography using a silica gel as a stationary phase and chloroform/methanol/ammonia solution (85:15:1) as a mobile phase to give a white amorphous solid mass. Yield (60%), mp 93 °C, UPLC-MS (UV) purity: 97%, RT:0.8 min, ESI-MS m/z calcd for $C_{39}H_{61}N_9O_7$: 767.47; found: 768.47 [M+H]$^+$. ^{1}H NMR (400 MHz, CD$_3$OD-d$_4$) δ 7.53 (s, 0H), 7.50 (dt, J = 7.9, 0.9 Hz, 1H), 7.35 (dt, J = 8.2, 1.0 Hz, 1H), 7.10 (ddd, J = 8.1, 7.0, 1.2 Hz, 1H), 7.05 − 6.99 (m, 1H), 6.97 (s, 1H), 5.60 (dd, J = 10.1, 4.4 Hz, 1H), 4.93 (dd, J = 10.8, 4.4 Hz, 1H), 4.75 (dd, J = 11.7, 3.6 Hz, 1H), 4.52 (dq, J = 6.5, 4.7, 3.8 Hz, 2H), 4.44 (t, J = 10.2 Hz, 1H), 3.45 − 3.33 (m, 1H), 3.23 − 3.05 (m, 2H), 3.02 − 2.89 (m, 2H), 2.77 (s, 2H), 2.68 (s, 1H), 2.61 (s, 2H), 2.36 (dd, J = 15.8, 4.4 Hz, 1H), 2.11 (dp, J = 8.4, 6.6 Hz, 1H), 1.94 − 1.40 (m, 9H), 1.08 − 0.79 (m, 12H), 0.74 − 0.65 (m, 1H), 0.51 − 0.32 (m, 6H), -0.57 (ddd, J = 13.2, 9.9, 3.4 Hz, 1H). ^{13}C NMR (101 MHz, CD$_3$OD-d$_4$) δ 173.31, 172.72, 172.54, 172.26, 171.37, 168.46, 168.11, 136.56, 126.97, 123.16, 121.29, 118.71, 117.71, 111.23, 109.01, 58.16, 56.53, 55.24, 52.26, 51.43, 50.23, 41.92, 39.04, 36.91, 34.53, 29.84, 28.92, 28.36, 28.16, 27.28, 24.74, 24.15, 23.02, 21.95, 21.90, 21.64, 21.30, 19.66, 18.33, 18.10, 16.94.

Synthesis of H₂N-Trp (Boc)-N-Me-Leu-D-Leu-N-Me-Val-Asn (Trt)-D-Orn (Boc)-COOH (25a)


SPPS approach was used to prepare **25a** according to the general procedure described under section 8.2. The synthesis was initiated from a resin loaded with Fmoc- D-Orn (Boc)-OH (0.33 g, 0.3 mmol). Crude % yield (92%), ESI-MS m/z calcd for $C_{68}H_{93}N_9O_{12}$: 1227.69; found: 1250.79 $[M+Na]^+$.

Synthesis of cyclo (Trp (Boc)-N-Me-Leu-D-Leu-N-Me-Val-Asn (Trt)-D-Orn (Boc)) (25b)
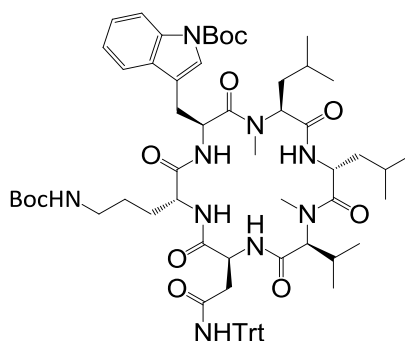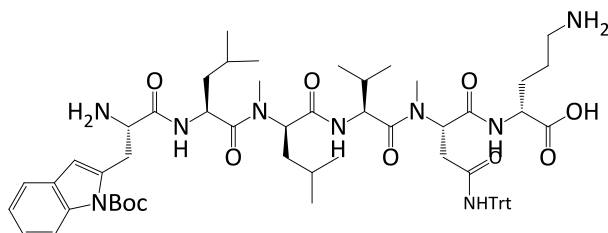

Compound **25b** was obtained through a macrocyclization of **25a** (0.34 g, 0.27 mmol) with HATU (0.31 g, 0.82 mmol), HOBt (0.11 g, 0.82 mmol) and DIPEA (0.48 mL, 2.73 mmol) according to the procedure described in section 8.3. The crude was purified by a column chromatography using a silica gel as a stationary phase and chloroform/methanol (49:1) as a mobile phase to give a white amorphous solid mass. Yield (73%), ESI-MS m/z calcd for $C_{68}H_{91}N_9O_{11}$: 1209.68; found: 1232.72 $[M+Na]^+$. R_f = 0.06 in CHCl₃/MeOH (49:1).

**Synthesis of cyclo (Trp-N-Me-Leu-D-Leu-N-Me-Val-Asn-D-Orn) (25c)**
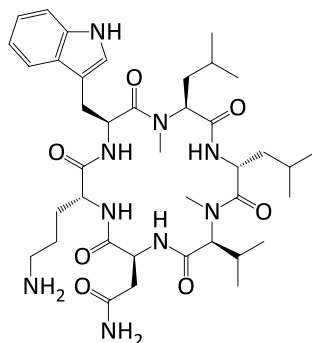
Compound **25b** (0.24 g, 0.2 mmol) was treated with 5 mL of TFA/TIPS/H$_2$O (95:2.5:2.5) for 3 h. The cleaving solution was removed under a strong pressure and the residue was purified by column chromatography using a silica gel as a stationary phase and chloroform/methanol/ammonia solution (80:20:1) as a mobile phase to give a white amorphous solid mass. Yield (60%), mp 85-87 °C, UPLC-MS (UV) purity: 99.9%, RT:0.82 min, ESI-MS m/z calcd for C$_{39}$H$_{61}$N$_9$O$_7$: 767.47; found: 768.47[M+H]$^+$. ^{1}H NMR (400 MHz, CD$_3$OD-d$_4$) δ 7.55 − 7.50 (m, 1H), 7.37 − 7.31 (m, 1H), 7.13 − 7.06 (m, 1H), 7.06 − 6.97 (m, 2H), 5.09 (dd, J = 10.6, 4.6 Hz, 1H), 4.76 − 4.71 (m, 1H), 4.58 − 4.43 (m, 3H), 3.79 (d, J = 10.5 Hz, 1H), 3.37 (dd, J = 13.5, 10.7 Hz, 1H), 3.16 − 3.08 (m, 1H), 3.07 (s, 3H), 3.02 − 2.88 (m, 3H), 2.77 (dd, J = 16.0, 8.3 Hz, 1H), 2.61 (s, 3H), 2.33 (dt, J = 10.5, 6.3 Hz, 1H), 1.88 − 1.44 (m, 9H), 1.39 − 1.28 (m, 1H), 1.02 − 0.83 (m, 12H), 0.43 (dd, J = 51.3, 6.6 Hz, 6H). ^{13}C NMR (101 MHz, CD$_3$OD-d$_4$) δ 174.21, 172.87, 172.82, 171.42, 170.85, 168.98, 136.54, 127.11, 123.28, 121.30, 118.72, 117.79, 111.27, 108.87, 58.42, 56.91, 51.87, 51.01, 49.97, 40.16, 38.95, 36.47, 34.66, 33.21, 33.19, 29.14, 28.37, 28.17, 26.28, 24.77, 24.35, 23.27, 21.66, 21.04, 20.04, 18.88, 18.82, 16.95, 16.78, 12.24.

Synthesis of H$_2$N-Trp (Boc)-Leu-N-Me-D-Leu-Val-N-Me-Asn (Trt)-D-Orn (Boc)-COOH (26a)


SPPS approach was used to prepare **26a** according to the general procedure described under section 8.2. The synthesis was initiated from a resin loaded with Fmoc- D-Orn (Boc)-OH (0.33 g, 0.3 mmol). Crude % yield (95%), ESI-MS m/z calcd for C$_{68}$H$_{93}$N$_9$O$_{12}$: 1227.69; found: 1250.74 [M+Na]$^+$.

**Synthesis of cyclo (Trp (Boc)-Leu-N-Me-D-Leu-Val-N-Me-Asn (Trt)-D-Orn (Boc)) (26b)**
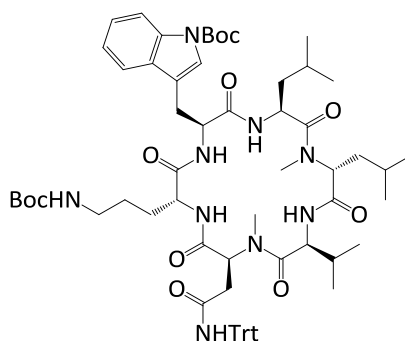
26b was obtained through a macrocyclization of **26a** (0.34 g, 0.28 mmol) with HATU (0.32 g, 0.84 mmol), HOBt (0.11 g, 0.84 mmol) and DIPEA (0.49 mL, 2.79 mmol) according to the procedure described in section 8.3. The crude was purified by a column chromatography using a silica gel as a stationary phase and chloroform/methanol (49:1) as a mobile phase to give a white amorphous solid mass. Yield (60%), ESI-MS m/z calcd for C$_{68}$H$_{91}$N$_9$O$_{11}$: 1209.68; found: 1232.69 [M+Na]$^+$. R$_f$ = 0.11 in CHCl$_3$/MeOH (49:1).

**Synthesis of cyclo (Trp-Leu-N-Me-D-Leu-Val-N-Me-Asn-D-Orn) (26c)**
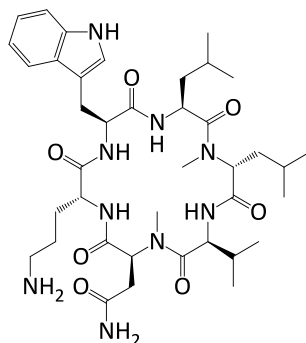
26b (0.08g, 0.07 mmol) was treated with 3 mL of TFA/TIPS/H$_2$O (95:2.5:2.5) for 3 h. The cleaving solution was removed under a strong pressure and the residue was purified by column chromatography using a silica gel as a stationary phase and chloroform/methanol/ammonia solution (80:20:1) as a mobile phase to give a white amorphous solid mass. Yield (63%), mp 93-95 °C, UPLC-MS (UV) purity: 98%, RT:0.82 min, ESI-MS m/z calcd for C$_{39}$H$_{61}$N$_9$O$_7$: 767.47; found: 768.47 [M+H]$^+$. ^{1}H NMR (400 MHz, CD$_3$OD-d$_4$) δ 7.68 (d, J = 7.8 Hz, 1H), 7.37 − 7.29 (m, 1H), 7.18 (s, 1H), 7.14 − 7.07 (m, 1H), 7.06 − 6.97 (m, 1H), 5.26 (dd, J = 8.7, 6.9 Hz, 1H), 4.92 (d, J = 4.3 Hz, 1H), 4.68 (dd, J = 9.8, 5.5 Hz, 1H), 4.60 (q, J = 8.2, 7.5 Hz, 1H), 4.39 (dq, J = 8.4, 4.9, 3.9 Hz, 1H), 4.28 (dd, J = 8.3, 5.3 Hz, 1H), 3.47 (dd, J = 14.6, 5.5 Hz, 1H), 3.31 (d, J = 5.4 Hz, 3H), 3.15 (dd, J = 16.4, 5.3 Hz, 1H), 3.09 − 3.00 (m, 1H), 2.97 (d, J = 5.8 Hz, 3H), 2.89 − 2.82 (m, 1H), 2.77 − 2.61 (m, 2H), 2.11 (dq, J = 11.2, 6.6 Hz, 1H), 1.78 − 1.54 (m, 4H), 1.42 (dddd, J = 24.0, 18.0, 9.2, 5.6 Hz, 6H), 1.07 − 0.78 (m, 18H). ^{13}C NMR (101 MHz, CD$_3$OD-d$_4$) δ 174.12, 172.91, 172.74, 172.06, 172.02, 170.39, 170.15, 136.69, 127.00, 123.64, 121.06, 118.47, 118.07, 110.92, 109.77, 61.68, 54.55, 54.05, 53.75, 52.00, 48.95, 40.21, 38.65, 38.03, 36.58, 33.37, 30.75, 29.53, 28.18, 27.37, 24.56, 24.29, 23.25, 21.87, 21.71, 21.22, 21.12, 19.24, 15.73.

Synthesis of H₂N- Trp (Boc)-D-Orn (Boc)-Asn (Trt)-Val-D-Leu-Leu-COOH (27a)
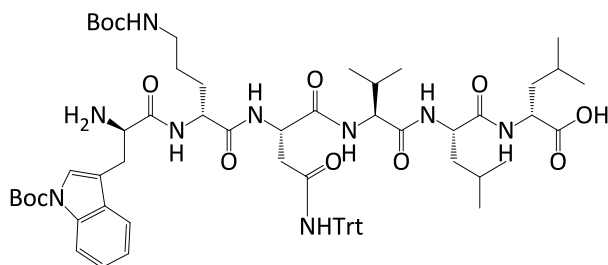

SPPS approach was used to prepare **27a** according to the general procedure described under section 8.2. The synthesis was initiated from a resin loaded with Fmoc-Leu-OH (0.63 g, 0.5 mmol). Crude % yield (92%), ESI-MS m/z calcd for $C_{66}H_{89}N_9O_{12}$:1199.66; found: 1222.71 $[M+Na]^+$.

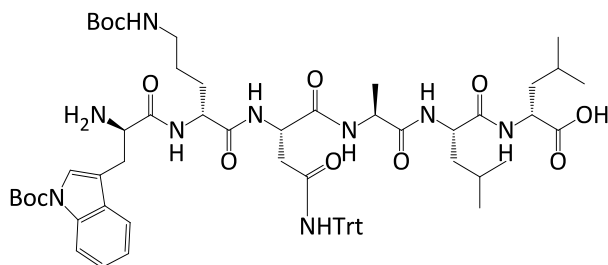**Synthesis of cyclo (Trp (Boc)-D-Orn (Boc)-Asn (Trt)-Val-D-Leu-Leu) (27b)**
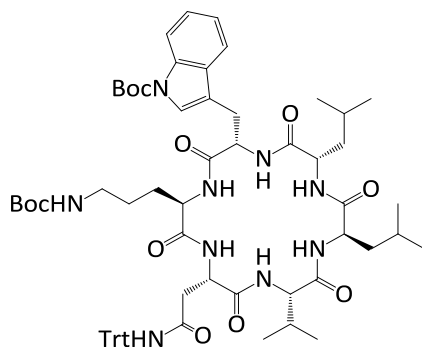
Compound **27b** was obtained through a macrocyclization of **27a** (0.2 g, 0.17 mmol) with HATU (0.19 g, 0.51 mmol), HOBt (0.07 g, 0.51 mmol) and DIPEA (0.19 g, 1.7 mmol) in DMF (170 mL) according to the procedure described in section 8.3. It was purified by a column chromatography using a silica gel as a stationary phase and chloroform/methanol (97:3) as a mobile phase to give a white amorphous solid mass. Yield (50 %), ESI-MS m/z calcd for $C_{66}H_{87}N_9O_{11}$: 1181.65; found: 1180.97$[M-H]^-$. R_f = 0.11 in $CHCl_3$/MeOH (97:3).

**Synthesis of cyclo (Trp-Val-Asn-D-Orn-D-Leu-Leu) (27c)**
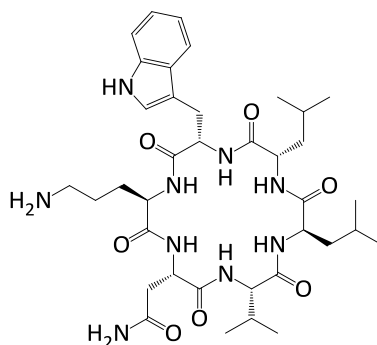
Compound **27b** (0.08g, 0.07 mmol) was treated with 3 mL of TFA/TIPS/H_2O (95:2.5/2.5/) for 3 h. The cleaving solution was removed under a strong pressure and the residue was purified by column chromatography using a silica gel as a stationary phase and chloroform/methanol/ammonia solution (80:20:1) as a mobile phase to give a white amorphous solid mass. Yield (89%), mp 142-145 °C, UPLC-MS (UV) purity: 97%, RT:0.78 min, ESI-MS m/z calcd for $C_{37}H_{57}N_9O_7$: 739.44; found: 740.44 [M+H]$^+$. ^{1}H NMR (400 MHz, CD_3OD-d_4) δ 7.62 (d, J = 7.9 Hz, 1H), 7.33 (d, J = 8.1 Hz, 1H), 7.14 − 7.04 (m, 2H), 7.00 (d, J = 7.3 Hz, 1H), 4.75 (t, J = 7.4 Hz, 1H), 4.61 (dd, J = 8.6, 4.2 Hz, 1H), 4.31 (d, J = 7.6 Hz, 1H), 4.25 − 4.12 (m, 2H), 4.02 (t, J = 7.5 Hz, 1H), 3.37 − 3.32 (m, 1H), 3.23 (dd, J = 14.3, 7.4 Hz, 1H), 2.84 (dd, J = 15.9, 4.2 Hz, 1H), 2.71 (dd, J = 15.8, 8.6 Hz, 1H), 2.55 (t, J = 7.2 Hz, 2H), 2.16 (h, J = 6.9 Hz, 1H), 1.68 − 1.20 (m, 10H), 1.01 − 0.77 (m, 18H). ^{13}C NMR (101 MHz, CD_3OD-d_4) δ 174.05, 173.44, 173.16, 172.49, 171.99, 171.50, 171.22, 136.56, 127.56, 123.09, 120.96, 118.28, 118.14, 110.87, 109.91, 58.01, 54.39, 53.42, 52.99, 52.16, 51.26, 39.77, 39.62, 39.36, 35.91, 31.59, 28.07, 26.76, 25.87, 24.59, 24.47, 22.25, 21.38, 21.32, 19.61, 17.99, 17.68.

Preparation of H$_2$N-Trp (Boc)-D-Orn (Boc)-Asn (Trt)-Ala-D-Leu-Leu-COOH (28a)


SPPS approach was used to prepare **28a** according to the general procedure described under section 8.2. The synthesis was initiated from a resin loaded with Fmoc-Leu-OH (0.38 g, 0.3 mmol). Crude % yield (93%), ESI-MS m/z calcd for C$_{66}$H$_{89}$N$_9$O$_{12}$:1171.63; found: 1194.58 [M+Na]$^+$.

Preparation of cyclo (Trp (Boc)-D-Orn (Boc)-Asn (Trt)-Ala-D-Leu-Leu) (28b)
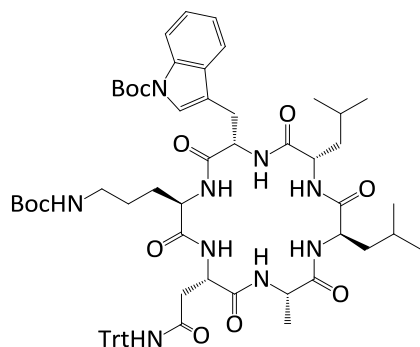
Compound **28b** was obtained through a macrocyclization of **28a** (0.2 g, 0.17 mmol) with HATU (0.19 g, 0.51 mmol), HOBt (0.07 g, 0.51 mmol) and DIPEA (0.19 g, 1.7 mmol) in DMF (170 mL) according to the procedure described in section 8.3. It was purified by a column chromatography using a silica gel as a stationary phase and chloroform/methanol (97:3) as a mobile phase to give a white amorphous solid mass. Yield (46%), ESI-MS m/z calcd for C$_{66}$H$_{87}$N$_9$O$_{11}$: 1153.62; found: 1176.63 [M+Na]$^+$. R$_f$ = 0.20 in CHCl$_3$/MeOH (95:5).

Preparation of cyclo(Trp-D-Orn-Asn-Ala-D-Leu-Leu) (28c)
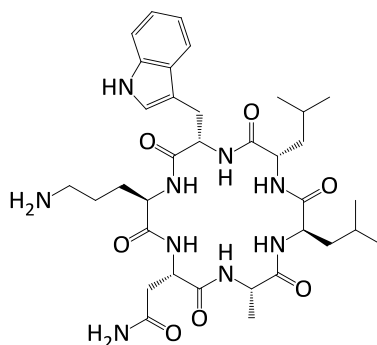
Compound **28b** (0.06 g, 0.05 mmol) was treated with 1 mL of TFA/TIPS/H$_2$O (95:2.5/2.5/) for 3 h. The cleaving solution was removed under a strong pressure and the residue was purified by column chromatography using a silica gel as a stationary phase and chloroform/methanol/ammonia solution (80:20:1) as a mobile phase to give a white amorphous solid mass. Yield (94%), mp 232-235 °C, UPLC-MS (UV) purity: 96%, RT:0.73 min, ESI-MS m/z calcd for C$_{35}$H$_{53}$N$_9$O$_7$: 711.41; found: 712.41 [M+H]$^+$. ^{1}H NMR (400 MHz, CD$_3$OD-d$_4$) δ 7.60 (dt, J = 7.9, 1.0 Hz, 1H), 7.33 (dt, J = 8.2, 0.9 Hz, 1H), 7.14 − 7.05 (m, 2H), 7.02 (ddd, J = 8.0, 7.0, 1.1 Hz, 1H), 4.68 (dd, J = 7.8, 6.8 Hz, 1H), 4.61 (dd, J = 9.1, 3.9 Hz, 1H), 4.48 (q, J = 6.8 Hz, 2H), 4.28 − 4.16 (m, 2H), 3.99 − 3.86 (m, 1H), 3.28 − 3.15 (m, 2H), 2.87 − 2.78 (m, 1H), 2.70 − 2.55 (m, 3H), 1.64 − 1.51 (m, 6H), 1.50 − 1.43 (m, 1H), 1.38 (d, J = 6.7 Hz, 3H), 1.25 (ddt, J = 10.0, 7.5, 5.0 Hz, 3H), 1.02 − 0.80 (m, 12H).

8.5.2. Synthesis of hirsutellides

Synthesis of (R)-2-hydroxy-3-phenylpropanoic acid (29)
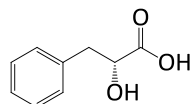
To an ice cooled solution of D-phenylalanine (6.6 gm, 40 mmol) in H_2SO_4 (1N, 45 mL) was added 40% $NaNO_2$ (12 mL) over a period of 1 hour. The reaction mixture was continued to be stirred at 0 ^{o}C for 8 h and kept at room temperature for additional 12 h. To push the reaction to completion, additional H_2SO_4 (1N, 10 mL) and 40% $NaNO_2$ (6 mL) were added in similar conditions as above and continued to be stirred for further 8 h. At the end of the reaction, the reaction mixture was saturated by NaCl, and extracted with EtOAc (3X60 mL). The combined EtOAc extract was washed by brine, dried with $MgSO_4$, filtered and evaporated to give a white crude solid mass which was recrystallized from diethyl ether to give the target compound. yield (68%), $[\alpha]_D^{20}$ = +20.4 (c 1, ethanol), R_f = 0.64 in MeOH., ESI-MS m/z calcd for $C_9H_{10}O_3$: 166.17; found: 165.22 [M-H]$^-$, ^{1}H NMR (400 MHz, Methanol-d4) δ 7.32 – 7.13 (m, 5H), 4.33 (dd, J = 8.0, 4.4 Hz, 1H), 3.09 (dd, J = 13.9, 4.4 Hz, 1H), 2.89 (dd, J = 13.9, 8.0 Hz, 1H).

**Synthesis of (R)-benzyl 2-hydroxy-3-phenylpropanoate (30)**
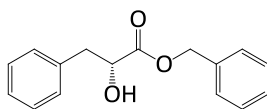
Into a 100-mL round-bottom flask equipped with a Stark and Dean distilling receiver were placed compound **29** (1.66 g, 10 mmol), p-toluenesulfonic acid monohydrate (0.069 g, .40 mmol), benzyl alcohol (1.6 mL, 15 mmol), and toluene (40 mL). The reaction mixture was heated under reflux (250 °C) for 4 h until water was no longer distilled off. After the reaction is completed, the mixture was allowed to cool at room temperature, 30 mL ether and 50 mL saturated Na_2CO_3 was added to set an organic and aqueous phase. The organic layer was separated and the aqueous layer was washed with ether (2X30 mL). The combined ether

extract was again washed with 100 mL brine, dried with MgSO$_4$, filtered and the solvent was evaporated under reduced pressure to get oily crude product. The crude product was then purified by column chromatography on silica gel using petroleum ether (40-60) and EtOAc (10:1) as a mobile phase to get a faint yellow oily product. yield (77%), R$_f$ = 0.11 in EtOAc /heptanes (1:1), ESI-MS m/z calcd for C$_{16}$H$_{16}$O$_3$: 256.30; found: 279.03 [M+Na]$^+$, ^{1}H NMR (400 MHz, CDCl$_3$-d) δ 7.47 – 7.11 (m, 10H), 5.20 (t, J = 1.9 Hz, 2H), 4.51 (ddd, J = 6.4, 4.7, 1.5 Hz, 1H), 3.15 (ddd, J = 14.0, 4.7, 1.6 Hz, 1H), 3.07 – 2.96 (m, 1H), 2.95 – 2.71 (bs, 1H).

Synthesis of (R)-benzyl 2-(2-((tert-butoxycarbonyl)(methyl)amino)acetoxy)-3-phenylpropanoate (31)
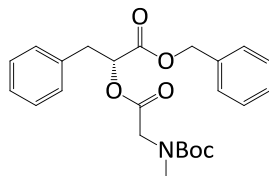
N-Me-Boc-Gly-OH (0.84 g, 4.45 mmol), **30** (1.14 g, 4.45 mmol) and DMAP (0.05 g, 4.45 mmol) were dissolved in 25 mL of dry DCM and allowed to cool to 0°C while stirring. EDC*HCl (1.02 g, 5.34 mmol) was added to the mixture and the whole reaction mixture continued to be stirred for 2 h in an ice bath (0 °C) and at room temperature for additional 24 h. Following the completion of the reaction, the contents were transferred to a separatory funnel. Three layers were formed when water (63 mL) and EtOAc (84 mL) were added to the separatory funnel. Upon shaking, the dichloromethane portion that sank down to the aqueous layer was re-extracted to the EtOAc layer to form an organic and aqueous phase. The organic phase was then separated and the aqueous layer was re-extracted twice by 50 ml EtOAc. Finally the combined organic extract was saturated by KHSO$_4$, washed with brine, dried by MgSO$_4$ and the solvent was removed under reduced pressure. The obtained oily mass was purified by column chromatography using silica gel as a stationary phase and petroleum ether/ EtOAc (1:1) as a mobile phase. Yield (90%), R$_f$ = 0.51 in EtOAc/hexane (1:1), ESI-MS m/z calcd for C$_{24}$H$_{29}$NO$_6$: 427.49; found: 450.02 [M+Na]$^+$, ^{1}H NMR (400 MHz, CDCl$_3$-d) δ 7.25 (m, 10H), 5.33 (dt, J = 9.0,

4.3 Hz, 1H), 5.21 − 5.04 (m, 2H), 4.14 − 3.96 (m, 1H), 3.93 (s, 1H), 3.15 (dtd, J = 22.4, 14.3, 8.9 Hz, 2H), 2.81, 2.79 (s, 3H, rotamers), 1.47, 1.33 (s, 9H, rotamers).

Synthesis of (R)-2-((1-(benzyloxy)-1-oxo-3-phenylpropan-2-yl)oxy)-N-methyl-2-oxoethanaminium (32)
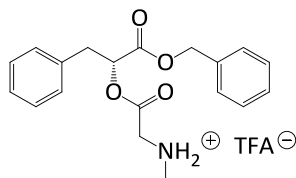
Compound **31** (1.73 g, 4.04 mmol) was dissolved in dry DCM (6 mL) and allowed to cool to 0 °C while stirring. TFA (2 mL, 26.04 mmol) was added drop wise and the reaction slowly allowed to warm to room temperature and stirred for 4 h. The product was concentrated under strong vacuum pressure to ensure complete removal of TFA. The obtained brownish crude mass was used directly for the next reaction without purification.

Synthesis of (R)-benzyl 2-(2-((2S,3R)-2-((tert-butoxycarbonyl)amino)-N,3-dimethylpentanamido)acetoxy)-3-phenylpropanoate (33)
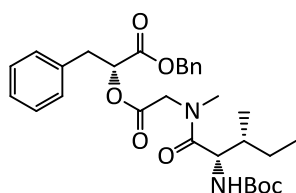

To a solution of **32** (1.1 g, 3.4 mmol) in dry DCM (30 mL) was added N-Boc-allo-Ile-OH (0.86 g, 4.4 mmol) and HATU (1.84 g, 4.8 mmol). The mixture was then allowed to be cooled to 0 °C and DIPEA (6.0 mL, 34.0 mmol) was added drop wise. The reaction slowly allowed to warm to room temperature and stirred for 14 h. It was then quenched by adding saturated ammonium chloride (2 mL) drop wise and followed by removal of the solvent under reduced pressure., The residue was then dissolved in 120 mL EtOAc and the organic phase was washed by saturated $NaHCO_3$ (2X100 mL) and brine (100 mL), dried with $MgSO_4$, filtered and the solvent was evaporated under reduced pressure. The obtained brownish yellow oily mass was then purified

by column chromatography using EtOAc/heptane (3:2) as a mobile phase and silica gel as a stationary phase. Yield (88%), R_f =0.48 in EtOAc/heptane (1:1), ESI-MS m/z calcd for $C_{30}H_{40}N_2O_7$: 540.65; found: 563.08 [M+Na]$^+$.

Synthesis of (6S,12R)-12-benzyl-6-((R)-sec-butyl)-2,2,8-trimethyl-4,7,10-trioxo-3,11-dioxa-5,8-diazatridecan-13-oic acid (33a)
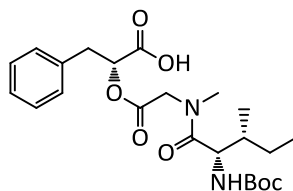

Compound **33** (0.89 g, 1.65 mmol) was dissolved in EtOAc (80 mL) and kept in a hydrogenator reaction vessel. 10% Pd (0.44 g) catalyst was added to the solution to form a suspension. The reaction mixture was then subjected to 5 atm hydrogen gas and stirred over night. After the end of the reaction, the catalyst was removed by filtration, and the filtrate was concentrated in vacuum to give **33a**. Yield (92%), ESI-MS m/z calcd for $C_{23}H_{34}N_2O_7$: 450.53; found: 449.23 [M-H]$^-$.

Synthesis of (2S,3R)-1-((2-(((R)-1-(benzyloxy)-1-oxo-3-phenylpropan-2-yl)oxy)-2-oxoethyl)(methyl)amino)-3-methyl-1-oxopentan-2-aminium (33b)
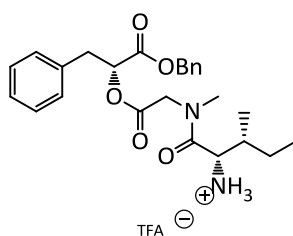
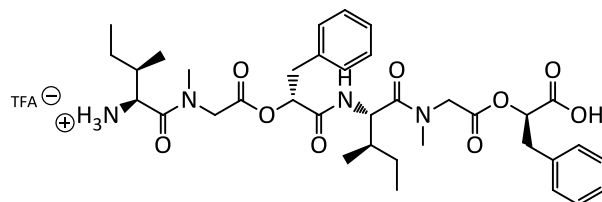Compound **33** (0.7 g, 1.3 mmol) was dissolved in dry DCM (10 mL) and allowed to cool to 0°C while stirring. TFA (2.0 mL, 26.14 mmol) was added drop wise and the reaction slowly allowed to warm to room temperature and stirred for 1 h. The product was concentrated under strong vacuum pressure to ensure complete removal of TFA. The obtained brownish crude mass was used directly for the next reaction without purification.

Synthesis of (R)-benzyl 2-(((6S,12R,15S)-12-benzyl-6,15-di((R)-sec-butyl)-2,2,8,17-tetramethyl-4,7,10,13,16-pentaoxo-3,11-dioxa-5,8,14,17-tetraazanonadecan-19-oyl)oxy)-3-phenylpropanoate (33c)
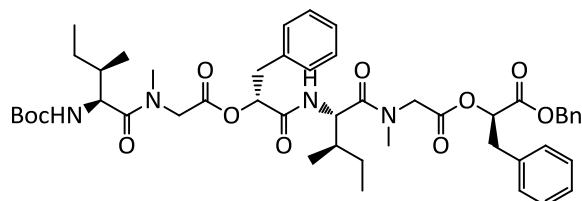
To a solution of **33b** (0.56 g, 1.3 mmol) in dry DCM (30 mL) was added **33a** (0.57 g, 1.3 mmol), BOP-Cl (0.36 g, 1.43 mmol) and HOBt (0.19 g, 1.43 mmol). The mixture was then allowed to be cooled to 0 °C and DIPEA (2.1 mL, 13.0 mmol) was added drop wise. The reaction slowly allowed to warm to room temperature and stirred for 20 h. It was then quenched by adding saturated ammonium chloride (2.5 mL) drop wise. The solvent was evaporated under reduced pressure and the residue was dissolved in 50 mL EtOAc with vigorous stirring. 50 mL saturated NaHCO$_3$ was added to the flask and continued to be stirred till all the contents get dissolve. The content was then transferred to 250 mL separatory flask. The EtOAc layer was again washed with 50 mL saturated NaHCO$_3$ and then by brine (50 mL), Dried with MgSO$_4$, filtered and the solvent was evaporated under reduced pressure. The obtained brownish yellow oily mass was then purified by column chromatography using heptane/EtOAc (3:2) as a mobile phase and silica gel as a stationary phase. Yield (45%), R$_f$ =0.13 in heptane /EtOAc (3:2), ESI-MS m/z calcd for C$_{48}$H$_{64}$N$_4$O$_{11}$: 873.04; found: 896.15 [M+Na]$^+$.

Synthesis of (2R,8S,11R,17S,18R)-11-benzyl-8-((R)-sec-butyl)-2-carboxy-6,15,18-trimethyl-

4,7,10,13,16-pentaoxo-1-phenyl-3,12-dioxa-6,9,15-triazaicosan-17-aminium (33d)

Compound **33c** (0.39 g, 0.44 mmol) was dissolved in EtOAc (60 mL) and kept in a hydrogenator reaction vessel 10% Pd (0.2 g) catalyst was added to the solution to form a suspension. The reaction mixture was subjected to 5 atm hydrogen gas and stirred over night. Afterwards, the catalyst was removed by filtration, and the filtrate was concentrated in vacuum to give **33d**, Yield (92%). It was then used directly for the next reaction

The compound obtained in the above step (0.32 g, 0.4 mmol) was dissolved in dry DCM (8 mL) and allowed to cool to 0 °C while stirring. TFA (2.0 mL, 26.14 mmol) was added drop wise and the reaction slowly allowed to warm to room temperature and stirred for 4 h.The product was concentrated under strong vacuum pressure to ensure complete removal of TFA. The obtained brownish crude mass was used directly for the next reaction without purification.

Synthesis of (6S,9R,15S,18R)-9,18-dibenzyl-6,15-di((R)-sec-butyl)-4,13-dimethyl-1,10-dioxa-4,7,13,16-tetraazacyclooctadecane-2,5,8,11,14,17-hexaone (33e)
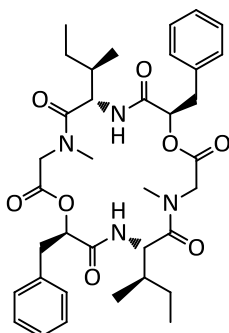

To a solution of **33d** (0.27 g, 0.4 mmol) in DMF (195 mL) was added HATU (0.46 g, 1.2 mmol) and HOBt (0.16 g, 1.2 mmol). The mixture was then allowed to be cooled to 0 °C and DIPEA (0.7 mL, 4.0 mmol) was added drop wise. The reaction slowly allowed to warm to room temperature and stirred for 3 days. Following that, the solvent was concentrated under reduced pressure, the residue dissolved in 50 mL EtOAc, washed by saturated NaHCO$_3$ (2X100 mL) and brine (100 mL), dried with MgSO$_4$, filtered and the solvent was removed under reduced pressure. The obtained brownish yellowish solid mass was then purified by column chromatography using heptane/EtOAc (1:1) as a mobile phase and silica gel as a stationary phase. Yield (50%). mp 254-257 °C, UPLC-MS (UV) purity: 98%, RT 1.29 min, ESI-MS m/z, calcd for C$_{36}$H$_{48}$N$_4$O$_8$: 664.35; found: 665.35[M+H]$^+$, ^{1}H NMR (400 MHz, CDCl$_3$-d) δ 7.53 (d, J = 9.7 Hz, 2H), 7.31 − 7.08 (m, 10H), 5.60 (dd, J = 11.7, 3.0 Hz, 2H), 4.87 (t, J = 10.1 Hz, 2H), 4.40 (d, J = 17.0 Hz, 2H), 3.65 (dd, J = 14.2, 3.0 Hz, 2H), 3.26 (s, 6H), 3.17 (d, J = 17.1 Hz, 2H), 2.73 (dd, J = 14.2, 11.8 Hz, 2H), 2.28 − 2.15 (m, 2H), 1.42 − 1.32 (m, 2H), 1.10 − 1.01 (m, 2H), 0.94 − 0.86 (m, 12H). ^{13}C NMR (101 MHz, cdcl$_3$) δ 174.18, 168.82, 166.76, 136.13, 129.07, 128.56, 127.10, 74.10, 52.95, 51.88, 38.72, 37.89, 36.39, 25.96, 14.32, 11.05.

Synthesis of (R)-benzyl 2-(2-((S)-2-((tert-butoxycarbonyl)amino)-N,4-dimethylpentanamido)acetoxy)-3-phenylpropanoate (34)
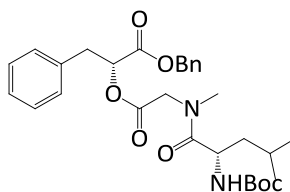

To a solution of **32** (1.31 g, 4.0 mmol) in dry DCM (25 mL) was added N-Boc-Leu-OH (1.02 g, 4.4 mmol) and HATU (1.84 g, 4.8 mmol). The mixture was then allowed to be cooled to 0 °C and TEA (5.6 mL, 39.8 mmol) was added drop wise. The reaction slowly allowed to warm to room temperature and stirred for 14 h. It was then quenched by adding saturated ammonium chloride (2 mL) drop wise and followed by removal of the solvent under reduced pressure. The residue was then dissolved in 150 mL EtOAc and the organic phase was washed by saturated $NaHCO_3$ (2X100 mL) and brine (100 mL), dried with $MgSO_4$, filtered and the solvent was evaporated under reduced pressure. The obtained brownish yellow oily mass was then purified by column chromatography using EtOAc/heptane (3:2) as a mobile phase and silica gel as a stationary phase. Yield (81%), R_f = 0.57 in EtOAc/hexane (1:1), ESI-MS m/z calcd for $C_{30}H_{40}N_2O_7$: 540.65; found: 563.11 $[M+Na]^+$, ^1H NMR (400 MHz, CD_3OD-d_4) δ 7.37 − 7.07 (m, 10H), 5.34 (ddd, J = 9.8, 7.4, 4.9 Hz, 1H), 5.18 − 5.02 (m, 2H), 4.73 − 4.57 (m, 2H), 4.40 (d, J = 17.4 Hz, 1H), 4.16 − 4.00 (m, 1H), 3.90 (dd, J = 17.5, 4.0 Hz, 1H), 3.22 − 3.05 (m, 2H), 3.02 (d, J = 1.7 Hz, 2H), 2.78 (s, 1H), 1.81 − 1.65 (m, 1H), 1.41 (m, 9H), 0.87 (ddd, J = 47.8, 14.8, 6.5 Hz, 6H).

Synthesis of (6S,12R)-12-benzyl-6-isobutyl-2,2,8-trimethyl-4,7,10-trioxo-3,11-dioxa-5,8-diazatridecan-13-oic acid (34a)
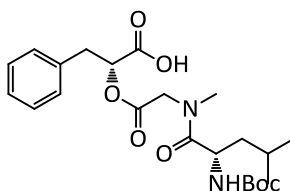
Compound **34** (0.8 g, 1.48 mmol) was dissolved in EtOAc (95 mL) and kept in a hydrogenator reaction vessel 10% Pd (0.8 g) catalyst was added to the solution to form a suspension. The reaction mixture was subjected to 5 atm hydrogen gas and stirred over night. Finally, the catalyst was removed by filtration, and the filtrate was concentrated in vacuum to give **34a**. Yield (66%), ESI-MS m/z calcd for $C_{23}H_{34}N_2O_7$: 450.53; found: 473.1 [M+Na]$^+$.

Synthesis of (S)-1-((2-(((R)-1-(benzyloxy)-1-oxo-3-phenylpropan-2-yl)oxy)-2-oxoethyl)(methyl)amino)-4-methyl-1-oxopentan-2-aminium (34b)
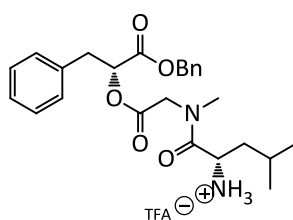
Compound **34** (0.75 g, 0.6 mmol) was dissolved in dry DCM (3.5 mL) and allowed to cool to 0 °C while stirring. TFA (0.82 mL, 10.72 mmol) was added drop wise and the reaction slowly allowed to warm to room temperature and stirred for 4 h.The product was concentrated under strong vacuum pressure to ensure complete removal of TFA. The obtained brownish crude mass was used directly for the next reaction without purification.

Synthesis of (R)-benzyl 2-(((6S,12R,15S)-12-benzyl-6,15-diisobutyl-2,2,8,17-tetramethyl-4,7,10,13,16-pentaoxo-3,11-dioxa-5,8,14,17-tetraazanonadecan-19-oyl)oxy)-3-phenylpropanoate (33c)
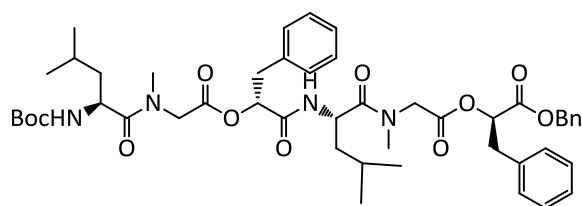

To a solution of **34a** (0.67 g, 1.48 mmol) in dry DCM (20 mL) was added **34b** (0.61 g, 1.39 mmol) and BOP-Cl (0.39 g, 1.53 mmol). The mixture was then allowed to be cooled to 0 °C and TEA (1.4
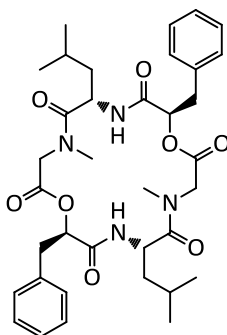
mL, 10.27 mmol) was added drop wise. The reaction slowly allowed to warm to room temperature and stirred for 14 h. It was then quenched by adding saturated ammonium chloride (2 mL) drop wise and followed by removal of the solvent under reduced pressure. The residue was then dissolved in 150 mL EtOAc and the organic phase was washed by saturated NaHCO$_3$ (2X100 mL) and brine (100 mL), dried with MgSO$_4$, filtered and the solvent was removed under reduced pressure. The obtained brownish yellow oily mass was then purified by column chromatography using petroleum ether/EtOAc (2:1) as a mobile phase and silica gel as a stationary phase. Yield (45%), R$_f$ = 0.49 in EtOAc, ESI-MS m/z calcd for C$_{48}$H$_{64}$N$_4$O$_{11}$: 873.04; found: 896.25 [M+Na]$^+$.

Synthesis of (2R,8S,11R,17S)-11-benzyl-2-carboxy-8-isobutyl-6,15,19-trimethyl-4,7,10,13,16-pentaoxo-1-phenyl-3,12-dioxa-6,9,15-triazaicosan-17-aminium (34d)
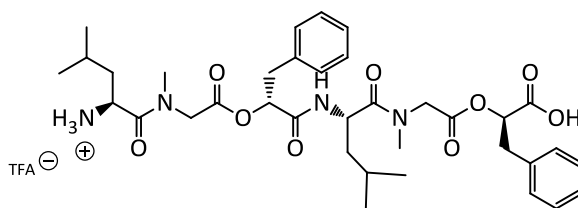
Compound **34c** (0.24 g, 0.28 mmol) was dissolved in EtOAc (30 mL) and kept in a hydrogenator reaction vessel 10% Pd (0.24 g) catalyst was added to the solution to form a suspension. The reaction mixture was subjected to 5 atm hydrogen gas and stirred over night. Finally, the catalyst was removed by filtration, and the filtrate was concentrated in vacuum to obtain the desired product. Yield (70%), ESI-MS m/z calcd for C$_{41}$H$_{58}$N$_4$O$_{11}$: 782.92; found: 805.2 [M+Na]$^+$.

The compound collected in the above step (0.15 g, 0.19 mmol) was dissolved in dry DCM (4 mL) and allowed to cool to 0 °C while stirring. TFA (0.11 mL, 1.25 mmol) was added drop wise and the reaction slowly allowed to warm to room temperature and stirred for 4 h. The product was concentrated under strong vacuum pressure to ensure complete removal of TFA. The obtained brownish crude mass was used directly for the next reaction without purification.

184

Synthesis of (6S,9R,15S,18R)-9,18-dibenzyl-6,15-diisobutyl-4,13-dimethyl-1,10-dioxa-4,7,13,16-tetraazacyclooctadecane-2,5,8,11,14,17-hexaone (34e)

To a solution of **34d** (0.13 g, 0.19 mmol) in DMF (195 ml) was added BOP-Cl (0.22 g, 0.86 mmol). The mixture was then allowed to be cooled to 0 °C and DIPEA (0.26 mL, 1.92 mmol) was added drop wise. The reaction slowly allowed to warm to room temperature and stirred for 3 days. It was then quenched by adding saturated ammonium chloride (2 mL) drop wise and followed by removal of the solvent under reduced pressure. The residue was then dissolved in 100 mL EtOAc and the organic phase was washed by saturated NH_4Cl (2X100 mL), saturated $NaHCO_3$ (2X100 mL) and brine (100 mL), dried with $MgSO_4$, filtered and the solvent was removed under reduced pressure. The obtained brownish yellow oily mass was then purified by column chromatography using petroleum ether/EtOAc (1:1) as a mobile phase and silica gel as a stationary phase. This gave a colorless oily mass. Yield (25%), UPLC-MS (UV) purity: 93%, RT 1.28 min, ESI-MS m/z calcd for $C_{36}H_{48}N_4O_8$: 664.35; found: 665.35 [M+H]$^+$, ^{1}H NMR (400 MHz, $CDCl_3$-d) δ 7.48 (d, *J* = 9.5 Hz, 2H), 7.31 − 7.11 (m, 10H), 5.61 (dd, *J* = 11.4, 3.2 Hz, 2H), 5.22 (dt, *J* = 9.6, 7.4 Hz, 2H), 4.43 (d, *J* = 17.2 Hz, 2H), 3.63 (dd, *J* = 14.2, 3.2 Hz, 2H), 3.26 (s, 6H), 3.18 (d, *J* = 17.2 Hz, 2H), 2.74 (dd, *J* = 14.2, 11.4 Hz, 2H), 1.77 (h, *J* = 6.6 Hz, 4H), 1.53 (dt, *J* = 13.5, 6.6 Hz, 2H), 0.99 − 0.86 (m, 12H).

Synthesis of (R)-benzyl 2-(2-((S)-2-((tert-butoxycarbonyl)amino)-N,3-dimethylbutanamido)acetoxy)-3-phenylpropanoate (35)
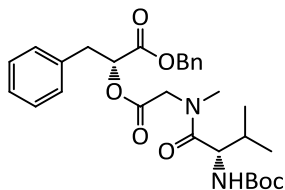
To a solution of **32** (2.1 g, 6.4 mmol) in dry DCM (30 mL) was added N-Boc-Val-OH (1.6 g, 7.04 mmol) and HATU (2.9 g, 7.68 mmol). The mixture was then allowed to be cooled to 0 °C and TEA (8.9 mL, 64.0 mmol) was added drop wise. The reaction slowly allowed to warm to room temperature and stirred for 24 h. It was then quenched by adding saturated ammonium chloride (2 mL) drop wise and followed by removal of the solvent under reduced pressure., The residue was then dissolved in 200 mL EtOAc and the organic phase was washed by saturated NaHCO$_3$ (2X100 mL) and brine (100 mL), dried with MgSO$_4$, filtered and the solvent was evaporated under reduced pressure. The obtained brownish yellow oily mass was then purified by column chromatography using EtOAc/ petroleum ether (1:2) as a mobile phase and silica gel as a stationary phase. Yield (88%), R$_f$ = 0.6 in EtOAc/petroleum ether (1:1), ESI-MS m/z, calcd for C$_{29}$H$_{38}$N$_2$O$_7$: 526.62; found: 549.16 [M+Na]$^+$, ^{1}H NMR (500 MHz, CDCl$_3$-d) δ 7.35 − 7.06 (m, 10H), 5.32 − 5.26 (m, 1H), 5.13 (d, J = 11.6 Hz, 2H), 5.03 (d, J = 12.2 Hz, 1H), 4.52 − 4.46 (m, 2H), 3.78 (dd, J = 17.3, 12.5 Hz, 1H), 3.14 − 3.06 (m, 3H), 2.96 (s, 2H), 2.93 (d, J = 1.4 Hz, 0H), 1.98 − 1.91 (m, 1H), 1.39 (t, J = 3.8 Hz, 9H), 0.96 (dd, J = 6.8, 2.4 Hz, 3H), 0.85 (dd, J = 10.4, 6.7 Hz, 3H).

Synthesis of (6S,12R)-12-benzyl-6-isopropyl-2,2,8-trimethyl-4,7,10-trioxo-3,11-dioxa-5,8-diazatridecan-13-oic acid (35a)
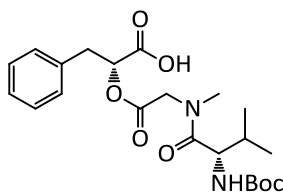
Compound **35** (0.59 g, 1.47 mmol) was dissolved in EtOAc (70 mL) and kept in a hydrogenator reaction vessel 10% Pd (0.59 g) catalyst was added to the solution to form a suspension. The reaction mixture was subjected to 5 atm hydrogen gas and stirred over night. Finally, the catalyst was removed by filtration, and the filtrate was concentrated in vacuum to give **35a**. Yield (90%), ESI-MS m/z calcd for $C_{22}H_{32}N_2O_7$: 436.50; found: 459.43 $[M+Na]^+$.

Synthesis of (S)-1-((2-(((R)-1-(benzyloxy)-1-oxo-3-phenylpropan-2-yl)oxy)-2-oxoethyl)(methyl)amino)-3-methyl-1-oxobutan-2-aminium (35b)
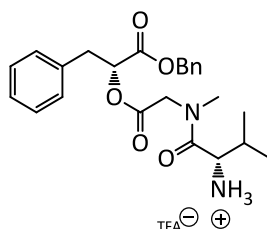
Compound **35** (0.52 g, 0.99 mmol) was dissolved in dry DCM (8 mL) and allowed to cool to 0 °C while stirring. TFA (1.15 mL, 15.0 mmol) was added drop wise and the reaction slowly allowed to warm to room temperature and stirred for 4 h. The product was concentrated under strong vacuum pressure to ensure complete removal of TFA. The obtained brownish crude mass was used directly for the next reaction without purification.

187

Synthesis of (R)-benzyl 2-(((6S,12R,15S)-12-benzyl-6,15-diisopropyl-2,2,8,17-tetramethyl-4,7,10,13,16-pentaoxo-3,11-dioxa-5,8,14,17-tetraazanonadecan-19-oyl)oxy)-3-phenylpropanoate (35c)
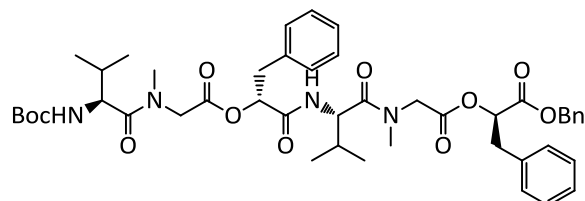
To a solution of **35a** (0.56 g, 1.01 mmol) in dry DCM (20 mL) was added **35b** (0.57 g, 0.99 mmol) and BOP-Cl (0.25 g, 1.0 mmol). The mixture was then allowed to be cooled to 0 °C and TEA (1.4 mL, 10.0 mmol) was added drop wise. The reaction slowly allowed to warm to room temperature and stirred for 24 h. It was then quenched by adding saturated ammonium chloride (2 mL) drop wise and followed by removal of the solvent under reduced pressure. The residue was then dissolved in 100 mL EtOAc and the organic phase was washed by saturated $NaHCO_3$ (2X100 mL) and brine (100 mL), dried with $MgSO_4$, filtered and the solvent was removed under reduced pressure. The obtained brownish yellow oily mass was then purified by column chromatography using EtOAc/heptane (1:1) as a mobile phase and silica gel as a stationary phase. Yield (50%), R_f = 0.19 in EtOAc/heptane (1:1), ESI-MS m/z calcd for $C_{46}H_{60}N_4O_{11}$: 844.99; found: 867.28 $[M+Na]^+$.

Synthesis of (2R,8S,11R,17S)-11-benzyl-2-carboxy-8-isopropyl-6,15,18-trimethyl-4,7,10,13,16-pentaoxo-1-phenyl-3,12-dioxa-6,9,15-triazanonadecan-17-aminium (35d)


Compound **35c** (0.27 g, 0.31 mmol) was dissolved in EtOAc (50 mL) and kept in a hydrogenator reaction vessel 10% Pd (0.27 g) catalyst was added to the solution to form a suspension. The

reaction mixture was subjected to 5 atm hydrogen gas and stirred over night. Finally, the catalyst was removed by filtration, and the filtrate was concentrated in vacuum to obtain the product, Yield (91%).

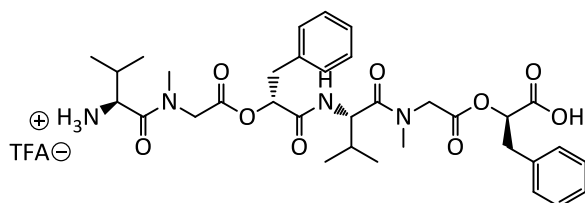The product obtained in the above step (0.22 g, 0.29 mmol) was dissolved in dry DCM (10 mL) and allowed to cool to 0°C while stirring. TFA (0.14 mL, 1.85 mmol) was added drop wise and the reaction slowly allowed to warm to room temperature and stirred for 4 h. The product was concentrated under strong vacuum pressure to ensure complete removal of TFA. The obtained brownish crude mass was used directly for the next reaction without purification.

Synthesis of (6S,9R,15S,18R)-9,18-dibenzyl-6,15-diisopropyl-4,13-dimethyl-1,10-dioxa-4,7,13,16-tetraazacyclooctadecane-2,5,8,11,14,17-hexaone (35e)
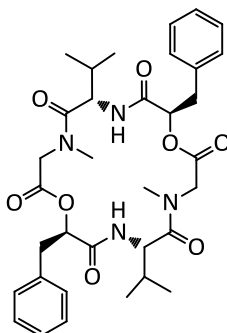
To a solution of **35d** (0.19 g, 0.29 mmol) in DMF (190 mL) was added HATU (0.33 g, 0.86 mmol) and HOBt (0.12 g, 0.86 mmol). The mixture was then allowed to be cooled to 0 °C and DIPEA (0.5 mL, 2.9 mmol) was added drop wise. The reaction slowly allowed to warm to room temperature and stirred for 3 days. Following that, the solvent was concentrated under reduced pressure, the residue dissolved in 50 mL EtOAc, washed by saturated NaHCO$_3$ (2X100 mL) and brine (160 mL), dried with MgSO$_4$, filtered and the solvent was removed under reduced pressure. The obtained brownish yellowish solid mass was then purified by column chromatography using heptane/EtOAc (1:1) as a mobile phase and silica gel as a stationary phase. Yield (39%), mp 215-217 °C, UPLC-MS (UV) purity: 98%, RT 1.17 min, ESI-MS m/z calcd for C$_{34}$H$_{44}$N$_4$O$_8$: 636.32; found: 637.32 [M+H]$^+$, ^{1}H NMR (500 MHz, CD$_3$OD-d$_4$) δ 7.70 (d, J = 9.7 Hz, 2H), 7.33 – 7.16 (m, 10H), 5.50 (dd, J = 11.2, 3.2 Hz, 2H), 4.88 – 4.78 (m, 2H), 4.31 (d, J = 17.3

Hz, 2H), 3.59 – 3.47 (m, 4H), 3.28 (s, 6H), 2.77 (dd, *J* = 14.1, 11.2 Hz, 2H), 2.36 – 2.28 (m, 2H), 0.98 – 0.85 (m, 12H). ^{13}C NMR (126 MHz, cd$_3$od) δ 173.81, 169.63, 167.26, 136.08, 128.90, 128.31, 126.84, 74.06, 54.23, 51.22, 38.27, 36.93, 30.40, 17.96, 17.29.

Synthesis of (R)-benzyl 2-(2-(2-((tert-butoxycarbonyl)amino)-N-methylacetamido)acetoxy)-3-phenylpropanoate (36)
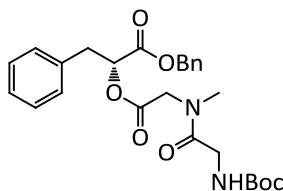
To a solution of **32** (1.0 g, 3.1 mmol) in dry DCM (20 mL) was added N-Boc-Gly-OH (0.6 g, 3.4 mmol) and HATU (1.4 g, 3.72 mmol). The mixture was then allowed to be cooled to 0 °C and TEA (4.3 mL, 31.0 mmol) was added drop wise. The reaction slowly allowed to warm to room temperature and stirred for 12 h. It was then quenched by adding saturated ammonium chloride (2 mL) drop wise and followed by removal of the solvent under reduced pressure., The residue was then dissolved in 120 mL EtOAc and the organic phase was washed by saturated NaHCO$_3$ (2X100 mL) and brine (100 mL), dried with MgSO$_4$, filtered and the solvent was evaporated under reduced pressure. The obtained faint yellow oily mass was then purified by column chromatography using EtOAc/ heptane (2:3) as a mobile phase and silica gel as a stationary phase. Yield (54%), R$_f$ = 0.11 in EtOAc/heptane (2:3). ESI-MS m/z calcd for C$_{27}$H$_{34}$N$_2$O$_7$: 498.57; found: 521.23 [M+Na]$^+$.

Synthesis of (R)-12-benzyl-2,2,8-trimethyl-4,7,10-trioxo-3,11-dioxa-5,8-diazatridecan-13-oic acid (36a)
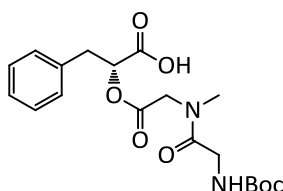
Compound **36** (0.38 g, 0.77 mmol) was dissolved in EtOAc (50 mL) and kept in a hydrogenator reaction vessel 10% Pd (0.09 g) catalyst was added to the solution to form a suspension. The reaction mixture was subjected to 5 atm hydrogen gas and stirred over night. The catalyst was removed by filtration, and the filtrate was concentrated in vacuum to give **36a**. Yield (96%), ESI-MS calcd for $C_{19}H_{26}N_2O_7$: 394.42; found: 393.11 [M-H]$^-$.

Synthesis of (R)-2-((2-((1-(benzyloxy)-1-oxo-3-phenylpropan-2-yl)oxy)-2-oxoethyl)(methyl)amino)-2-oxoethanaminium (36b)
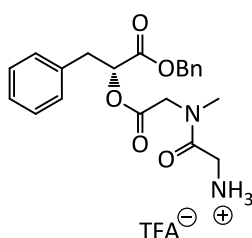
Compound **36** (0.35 g, 0.72 mmol) was dissolved in dry DCM (2 mL) and allowed to cool to 0 °C while stirring. TFA (0.4 mL, 5.1 mmol) was added drop wise and the reaction slowly allowed to warm to room temperature and stirred for 1 h. The product was concentrated under strong vacuum pressure to ensure complete removal of TFA. The obtained brownish crude mass was used directly for the next reaction without purification.

Synthesis of (R)-benzyl 2-(((R)-12-benzyl-2,2,8,17-tetramethyl-4,7,10,13,16-pentaoxo-3,11-dioxa-5,8,14,17-tetraazanonadecan-19-oyl)oxy)-3-phenylpropanoate (36c)
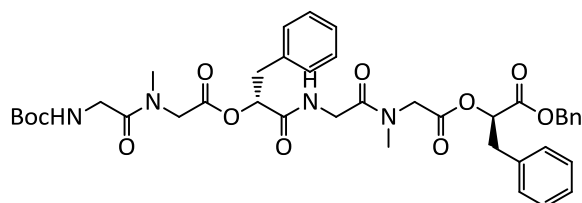
To a solution of **36a** (0.31 g, 0.78 mmol) in dry DCM (15 mL) was added **36b** (0.28 g, 0.72 mmol) and BOP-Cl (0.25 g, 1.0 mmol). The mixture was then allowed to be cooled to 0 °C and DIPEA (1.36 mL, 7.8 mmol) was added drop wise. The reaction slowly allowed to warm to room

temperature and stirred for 8 h. It was then quenched by adding saturated ammonium chloride (2 mL) drop wise and followed by removal of the solvent under reduced pressure. The residue was then dissolved in 100 mL EtOAc and the organic phase was washed by saturated NaHCO$_3$ (2X100 mL) and brine (100 mL), dried with MgSO$_4$, filtered and the solvent was removed under reduced pressure. The obtained yellowish oily mass was then purified by column chromatography using heptane/EtOAc (2:3) as a mobile phase and silica gel as a stationary phase. Yield (40%), R$_f$ = 0.28 in EtOAc, ESI-MS m/z calcd for C$_{40}$H$_{48}$N$_4$O$_{11}$: 760.83; found: 783.21 [M+Na]$^+$.

Synthesis of (7R,16R)-7-benzyl-16-carboxy-3,12-dimethyl-2,5,8,11,14-pentaoxo-17-phenyl-6,15-dioxa-3,9,12-triazaheptadecan-1-aminium (36d)
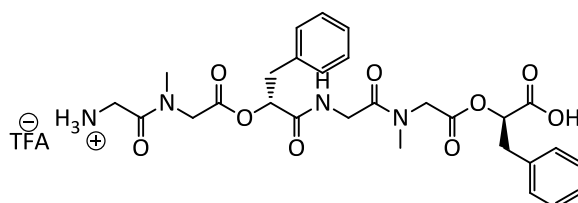

Compound **36c** (0.17 g, 0.23 mmol) was dissolved in EtOAc (40 mL) and kept in a hydrogenator reaction vessel 10% Pd (0.05 g) catalyst was added to the solution to form a suspension. The reaction mixture was subjected to 5 atm hydrogen gas and stirred over night. Finally, the catalyst was removed by filtration, and the filtrate was concentrated in vacuum to obtain the product, Yield (96%).

The obtained product (0.15 g, 0.22 mmol) was dissolved in dry DCM (2 mL) and allowed to cool to 0 °C while stirring. TFA (0.12 mL, 1.52 mmol) was added drop wise and the reaction slowly allowed to warm to room temperature and stirred for 4 h. The product was concentrated under strong vacuum pressure to ensure complete removal of TFA. The obtained brownish crude mass was used directly for the next reaction without purification.

Synthesis of (9R,18R)-9,18-dibenzyl-4,13-dimethyl-1,10-dioxa-4,7,13,16-

tetraazacyclooctadecane-2,5,8,11,14,17-hexaone (36e)

To a solution of **36d** (0.12 g, 0.21 mmol) in DMF (150 mL) was added HATU (0.24 g, 0.63 mmol). The mixture was then allowed to be cooled to 0 °C and DIPEA (0.37 mL, 2.1 mmol) was added dro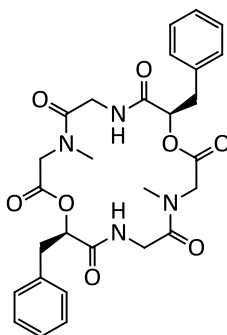p wise. The reaction slowly allowed to warm to room temperature and stirred for 3 days. Following that, the solvent was concentrated under reduced pressure, the residue dissolved in 50 mL EtOAc, washed by saturated $NaHCO_3$ (2X100 mL) and brine (160 mL), dried with $MgSO_4$, filtered and the solvent was removed under reduced pressure. The obtained brownish yellowish solid mass was then purified by column chromatography using EtOAc/methanol (9:1) as a mobile phase and silica gel as a stationary phase. Yield (43%), UPLC-MS (UV) purity: 99.9%, RT 0.92 min, ESI-MS m/z calcd for $C_{28}H_{32}N_4O_8$: 552.22; found: 553.22 [M+H]$^+$, ^{1}H NMR (500 MHz, CD$_3$OD-d$_4$) δ 7.33 − 7.18 (m, 10H), 5.43 (dd, *J* = 7.7, 4.2 Hz, 2H), 4.20 (d, *J* = 17.5 Hz, 2H), 4.09 − 3.96 (m, 4H), 3.91 (d, *J* = 16.3 Hz, 2H), 3.25 (dd, *J* = 14.3, 4.2 Hz, 2H), 3.15 (q, *J* = 6.6 Hz, 2H), 3.11 (s, 6H). ^{13}C NMR (126 MHz, cd$_3$od) δ 169.93, 169.86, 168.51, 135.99, 129.21, 128.05, 126.63, 74.26, 51.44, 47.99, 40.05, 37.48, 35.60.

Synthesis of (5S,8R,14S,17R)-8-benzyl-5,14-di((S)-sec-butyl)-17-hydroxy-4,7,10,13,16-pentaoxo-18-phenyl-9-oxa-3,6,12,15-tetraazaoctadecan-1-oic acid (37a)
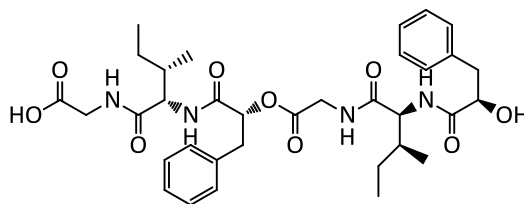
SPPS approach was used to prepare **37a** according to the general procedure described under section 8.2. The synthesis was initiated from a resin loaded with Fmoc-Gly-OH (0.45 g, 0.5 mmol). Crude yield (40%), ESI-MS calcd for $C_{34}H_{46}N_4O_9$: 654.75; found: 653.90 $[M-H]^-$.

Synthesis of (6S,9R,15S,18R)-9,18-dibenzyl-6,15-di((R)-sec-butyl)-1,10-dioxa-4,7,13,16-tetraazacyclooctadecane-2,5,8,11,14,17-hexaone (37b)
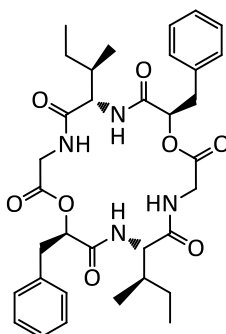
To degassed and stirred solution of MNAB (0.08 g, 0.24 mmol) and DMAP (0.06 g, 0.47 mmol) in 10 mL DCM, a solution of **37a** (0.05 g, 0.08 mmol) in DCM (70 mL) was slowly added under argon over a period of 8 h using a syringe pump. The reaction mixture was further stirred for additional 16 h at room temperature. When the reaction get completed, the solvent was removed under reduced pressure and the crude mass was purified by column chromatography using silica gel as a stationary phase and EtOAc/hexane (3:1) as a mobile phase. This gave a colorless oily product. Yield (45%), UPLC-MS (UV) purity: 99.9%, RT:1.13 min, ESI-MS m/z calcd for $C_{34}H_{44}N_4O_8$: 636.32; found: 637.32 $[M+H]^+$, ^{1}H NMR (400 MHz, CDCl$_3$-d) δ 7.46 (d, J = 8.8 Hz, 2H), 7.32 − 7.11 (m, 10H), 7.01 (t, J = 5.8 Hz, 2H), 5.73 (dd, J = 10.9, 3.7 Hz, 2H), 4.18 (dd, J =

10.9, 8.8 Hz, 2H), 4.04 (dd, *J* = 17.4, 5.2 Hz, 2H), 3.66 (dd, *J* = 14.3, 3.7 Hz, 2H), 3.39 (dd, *J* = 17.4, 6.2 Hz, 2H), 2.82 (dd, *J* = 14.3, 10.9 Hz, 2H), 2.31 (ttd, *J* = 13.1, 6.7, 3.0 Hz, 2H), 1.54 (dqd, *J* = 14.9, 7.3, 3.1 Hz, 2H), 1.20 − 1.10 (m, 2H), 0.96 − 0.79 (m, 12H). ^{13}C NMR (101 MHz, cdcl$_3$) δ 173.30, 169.64, 166.81, 135.96, 129.08, 128.62, 127.08, 73.41, 57.04, 42.34, 38.06, 32.76, 24.33, 15.68, 9.97.

Synthesis of H₂N-ᴅ-Phe-*allo*-Ile-Sar-ᴅ-Phe-*allo*-Ile-Sar-COOH (38a)
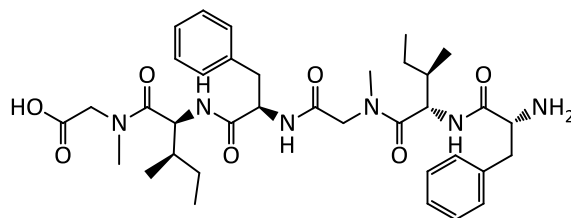
SPPS approach was used to prepare **38a** according to the general procedure described under section 8.2. The synthesis was initiated from a resin loaded with Fmoc-Sar-OH (0.45 g, 0.5 mmol). Crude yield (72%), ESI-MS m/z calcd for C$_{36}$H$_{52}$N$_6$O$_7$: 680.83; found: 681.13 [M+H]$^+$.

Synthesis of cyclo (ᴅ-Phe-*allo*-Ile-Sar-ᴅ-Phe-*allo*-Ile-Sar) (38b)
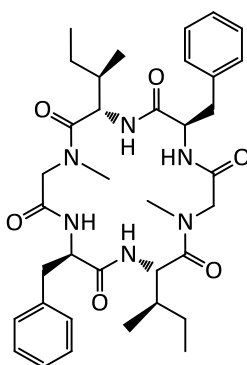
Compound **38b** was obtained through a macrocyclization of **38a** (0.19 g, 0.28 mmol) with HATU (0.32 g, 0.84 mmol), HOBt (0.11 g, 0.84 mmol) and DIPEA (0.49 mL, 2.8 mmol) according to the procedure described in section 8.3. The crude was purified by a column chromatography using a silica gel as a stationary phase and chloroform/methanol (49:1) as a mobile phase to give a white amorphous solid mass. Yield (30%), mp 270-272 °C, UPLC-MS (UV) purity: 99.9%, RT:1.11

min, ESI-MS m/z calcd $C_{36}H_{50}N_6O_6$: 662.38; found: 663.38.90 $[M+H]^+$. ^{1}H NMR (500 MHz, CDCl$_3$-d) δ 7.42 – 7.18 (m, 12H), 7.07 (d, J = 7.4 Hz, 2H), 5.00 (s, 2H), 4.77 (td, J = 9.2, 6.2 Hz, 2H), 4.27 (t, J = 8.1 Hz, 2H), 3.39 (dd, J = 14.2, 9.9 Hz, 2H), 3.27 (dd, J = 14.3, 6.0 Hz, 2H), 3.17 – 3.06 (m, 2H), 3.03 (s, 6H), 1.79 (dtt, J = 9.9, 6.6, 3.5 Hz, 2H), 1.40 (dtd, J = 11.3, 7.5, 4.0 Hz, 2H), 1.15 – 1.04 (m, 2H), 1.01 (d, J = 6.6 Hz, 6H), 0.89 (t, J = 7.3 Hz, 6H). ^{13}C NMR (126 MHz, cdcl$_3$) δ 173.34, 172.08, 169.65, 137.41, 129.46, 128.41, 126.62, 55.17, 52.91, 51.92, 36.53, 35.99, 34.77, 25.83, 15.46, 11.50.

Synthesis of H₂N-D-Phe(4-Cl)-*allo*-Ile-Sar-D-Phe(4-Cl)-*allo*-Ile-Sar-COOH (39a)

SPPS approach was used to prepare **39a** according to the general procedure described under section 8.2. The synthesis was initiated from a resin loaded with Fmoc-Sar-OH (0.27 g, 0.3 mmol). Crude yield (45%), ESI-MS calcd for $C_{36}H_{50}Cl_2N_6O_7$: 749.72, found: 772.38 $[M+Na]^+$.

Synthesis of cyclo (D-Phe(4-Cl)-*allo*-Ile-Sar-D-Phe (4-Cl)-*allo*-Ile-Sar) (39b)
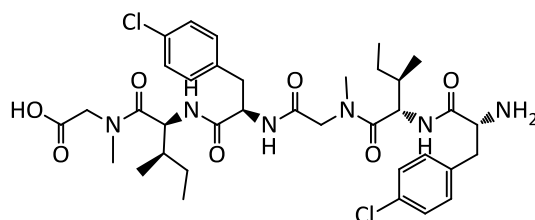

Compound **39b** was obtained through a macrocyclization of **39a** (0.09 g, 0.124 mmol) with HATU (0.14 g, 0.37 mmol), HOBt (0.05 g, 0.37 mmol) and DIPEA (0.22 mL, 1.24 mmol) according

to the procedure described in section 8.3. The crude was purified by a column chromatography using a silica gel as a stationary phase and chloroform/methanol (97:3) as a mobile phase to give a white amorphous solid mass. Yield (50%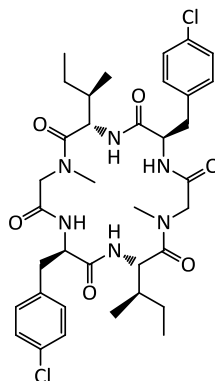), mp 270-273 °C, UPLC-MS (UV) purity: 98%, RT:1.24 min, ESI-MS m/z calcd $C_{36}H_{48}Cl_2N_6O_6$: 730.3; found: 731.3 $[M+H]^+$. ^{1}H NMR (400 MHz, CDCl$_3$-d) δ 7.36 – 7.22 (m, 8H), 7.22 – 7.10 (m, 2H), 7.10 (s, 2H), 4.97 (d, J = 14.9 Hz, 2H), 4.70 (tt, J = 10.1, 6.4 Hz, 2H), 4.24 (dd, J = 9.0, 4.6 Hz, 2H), 3.34 (dd, J = 14.2, 10.0 Hz, 2H), 3.23 – 3.06 (m, 4H), 3.03 (s, 6H), 1.77 (qt, J = 10.4, 6.7 Hz, 2H), 1.39 (dqd, J = 14.1, 7.3, 3.8 Hz, 2H), 1.15 – 1.04 (m, 2H), 1.00 (d, J = 6.7 Hz, 6H), 0.88 (t, J = 7.3 Hz, 6H). ^{13}C NMR (101 MHz, cdcl$_3$) δ 173.23, 171.93, 169.89, 135.84, 132.51, 130.79, 128.54, 55.13, 52.64, 51.92, 36.58, 35.95, 33.91, 25.80, 15.46, 11.49.

Synthesis of H$_2$N-D-Phe(4-OMe)-*allo*-Ile-Sar-D-Phe(4-OMe)-*allo*-Ile-Sar-COOH (40a)

SPPS approach was used to prepare **40a** according to the general procedure described under section 8.2. The synthesis was initiated from a resin loaded with Fmoc-Sar-OH (0.27 g, 0.3 mmol). Crude yield (47%), ESI-MS calcd for $C_{38}H_{56}N_6O_9$: 740.89, found: 763.54 $[M+H]^+$.
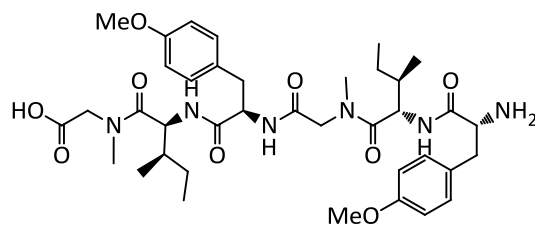
Synthesis of cyclo (D-Phe(4-OMe)-*allo*-Ile-Sar-D-Phe(4-OMe)-*allo*-Ile-Sar) (40b)

Compound **40b** was obtained through a macrocyclization of **40a** (0.16 g, 0.21 mmol) with HATU (0.24 g, 0.64 mmol), HOBt (0.09 g, 0.64 mmol) and DIPEA (0.37 mL, 2.13 mmol) according to the procedure described in section 8.3. The crude was purified by a column chromatography using a silica gel as a stationary phase and chloroform/methanol (97:3) as a mobile phase to give a white amorphous solid mass. Yield (50%), mp 245-247 °C, UPLC-MS (UV) purity: 99.9%, RT:1.06 min, ESI-MS m/z calcd $C_{38}H_{54}N_6O_8$: 722.4; found: 723.4 $[M+H]^+$, ^{1}H NMR (400 MHz, CDCl$_3$-d) δ 7.34 – 7.22 (m, 4H), 7.18 (d, J = 8.7 Hz, 2H), 7.04 (d, J = 7.1 Hz, 2H), 6.88 – 6.75 (m, 4H), 4.99 (d, J = 17.6 Hz, 2H), 4.69 (td, J = 9.1, 6.3 Hz, 2H), 4.30 – 4.19 (m, 2H), 3.78 (s, 6H), 3.35 – 3.25 (m, 2H), 3.22 – 3.07 (m, 4H), 3.04 (s, 6H), 1.77 (tdd, J = 9.7, 6.4, 3.6 Hz, 2H), 1.38 (ttd, J = 11.4, 7.7, 3.7 Hz, 2H), 1.12 – 1.03 (m, 2H), 0.99 (d, J = 6.7 Hz, 6H), 0.87 (t, J = 7.3 Hz, 6H). ^{13}C NMR (101 MHz, cdcl$_3$) δ 173.35, 172.01, 169.56, 158.34, 130.41, 129.36, 113.81, 55.23, 53.09, 51.93, 36.58, 35.94, 33.99, 25.82, 15.42, 11.48.

Synthesis of H₂N-D-Leu-*allo*-Ile-Sar-D-Leu-*allo*-Ile-Sar-COOH (41a)

SPPS approach was used to prepare **41a** according to the general procedure described under section 8.2. The synthesis was initiated from a resin loaded with Fmoc-Sar-OH (0.27 g, 0.3 mmol). Crude yield (54%), ESI-MS m/z calcd for $C_{30}H_{56}N_6O_7$: 612.42, found: 635.45 [M+Na]⁺.

Synthesis of cyclo (D-Leu-*allo*-Ile-Sar-D-Leu-*allo*-Ile-Sar) (41b)
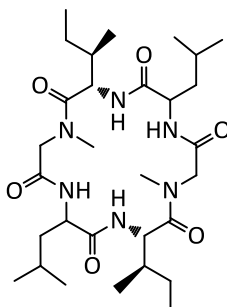
Compound **41b** was obtained through a macrocyclization of **41a** (0.2 g, 0.26 mmol) with HATU (0.3 g, 0.78 mmol), HOBt 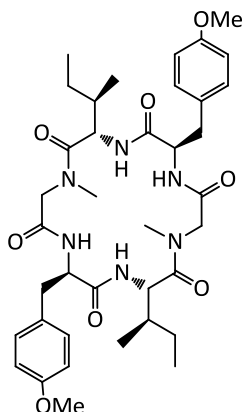(0.11 g, 0.78 mmol) and DIPEA (0.45 mL, 2.6 mmol) according to the procedure described in section 8.3. The crude was purified by a column chromatography using a silica gel as a stationary phase and chloroform/methanol 24:1) as a mobile phase to give a colorless oily product. Yield (45%), UPLC-MS (UV) purity: 93%, RT:1.13 min, ESI-MS m/z calcd $C_{38}H_{54}N_6O_8$: 594.41; found: 595.41 [M+H]⁺, ¹H NMR (400 MHz, CDCl₃-d) δ 7.04 (dd, *J* = 18.1, 7.9 Hz, 4H), 5.06 (s, 2H), 4.51 (q, *J* = 8.0 Hz, 2H), 4.24 (t, *J* = 8.2 Hz, 2H), 3.39 – 3.11 (m, 8H), 1.88 – 1.65 (m, 6H), 1.62 – 1.50 (m, 2H), 1.43 (ddt, *J* = 14.9, 11.5, 5.3 Hz, 2H), 1.12 (dtd, *J* = 16.2, 7.9, 4.6 Hz, 2H), 1.05 – 0.81 (m, 24H).

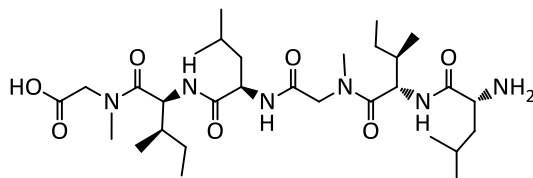**Synthesis of H$_2$N-D-Phe-*allo*-Ile-Pro-D-Phe-*allo*-Ile-Pro-COOH (42a)**

SPPS approach was used to prepare **42a** according to the general procedure described under section 8.2. The synthesis was initiated from a resin loaded with Fmoc-Pro-OH (0.25 g, 0.3 mmol). Crude yield (80%), ESI-MS m/z calcd for C$_{40}$H$_{56}$N$_6$O$_7$: 732.91, found: 733.38 [M+H]$^+$.

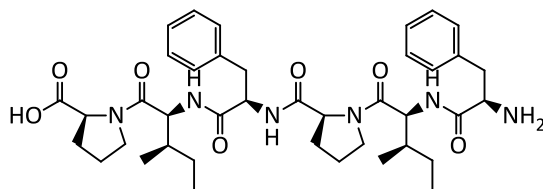**Synthesis of cyclo (D-Phe-*allo*-Ile-Pro-D-Phe-*allo*-Ile-Pro) (42b)**
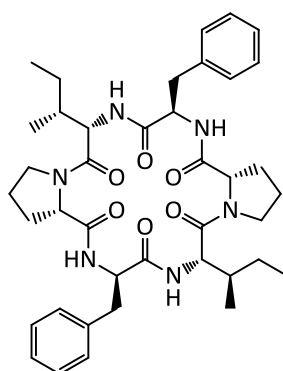
Compound **42b** was obtained through a macrocyclization of **42a** (0.18 g, 0.25 mmol) with HATU (0.29 g, 0.75 mmol), HOBt (0.1 g, 0.75 mmol) and DIPEA (0.44 mL, 2.5 mmol) according to the procedure described in section 8.3. The crude was purified by a column chromatography using a silica gel as a stationary phase and chloroform/methanol (97:3) as a mobile phase to give a white amorphous solid mass. Yield (43%), UPLC-MS (UV) purity: 90%, RT:1.07 min, ESI-MS m/z calcd C$_{40}$H$_{54}$N$_6$O$_6$: 714.41; found: 715.41[M+H]$^+$, ^{1}H NMR (400 MHz, CDCl$_3$-d) δ 7.45 (d, J = 8.1 Hz, 2H), 7.25 − 7.12 (m, 10H), 6.22 (d, J = 9.6 Hz, 2H), 4.90 (ddd, J = 9.6, 7.0, 5.9 Hz, 2H), 4.79 (dd, J = 8.1, 2.8 Hz, 2H), 3.99 (dd, J = 9.5, 6.8 Hz, 2H), 3.61 (t, J = 8.6 Hz, 2H), 3.50 (td, J = 10.1, 5.9 Hz, 2H), 3.17 (qd, J = 14.0, 6.5 Hz, 4H), 2.09 (dq, J = 14.5, 8.3, 7.1 Hz, 2H), 1.99 (ddd, J = 12.2, 9.6, 6.3 Hz, 2H), 1.93 − 1.77 (m, 6H), 1.42 (dp, J = 14.2, 7.2 Hz, 2H), 1.19 − 1.08 (m, 2H), 0.93 (t, J = 7.3 Hz, 6H), 0.65 (d, J = 6.8 Hz, 6H).

8.6. Biological assay

8.6.1. Agar diffusion assay

The inocula of *E. coli* SG 458, *B. subtilis* ATCC 6633, *M. aurum* SB 66, *M. smegmatis* SG987, *M. vaccae* IMET 10670 and *P. aeruginosa* K799/61 were prepared by incubating a few well-isolated colonies from an angular agar culture with 3 mL of nutrient solution for 16 h at 37 °C. The solution was diluted with aqueous NaCl (0.9 %) to a bacterial density (turbidity of solution) compared to McFarland standard 0.5 (Biomerieux). The test compound (1 mg) was dissolved in 1 mL DMSO and this stock solution diluted with methanol to a test concentration of 100 μg/mL. Reference compound was ciprofloxacin (5 μg/mL).

Culture plates for antibacterial activity were filled with 34 mL standard culture broth (Merck NA1) and inoculated with the corresponding microorganism inoculum so that the cell count is approximately 10^7. Plates were set aside on a flat surface for drying. Subsequently, holes of 9 mm diameter were punched into the culture medium in which 50 μL of the test compound solution was injected. Inoculated plates were incubated at 37 °C for 24 h. Determination of antibacterial and antifungal activity was performed optically by measuring diameters of inhibition zones.

8.6.2. MIC determination

MIC against *M. vaccae* (HKI Jena)

MIC against *M. vaccae* was determined by the micro broth dilution method in Mueller- Hinton broth according to NCCLS guidelines.

Preparation of inoculum: 20 mL culture medium for Mycobacteria (glycerol 1%, meat extract 0.5%, peptone (pancreatic from casein) 0.5%, NaCl 0.3%, aqueous destilled, pH 7.0) were inoculated with 0.5 mL preparatory culture and incubated at 32°C for 48 h. The inoculum was adjusted to McFarland standard 0.5 (Biomerieux) and diluted to 10^6 CFU/mL.

Stock solutions of the test compounds (1 mg in 1 mL DMSO) were diluted with methanol to a starting concentration of 400 µg/mL. 50 µl of these drug solutions were added to row 1, column A-E of 96-well microtiter plates, prepared with 50 µL Mueller-Hinton broth. Similarly, 50 µLl of the reference compound (ciprofloxacin) was added to column F, row 1 (final concentration of reference compound in row 1 = 100 µg/mL). Columns G and H were reserved for solvent control and growth control. Twelve twofold dilutions of test compound solutions were performed from row 1 to row 12 in order to achieve final test concentrations of 100 µg/mLl in row 1 and 0.05 µg/ml in row 12 on microtiter plates. Finally, 50 µL of inoculum were added to each vial of the 96-well microtiter plate. The final concentration of inoculum was $5*10^5$ CFU/mL.

Plates were incubated at 37 °C for 48 h. 30 µL of a resazurin solution (0.01 % in aqueous destilled) were added to each well and plates incubated for another 24 h at 37 °C. Fluorescence was detected after 72 h with a Nephelocan Ascent 1.4 automatic plate reader (Labsystems, Vantaa, Finland) at λ = 630 nm. The MIC was the lowest compound concentration where no viable cells of *M. vaccae* are detectable (color change of indicator dye resazurin from pink to blue).

MIC against *Mtb H37Rv* (Tres Cantos)

The measurement of the MIC for each tested compound was performed in 96-well flat-bottomed, polystyrene microtiter plates. Ten 2-fold drug dilutions were performed in neat DMSO. Then 5 µL of these drug solutions were added to 95 µL of Middlebrook 7H9 medium (Difco catalogue ref 271310). Isoniazid was used as the positive control: eight 2-fold dilutions of isoniazid were prepared, starting at 160 µg/mL, and 5 µL of this control curve was added to 95 µL of Middlebrook 7H9 medium. Likewise, 5 µL of neat DMSO were used as the growth and blank controls. The inoculum was standardized to approximately 1×10^7 CFU/mL and diluted 1 in 100 in Middlebrook 7H9 broth (10% ADC; Becton Dickinson BBL catalogue ref. 211887) and 0.025% Tween 80, to produce the final inoculum. Following this, 100 µL of this inoculum was added to the entire plate, except for the blank controls. All of the plates were placed in a sealed box to prevent drying out of the peripheral wells, and they were incubated at 37 °C without

shaking for 6 days. A resazurin solution was prepared by dissolving one tablet of resazurin (Resazurin Tablets for Milk Testing; ref 330884Y, VWR International Ltd.) in 30 mL of sterile phosphate-buffered saline. Of this solution, 25 μL was added to each well. Fluorescence was measured (Spectramax M5, Molecular Devices, excitation 530 nm, emission 590 nm) after 48 h, to determine the MIC values. For each compound, the average value of the duplicate samples was calculated.

8.6.3. HepG2 cytotoxicity assay

Actively growing HepG2 cells were removed from a T-175 TC flask using 5 mL Eagle's MEM (containing 10% FBS, 1% NEAA, 1% penicillin/streptomycin) and dispersed in the medium by repeated pipetting. Seeding density was checked to ensure that new monolayers were not > 50% confluent at the time of harvesting. Cell suspension was added to 500 mL of the same medium at a final density of $1.2x10^5$ cells/ per mL. This cell suspension (25 μL, typically 3000 cells per well) was dispensed into the wells of 384-well clear-bottom plates (Greiner, cat. # 781091) using a Multidrop instrument. Prior to addition of the cell suspension, the screening compounds (250 nL) were dispensed into the plates with an Echo 555 instrument. Plates were allowed to incubate at 37 °C at 80% relative humidity for 48 h under 5% CO_2. After the incubation period, the plates were allowed to equilibrate at room temperature for 30 min before proceeding to develop the luminescent signal. The signal developer, CellTiter-Glo (Promega) was equilibrated at room temperature for 30 min and added to the plates (25 μL per well) using a Multidrop. The plates were left for 10 min at room temperature for stabilization and were subsequently read using a View Lux instrument (PerkinElmer). The human biological samples were sourced ethically and their research use was in accord with the terms of the informed consents.

8.6.4. *In vivo* efficacy testing and blood exposure study

Specific pathogen-free, 8-10 week-old female C57BL/6 mice were purchased from Harlan Laboratories and were allowed to acclimate for one week. Mice were intratracheally infected

with approximately 100.000 CFU/mouse (*Mtb* H37Rv). Test substances were administered once a day since day 1 to day 8 after infection by intraperitoneal route. Moxifloxacin was administrated by oral route and was used as a positive control. Mice could eat and drink *ad libitum*. Lungs were harvested on day 9 after infection. All lung lobes were aseptically removed, homogenized and frozen. Homogenates were unfrozen and plated in 10% OADC-7H11 medium + 0.4% activated charcoal for 18 days at 37 °C.

Blood samples were collected at different time points from infected mice to measure the levels of the tested compounds. All animal studies were ethically reviewed and carried out in accordance with European Directive 2010/63/EU and the GSK Policy on the Care, Welfare and Treatment of Animals.

.

8.7. Physicochemical properties

8.7.1. Chemi-Luminescent Nitrogen Detection (CLND) solubility assay

GSK in-house kinetic solubility assay: 5 µL of 10 mM DMSO stock solution diluted to 100 µL with pH = 7.4 phosphate buffered saline, equilibrated for 1 h at room temperature, filtered through Millipore Multiscreen HTS-PCF filter plates (MSSL BPC).

The filtrate is quantified by suitably calibrated flow injection CLND. The standard error of the CLND solubility determination is ±30 µM, the upper limit of the solubility is 500 µM when working from 10 mM DMSO stock solution.

8.7.2. Chrom logD assay

The Chromatographic Hydrophobicity Index (CHI) values were measured using a reversed phase HPLC column (50 x 2 mmx 3 µM Gemini NX C18, Phenomenex, UK) with fast acetonitrile gradient at starting mobile phase of 100% pH = 7.4 buffer. CHI values are derived directly from the gradient retention times by using a calibration line obtained for standard compounds. The CHI value approximates to the volume % organic concentration when the compound elutes. CHI is linearly transformed into Chrom logD by the formula:

$$\text{Chrom log D} = 0.0857\ \text{CHI} - 2.00$$

The average error of the assay is ±3 CHI unit or ±0.25 Chrom logD.

8.7.3. Artificial membrane permeability assay

A 8% L-a-phosphatidylcholine (EPC) in 1% cholesterol decane solution and a 1.8% EPC in cholesterol decane solution were prepared. The lipid solution was then aliquoted into 4 mL capped vials, sealed with parafilm and stored in -20 °C freezer. The lipid solution was then transferred from 4 mL vial into 96-well half area plate (130 µL/well) for daily assay usage. An additional 50 mM phosphate buffer with 0.5% encapsin, pH at 7.4 was prepared. The assay was

run by the Biomek FX and Biomek software. The assay procedure is written under the Biomek software. For one batch assay, it can test two 96-well sample plates with at least one standard on each sample plate. The total assay time was about 4 h. 3.5 µL of lipid solution were added to the filler plate, shaken for 12 seconds, and 250 µL of buffer were added to donor side and 100 µL to the receiver side. The assay plate was shaken for 45 min before adding the compounds. The test compounds (2.5 µL) were added to the donor side. The assay was run as replicates: Assay plates1 and 2 tested the sample plate 1; assay plates 3 and 4 tested the sample plate 2. The assay plates were then incubated and shaken for 3 hours at room temperature.

The assay samples were transferred to the HPLC analysis plates and 100 µL of receiver solution were aspirated and transferred to the receiver for analysis. Similarly, another 100 µL from the donor solution were transferred to the donor analysis plate. Compound concentration was measured by HPLC at different time-points and permeability was established as nm/sec.

8.7.4. Human serum albumin (HSA) binding assay

HSA binding assay was performed according to the method described by Valko K, et al[183]. The basic principle of the measurements is the determination of gradient retention times of compounds on immobilized HSA column and converting these retention times to the appropriate property values using calibration. The peaks are detected and identified by UV. Calibration sets of compounds are measured before each run for which the HSA binding values are known. The retention times of the calibration set of compounds are plotted against these known values. The slope and the intercept of the obtained straight lines are used to calculate the HSA binding for the unknown compounds.

8.7.5. Plasma stability assay

Plasma stability of the compounds was assessed in CD1 mouse and human plasma. Plasma was spiked with 1 µL of a 10 mM of each test compound solution to produce a 1 µM incubation. Three separate 300 µl aliquots were then taken from each tube and incubated at 37 °C for 2 h. At each time point (0, 15, 30, 60 and 120 min), 50 µL of plasma were collected from each sample. Samples were extracted by protein precipitation with 250 µL of 0.1% acetic acid in acetonitrile/methanol 3-1 (v/v) containing 1µM internal standard and centrifuged for 10 min at 2800 rpm. Supernatants were collected prior the injection onto an LC-MS/MS system. Analyte/Internal standard peak area ratios were referenced to the zero time-point samples as 100% in order to determine the percentage of compound remaining for each time-point. Ln plots of the % remaining for each compound were used to determine the half-life for the plasma incubations.

The human biological samples were sourced ethically, and their research use was in accord with the terms of the informed consents.

8.7.6. Intrinsic clearance (CL$_{int}$) assay

Pooled mouse and human liver microsomes are purchased from Xenotech. Microsomes (final protein concentration 0.5 mg/mL), MgCl$_2$ (final concentration = 5 mM) and test compound (final substrate concentration = 0.5 M; final DMSO concentration = 0.5%) in 0.1 M phosphate buffer pH 7.4 are pre-incubated at 37 °C prior to the addition of NADPH (final concentration = 1 mM) to initiate the reaction. The final incubation volume is 600 µL.

Control incubation is included for each compound tested where 0.1 M phosphate buffer pH 7.4 is added instead of NADPH (minus NADPH). One control compound is included with each species. All incubations are performed singularly for each test compound. Each compound is incubated for 45 min and samples (100 µL) of incubate are taken at 0, 5, 15, 30 and 45 min. The control (minus NADPH) is sampled at 30 min only. The reactions are stopped by the addition of sample to 200 µL acetonitrile: methanol (3:1) containing internal standard. The terminated

samples are centrifuged at 2,500 rpm for 20 min at 4 °C to precipitate the protein. Quantitative analysis: following protein precipitation, the samples were analyzed using specific LC-MS/MS conditions. Data analysis: from a plot of ln peak area ratio (compound peak area/internal standard peak area) against time, the gradient of the line was determined. Subsequently, half-life and intrinsic clearance were calculated using the equations below:

$$\text{Elimination rate constant (K)} = (-\text{gradient})$$

$$\text{Half life } (t_{1/2}) \text{ (min)} = \frac{0.693}{K}$$

$$\text{Cli (mL/ min/g protien)} = \frac{V \times 0.693}{t_{1/2}}$$

Where V = Incubation volume (ml/g microsomal protien)

9. References

1. WHO. Global tuberculosis report 2015, **2015**.

2. http://www.bbc.com/news/uk-england-london-34637968.

3. http://wiat.com/2016/01/07/3-dead-after-tuberculosis-outbreak-in-perry-county/.

4. Diel, R.; Loddenkemper, R.; Nienhaus, A. *J. Occup. Med. Toxicol.* **2016**, *11*, 4.

5. Ahsan, M. J.; Ansari, M. Y.; Yasmin, S.; Jadav, S. S.; Kumar, P.; Garg, S. K.; Aseri, A.,; Khalilullah, H. *Infect. Disord. Drug Targets*. **2015,** *15*, 32-41.

6. Forrellad, M. A.; Klepp, L. I.; Gioffré, A.; Sabio y García, J.; Morbidoni, H. R.; de la Paz Santangelo, M.; Cataldi, A. A.; Bigi, F. *Virulence.* **2013**, *4*, 3–66.

7. Kieser, K. J.; Rubin, E. J. *Nat. Rev. Microbiol.* **2014**, *12*, 550–562.

8. Brennan, P. J. *Tuberculosis.* **2003**, *83*, 91–97.

9. Pinho, M. G.; Kjos, M.; Veening, J.-W. *Nat. Rev. Microbiol.* **2013**, *11*, 601–14.

10. Hett, E. C.; Rubin, E. J. *Microbiol. Mol. Biol. Rev.* **2008**, *72*, 126–156.

11. Riley, L. W. *J. Clin. Invest.* **2006**, *116*, 4–7.

12. Balasubramanian, V.; Wiegeshaus, E. H.; Taylor, B. T.; Smith, D. W. *Tuber. Lung Dis.* **1994**, *75*, 168–178.

13. Pieters, J. *Cell Host Microbe.* **2008**, *3*, 399–407.

14. Ernst, J. D. *Infect. Immun.* **1998**, *66*, 1277–1281.

15. Armstrong, J. A.; Hart, P. D. *J. Exp. Med.* **1975**, *142*, 1–16.

16. Kang, P. B.; Azad, A. K.; Torrelles, J. B.; Kaufman, T. M.; Beharka, A.; Tibesar, E.; DesJardin, L. E.; Schlesinger, L. S. *J. Exp. Med.* **2005**, *202*, 987–99.

17. Pieters, J. *Cell Host Microbe.* **2008**, *3*, 399–407.

18. Wong, D.; Bach, H.; Sun, J.; Hmama, Z.; Av-Gay, Y. *Proc. Natl. Acad. Sci. U.S.A.* **2011**, *108*, 19371–6.

19. Lukacs, G. L.; Rotstein, O. D.; Grinstein, S. *J. Biol. Chem.* **1990**, *265*, 21099–21107.

20. van Crevel, R.; Ottenhoff, T. H. M.; van der Meer, J. W. M. *Clin. Microbiol. Rev.* **2002**, *15*, 294–309.

21. Meraviglia, S.; El Daker, S.; Dieli, F.; Martini, F.; Martino, A. *Clin. Exp. Immunol.* **2011**, *2011*, 587315.

22. van Crevel, R.; Ottenhoff, T. H. M.; van der Meer, J. W. M. *Adv. Exp. Med. Biol.* **2003**, *531*, 241–247.

23. McCune, R. M.; Feldmann, F. M.; McDermott, W. *J. Exp. Med.* **1966**, *123*, 469–486.

24. Kim, M. J.; Wainwright, H. C.; Locketz, M.; Bekker, L. G.; Walther, G. B.; Dittrich, C.; Visser, A.; Wang, W.; Hsu, F. F.; Wiehart, U.; Tsenova, L.; Kaplan, G.; Russell, D. G. *EMBO Mol. Med.* **2010**, *2*, 258–274.

25. Sakamoto, K. *Vet. Pathol.* **2012**, *49*, 423–439.

26. Comstock, G. W. *Am. J. Epidemiol.* **1975**, *101*, 363–382.

27. Tufariello, J. A. M.; Chan, J.; Flynn, J. A. L. *Lancet Infect. Dis.* **2003**, *3*, 578–590.

28. Andrews, J. R.; Noubary, F.; Walensky, R. P.; Cerda, R.; Losina, E.; Horsburgh, C. R. *Clin. Infect. Dis.* **2012**, *54*, 784–791.

29. Bates, J. H. *Clinic. Chest Med 1.* **1980**, 167-174.

30. Zumla, A.; Nahid, P.; Cole, S. T. *Nat. Rev. Drug Discov.* **2013**, *12*, 388–404.

31. Keshavjee, S.; Farmer, P. E. *N. Engl. J. Med.* **2012**, *367*, 931–6.

32. Wayne, L. G.; Sramek, H. A. *Antimicrob. Agents Chemother.* **1994**, *38*, 2054–2058.

33. Timmins, G. S.; Deretic, V. *Mol. Microbiol.* **2006**, *62*, 1220–1227.

34. Lei, B.; Wei, C. J.; Tu, S. C. *J. Biol. Chem.* **2000**, *275*, 2520.

35. Fu, L. M.; Shinnick, T. M. *Tuberculosis.* **2007**, *87*, 63–70.

36. Cade, C. E.; Dlouhy, A. C.; Medzihradszky, K. F.; Salas-Castillo, S. P.; Ghiladi, R. A. *Protein Sci.* **2010**, *19*, 458–474.

37. Vilchèze, C.; Jacobs Jr, W. R. *Microbiol. Spectr.* **2014**, *2*, 1–21.

38. Sensi, P. *Rev. Infect. Dis.* **1983**, *5*, S402–S406.

39. Sensi, P. *Pure Appl. Chem.* **1975**, 15–29.

40. Hartmann, B. G. R.; Heinrich, P.; Kollenda, M. C.; Skrobranek, B.; Tropschug, M.; Weid, W. *Angewandte Chemie.* **1985**, *24*, 1009–1014.

41. Campbell, E. A.; Korzheva, N.; Mustaev, A.; Murakami, K.; Nair, S.; Goldfarb, A.; Darst, S. A. *Cell.* **2001**, *104*, 901–12.

42. Alifano, P.; Palumbo, C.; Pasanisi, D.; Talà, A. *J. Biotechnol.* **2015**, *202*, 60–77.

43. Goldstein, B. P. *J. Antibiot.* **2014**, *67*, 625–30.

44. Singh, P.; Mishra, A. K.; Malonia, S. K.; Chauhan, D. S.; Sharma, V. D.; Venkatesan, K.; Katoch, V. M. *J. Com. Dis.* **2006**, *38*, 288–298.

45. Somoskovi, A; Parsons, L. M.; Salfinger, M. *Resp. Res.* **2001**, *2*, 164–168.

46. Scorpio, A.; Zhang, Y. *Nat. Med.* **1996**, *2*, 662–667.

47. Boshoff, H. I.; Mizrahi, V.; Barry, C. E. *J. Bacteriol.* **2002**, *184*, 2167–2172.

48. Wilkinson, R. G.; Shepherd, R. G.; Thomas, J. P.; Baughn, C. *J. Am. Chem. Soc.* **1961**, *83*, 2212–2213.

49. Takayama, K.; Kilburn, J. O. *Antimicrob. Agents Chemother.* **1989**, *33*, 1493–1499.

50. Forbes, M.; Kuck, N. A.; Peets, E. A. *J. Bacteriol.* **1962**, *84*, 1099–1103.

51. Starks, A. M.; Gumusboga, A.; Plikaytis, B. B.; Shinnick, T. M.; Posey, J. E. *Antimicrob. Agents Chemother.* **2009**, *53*, 1061–1066.

52. Wainwright, M. *Hist. Philos. Life Sci.* **1991**, *13*, 97–124.

53. Schatz, A.; Bugie, E.; Waksman, S. *Clin. Orthop. Relat. Res.* **2005**, *55*, 3–6.

54. Streptomycin in Tuberculosis Trials Committee. *A medical counsel investigation. Br. Med. J.* **1948**, *2*, 769–782.

55. Davis, B. D. *Microbiol. Rev.* **1987**, *51*, 341–350.

56. Springer, B.; Kidan, Y. G.; Prammananan, T.; Ellrott, K.; Böttger, E. C.; Sander, P. *Antimicrob. Agents Chemother.* **2001**, *45*, 2877–2884.

57. Honore, N.; Cole, S. T. *Antimicrob. Agents Chemother.* **1994**, *38*, 238–242.

58. Scholar, E. In *xPharm: The Comprehensive Pharmacology Reference*; **2007**; pp. 1–5 (Print).

59. J. Brennen, P. *Tuberculosis.* **2008**, *88*, 117–8.

60. Ho, O.; Nh, H. O.; Nh, H. O.; Oh, H. O.; Nh, G.; Dodge, F.; Squibb, B.; Carlo, S.; Squibb, B. *Tuberculosis.* **2008**, *88*, 87–8.

61. Allen, B. W.; Mitchison, D. A.; Chan, Y. C.; Yew, W. W.; Allan, W. G. L.; Girling, D. J. *Tubercle.* **1983**, *64*, 111–118.

62. Donald, P. R.; Diacon, A. H. *Lancet Infect. Dis.* **2015**, *15*, 1091–1099.

63. Zheng, J.; Rubin, E. J.; Bifani, P.; Mathys, V.; Lim, V.; Au, M.; Jang, J.; Nam, J.; Dick, T.; Walker, J. R.; Pethe, K.; Camacho, L. R. *J. Biol. Chem.* **2013**, *288*, 23447–23456.

64. Rengarajan, J.; Sassetti, C. M.; Naroditskaya, V.; Sloutsky, A.; Bloom, B. R.; Rubin, E. J. *Mol.*

Microbiol. **2004**, *53*, 275–282.

65. Marshall, E. *Science.* **2008**, *321*, 364.

66. Lambert, M. P.; Neuhaus, F. C. *J. Bacteriol.* **1972**, *110*, 978–987.

67. Prosser, G. A.; De Carvalho, L. P. S. *ACS Med. Chem. Lett.* **2013**, *4*, 1233–1237.

68. Cáceres, N. E.; Harris, N. B.; Wellehan, J. F.; Feng, Z.; Kapur, V.; Barletta, R. G. *J. Bacteriol.* **1997**, *179*, 5046–55.

69. Lin, Y.; Li, Y.; Zhu, N.; Han, Y.; Jiang, W.; Wang, Y.; Si, S.; Jiang, *J. Antimicrob. Chemother.* **2014**, *58*, 2038–2044.

70. Johansen, S. K.; Maus, C. E.; Plikaytis, B. B.; Douthwaite, S. *Mol. Cell.* **2006**, *23*, 173–182.

71. Walwaikar, P. P.; Morye, V. K.; Gawde, A. S. *J. Indian Med. Assoc.* **2003**, *101*, 210–212.

72. Johnson, J. L.; Hadad, D. J.; Boom, W. H.; Daley, C. L.; Peloquin, C. A.; Eisenach, K. D.; Jankus, D. D.; Debanne, S. M.; Charlebois, E. D.; Maciel, E.; Palaci, M.; Dietze, R. *Int. J. Tuberc. Lung Dis.* **2006**, *10*, 605–612.

73. Hooper, D. C. *Clin. Infect. Dis.* **2000**, *31 Suppl 2*, S24-8.

74. Drlica, K.; Malik, M. *Curr. Top. Med. Chem.* **2003**, *3*, 249–82.

75. D 'ambrosio, L.; Centis, R.; Sotgiu, G.; Pontali, E.; Spanevello, A.; Migliori, G. B. *ERJ Open Res.* **2015**, *1*, 10–2015.

76. Chahine, E. B.; Karaoui, L. R.; Mansour, H. *Ann. Pharmacother.* **2014**, *48*, 107–115.

77. Hards, K.; Robson, J. R.; Berney, M.; Shaw, L.; Bald, D.; Koul, A.; Andries, K.; Cook, G. M. *J. Antimicrob. Chemother.* **2014**, *70*, 2028–2037.

78. Xavier, A S.; Lakshmanan, M. *J. Pharmacol. Pharmacother.* **2014**, *5*, 222–224.

79. Reviriego, C. *Drugs Future.* **2013**, *38*, 7.

80. Wallis, R. S.; Maeurer, M.; Mwaba, P.; Chakaya, J.; Rustomjee, R.; Migliori, G. B.; Marais, B.; Schito, M.; Churchyard, G.; Swaminathan, S.; Hoelscher, M.; Zumla, A. *Lancet Infect. Dis.* **2016**, *16*, e34–e46.

81. Hancock, R. E. W.; Lehrer, R. *Trends Biotechnol.* **1998**, *16*, 82–88.

82. Hancock, R. E. W.; Sahl, H. *Nat. Biotechnol.* **2006**, *24*, 1551–1557.

83. Epand, R. M.; Vogel, H. J. *BBA Biomemb.* **1999**, *1462*, 11–28.

84. Shai, Y. *Biopolymers - Pept. Sci.* **2002**, *66*, 236–248.

85. Guilhelmelli, F.; Vilela, N.; Albuquerque, P.; Derengowski, L. da S.; Silva-Pereira, I.; Kyaw, C. M. *Front. Microbiol.* **2013**, *4*, 1–12.

86. Hancock, R. E. *Lancet.* **1997**, *349*, 418–422.

87. Strøm, M. B.; Haug, B. E.; Skar, M. L.; Stensen, W.; Stiberg, T.; Svendsen, J. S. *J. Med. Chem.* **2003**, *46*, 1567–1570.

88. Taira, J.; Kida, Y.; Yamaguchi, H.; Kuwano, K.; Higashimoto, Y.; Kodama, H. *J. Pept. Sci.* **2010**, *16*, 607–612.

89. Datrie, M.; Schumann, M.; Wieprecht, T.; Winkler, A.; Beyermann, M.; Krause, E.; Matsuzaki, K.; Murase, O.; Bienert, M. *Biochemistry.* **1996**, *35*, 12612–12622.

90. Tang, M.; Waring, A. J.; Hong, M. *J. Am. Chem. Soc.* **2007**, *129*, 11438–11446.

91. Padhi, A.; Sengupta, M.; Sengupta, S.; Roehm, K. H.; Sonawane, A. *Tuberculosis* **2014**, *94*, 363–373.

92. Carroll, J.; O'Mahony, J. *Bioeng. Bugs.* **2011**, *2*, 241–246.

93. Teng, T.; Liu, J.; Wei, H. *Cell. Physiol. Biochem.* **2015**, *35*, 452–466.

94. Abedinzadeh, M.; Gaeini, M.; Sardari, S. *J. Antimicrob. Chemother.* **2014**, *70*, 1285–1289.

95. Garcia, A.; Bocanegra-Garcia, V.; Palma-Nicolis, J. P.; Rivera, G. *Eur. J. Med.Chem.* **2012**, *49*, 1–23.

96. Gutsmann, T. *BBA Biomemb.* **2016**, *1858*, 1034–1043.

97. Okunade, A. L.; Elvin-Lewis, M. P. F.; Lewis, W. H. *Phytochemistry.* **2004**, *65*, 1017–1032.

98. Wang, G.; Li, X.; Wang, Z. Nucleic Acids Res. **2016**, *44*, D1087–D1093.

99. Kalita, A.; Verma, I.; Khuller, G. K. *J. Infect. Dis.* **2004**, *190*, 1476–80.

100. Kisich, K. O.; Heifets, L.; Higgins, M.; Diamond, G. *Infect. Immun.* **2001**, *69*, 2692–2699.

101. Sow, F. B.; Florence, W. C.; Satoskar, A. R.; Schlesinger, L. S.; Zwilling, B. S.; Lafuse, W. P. *J. Leukoc. Biol.* **2007**, *82*, 934–45.

102. Jena, P.; Mishra, B.; Leippe, M.; Hasilik, A.; Griffiths, G.; Sonawane, A. *Peptides.* **2011**, *32*, 881–887.

103. Gansert, J. L.; Kiessler, V.; Engele, M.; Wittke, F.; Rollinghoff, M.; Krensky, A. M.; Porcelli, S. A.; Modlin, R. L.; Stenger, S. *J. Immunol.* **2003**, *170*, 3154–3161.

104. Pulido, D.; Torrent, M.; Andreu, D.; Nogues, M. V.; Boix, E. *Antimicrob. Agents Chemother.* **2013**, *57*, 3797–3805.

105. Alonso, S.; Pethe, K.; Russell, D. G.; Purdy, G. E. *Proc. Natl. Acad. Sci. U.S.A.* **2007**, *104*, 6031–6036.

106. Donaghy, J. *Bioeng. Bugs.* **2010**, *1*, 437–439.

107. Sosunov, V.; Mischenko, V.; Eruslanov, B.; Svetoch, E.; Shakina, Y.; Stern, N.; Majorov, K.; Sorokoumova, G.; Selishcheva, A.; Apt, A. *J. Antimicrob. Chemother.* **2007**, *59*, 919–925.

108. Kling, A.; Lukat, P.; Almeida, D. V.; Bauer, A.; Fontaine, E.; Sordello, S.; Zaburannyi, N.; Herrmann, J.; Wenzel, S. C.; Konig, C.; Ammerman, N. C.; Barrio, M. B.; Borchers, K.; Bordon-Pallier, F.; Bronstrup, M.; Courtemanche, G.; Gerlitz, M.; Geslin, M.; Hammann,

P.; Heinz, D. W.; Hoffmann, H.; Klieber, S.; Kohlmann, M.; Kurz, M.; Lair, C.; Matter, H.; Nuermberger, E.; Tyagi, S.; Fraisse, L.; Grosset, J. H.; Lagrange, S.; Muller, R. *Science.* **2015**, *348*, 1106–1112.

109. Isshiki, k.; Sawa, T.; Naganawa, H.; Koizumi, Y.; Matsuda, N.; Hamada, M.; Takeuchi, T.; Iijima, M.; Osono, M.; Masuda, T.; Ishizuka, M. *J. Antibiot.* 1990, 43, 1195-1198.

110. Cai, G.; Napolitano, J. G.; McAlpine, J. B.; Wang, Y.; Jaki, B. U.; Suh, J. W.; Yang, S. H.; Lee, I. A.; Franzblau, S. G.; Pauli, G. F.; Cho, S. *J. Nat. Prod.* **2013**, *76*, 2009–2018.

111. Müller, D.; Krick, A.; Kehraus, S.; Mehner, C.; Hart, M.; Küpper, F. C.; Saxena, K.; Prinz, H.; Schwalbe, H.; Janning, P.; Waldmann, H.; König, G. M. *J. Med. Chem.* **2006**, *49*, 4871–4878.

112. Hartkoorn, R. C.; Sala, C.; Neres, J.; Pojer, F.; Magnet, S.; Mukherjee, R.; Uplekar, S.; Boy-Röttger, S.; Altmann, K. H.; Cole, S. T. *EMBO Mol. Med.* **2012**, *4*, 1032–1042.

113. Vongvanich, N.; Kittakoop, P.; Isaka, M.; Trakulnaleamsai, S.; Vimuttipong, S.; Tanticharoen, M.; Thebtaranonth, Y. *J. Nat. Prod.* **2002**, *65*, 1346–1348.

114. Khalil, Z. G.; Salim, A. A.; Lacey, E.; Blumenthal, A.; Capon, R. J. *Org. Lett.* **2014**, *16*, 5120–5123.

115. Hoagland, D.; Liu, J.; Lee, R. B.; Lee, R. E. *Adv. Drug Deliv. Rev.* **2016**, 1–18.

116. Walther, T.; Renner, S.; Waldmann, H.; Arndt, H. D. *Chem. Bio. Chem.* **2009**, *10*, 1153–1162.

117. Narayanaswamy, V. K.; Albericio, F.; Coovadia, Y. M.; Kruger, H. G.; Maguire, G. E. M.; Pillay, M.; Govender, T. *J. Pept. Sci.* **2011**, *17*, 683–689.

118. Hartkoorn, R. C.; Pojer, F.; Read, J. A; Gingell, H.; Neres, J.; Horlacher, O. P.; Altmann, K.-H.; Cole, S. T. *Nat. Chem. Biol.* **2014**, *10*, 96–8.

119. Horlacher, O. P.; Hartkoorn, R. C.; Cole, S. T.; Altmann, K. H. *ACS Med. Chem. Lett.* **2013**,

4, 264–268.

120. Gerard, J.; Lloyd, R.; Barsby, T.; Haden, P.; Kelly, M. T.; Andersen, R. J. *J. Nat. Prod.* **1997**, *60*, 223–229.

121. Xu, Y.; Chen, L.; Duan, X.; Meng, Y.; Jiang, L.; Li, M.; Zhao, G.; Li, Y. *Tetrahedron Lett.* **2005**, *46*, 4377–4379.

122. Hancock, R. E. W.; Chapple, D. S. *Antimicrob. Agents Chemother.* **1999**, *43*, 1317–1323.

123. Wenzel, M.; Chiriac, A. I.; Otto, A.; Zweytick, D.; May, C.; Schumacher, C.; Gust, R.; Albada, H. B.; Penkova, M.; Krämer, U.; Erdmann, R.; Metzler-Nolte, N.; Straus, S. K.; Bremer, E.; Becher, D.; Brötz-Oesterhelt, H.; Sahl, H. G.; Bandow, J. E. *Proc. Natl. Acad. Sci. U.S.A.* **2014**, *111*, E1409-18.

124. Kimmerlin, T.; Seebach, D. *J. Pept. Res.* **2005**, *65*, 229–60.

125. du Vigneaud, V.; Ressler, C.; Swan, J. M.; Roberts, C. W.; Katsoyannis, P. G. *J. Am. Chem. Soc.* **1954**, *76*, 3115–3121.

126. Mitchell, A. R. *Biopolymers - Pept. Sci.* **2008**, *90*, 175–184.

127. Amblard, M.; Fehrentz, J. A.; Martinez, J.; Subra, G. *Mol. Biotechnol.* **2006**, *33*, 239–254.

128. Sarin, V. K.; Kent, S. B. H.; Merrifield, R. B. *J. Am. Chem. Soc.* **1980**, *102*, 5463–5470.

129. Palomo, J. M. *RSC Adv.* **2014**, *4*, 32658–32672.

130. Dax, S. L. General Overview, in Linker Strategies in Solid-Phase Organic Synthesis. In: Scott, P. J. H. eds. Linker Strategies in Solid-Phase Organic Synthesis Chichester, UK. John Wiley & Sons, Ltd; 2009:1-23..

131. Shelton, P. T.; Jensen, K. J. *Methods Mol. Biol.* **2013**, *1047*, 23–41.

132. Carpino, L. A.; Han, G. Y. *J. Am. Chem. Soc.* **1970**, *92*, 5748–5749.

133. Schnölzer, M.; Alewood, P.; Jones, A.; Alewood, D.; Kent, S. B. H. *Int. J. Pept. Res. Ther.*

2007, *13*, 31–44.

134. Han, S. Y.; Kim, Y. A. *Tetrahedron.* **2004**, *60*, 2447–2467.

135. Al-Warhi, T. I.; Al-Hazimi, H. M. A.; El-Faham, A. *J. Saudi Chem. Soc.* **2012**, *16*, 97–116.

136. Knorr, R.; Trzeciak, A.; Bannwarth, W.; Gillessen, D. *Tetrahedron Lett.* **1989**, *30*, 1927–1930.

137. El-Faham, A.; Albericio, F. *Chem. Rev.* **2011**, *111*, 6557–6602.

138. Montalbetti, C. A. G. N.; Falque, V. *Tetrahedron.* **2005**, *61*, 10827–10852.

139. Caprino, L. A. *J. Am. Chem. Soc.* **1993**, *115*, 4397–4398.

140. Isidro-Llobet, A.; Álvarez, M.; Albericio, F. *Chem. Rev.* **2009**, *109*, 2455–2504.

141. Chatterjee, J.; Laufer, B.; Kessler, H. *Nat. Protoc.* **2012**, *7*, 432–444.

142. Hoekstra, W. J. *Curr. Med. Chem.* **2001**, *8*, 715–9.

143. Barlos, K.; Chatzi, O.; Gatos, D.; Stavropoulos, G. *Int. J. Pept. Protein Res.* **1991**, *37*, 513–520.

144. Collins, J. M.; Porter, K. A; Singh, S. K.; Vanier, G. S. *Org. Lett.* **2014**, *16*, 940–943.

145. Bollhagen, R.; Schmiedberger, M.; Barlos, K.; Grell, E. *J. Chem. Soc. Chem. Comm.* **1994**, 2559–2560.

146. Mergler, M.; Dick, F. *J. Pept. Sci.* **2005**, *11*, 650–657.

147. Ruczyński, J.; Lewandowska, B.; Mucha, P.; Rekowski, P. *J. Pept. Sci.* **2008**, *14*, 335–341.

148. Subir os-Funosas, R.; El-Faham, A.; Albericio, F. *Tetrahedron.* **2011**, *67*, 8595–8606.

149. White, C. J.; Yudin, A. K. *Nat. Chem.* **2011**, *3*, 509–24.

150. Davies, J. S. *J. Pept. Sci.* **2003**, *9*, 471–501.

151. Sanchez, J. G. B.; Kouznetsov, V. V. *Braz. J. Microbiol.* **2010**, *41*, 270–277.

152. Inderlied, C. B. *Eur. J. Clin. Microbiol. Infect. Dis.* **1994**, *13*, 980–993.

153. Medeiros, M. A.; Dellagostin, O. A.; Armôa, G. R. G.; Degrave, W. M.; de Mendonça-Lima, L.; Lopes, M. Q.; Costa, J. F.; Mcfadden, J.; McIntosh, D. *Microbiology.* **2002**, *148*, 1999–2009.

154. Pitta, E.; Rogacki, M. K.; Balabon, O.; Huss, S.; Cunningham, F.; Lopez-Roman, E. M.; Joossens, J.; Augustyns, K.; Ballell, L.; Bates, R. H.; Van Der Veken, P. *J. Med. Chem.* **2016**, *59*, 6709–6728.

155. Di, L.; Kerns, E. H. *Curr. Opin. Chem. Biol.* **2003**, *7*, 402–408.

156. Chao, P.; Uss, A.; Cheng, K. *Expert Opin. Drug Metab. Toxicol.* **2010**, *6*, 189.

157. Morrison, K. L.; Weiss, G. A. *Curr. Opin. Chem. Biol.* **2001**, *5*, 302–307.

158. Danial, M.; Perrier, S.; Jolliffe, K. A. *Org. Biomol. Chem.* **2015**, *13*, 2464–2473.

159. Waring, M. J. *Bioorg. Med. Chem. Lett.* **2009**, *19*, 2844–2851.

160. Bagheri, M.; Keller, S.; Dathe, M. *Antimicrob. Agents Chemother.* **2011**, *55*, 788–797.

161. Brecik, M.; Centárová, I.; Mukherjee, R.; Kolly, G. S.; Huszár, S.; Bobovská, A.; Kilacsková, E.; Mokošová, V.; Svetlíková, Z.; Šarkan, M.; Neres, J.; Korduláková, J.; Cole, S. T.; Mikušová, K. *ACS Chem. Biol.* **2015**, 10, 1631-1636.

162. Dathe, M.; Nikolenko, H.; Klose, J.; Bienert, M. *Biochemistry.* **2004**, *43*, 9140–9150.

163. Yau, W. M.; Wimley, W. C.; Gawrisch, K.; White, S. H. *Biochemistry.* **1998**, *37*, 14713–14718.

164. Chan, D. I.; Prenner, E. J.; Vogel, H. J. *BBA Biomemb.* **2006**, *1758*, 1184–1202.

165. Klein-Seetharaman, J.; Oikawa, M.; Grimshaw, S. B.; Wirmer, J.; Duchardt, E.; Ueda, T.; Imoto, T.; Smith, L. J.; Dobson, C. M.; Schwalbe, H. *Science.* **2002**, *295*, 1719–1722.

166. Strøm, M. B.; Rekdal, Ø.; Svendsen, J. S. *J. Pept. Sci.* **2002**, *8*, 431–437.

167. Wu, G.; Bazer, F. W.; Davis, T. A.; Kim, S. W.; Li, P.; Marc Rhoads, J.; Carey Satterfield, M.; Smith, S. B.; Spencer, T. E.; Yin, Y. *Amino Acids.* **2009**, *37*, 153–168.

168. Dechantsreiter, M. A.; Planker, E.; Matha, B.; Lohof, E.; Jonczyk, A.; Goodman, S. L.; Kessler, H. *J. Med. Chem.* **1999**, 3033–3040.

169. Ovadia, O.; Greenberg, S.; Chatterjee, J.; Laufer, B.; Opperer, F.; Kessler, H.; Gilon, C.; Hoffman, A. *Mol. Pharm.* **2011**, *8*, 479–487.

170. Biron, E.; Chatterjee, J.; Ovadia, O.; Langenegger, D.; Brueggen, J.; Hoyer, D.; Schmid, H. A.; Jelinek, R.; Gilon, C.; Hoffman, A.; Kessler, H. *Angew. Chem., Int. Ed.* **2008**, *47*, 2595–2599.

171. Collins, L. A.; Franzblau, S. G. *Antimicrob. Agents Chemother.* **1997**, *41*, 1004–1009.

172. Mead, A. N.; Amouzadeh, H. R.; Chapman, K.; Ewart, L.; Giarola, A.; Jackson, S. J.; Jarvis, P.; Jordaan, P.; Redfern, W.; Traebert, M.; Valentin, J. P.; Vargas, H. M. *Regul. Toxicol. Phar.* **2016**, *80*, 348–357.

173. Ludden, T. M. *Clin. Pharmacokinet.* **1991**, *20*, 429–46.

174. Degerbeck, F.; Fransson, B.; Grehn, L.; Ragnarsson, U. *J. Chem. Soc. Perkin Trans. 1* **1992**, 245–253.

175. Khumtaveeporn, K.; Ullmann, A.; Matsumoto, K.; Davis, B. G.; Jones, J. B. *Tetrahedron Asymmetry.* **2001**, *12*, 249–261.

176. Zervas, L.; Winitz, M.; Greenstein, J. P. *J. Org. Chem.* **1957**, *22*, 1515–1521.

177. Xu, Y.; Duan, X.; Li, M.; Jiang, L.; Zhao, G.; Meng, Y.; Chen, L. *Molecules.* **2005**, *10*, 259–264.

178. Martinez, J.; Tolle, J. C.; Bodanszky, M. *Int. J. Pept. Protein Res.* **1979**, *13*, 22–27.

179. Shiina, I.; Katoh, T.; Nagai, S.; Hashizume, M. *Chem. Rec.* **2010**, *9*, 305–320.

180. Pedroso, E.; Grandas, A.; de las Heras, X.; Eritja, R.; Giralt, E.; de las Heras, F. X. C. *Tetrahedron Lett.* **1986**, *27*, 743–746.

181. Xu, Y. J.; Chen, L. G.; Duan, X. M.; Meng, Y.; Jiang, L. Q.; Li, M. L.; Zhao, G. L.; Li, Y. *Tetrahedron Lett.* **2007**, *48*, 733–735.

182. Bahar, F. G.; Ohura, K.; Ogihara, T.; Imai, T. *J. Pharm. Sci.* **2012**, *101*, 3979–3988.

183. Valko, K.; Nunhuck, S.; Bevan. C.; Abraham, H. M.; Reynolds, P. D. *J.Pharm. Sci.* **2003**, 92,2236-2248.

10. Appendices

Acknowledgements

My heartfelt gratitude and appreciation goes to my supervisor Prof. Dr. Peter Imming who trusted me and gave me the chance to join his working group; helped unreservedly for the success of my DAAD scholarship application; created conducive working environment throughout my stay. This was on top of his continuous support, guidance, encouragement and constructive feedback related to my project. I truly appreciate all what you have done to me.

I am sincerely indebted to our collaborative partner, the Open Lab Foundation of GSK Tres Cantos, Spain for running the biological and pharmacokinetic assays for my synthetic compounds, punctually providing test results, and financially supporting part of my PhD project. In particular, I am thankful to Dr. Maria Santos Martinez-Martinez, Dr. Fraser Cunningham and Dr. Katja Laqua who were involved in registering of the test compounds, closely following up the assays and supporting me in interpreting the results. I am thankful to Dr. Lluis Ballell-Pages and Dr. Juan Carlos Cuevas-Zurita for facilitating all the administrative works.

My thank also goes to the other collaborative partner, Microbial Resource Collection, Leibniz-Institut für Naturstoff-Forschung und Infektionsbiologie - Hans-Knöll-Institut, Jena (Germany) for testing the *in vitro* antimicrobial activities of my synthetic compounds, promptly providing the results with the necessary explanations. Especially, my thanks go to Dr. Kerstin Voigt and Christiane Weigel who were always collaborative whenever asked to run the assay.

The German Academic Exchange Service (DAAD) is hearted fully acknowledged for financially supporting me throughout the study period.

I would like to express my deep gratitude to the young intelligent colleague Adrian Richter who introduced me in the synthetic lab and for being always cooperative whenever I needed his help in and out of the lab. My gratitude also goes to Dr. Andreas for introducing me to a solid phase peptide synthesis approach.

Curriculum vitae

PERSONAL INFORMATION

Name	Henok Asfaw Sahile
Date/place of birth	02/12/1984, Enewari, Ethiopia
Nationality	Ethiopian
Residence address	Kattowitzer str. 26,
	06128, Halle (saale), Germany

WORK EXPERIENCE

03/2010-05/2012	Lecturer, Addis Ababa University, College of health science, Department of pharmaceutical chemistry, Addis Ababa, Ethiopia
10/2007-03/2010	Assistant lecturer, Addis Ababa University, School of Pharmacy, Department of pharmaceutical chemistry, Addis Ababa, Ethiopia
10/2016-10/2007	Graduate assistant, Addis Ababa University, School of Pharmacy, Department of pharmaceutical chemistry, Addis Ababa, Ethiopia

EDUCATION AND TRAINING

01/2013-03/2017	PhD in medicinal chemistry, Martin Luther University Halle-Wittenberg, Department of Pharmaceutical Chemistry, Halle (Saale), Germany Title of the thesis: Design, synthesis and biological evaluation of two classes of antimycobacterial cyclic hexa(depsi)peptides
10/2007-01/2010	Master of sciences in medicinal chemistry, Addis Ababa University, School of Pharmacy, Department of pharmaceutical chemistry, Addis Ababa, Ethiopia Title of master thesis: Design, synthesis and biological evaluation of pyrazoles as antimalarial agents
10/2001-08/2006	Bachelor of pharmacy, Addis Ababa University, School of Pharmacy, Addis Ababa, Ethiopia

Publication

- Adnan A. Bekhit, Ariaya Hymete, <u>Henok Asfaw,</u> and Alaa El-Din A. Bekhit. Synthesis and biological evaluation of some pyrazole derivatives as anti-Malarial Agents. Arch. Pharm. Chem. Life Sci. **2012**, 345, 147–154.

- <u>Henok Asfaw</u>, Katja Laqua, Anna Maria Walkowska, Fraser Cunningham, Maria Santos Martinez-Martinez, Juan Carlos Cuevas-Zurita, Lluís Ballell-Pages, Peter Imming. Design, synthesis and structure-activity relationship study of wollamide B; a new potential anti TB agent. **Ready to be submitted**

Conference Participation and Poster Presentation

- Poster Presenter at Tres Cantos Open Lab Foundation (TCOLF) board meeting held 10/11/2016 at Tres Cantos, Madrid, Spain.
  Presented poster titled: Turning small potent antimycobacterial cyclo(depsi)peptides into drug-like scaffolds

- Poster Presenter at the International Meeting on Antimicrobial Peptides (IMAP) held 31/08/2016 - 03/09/2016 at Leipzig, Germany.
  Presented poster titled: Investigating the SAR of Hirsutellide A, a natural antimycobacterial cyclodepsipeptide

- Poster Presenter at the Gordon Research Conference on Tuberculosis Drug Discovery & Development held 07/12/2015 - 07/17/2015 at Melia Golf Vichy Catalan Business and Convention Center in Girona Spain.
  Presented poster titled: Synthesis and SAR investigations of the natural antimycobacterial cyclodepsipeptide: Hirsutellide A

- Poster Presenter at the German Pharmaceutical Society (*DPhG*) held 24/09/2014 - 26/09/2014 at Goethe University in Frankfurt/Main, Germany.
  Presented poster titled: Synthesis of cyclodepsipeptides analogous to hirsutellide A using solid phase peptide synthesis for antimycobacterial activity testing

Declaration of academic integrity

With this statement I declare, that I have independently completed the above PhD thesis entitled Design, synthesis and biological evaluation of two classes of antimycobacterial cyclic hexa(depsi)peptides. The thoughts taken directly or indirectly from external sources are properly marked as such. This thesis was not previously submitted to another academic institution and has also not yet been published.

Halle (Saale), _____   Henok Asfaw Sahile